

A dark blue BMW i3 electric car is parked on a city street. The car is in the foreground, angled slightly towards the right. The background features tall, modern buildings with many windows, some palm trees, and a construction crane. A traffic light and a 'ONE WAY' sign are visible on the right side of the street. The scene is set during the day with bright sunlight.

Improving the range of EVs through urban data

The impacts of environmental variables, driving style and route choice on the energy efficiency of electric vehicles

A.J.A. Donkers, 2019
Construction Management & Engineering

Improving the range of EVs through urban data

The impacts of environmental variables and route choice on the energy efficiency of electric vehicles

A.J.A. Donkers

0847991

20-08-2019

Master Thesis

*MSc Construction Management and Engineering
Eindhoven University of Technology*

Graduation Committee

Chair

Prof. Dr. Ir. Bauke de Vries

*Information Systems in the Built Environment
Eindhoven University of Technology*

First supervisor

Dr. Dujuan Yang

*Information Systems in the Built Environment
Eindhoven University of Technology*

Second supervisor

Milos Viktorovic MSc

Doctoral Candidate

*Information Systems in the Built Environment
Eindhoven University of Technology*

External advisor

Ir. Jeroen Quee

*Senior Consultant Chain Mobility and Parking
Sweco Nederland B.V.*

Company

Sweco Nederland B.V.

De Holle Bilt 22

3732 HM, De Bilt

Table of Contents

Table of Contents	i
Preface.....	v
Summary	vi
Samenvatting	viii
Abstract	x
Abbreviations.....	xi
List of figures.....	xii
List of tables	xv
Chapter 1. Introduction.....	2
1.1 Background	2
1.2 Research gap	3
1.3 Outline	4
Chapter 2. Literature review.....	6
2.1 Energy prediction modelling.....	6
2.1.1 Velocity prediction models.....	6
2.1.2 Energy prediction models.....	8
2.2 Energy consumption model	10
2.2.1 Energy consumption modelling principles	11
2.2.2 Regenerative braking	14
2.2.3 Auxiliary energy use	15
2.3 Microscopic traffic modelling	17
2.3.1 Different traffic modelling scales	17
2.3.2 Car-following models.....	18
2.3.3 Lane-changing models.....	19
2.3.4 Route choice models.....	20
2.3.5 Additional models.....	22
2.3.6 Microscopic modelling tools	22
2.3.7 Microscopic modelling principles	23
2.3.8 Limitations of microsimulation.....	23
2.4 Modelling the influence of driving style	24
2.5 Modelling the influence of environmental variables.....	25
2.6 Modelling the influence of infrastructural design elements.....	26

2.6.1	Road type and rolling resistance	26
2.6.2	Road curvature	28
2.6.3	Road slopes and hilly driving.....	29
2.6.4	Traffic calming measures.....	29
2.6.5	Signalized intersections	31
2.7	Modelling the influence of traffic intensity	31
2.7.1	Measuring traffic flow	32
2.7.2	Level of Service	32
2.7.3	Implications of traffic flow on energy consumption	33
2.7.4	Decreasing time headway and platoons.....	34
Chapter 3.	Methodology	36
3.1	Research methodology	36
3.2	Data collection	37
3.3	VISSIM modelling methodology	38
3.3.1	Driving behavior modelling.....	39
3.3.2	Infrastructure modelling.....	41
3.3.3	Excel model	43
Chapter 4.	Individual elements.....	46
4.1	Influence of elements related to driving style	46
4.1.1	Speed differences	46
4.1.2	Acceleration and deceleration.....	48
4.1.3	Speed oscillations.....	52
4.2	Influence of elements related to environmental variables.....	55
4.2.1	Temperature	55
4.2.2	Wind	58
4.2.3	Daytime and nighttime driving.....	59
4.3	Influence of elements related to infrastructural design.....	60
4.3.1	Road type.....	60
4.3.2	Road curvature	63
4.3.3	Hilly driving.....	66
4.3.4	Traffic calming measures.....	70
4.3.5	Signalized intersections	87
Chapter 5.	Nieuwegein case study.....	94
5.1	Model and methodology.....	94
5.1.1	Routes	94

5.1.2	Scenarios.....	95
5.1.3	Traffic intensity	95
5.1.4	Slope	97
5.2	Results	98
5.2.1	Scenario 1: Driving on an empty network	98
5.2.2	Scenario 2: Driving during the morning peak hour.....	99
5.2.3	Scenario 3: Driving in an all-eco scenario	100
5.2.4	Scenario 4: Driving during a winter morning peak hour	104
5.3	Power breakdown	105
5.3.1	Power breakdown when driving in an empty network	105
5.3.2	Power breakdown when driving during a morning peak hour	107
5.3.3	Power breakdown when driving during a winter morning peak hour	109
5.4	Route optimization	112
5.4.1	Charging costs	112
5.4.2	Travel time.....	112
5.4.3	CO ₂ -emissions	113
5.4.4	Generalized cost model.....	113
5.4.5	Route optimization results	113
5.5	Validation.....	115
5.5.1	Validation against laboratory measurements	115
5.5.2	Validation against driving test measurements	116
5.5.3	Validation against BMW measurements.....	118
Chapter 6.	Conclusion and discussion	122
6.1	Conclusion.....	122
6.2	Discussion	125
6.2.1	Application for navigation companies	125
6.2.2	Application for car manufacturers	126
6.2.3	Application for traffic engineers.....	126
6.2.4	Data.....	126
6.2.5	Limitations	127
References.....	128
Appendices.....	141
	Appendix A - Routes in Nieuwegein.....	142
	Appendix B – VISSIM model of Nieuwegein.....	143
	Appendix C - Desired speed distributions	144

Appendix D – Driving tests	146
Appendix E – Nieuwegein results: Scenario 1.....	149
Appendix F – Nieuwegein results: Scenario 2	153
Appendix G – Nieuwegein results: Scenario 3.....	157
Appendix H – Nieuwegein results: Scenario 4	161

Preface

Eindhoven, July 2019

Dear reader,

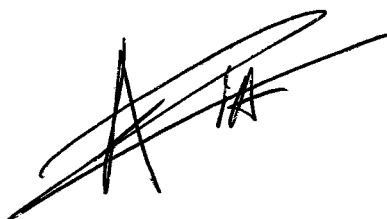
After six years of studying, the big moment is almost there. Studying at the Eindhoven University of Technology has been a rollercoaster, one in which I learned how much passion I've got for the urban environment and how much I love technology. One in which I had the opportunity to meet wonderful bright minds and made friends for life. One which stimulated me to get the most out of my studies while also performing in a rich amount of extracurricular activities. It was tough sometimes, but it has always been fun.

This thesis is the masterpiece of this six years of studying. I'm very glad that I could perform a research which is so close to the topics I'm most interested in. Combining interest for energy, mobility and urban environments was hard, but gave me the opportunity to research on a topic which is innovative and socially relevant at the same time. I truly believe that combining these interests can play a vital role in making our living environments a better and more fun place to live.

This thesis wouldn't be there without a lot of people. I'm grateful for having such an amazing group of people who stimulated me to get the most out of this research. The true quality of this thesis lies in the fact that you shared your critical opinions, and I'm very thankful for that. First, I'd like to thank my supervisors from the Eindhoven University of Technology, Djujan and Milos. I've never had such inspiring brainstorming about a topic than the ones with you two. Your sharp and honest advice helped me to get this thesis to a higher level. Second of all, I'd like to thank my supervisors from Sweco, Jeroen and Luuk, for being so resourceful during the last six months. I'd like to thank my other colleagues at Sweco for showing a lot of interest and for the fun moments during the office hours. Most important would be to thank my friends and family for the support they gave me during my entire studies. Your love and understanding encouraged me to do the things I'm very passionate about. I owe you the world.

I hope this thesis inspires you to work on more innovative, but above all fun projects.

Alex Donkers

A handwritten signature in black ink, consisting of a large, stylized 'A' followed by a smaller, more complex mark that appears to be 'JA' or a similar monogram.

Summary

Internal combustion engine vehicles produce a large portion of the total GHG-emissions, noise nuisance and particulate matter. Electrification of transport modes is expected to reduce such problems and enhance economies. However, the market penetration of plug-in electric vehicles is still small and growth rates are modest in many EU countries. This is mainly caused by the high initial price, lack of charging infrastructure and the low driving range. Using less energy could reduce range anxiety on the short term but requires insights in the energy consumption of BEVs.

In the academic field, many energy prediction models have been created to predict the energy consumption of BEVs. Many models use historical speed data and aren't able to predict the energy consumption upfront. This limits the prediction due to a lack of historical data. More recent models have been created based on microscopic energy prediction models, however, they often use standardized energy parameters to model the influence of the built environment. Therefore, these models often lack the microscopic influence of the built environment on the energy consumption of BEVs. Microscopic traffic software has been established for many years and proved to be able to predict microscopic driving behavior and vehicle processes. The software uses mathematical models to predict microscopic driving behavior and is able to model the driving speed of a vehicle based on many variables. This creates new possibilities for predicting the energy consumption of BEVs.

A research gap has been found in the influence of the built environment on the energy consumption of BEVs. Current energy consumption models in vehicles base the prediction on historical energy consumption and lack route, weather and traffic information. Combining microscopic traffic simulations and energy prediction models gives more insight in the influence of the built environment on the energy consumption of BEVs. The main research question this thesis answered arises from this gap in academic knowledge about the energy consumption of electric vehicles, and reads: *To what extent do driving style, environmental variables, infrastructural design and traffic intensity have an effect on the energy efficiency of electric vehicles and how could route optimization reduce the energy consumption within a driver's time constraints?* By answering this question, this thesis strives to contribute to the knowledge about the influence of the built environment on the energy consumption of BEVs and how that would influence the energy efficiency of different routes. Furthermore, it's a goal to give policy makers and companies in the mobility sector new insights related to the energy consumption of electric vehicles, so that these could be a basis for sustainable measures on the long term.

To answer this question, a combination of methods has been used originating from different fields of science. After performing a literature research, an energy consumption model has been created which could predict the energy consumption of an electric vehicle based on its speed profile. Thereafter, a research has been performed into the possible influences of driving style, environmental variables and infrastructural design and traffic intensity. Based on literature, variables representing these four categories have been selected and quantified. First, the influence of these variables on the energy consumption has been calculated individually. Speed profiles have been created manually and by using VISSIM, after which the energy consumption model has been used to calculate the energy consumption in different situations. Secondly, these individual variables have been combined in a case study by modeling the southern part of Nieuwegein, Utrecht (the Netherlands) in VISSIM. The model combines influences from driving styles, the environment and infrastructural design. The first scenario, in which only one BEV is driving on the road network, gives insight in the influence of the built environment on the energy consumption of BEVs. The VISSIM model has also been used to calculate the influence of traffic intensity, by adding other traffic. The second scenario runs

simulations during the morning peak. The third scenario tests the same morning peak; however, all other vehicles are set to be eco-drivers, thus testing the influence of a large-scale eco-driving strategy. Finally, a simulation has been performed with an ambient temperature of 0°C to test the influence of the winter. The efficiency of route optimization has been tested by creating a generalized cost model based on charging costs, travel time valuation and a price for CO₂-emissions. Different scenarios have been calculated, based on driving style, environmental variables, infrastructural design and traffic intensity. Furthermore, the trip purpose and driver's income are included in the model to evaluate travel time preferences.

Regarding driving style, this research found that a combination of eco-driving strategies, such as driving a lower speed, calmer acceleration and lower speed oscillations led to a significant reduction in energy consumption compared to an aggressive driving style. Weather influences the energy consumption through temperature, with a significantly higher energy consumption at 0°C compared to 12°C ambient temperature. Wind also has an influence on the energy consumption, regardless of the driving speed. Infrastructure influences the energy consumption through the road type, slope and curvature, but also through stop-and-go situations, such as speed bumps and signalized junctions. The influence of signalized junctions becomes bigger during winter due to the high energy consumption during idling.

The Nieuwegein VISSIM model has been used to test different scenarios. As expected, in the empty network, the results show a higher energy consumption for aggressive drivers compared to eco-/normal drivers, and longer travel times for eco-drivers. Increasing the intensity mainly led to longer travel times. Striking is the fact that the energy-efficiency increased on the motorway in the high traffic intensity scenario due to the lower average driving speeds. In the all-eco scenario, the eco-drivers remained more efficient than aggressive drivers, however, their calm acceleration and lower average speeds resulted in congestions. For many roads, an eco-strategy could therefore only be implemented after increasing the capacity of the road or by using new vehicle technologies, such as driving in platoons. Testing the Nieuwegein network at 0°C compared to 12°C resulted in an increase of 25% in energy consumption. The relative influence was bigger for eco-drivers than for aggressive drivers. Different forces turned out to be dominant for different routes and scenarios. In example, the aerodynamic drag forces are dominant on the motorway route, while at 0°C, the auxiliary energy is dominant on the residential route caused by the climate system. Concluding from this, different sustainability strategies would be preferable for different routes. Based on the generalized cost model, different scenarios, related to both energy efficiency and travel time preferences, led to different optimal routes. This demonstrates that optimal routes are influenced by all these variables and that route optimization could definitely influence the energy consumption.

A validation study has been performed. Under Dutch circumstances, the model has been able to predict laboratory measurements with an accuracy of 97%. Next to this, 30 driving tests have been performed in Nieuwegein. The mean absolute percentage error (MAPE) of these measurements is 7,8% for short trips (<5 km) and 3,4% for longer trips (5-20 km). The main accuracy losses are found on motorway driving with the climate system running. A critical note has been expressed towards the current standard used for the technical specification of a vehicle's range.

The thesis ends with a conclusion and discussion, in which recommendations for further research have been given. Next to this, the limitations of this research have been critically discussed, and finally the most relevant information for different sectors has been emphasized.

Samenvatting

Voertuigen met verbrandingsmotoren produceren een groot deel van de totale broeikasgassen, geluidsoverlast en uitstoot van fijnstof. Van elektrische voertuigen wordt verwacht dat ze deze problemen verminderen en tevens een positieve impuls voor de economie zijn. De marktpenetratie van deze voertuigen in de EU laat achter, voornamelijk door te hoge kosten, het gebrek aan laadinfrastructuur en de te lage actieradius. Door minder energie te gebruiken kan de onzekerheid ('range anxiety') van bestuurders worden teruggedrongen op korte termijn. Hiervoor is meer inzicht in het energieverbruik van elektrische voertuigen nodig.

In de academische wereld zijn verschillende modellen gemaakt om het energieverbruik van elektrische voertuigen te berekenen. Veel modellen gebruiken historische data en zijn niet in staat om een voorspelling vooraf te maken. De kwaliteit van de voorspelling wordt beperkt door een tekort aan historische data. Nieuwere modellen gebruiken microscopische energievoorspellingsmodellen. Echter, gestandaardiseerde parameters worden gebruikt om de invloed van de gebouwde omgeving te modelleren. Daarom zijn deze modellen beperkt in de microscopische invloed van de gebouwde omgeving op het energieverbruik. Microscopische verkeerssoftware is al jaren een bewezen kracht in het voorspellen van microscopisch verkeers- en rijgedrag. Deze software gebruikt wiskundige modellen die het microscopisch gedrag voorspellen en zijn geschikt om de rijsnelheid te voorspellen aan de hand van vele variabelen. Dit brengt nieuwe mogelijkheden met zich mee voor de voorspelling van het energieverbruik van elektrische voertuigen.

Er bestaat wetenschappelijke onduidelijkheid over de invloed van de gebouwde omgeving op het energieverbruik van elektrische voertuigen. Huidige energievoorspellingsmodellen baseren de voorspelling op historische data en gebruiken maar beperkt route-, weer- en verkeersinformatie. Het combineren van microscopische verkeerssimulaties en energievoorspellingsmodellen geeft meer inzicht in de invloed van de gebouwde omgeving op het energieverbruik van elektrische voertuigen. Om dit gat in wetenschappelijke kennis te dichten is de volgende onderzoeksvraag gesteld: *In welke mate hebben rijstijl, weersomstandigheden, infrastructureel ontwerp en verkeersintensiteit invloed op de energie-efficiëntie van elektrische voertuigen en hoe kan routeoptimalisatie het energieverbruik verminderen zonder tekort te doen aan de gewenste reistijd?* Door antwoord te geven op deze vraag hoopt deze thesis bij te dragen aan de kennis over de gebouwde omgeving en haar invloed op het energieverbruik en hoe dit de energie-efficiëntie van verschillende routes beïnvloed. Tevens is het doel om beleidsmakers en bedrijven in de mobiliteitssector kwantitatieve inzichten te geven in elektriciteitsverbruik van voertuigen, om zo op langere termijn een basis te kunnen zijn voor verduurzamende maatregelen.

Om deze onderzoeksvraag te beantwoorden is een combinatie van methodes gebruikt uit verschillende wetenschapsrichtingen. Na een literatuuronderzoek is er een energievoorspellingsmodel opgesteld waarmee het energieverbruik van een elektrisch voertuig kan worden bepaald aan de hand van een snelheidsprofiel. Vervolgens is er onderzoek gedaan naar de mogelijke invloed van rijstijl, weersomstandigheden, infrastructureel ontwerp en verkeersintensiteit. Op basis van literatuuronderzoek zijn per categorie variabelen opgesteld en gekwantificeerd. Allereerst is de invloed van deze individuele variabelen op het energieverbruik berekend. Snelheidsprofielen zijn handmatig en met behulp van VISSIM opgesteld, waarna het energievoorspellingsmodel is gebruikt om de energieconsumptie te berekenen voor verschillende situaties. Daarna zijn deze individuele variabelen gecombineerd in een case study door het zuiden van Nieuwegein, Utrecht (Nederland) te modelleren in VISSIM. Het model combineert invloeden van rijstijlen, weer en infrastructureel ontwerp. Het eerste scenario, waarin enkel één voertuig is gesimuleerd, geeft inzicht in de invloed van de gebouwde omgeving op het energieverbruik van elektrische voertuigen. Het tweede scenario is een simulatie van de

ochtendspits en meet de invloed van verkeersintensiteit. Het derde scenario test dezelfde ochtendspits, maar dan met alle auto's rijdend met een eco-rijstijl, om zodoende de invloed van een grootschalige eco-strategie te testen. Als laatste is er een simulatie voltooid met een buitentemperatuur van 0°C om de invloed van de winter te testen. De efficiëntie van routeoptimalisatie is getest door een gegeneraliseerd kostenmodel te maken gebaseerd op laadkosten, reistijd en CO₂-uitstoot. Verschillende scenario's zijn doorberekend, gebaseerd op verschillende rijstijlen, weersomstandigheden, infrastructuur en verkeersdruk. Verder zijn het reisdoel en het inkomen van de bestuurder meegenomen om persoonlijke voorkeuren voor reistijd te modelleren.

Dit onderzoek vond dat een combinatie van eco-rijstijl strategieën, zoals een lagere snelheid, kalmere acceleratie en minder snelheidsschommelingen zorgen voor een significante reductie in energieconsumptie vergeleken met een agressievere rijstijl. Weer beïnvloedt de energieconsumptie door temperatuur, met een significant hogere energieconsumptie bij een buitentemperatuur van 0°C vergeleken met 12°C. Wind heeft ook een invloed op de energieconsumptie, onafhankelijk van de rijnsnelheid. De infrastructuur beïnvloedt de energieconsumptie door verschillende wegtypes, hellingen en bochten, maar ook door 'stop-and-go' situaties zoals verkeersdrempels en verkeerslichten. De invloed van verkeerslichten wordt groter naarmate het kouder wordt buiten door de hoge energieconsumptie van het klimaatsysteem tijdens het wachten.

Het Nieuwegein VISSIM-model is getest op verschillende scenario's. Zoals verwacht is in het lege netwerk de energieconsumptie lager voor eco-bestuurders dan voor agressieve bestuurders, terwijl de reistijd hoger is voor eco-bestuurders. Het verhogen van verkeersintensiteit leidde voornamelijk tot langere reistijden. Opvallend is dat de energie-efficiëntie op de snelweg soms zelfs hoger werd door de lagere gemiddelde snelheid in de spits. In het derde scenario, waarin een grootschalige eco-rijstijl implementatie werd getest, bleven de eco-bestuurders energie-efficiënter dan de agressieve bestuurders. Echter zorgde de kalme acceleratie en lagere rijnsnelheid voor files. Voor veel wegen is het daarom aan te raden om een bij een grootschalige eco-strategie nauwlettend de capaciteit van de wegen te monitoren of zelfs te vergroten. Dit kan door extra asfalt, maar ook door slimme technologieën, zoals het rijden in pelotons. Het testen van het Nieuwegein model met een buitentemperatuur van 0°C vergeleken met 12°C resulteerde in 25% meer energieverbruik. De relatieve invloed was groter voor eco-bestuurders dan voor agressieve bestuurders. Het onderzoek vond dat verschillende krachten dominant waren op verschillende routes en scenario's. Zo is de aerodynamische weerstand dominant op de snelweg, terwijl bij een buitentemperatuur van 0°C het klimaatsysteem bepalend is voor het energieverbruik op de residentiële route. Hieruit kan geconcludeerd worden dat verschillende duurzaamheidsstrategieën gebruikt dienen te worden voor verschillende routes en scenario's. Gebaseerd op een gegeneraliseerd kostenmodel bleken verschillende scenario's (gebaseerd op zowel energie-efficiëntie als reistijd) tot verschillende optimale routes te leiden. Dit demonstreert dat de optimale route wordt beïnvloed door al deze verschillende variabelen en dat route-optimalisatie gebruikt kan worden om de energieconsumptie te verminderen.

Een validatiestudie is uitgevoerd, waarin het model onder Nederlandse omstandigheden bewezen heeft dynamometer metingen met een nauwkeurigheid van 97% te kunnen voorspellen. Hiernaast zijn 30 rijtesten uitgevoerd in Nieuwegein. De 'mean absolute percentage error' (gemiddelde absolute procentuele afwijking) is 7,8% voor kortere ritten (<5km) en 3,4% voor langere ritten (5-20 km). De grootste afwijkingen zijn gevonden op de snelweg tijdens het rijden met het klimaatsysteem aan. Een kritische noot is geuit naar de huidige standaard voor de technische specificatie van de actieradius van voertuigen.

De thesis eindigt met een conclusie en discussie, waarin aanbevelingen voor toekomstig onderzoek worden gedaan. Tevens worden hier de limitaties van het onderzoek besproken, en wordt kort de relevante informatie voor verschillende sectoren besproken.

Abstract

Increasing the market penetration of electric vehicles is necessary to reduce negative externalities of mobility. This penetration is still small thanks in part to range anxiety. Gaps in the academic understanding of energy consumption of electric vehicles have been found, increasing this range anxiety. New ICT developments and the availability of data made it possible to create complex prediction models in order to gain more insights in the energy consumption. These insights could on the short-term lead to better range predictions, while on the long term they could be the basis of sustainability strategies and new business models. This research gives both qualitative and quantitative insight in the influence of driving styles, environmental variables, infrastructural design and traffic intensity on the energy consumption of electric vehicles. An energy consumption model has been used to calculate the influence of individual elements on the energy consumption. Afterwards, the southern part of Nieuwegein has been modeled by using the microscopic traffic simulator VISSIM. The relationship between all individual elements for three driving styles has been measured by using the energy consumption model. Furthermore, different scenarios have been tested to measure the influence of traffic intensity, winter and eco-driving strategies, resulting in qualitative insights in energy consumption and travel time. A power breakdown graph gives more insight in the specific energy consumption in different scenarios. Afterwards, a generalized cost model has been used to measure the influence of different scenarios and travel time preferences on the optimal routes. A significant influence of these scenarios and preferences on the route choice and energy consumption has been found. The model has been satisfyingly validated by using laboratory measurements and 30 driving tests in Nieuwegein, using a BMW i3.

Keywords

Battery electric vehicle, Energy prediction model, Driving style, Weather, Infrastructure, Traffic intensity

Abbreviations

AC	Alternating current
AHN	Actueel hoogtebestand Nederland (actual height map of the Netherlands)
ANL	Argonne National Laboratory
ANN	Artificial neural network
AV	Autonomous vehicle
BEV	Battery electric vehicle
CMEM	Comprehensive Modal Emissions Model
CROW	Centrum voor Regelgeving en Onderzoek in de Grond-, Water en Wegenbouw en de verkeerstechniek (center for regulations and research in ground, water, road and traffic engineering)
DC	Direct current
DLC	Discretionary lane change
EREV	Extended range electric vehicle
EV	Electric vehicle
GHG	Greenhouse gas
HEV	Hybrid electric vehicle
Hwy	Highway
ICE	Internal combustion engine
ICEV	Internal combustion engine vehicle
ITS	Intelligent transport systems
KNMI	Royal Dutch meteorological institute
LCA	Life-cycle analysis
LOS	Level of Service
MaaS	Mobility as a service
MLC	Mandatory lane change
MOE	Measure of effectiveness
MVEI	Motor vehicle emission inventory model
na	Not applicable
OD	Origin-destination
OD	Origin-destination
PHEV	Plug-in hybrid electric vehicle
RPA	Relative positive acceleration
SAE	Society for automobile engineers
SOC	State of charge
T2W	Tank-to-wheel
THW	Time headway
TNO	Dutch organization for applied scientific research
UDDS	Urban Dynamometer Driving Schedule
USo6	USo6 Supplemental Federal Test Procedure
VoT	Value of time
VRU	Veiligheidsregio Utrecht (safety region Utrecht)
W2W	Well-to-wheel
WLTP	Worldwide Harmonised Light Vehicle Test Procedure

List of figures

Figure 2.1 Conceptual model	11
Figure 2.2 Tractive forces on a vehicle	11
Figure 2.3 Energy flows inside an EV from battery to wheels	13
Figure 2.4 Powertrain configuration of a vehicle including the internal energy losses	15
Figure 2.5 Climate control power for different ambient temperatures	16
Figure 2.6 Wiedemann car-following model	19
Figure 2.7 Vehicle type structure in VISSIM	23
Figure 2.8 Rolling resistance coefficient for different temperatures and road types	27
Figure 2.9 Rolling resistance coefficient of the BMW i3 for different road types and temperatures	28
Figure 2.10 Lateral acceleration for different driving speeds	28
Figure 2.11 Assumed lateral acceleration for different driving speeds and styles	29
Figure 2.12 Different types of traffic calming measures	30
Figure 2.13 Schematic representation of the two used traffic calming measure models	31
Figure 2.14 Speed flow curve of a motorway for different intensities and road layouts	33
Figure 2.15 Individual vehicle traces	34
Figure 3.1 Structure of vehicle classes, types and behaviors	39
Figure 3.2 Desired speed distributions for a 50 km/h road	40
Figure 3.3 Desired acceleration for eco-drivers	40
Figure 3.4 Average desired acceleration for different driving styles	41
Figure 3.5 Detector layout for cars, busses and trucks	42
Figure 3.6 Detector layout for trams	42
Figure 3.7 Reduced speed area on a curved road segment	43
Figure 3.8 Different bus stop configurations	43
Figure 4.1 Energy consumption for different desired speeds	47
Figure 4.2 Percentual differences in energy consumption for different desired speeds	47
Figure 4.3 Two ways of measuring the energy consumption during acceleration	48
Figure 4.4 Differences in energy consumption while accelerating	50
Figure 4.5 Differences in energy consumption while decelerating with $P_{aux}=960$ W	51
Figure 4.6 Differences in energy consumption while decelerating with $P_{aux}=350$ W	52
Figure 4.7 Different speed oscillations for eco-driving	53
Figure 4.8 Different speed oscillations for normal driving	53
Figure 4.9 Different speed oscillations for aggressive driving	53
Figure 4.10 Total energy consumption per driving style for high speed oscillations	53
Figure 4.11 Speed distribution for different driving styles with speed oscillations	54
Figure 4.12 Energy consumption for different driving styles due to speed oscillations	55
Figure 4.13 Energy consumption for different ambient temperatures when driving at 30 km/h	56
Figure 4.14 Energy consumption for different ambient temperatures when driving at 130 km/h	57
Figure 4.15 Energy consumption for different wind speeds when driving at 30 km/h	58
Figure 4.16 Energy consumption for different wind speeds when driving at 130 km/h	59
Figure 4.17 Influence of daytime and nighttime driving and LED lighting on the energy consumption	60
Figure 4.18 Energy consumption per 500 m for different road types	62
Figure 4.19 Energy consumption per 500 m for different road types and speeds	63
Figure 4.20 Influence of radius on maximum driving speed for different lateral accelerations	64
Figure 4.21 Speed profile for a 90 degrees curve with a radius of 30 meter	65
Figure 4.22 Energy consumption for a 90 degrees curve with a radius of 30 meter	65
Figure 4.23 Speed profile for a 90 degrees curve with a radius of 20 meter	65
Figure 4.24 Energy consumption for a 90 degrees curve with a radius of 20 meter	66
Figure 4.25 Influence of radius on the energy consumption per driving style	66
Figure 4.26 Influence of up- and downhill driving on the energy consumption when driving 30 km/h	67

Figure 4.27 Influence of up- and downhill driving on the energy consumption when driving 130 km/h	68
Figure 4.28 Uphill-downhill with a slope of 1°, compared to baseline	69
Figure 4.29 Downhill-uphill with a slope of 1°, compared to baseline	70
Figure 4.30 Uphill-downhill with a slope of 10°, compared to baseline	70
Figure 4.31 Downhill-uphill with a slope of 10°, compared to baseline	70
Figure 4.32 Energy consumption at different traffic calming measures	71
Figure 4.33 Relation between speed reduction and increase in energy consumption	72
Figure 4.34 Energy consumption at the speed bump	73
Figure 4.35 Energy consumption breakdown at the speed bump	73
Figure 4.36 Speed profiles at the speed bump	73
Figure 4.37 Energy consumption at the speed bump	74
Figure 4.38 Energy consumption at the Watts speed bump	74
Figure 4.39 Energy consumption breakdown at the Watts speedbump	74
Figure 4.40 Speed profiles at the Watts speed bump	75
Figure 4.41 Energy consumption at the Watts speed bump	75
Figure 4.42 Energy consumption at the Seminole speed bump	75
Figure 4.43 Energy consumption breakdown at the Seminole speed bump	76
Figure 4.44 Speed profiles at the Seminole speed bump	76
Figure 4.45 Energy consumption at the Seminole speed bump	77
Figure 4.46 Energy consumption at the speed slot	77
Figure 4.47 Energy consumption breakdown at the speed slot	78
Figure 4.48 Speed profiles at the speed slot	78
Figure 4.49 Energy consumption at the speed slot	79
Figure 4.50 Energy consumption at the speed cushion	79
Figure 4.51 Energy consumption breakdown at the speed cushion	80
Figure 4.52 Speed profiles at the speed cushion	80
Figure 4.53 Energy consumption at the speed cushion	80
Figure 4.54 Three scenarios for driving at a sequence of traffic calming measures	81
Figure 4.55 Speed profiles of the eco-driver for different distances between two speed bumps	83
Figure 4.56 Speed profiles of the normal driver for different distances between two speed bumps	83
Figure 4.57 Speed profiles of the aggressive driver for different distances between two speed bumps	83
Figure 4.58 Total energy consumption with two speed bumps with 50 m spacing	84
Figure 4.59 Total energy consumption at two speed bumps with 70 m spacing	84
Figure 4.60 Total energy consumption at two speed bumps with 90 m spacing	85
Figure 4.61 Total energy consumption at two speed bumps with 110 m spacing	85
Figure 4.62 Comparison of energy consumption at traffic lights for different initial speeds	88
Figure 4.63 Comparison of energy consumption at traffic lights for different ambient temperatures	89
Figure 4.64 Speed profile with stops at two traffic lights at d=100m and d=200m	90
Figure 4.65 Total energy consumption with stops at two traffic lights at d=100m and d=200m	90
Figure 4.66 Total energy consumption with stops at two traffic lights at d=100m and d=200m during winter	90
Figure 4.67 Total energy consumption with stops at two traffic lights at d=100m and d=200m when waiting 30s	91
Figure 4.68 Total energy consumption with stops at two traffic lights at d=100m and d=200m when waiting 30s during winter	91
Figure 5.1 Schematic representation of zones calculated manually and by using OmniTRANS	97
Figure 5.2 Locations of the slopes in the Nieuwegein model	98
Figure 5.3 Average travel times and energy consumptions for scenario 1	99
Figure 5.4 Average travel times and energy consumptions for scenario 2	100
Figure 5.5 Average travel times and energy consumptions for scenario 3	101
Figure 5.6 Travel time for different starting times when driving the residential route	102
Figure 5.7 Energy consumption for different starting times when driving the residential route	102
Figure 5.8 Travel time for different starting times when driving the city center route	103

Figure 5.9	Energy consumption for different starting times when driving the city center route	103
Figure 5.10	Travel time for different starting times when driving the motorway route	104
Figure 5.11	Energy consumption for different starting times when driving the motorway route	104
Figure 5.12	Average travel times and energy consumptions for scenario 4	105
Figure 5.13	Power breakdown of the three different routes when driving in an empty network	106
Figure 5.14	Power breakdown of a normal driver on the residential route	106
Figure 5.15	Power breakdown of a normal driver on the city center route	107
Figure 5.16	Power breakdown of a normal driver on the motorway route	107
Figure 5.17	Power breakdown of the three different routes when driving in a morning peak	108
Figure 5.18	Power breakdown of a normal driver on the residential route	108
Figure 5.19	Power breakdown of a normal driver on the motorway route	109
Figure 5.20	Power breakdown of a normal driver on the motorway route	109
Figure 5.21	Power breakdown of the three different routes when driving in a winter morning peak	110
Figure 5.22	Power breakdown of a normal driver on the residential route in a winter morning peak ...	110
Figure 5.23	Power breakdown of a normal driver on the city center route in a winter morning peak	111
Figure 5.24	Power breakdown of a normal driver on the motorway route in a winter morning peak	111
Figure 5.25	Price development of CO ₂ emission allowances since the Paris Agreement	113
Figure 5.26	Speed profile of the ANL tests	115
Figure 5.27	Difference between measured and predicted energy consumption	117
Figure 5.28	Influence of the climate system on the energy efficiency	118
Figure 5.29	Speed profile of the WLTC (class 3) driving cycle	118

List of tables

Table 2.1 Definitions of speed.....	6
Table 2.2 Variables used to determine operational speed in speed models from EU countries	7
Table 2.3 Variables used in energy prediction models	9
Table 2.4 Lighting systems and their power use	16
Table 2.5 Wiedemann parameters	19
Table 2.6 Model settings for driving styles	25
Table 2.7 Weather scenarios.....	25
Table 2.8 Types of traffic calming measures	30
Table 2.9 Typical traffic intensity values for different levels of service	32
Table 4.1 Energy consumption after driving 500 m	46
Table 4.2 Energy consumption during different accelerations, model 1.....	48
Table 4.3 Energy consumption during different accelerations, model 2	49
Table 4.4 Energy consumption during acceleration for different driving styles.....	49
Table 4.5 Energy consumption during deceleration for $P_{aux} = 906 \text{ W}$	50
Table 4.6 Energy consumption during deceleration for $P_{aux} = 350 \text{ W}$	51
Table 4.7 Influence of speed oscillations on the energy consumption for different driving styles.....	52
Table 4.8 Effect of speed oscillations on energy consumption, VISSIM results	54
Table 4.9 Influence of ambient temperature on the energy consumption while driving at 30 km/h	56
Table 4.10 Influence of ambient temperature on the energy consumption while driving at 130 km/h ...	57
Table 4.11 Influence of head- and tailwind on the energy consumption when driving at 30 km/h.....	58
Table 4.12 Influence of head- and tailwind on the energy consumption when driving at 130 km/h	59
Table 4.13 Influence of daytime and nighttime driving and LED lighting on the energy consumption ..	60
Table 4.14 Rolling resistance scenario for different road types, road segments of 500 m	61
Table 4.15 Rolling resistance scenario for different road types and speeds, road segments of 500 m	62
Table 4.16 Energy consumption for different curved road segments.....	64
Table 4.17 Influence of up- and downhill driving on the energy consumption when driving 30 km/h ...	67
Table 4.18 Influence of up- and downhill driving on the energy consumption when driving 130 km/h..	68
Table 4.19 Hilly driving scenarios	69
Table 4.20 Results of the individual calculations	71
Table 4.21 Results of the VISSIM simulations.....	72
Table 4.22 Different distances between two traffic calming measures before the critical point	82
Table 4.23 Energy consumption for different scenarios of 'alternative scenario 1'	82
Table 4.24 Energy consumption for different scenarios of 'alternative scenario 2'	86
Table 4.25 Influence of a traffic light when driving 30 km/h.....	87
Table 4.26 Influence of a traffic light when driving 80 km/h	87
Table 4.27 Influence of traffic lights on the energy consumption.....	88
Table 4.28 Influence of traffic lights on the energy consumption during winter	89
Table 5.1 Comparison of routes based on Google Maps data.....	95
Table 5.2 Tested scenarios in Nieuwegein	95
Table 5.3 Slopes in the Nieuwegein model	98
Table 5.4 Output of the generalized cost model for different scenarios and driving styles	114
Table 5.5 Validating the results against the ANL measurements	115
Table 5.6 Driving test results.....	116
Table 5.7 Electricity consumption of 59 BMW i3's.....	118

A photograph of a modern building with a light-colored stone or brick facade. The building has several large, dark-framed windows. A brown car is parked on the street in front of the building. The scene is lit with warm, golden light, suggesting late afternoon or early morning. The text "Chapter 1 Introduction" is overlaid in the bottom left corner.

Chapter 1 Introduction

Chapter 1. Introduction

1.1 Background

Internal combustion engine (ICE) vehicles produce a large portion of the total GHG-emissions (IPCC, 2014; EPA, n.d.; Clarke, 2017), noise and fine particles (Jochem et al., 2016). Electrification of transport modes is expected to reduce these problems and enhances economies (OECD/IEA, 2018). Electric vehicles are expected to play a key role in the contribution to energy transition in the EU green policy agenda. However, the market share of plug-in electric vehicles is still small and growth rates are modest in many EU countries.

The low adaptation rates are mainly caused by three consumer concerns, which are driving range, lack of charging infrastructure and a high initial price (Deloitte, 2019). The driving range has been extensively discussed in literature. Many researchers show that the concern of not reaching a destination on time while traveling in a plug-in electric vehicle is caused by the battery capacity (Tate, Harpster & Savagian, 2008; Brady, 2010; Sonnenschein, 2010), long charging time (Agasal, 2009; Wynn & Lafleur, 2009), and lack of charging infrastructure (Deloitte, 2019; Nilsson, 2011). This prevents consumers from adapting to electric vehicles. Due to these concerns, most plug-in electric vehicles are bought as a second car in a multi-vehicle household (Shahan, 2017). Especially in North-America, where distances are relatively long, only about 11-17% of the electric vehicles are bought in single-vehicle households. Khan and Kockelman (2012) showed that the range of current plug-in electric vehicles such as Nissan LEAF, BMW i3 and the Fiat 500e could serve 69% of driving demand considering a range of 160 km, which would meet half of single-car households preferences and 80% of multi-vehicle households.

The battery capacity of electric vehicles is improving (Yong et al., 2015), however, real breakthroughs are not solving range anxiety problems on the short term (Yong et al., 2015; Cluzel and Douglas, 2012) and batteries are expected to be constrained by weight and cost issues (Wang et al., 2017). Simultaneously, Cuijpers et al. (2016) expect that in 2035, the Netherlands would need 2.700.000 charging points, while most people prefer private charging over public charging (Mathieu, 2018; Cuijpers et al., 2016). Significant peak grid demands are likely to occur due to private charging peaks (Morrissey et al., 2016). European Automobile Manufacturers Association ACEA oversees practical and legislative problems in the realization of all these charging points (ACEA, 2018).

The most fundamental rule of Trias Energetica might be an outcome: using less energy. Ericsson et al. (2006) measured the energy consumption of 109 vehicles in Sweden. 46% of these vehicles didn't use the most energy-efficient route and would've saved 8,2% by changing to a more sustainable route. Creating insights in the energy consumption of electric vehicles is a necessary first step. Many energy prediction models have been created, such as MVEI and MOBILE (Barth et al., 2000). Most of these have been based on macroscopic traffic models (Barth et al., 2000, Barth and Boriboonsomsin, 2009). Although these are able to get an insight in the total emissions at road segments, they don't cover individual driving characteristics (Burghout, 2004; Hamdar, 2012). Microscopic models have been developed to simulate these individual characteristics (Barth et al., 2000; Scora and Barth, 2006). As Barth and Boriboonsomsin (2009) mentioned: "If the microscopic effects can be determined, then it will be possible to estimate vehicle emissions and energy consumption impacts of various speed and acceleration modification techniques for a variety of roadway conditions." This formed the basis of many research projects (Ericsson, 2001; Brundell-Freij and Ericsson, 2005, Boriboonsomsin et al., 2012; Barth and Boriboonsomsin, 2009; Fukushima et al., 2018). Multiple microscopic

influences have been individually identified, such as rolling resistance (Michelin, 2003; Goubert and Sandberg, 2016; Esjmont, 2016), hilly driving (Liu et al., 2017), traffic calming elements (Johnson and Nedzesky, 2004; Ahn and Rahka, 2009; Gupta, 2014), traffic intensity (Sugiyama et al., 2008), vehicle automation (Hoogendoorn and Knoop, 2013; Heijne, 2014; Schoenmakers, 2018), driving style (Gundana et al., 2018; Boriboonsomsin et al., 2012; Kedar-Dongarkar and Das, 2012; Fonseca et al., 2010; Zhu et al., 2018) and environmental influences (Wang et al., 2017, Evtimov et al., 2017; Geringer and Tober, 2012; Kavalchuk et al., 2015).

1.2 Research gap

The rise of ICT and the availability of data creates a stimulus to use data to create more complex energy prediction models. Due to the development of microscopic traffic simulation software, microscopic traffic behavior could be better predicted, and more vehicle operations could be modeled nowadays (Barth and Boriboonsomsin, 2009). A research gap has been found in the influence of the built environment on the energy consumption of EVs. Current energy consumption models in vehicles base the prediction on historical energy consumption and lack route, weather and traffic information (Wang et al., 2017). Creating insights in the influence of the built environment on the energy consumption of BEVs is a fundamental step towards more efficient routes and driving styles. Interesting is the rise of vehicle automation, however, a lot of research is necessary before efficient commercial AVs enter the market (Fagnant and Kockelman, 2015; Gao et al., 2016). The use of urban data in complex microscopic energy prediction models could therefore not only be used to create more efficient electric vehicles on the short term, but also to improve autonomous driving on the long term. The motive of this thesis is to research the influence of driving styles, environmental variables, infrastructural design and traffic intensity on the energy consumption of BEVs and how they would influence the energy efficiency of different routes. The research question which fits best to this motive and which this thesis aims to answer is:

To what extent do driving style, environmental variables, infrastructural design and traffic intensity have an effect on the energy efficiency of electric vehicles and how could route optimization reduce the energy consumption within a driver's time constraints?

In order to answer this research question, several sub-questions need to be reviewed. These will be:

1. What is the effect of different driving styles on the energy efficiency of electric vehicles?
2. Which environmental variables do have an effect on the energy efficiency of electric vehicles and to what extent?
3. What is the influence of different infrastructural elements on the energy efficiency of electric vehicles?
4. What is the effect of traffic intensity (intensity/capacity) on the energy efficiency of electric vehicles?
5. Can route optimization and style optimization make more energy efficient routes within a driver's time constraints, and if yes, to what extent?
6. To what extent does this predicted efficiency correspond to reality?

By answering this question, this thesis strives to contribute to the knowledge about these different elements and their influence on the energy consumption, in order to provide drivers with information about the optimal route based on real-time data. Furthermore, it's a goal to give policy makers and companies in the mobility sector new insights related to the energy consumption of electric vehicles, so that these could be a basis for sustainable measures on the long term.

1.3 Outline

This thesis is structured such that a better understanding of the relationship between driving circumstances and energy consumption will be created bit by bit. Chapter 2 aims to create a basic understanding of the fundamental theory behind traffic modelling and energy prediction models through a literature review. Following on this, the literature review will explain different methods to model the various influences by using an energy consumption model. After creating a theoretical base, the methodology of the research will be explained in Chapter 3. This chapter will indicate the different methods which have been used to answer the research question and sub questions, globally. More in depth methodologies will be emphasized in Chapter 4 and 5. Chapter 4 focusses on the influence of individual elements related to driving style, environmental effects and infrastructural design. It explains how these individual elements have been modeled and shows results of both manual calculations and VISSIM measurements. Chapter 5 combines these individual elements in a case study of Nieuwegein. Again, a methodological framework will be sketched after which different scenarios will be explained. By using a generalized cost model, optimal routes will be chosen for different personal preferences and circumstances. In order to measure the accuracy of the model, all the results are validated in threefold. First, the model is validated against measurements from the Argonne National Laboratory. Second, 30 real driving tests with a BMW i3 in Nieuwegein are compared against the predicted scenarios. Finally, the results are compared against the technical specifications used by BMW itself. Chapter 6 closes this research with a conclusion and a discussion. It emphasizes both the scientific and societal relevance and critically discusses the limitations of this research. The thesis ends with recommendations for further research.



Chapter 2

Literature review

Chapter 2. Literature review

Fundamental knowledge in traffic modeling and energy prediction models is essential for evaluating the microscopic influence of different built environment variables on the energy consumption of BEVs. In order to obtain this knowledge, a literature review has been conducted. First, current speed and energy prediction models are being discussed, after which a mathematical energy consumption model will be created based on the literature. Afterwards, the literature review will focus on microscopic traffic modeling as a tool to predict microscopic vehicle behavior. After combining the energy consumption model and the microscopic traffic modeling methods, the literature review will describe how driving style, environmental variables, infrastructural design and traffic intensity might influence the energy consumption based on the energy consumption model and microscopic traffic modeling.

2.1 Energy prediction modelling

Boriboonsomsin et al. (2012) found that the shortest path isn't always the most eco-efficient and that 46% of the trips in Sweden could save energy by choosing a different route. Therefore, it is relevant to take a deeper look into predicting the energy consumption. The first subchapter compares models for predicting driving speed and behavior in different situations, since these affect the energy consumption directly. Different energy prediction models are being emphasized in the second subchapter. They form the basis for the setup of the energy consumption model used in this thesis.

2.1.1 Velocity prediction models

The largest amount of energy consumed in a vehicle is of course related to the movement of the vehicle. Energy is necessary to accelerate the car to a certain speed according to Newton's second law, and to keep it driving in a certain speed due to the resistance forces working on the vehicle. Since the speed of the car has a direct relationship with the energy related to motion, the first models which will be assessed are the velocity prediction models.

Many definitions for vehicle speed exist for many different purposes and uses. Bysveen (2017) captured multiple definitions, based on a survey by Fitzpatrick et al. (2000). Added to these definitions is the desired speed which is often used in simulation software (PTV Group, n.d.). Table 2.1 (Bysveen, 2017) shows these definitions. The most interesting speed to predict is the operating speed, since this operating speed is the 'real' driving speed and thus says the most about the energy consumption. Since it's impossible to measure the real speed of all vehicles, predictions are often made based on the other concepts.

Table 2.1 Definitions of speed

Concept	Definition
Design speed	Speed related to the design of a road type (e.g. 30 km/h, 50 km/h)
Free flow speed	Speed of a vehicle when not being affected by other vehicles
Operating speed	Measured or observed speed of drivers in real situations
Running speed	Length of the road section divided by the time a vehicle drives on it
Average running speed	Average running speeds of all vehicles on a single road section
Posted speed limit	Maximum speed of a road regulated by law
Desired speed	Speed distribution of the speeds individual vehicles want to drive

The Transportation Research Board (2011) brought together many speed prediction models from North America and Europe. In most cases, the operating speed is being affected by the speed and the shape and presence of curves. Furthermore, the geographic shape of the infrastructure, such as width, road type, rolling resistance and road slope seems to be relevant. Table 2.2 shows the variables used in 22 European speed prediction models:

Table 2.2 Variables used to determine operational speed in speed models from EU countries

	Country*	Lane width	Curve shape	Curvature change rate	Posted speed limit	Sight distance	Slope	Acceleration/Deceleration	Road type/rolling resistance
Dilling	GE	X	X	X	X				
Lamm	GE		X		X	X			
Trapp and Oellers	GE	X		X	X	X	X		
Koeppel and Bock	GE	X		X	X	X			
Al-Kassar et al.	GE	X		X	X		X		
Durth et al.	GE		X		X				
Biedermann	GE		X		X				
Koeppel	GE	X		X	X				
Buck	GE		X			X	X		
Lippold	GE	X	X						
Swiss Guide	SW		X	X	X	X		X	X
Italian official approach	IT		X		X		X	X	X
Cafiso et al.	IT	X	X	X	X				
Marchionna and Perco	IT		X	X	X			X	
UK official approach	UK		X	X	X	X			
Kerman et al.	UK		X		X				
French Guide	FR	X	X		X		X		X
Austrian Guide	AU		X		X		X		
OMOE-X	GR	X		X	X		X		X
Kanellaidis et al.	GR		X	X	X		X		X
Total		9	15	11	20	6	8	3	5

* GE = Germany, SW = Switzerland, IT = Italy, UK = United Kingdom, FR = France, AU = Austria, GR = Greece

The 22 prediction models are hardly comparable, since the traffic situation in many countries is very different. These situations differ due to behavioral differences, infrastructural differences, different geographical characteristics and differences in laws and regulations. However, the synthesis table shows which elements are often considered when modelling speed.

Lately, due to the increasing amounts of traffic data and computational power, new types of speed prediction models occurred by using this data to find certain patterns and predict future situations. Csikós et al. (2015) used artificial neural networks to predict traffic speed and congestions by training the ANN with VISSIM outputs. Lin et al. (2018) used a Gaussian Process Model to combine different data sources, such as the geodata from twitter tweets and the trajectory sensors from traffic service platforms to predict trajectory speed, while Tang et al. (2017) used a Fuzzy Neural Network to predict traffic speed. They predicted the speed more accurately than traditional models, due to the learning ability of the machine learning tools. Although these prediction models are still in their infancy and not ready to be used on a large

scale, they do show how new technology could make prediction models better. It's interesting to follow this development.

2.1.2 Energy prediction models

Besides predicting velocity, many researchers proposed models to predict the energy consumption on roads. Two types of energy prediction models could be distinguished: instantaneous models and aggregated models (Guo et al., 2015). In instantaneous models, the input is always done in very small discrete time-intervals (often second-to-second data) and comprises velocity and acceleration. The output of these models is usually GHG-emissions or energy consumption and could be calculated per second. Aggregated models are more of a macroscopic nature. Their input is aggregated data over multiple vehicles, such as average speed, and also gives an aggregated output.

During the last century, two models seemed to be most reliable for modelling vehicle emissions: MOBILE and MVEI (Barth et al., 2000). Both models used average trip speeds to calculate emissions, based on large emission testing datasets. These models were intended to predict emissions on larger scales; the nature of the models isn't suitable for individual (microscopic) predictions (EPA, n.d.-b; Barth et al., 2000). The models lacked the ability to assess complex vehicle operations and ITS strategies.

Because there was more need for mesoscopic and microscopic emission models, the University of California-Riverside, the University of Michigan, Lawrence Berkeley National Laboratory and the National Cooperative Highway Research Program started a research project to build a better prediction model. The outcome was one of the most comprehensive models in that period: the Comprehensive Modal Emissions Model (CMEM) (Barth et al., 2000; Scora and Barth, 2006). The model is based on a physical modelling approach. What was new was the use second-to-second speed and acceleration data. Researchers did already find the influence of this second-to-second data on emissions (Joumard et al., 1995) but the CMEM putting this effect into a modelling environment was a breakthrough (Barth et al., 2000).

Principles of the CMEM model have been used by many researchers around the globe. A lot of research found uses car data to do a post-trip analysis of the energy consumption (Ericsson, 2001; Brundell-Freij and Ericsson, 2005; Boriboonsomsin et al., 2012; Barth and Boriboonsomsin, 2009; Fukushima et al., 2018). The first developed models focused on ICE vehicles. Ericsson (2001) set up a very extensive conceptual model to determine total energy use and exhaust emissions. This model has been further developed by Ericsson (2006) and Ericsson and Brundell-Freij (2005). Barth (2000, 2006, 2009) also further developed the CMEM model. However, these researches clearly lack real-time environmental influences. Pan et al. (2017) used a kernel principal component feature to select parameters for the model and Fuzzy C means clustering to cluster these parameters. Based on the results of a Markov model, these parameters are being translated in an energy prediction using MATLAB/Simulink. Although the results of the prediction are relatively accurate, the model lacks environmental factors, street characteristics and driving style characteristics and thus does not give enough insight in how these variables influence the energy consumption.

More recent projects developed models based on the CMEM model focus on BEV's (Table 2.6). Wu et al. (2015) and Fukushima et al. (2018) used historical speed measurements but were not able to predict the energy consumption upfront due to a lack of historical data. Boriboonsomsin et al. (2012) made use of historical route and standardized energy parameters based on roadway characteristics and Wang et al. (2017) created an online and offline algorithm to predict energy consumption, based on route data, road slope and weather data. It shows impressive results in terms of accuracy, however, both models by Boriboonsomsin et al. (2012) and Wang et al. (2017) lack the microscopic influence of driving behavior and traffic intensity on the driving speed. The model by Wang et al (2017) has been mainly tested on motorways, since predicting speed profiles for inner city areas is very hard. More information on the effects

of street characteristics on the speed profile are necessary in order to make inner city predictions.

Like in velocity prediction, energy prediction models start to use machine learning methodologies more often. Fukushima et al. (2018) used machine learning techniques to predict energy consumption of EVs to recommend charging spot locations, Foiadelli et al. (2018) used the Multi-Layer Perceptron neural network methodology to predict energy consumption based on route information, vehicle information, driver information and environmental variables. The use of machine learning models and especially their learning ability is promising, though a lot of data is necessary to generate accurate results. Very intensive data collection is still needed to create these models, which limits the contemporary use up till now.

Although the prediction model of this thesis won't take sociodemographic variables into consideration, it will be discussed shortly since these sociodemographic influences might explain some of the outcomes of the results. Brundell-Freij and Ericsson (2005) found that males tend to drive a bit faster than females. Though, the difference is very small and would be insignificant for the calculation. An increasing age would on its turn decrease the average driving speed significantly. With a mean of 46 km/h, Brundell-Freij and Ericsson (2005) found an effect of -12 km/h for elderly.

The variables used in different researches have been assessed and summarized in Table 2.3.

Table 2.3 Variables used in energy prediction models

	Brundell-Freij and Ericsson (2005)	Ericsson (2001, 2006)	Wang et al. (2018)	Boriboonsinsin et al. (2012)	Lee (2011)	Barth et al. (2000, 2006, 2009) *	Wu et al. (2015)	Total
EV/PHEV/ICEV	ICEV	ICEV	EV	EV	PHEV	ICEV	EV/ICEV	
Infrastructure								
Junctions with traffic lights	X		X	X		X	X	5
Speed limit	X	X	X	X		X	X	6
Type of neighborhood	X	X						2
Type of road	X	X	X	X		X	X	6
Junctions without traffic lights	X	X	X	X		X	X	6
Intensity (vehicles/lane*hour)	X	X		X		X		4
Number of lanes	X	X				X		3
Traffic management		X						1
Street function		X		X				2
Road slope			X	X		X	X	4
Rolling resistance			X	X			X	3
Road curvature			X	X		X	X	4

Driving style

Relative positive acceleration	X	X		X	X			4
Deceleration	X	X	X	X	X	X	X	7
Stops	X	X	X	X	X	X	X	7
Speed oscillation	X	X	X	x	X	X	X	7
Engine speed (rpm)	X	X		X				3
(Extreme) acceleration	X	X	X	X	X		X	6
Speed	X	X	X	X	X		X	6
Late gear changing	X	X						2
Cruise time (%)				X	X			2

Environment

Temperature		X	X	X			X	4
Humidity		X	X	X			X	4
Air density			X	X			X	3
Rainfall		X						1
Snow		X						1
Head wind			X				X	2

Car performance

Car power/mass	X	X			X	X		4
Rolling resistance coefficient			X			X	X	3
Mass			X	X		X	X	4
Aerodynamic drag force			X			X	X	3
Acceleration force			X			X	X	3
Wheel inertia			X			X	X	3
Tire radius			X			X	X	3
Gearbox			X			X	X	3
Drivetrain			X			X	X	3
Auxiliary energy			X			X	X	3

* CNEM uses car categories, which are based on average car performance characteristics of the cars within the group. Therefore, some accuracy losses will likely occur.

2.2 Energy consumption model

Based on the models which have been compared in 2.1.1 and 2.1.2, a conceptual model has been created as could be seen in Figure 2.1. Different variables related to the environment, infrastructural design and traffic intensity, as well as personal preferences related to driving style and the technical performance of a vehicle determine the speed profile on a certain route. Based on this speed profile, and some variables related to the environment and the car performance, the energy consumption could be calculated by using an energy consumption model.

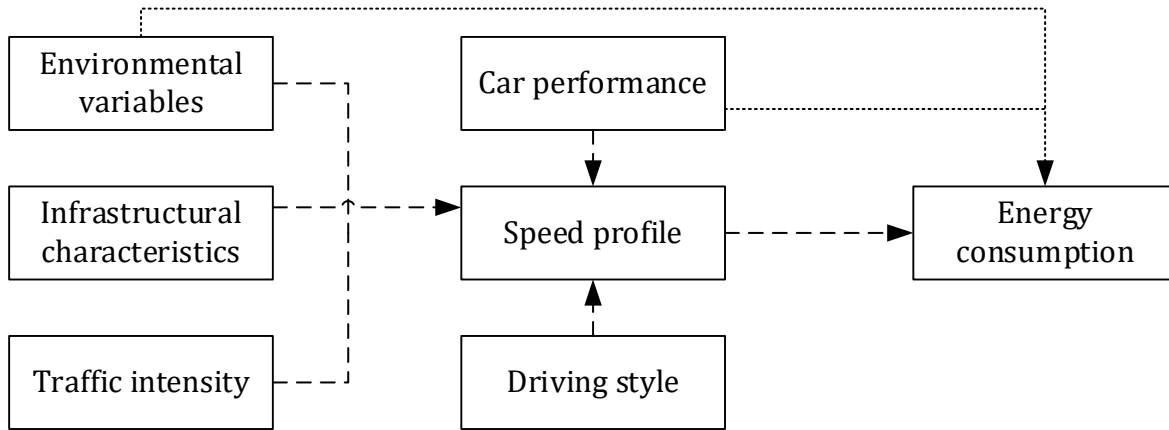


Figure 2.1 Conceptual model

Various energy prediction models have been compared (Table 2.3). Based on these models, an energy consumption model could be created which is able to predict the energy consumption at different routes. The following subchapters show the basic principles of this model.

2.2.1 Energy consumption modelling principles

Basic physical theory shows that the tractive forces of a vehicle are determined by the rolling resistance, the aerodynamic resistance, gravity, and acceleration force. The tractive force is also called the longitudinal dynamic force. This principle is shown in equation 1 and Figure 2.2 (Wang et al., 2015).

$$F_{tr} = F_r + F_{aero} + F_g + F_m \quad [1]$$

where F_r is the rolling resistance force caused by the rolling resistance between the wheels and the road surface, F_{aero} the aerodynamic drag force caused by aerodynamic resistance and wind, F_g the gravity or grade force caused by the gravity and the road slope and F_m the acceleration force caused by the acceleration and vehicle inertia.

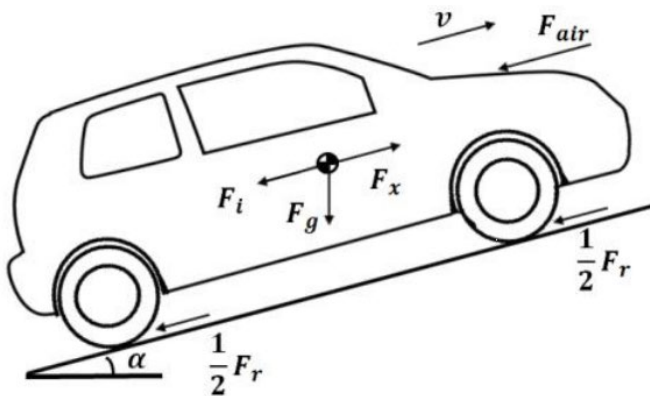


Figure 2.2 Tractive forces on a vehicle

2.2.1.1 Rolling resistance

The rolling resistance force of a vehicle could be explained by the rolling resistance of the wheels on a road surface, multiplied by the mass and the gravitational constant. The equation for the rolling resistance force is:

$$F_r = f_r mg \cos(\theta) \quad [2]$$

Where f_r is the rolling resistance coefficient, m represents the mass of the vehicle in kg, g is the gravitational constant which is $9,81 \text{ m/s}^2$ and θ represents the slope on which the vehicle is driving (in rad).

2.2.1.2 Aerodynamic drag force

The aerodynamic drag force is the component of the force which is caused by air resistance while driving. The aerodynamic drag force is dependent on the air density, the size of the vehicle and its aerodynamic performance. Wind also influences the aerodynamic forces on a car. The equation of aerodynamic drag force is:

$$F_{aero} = \frac{1}{2} \rho A C_d (v - w)^2 \quad [3]$$

With ρ being the air density in kg/m^3 , A being the frontal area of the vehicle, C_d being the aerodynamic drag coefficient representing the aerodynamic performance of the car, v being the velocity of the vehicle in m/s and w being the wind speed in the driving direction of the car in m/s . This wind speed reduces the amount of aerodynamic drag, since air particles will move in the same direction as the car and thus cause less air resistance.

2.2.1.3 Gravitational force

The gravitational force of the vehicle is the force component of gravity that pulls the vehicle towards the earth. When driving on a slope, the vehicle will either get positive or negative gravitational force, depending on the driving direction. The gravitational force is also called the hill climbing force (Genikomsakis and Mitrentsis, 2017) and could be calculated with the following equation:

$$F_g = mg \sin(\theta) \quad [4]$$

with m being the mass in kg, g being the gravitational constant $9,81 \text{ m/s}^2$ and θ representing the slope on which the vehicle is driving (in rad).

2.2.1.4 Acceleration force

Newton's second law of motion states that the net force needed to bring an object in motion is calculated by multiplying the mass of the object and the acceleration of the object. This same principle is being used to formulate the force which is used to linearly accelerate a vehicle:

$$F_m = ma \quad [5]$$

The inertia of the wheels and the motor causes forces as well. According to Wang et al. (2018) these could be described as follows:

$$F_i = \left(\frac{4J_w}{r^2} + \frac{J_m l_g^2}{r^2} \right) a \quad [6]$$

Where J_w is the wheel inertia, J_m is the motor inertia, g is the gravitational constant, r is the radius of the tires, i_g is the gearbox ratio and a is the acceleration. For most vehicles, the inertia is hard to calculate due to unknown variables (Genikomsakis and Mitrentsis, 2016). However, Larminie and Lowry (2012) found that the inertia is approximately 5% of the total vehicle mass. Therefore, the equation for acceleration force, corrected for the inertia, will be:

$$F_m = 1,05 * ma \quad [7]$$

2.2.1.5 Substitution

Substituting the above formulas into equation 8 gives a detailed equation of the tractive forces of the vehicle:

$$F_{tr} = f_r mg \cos(\theta) + \frac{1}{2} \rho A C_d (v - w)^2 + mg \sin(\theta) + 1,05 * ma \quad [8]$$

Multiplying the longitudinal force (in N) with the velocity (in m/s) results in the tractive power (in W). Multiplying this power with the time gives the tractive energy. Since velocity multiplied by time represents distance, the tractive energy could be calculated by multiplying the tractive forces by the driven distance.

$$P_{tr} = F_{tr} * v \quad [9]$$

$$E_{tr} = P_{tr} * t \quad [10]$$

$$E_{tr} = (f_r mg \cos(\theta) + \frac{1}{2} \rho A C_d (v - w)^2 + mg \sin(\theta) + 1,05 * ma) * d \quad [11]$$

Within every car, mechanical losses appear during transmission of energy from the battery to the wheels. These losses are referred to as powertrain losses (Wang et al., 2017). Based on energy conversion efficiency laws, the tank-to-wheel energy consumption of a car could be calculated. Figure 2.3 shows the process of energy flows from the battery to the wheels.

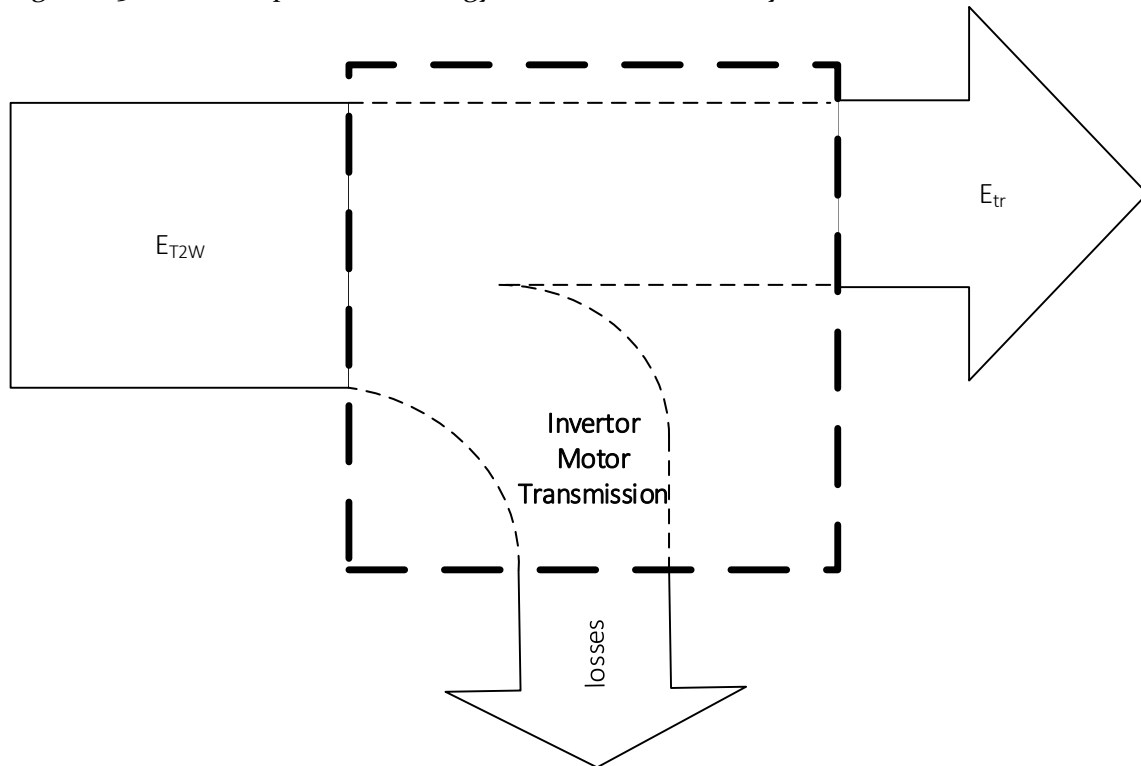


Figure 2.3 Energy flows inside an EV from battery to wheels

The equation to calculate the tank-to-wheel energy, based on the energy flows, will be:

$$E_{T2W} = \frac{E_{tr}}{\eta_{powertrain}} \quad [12]$$

Where $\eta_{drivetrain}$ is the powertrain efficiency. Powertrain efficiency is usually calculated by using dynamometer measurements. A dynamometer is a measuring equipment which is able to measure the rotational speed and the torque of a vehicle (Irimescu et al. 2011). Based on the measurements by Argonne National Laboratory (2015) and measurements of other comparable vehicles, such as the Nissan Leaf (Lohse-Busch et al., 2013), the powertrain efficiency has been set to 85%.

2.2.2 Regenerative braking

EVs largely differ from ICEVs by their powertrains, since EVs use an electromotor and ICEVs an internal combustion engine. This electromotor has the potential to regenerate electric energy during braking, which is called regenerative braking. In regenerative braking, the kinetic energy is converted into chemical energy (Figure 2.4). Normally, kinetic energy is being converted to heat and thus lost. Regenerative braking uses the kinetic energy to power the drivetrain with chemical energy from an internal battery (Xu et al., 2016; Solberg, 2007; Clarke, 2017). Formula 13 shows the equation for kinetic energy:

$$E_k = \frac{1}{2}mv^2 \quad [13]$$

The amount of energy regenerative braking could produce is dependent on the rolling resistance and aerodynamic forces, since part of the kinetic energy is lost due to these resistances. As Fiori et al. (2018) mention, “the most energy efficient route assignment for BEVs could be significantly affected by the regenerated energy”.

A lot of future work will be needed to increase the regenerative braking efficiency, while maintaining safety during braking (Xu et al., 2016). It's also common that new EV users need some adaptation time to get used to this way of braking (Llana, 2015; Cocron et al., 2013) while also differences in user preferences need to be considered (Solberg, 2007). Though, overall, users seem to be very positive about regenerative braking after some adaptation time (Cocron et al., 2013). Schmitz et al. (2012) found that drivers prefer combined pedal solutions (where electric braking is done by the acceleration pedal) over split pedal solutions.

Regenerative braking strategies are typically useful in stop-and-go situations, which in most cases refers to urban driving (Lv et al., 2015; Cocron et al., 2013). There's also a lot of potential for hilly driving (Romm and Frank, 2006). It's first use was in railway situations to regenerate the energy lost during braking (Gonzalez-Gil et al., 2014), but gained interest in the car transportation field lately. For trains, energy reductions of about 30% were found. For cars, the regenerative braking efficiency highly depends on the driving style (Walsh et al., 2010), however, the energy improvement is of about the same order (Wager et al., 2018; Walsh et al., 2010; Romm and Frank, 2006).

The model created by Besselink (2019), which is also used by Wang et al. (2017) assumes a fixed regenerative braking efficiency while the efficiency is highly dependent on driving style. Tests done by Walsh et al. (2010) found regenerative braking efficiencies ranging from 15-93% after measuring different drivers on different scenarios. The highest efficiency was reached by a trained eco-driver, suggesting that training people to use regenerative braking could lead to serious efficiency improvements. In their analysis, approximately 50% of the variation relates to the differences in tracks, while the rest of the variation is driver-specific. Gao et al. (2008) found

that the maximum efficiency of regenerative braking is 86% in 2007 based on five standard driving cycles.

When decelerating slowly, the deceleration could be realized by only using the regenerative braking system, regenerating most of the kinetic energy to electrical energy. Extreme deceleration, as might be seen at aggressive driving styles, requires deceleration realized by a mechanical braking system. Parts of the braking process would still be done by the regenerative braking system, but the aggressive deceleration reduces the regenerative braking efficiency significantly (Evtimov et al., 2017).

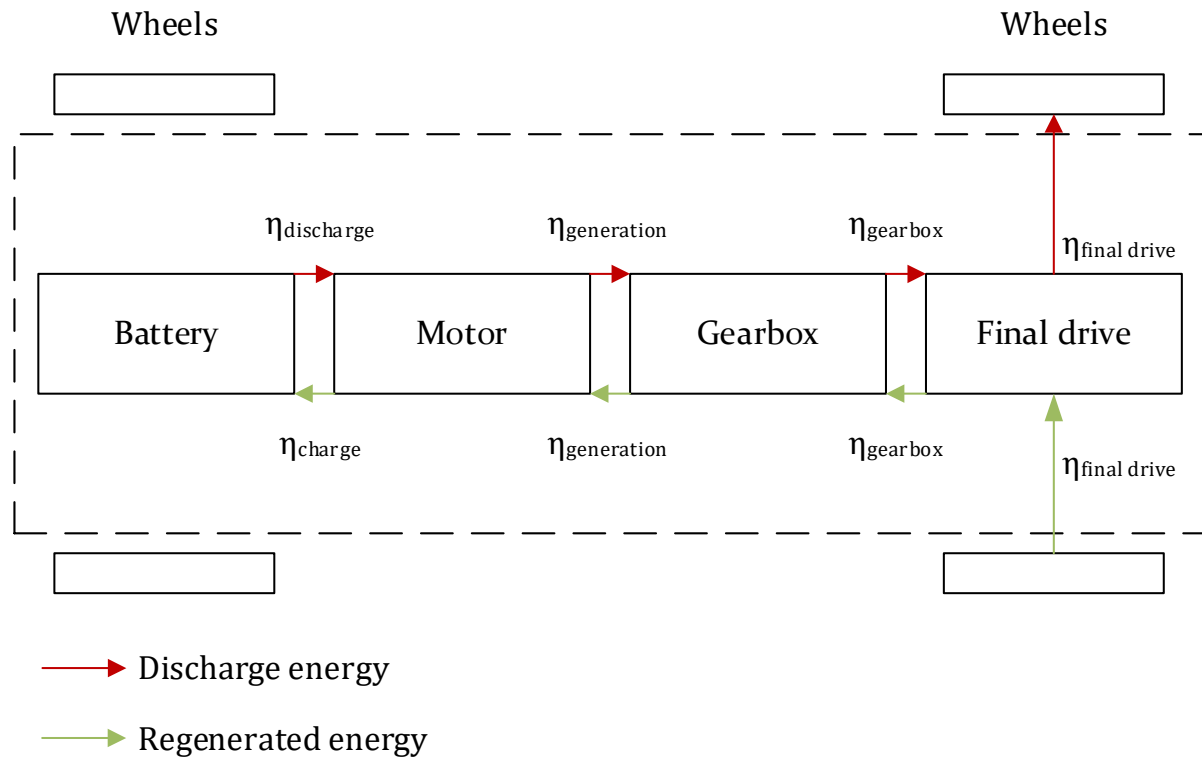


Figure 2.4 Powertrain configuration of a vehicle including the internal energy losses

2.2.3 Auxiliary energy use

Operating vehicles requires more power than only tractive power. Other processes, such as turning on the lights, blowing a fan and putting on the heating require energy. The power this energy causes, which from now on is called *auxiliary power* or P_{aux} , could be measured during standstill or idling. The biggest difference between ICEVs and EVs is that in most ICEVs, the motor keeps running even when the car is idling, which requires energy. Literature calls this idling energy (Boriboonsomsin et al., 2012). Electric vehicles are simpler in the sense that no energy is used in the motor when the car is idling. However, some energy is needed to keep the battery on working temperature.

Auxiliary systems do have a significant impact on the energy use. Evtimov et al. (2017) describe five types of auxiliary systems: climate control, lights and horn, audio system, window cleaning system and seat heating and other systems. As electric vehicles don't produce enough heat to control a comfortable temperature in the car themselves, active climate control is necessary (Kavalchuk et al., 2015). Evtimov et al. (2017) estimated the needed power to bridge a temperature difference of 22 degrees Celsius to be about 2 kW. This not only includes the heating, but also fans which defog windows and window heating devices. The last one requires relatively much power (about 200W per window), though, the running time is usually very short (Kavalchuk et al., 2015). Other climate systems exist in modern, luxurious cars, such as seat

heaters (about 200W per seat) and a steering wheel heater (50W). For modelling purposes, these are not considered. It is however good to mention that only the seat heaters and steering wheel heater could be using about 0,25 kWh on a trip from Eindhoven University of Technology to the Sweco Netherlands main office (a typical 1-hour drive of about 90 km), while this trip would normally use about 12 kWh (based on technical specifications. BMW, 2018). Based on Reichmuth (2016), the energy used to cool the vehicle is about half the energy to heat it. Since the targeted internal temperature is assumed to be 20 degrees, the relation between climate control power and ambient temperature will be used as shown in Figure 2.5.

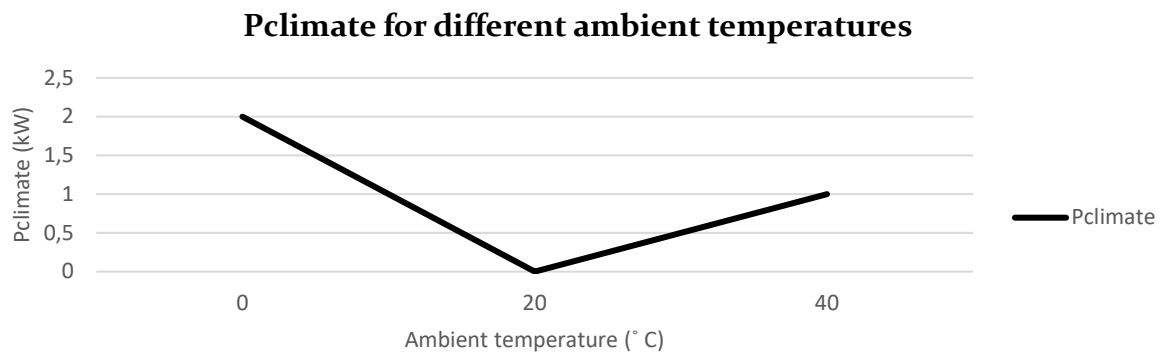


Figure 2.5 Climate control power for different ambient temperatures

The power used by the light system has been captured by Vražić et al. (2014) and Schoettle et al. (2008) and summarized by Evtimov et al. (2017) as could be seen in Table 2.4 (based on Evtimov et al., 2017; Vražić et al., 2014; Schoettle et al., 2008). Based on this data, an average use during daytime and nighttime driving could be estimated. The estimated power for conventional lighting systems is 76 W during daytime and 95 W during nighttime driving. LED lighting systems significantly drop power consumption to 16 W during daytime and 64 W during nighttime driving.

Table 2.4 Lighting systems and their power use

Element	Time of the day	Power consumption [W]	Power consumption (LED) [W]	Use ratio [%]
Daily lights	Day	40	8	100
Long lights	Night	60	34,4	8,4
Short lights	Night	55	54	97,6
Left blinker	Day & night	21	6,9	5,8
Right blinker	Day & night	21	6,9	4,6
Stop-lights	Day & night	21	5,6	3,9
Stop-lights (central)	Day & night	21	3	16,2
Rear-lights	Day & night	5	1,7	92,2
Registration	Day & night	5	0,5	92,2
table lights				
Reverse motion light	Day & night	21	5,2	0,8
Cabin lights	Day & night	20	5	100

The audio system could reach 200 W according to Evtimov et al. (2017). According to measurements done by Geringer and Tober (2012) not surpass 20 W. The use ratio would be about 75% of the time. Therefore, the estimated power for the radio system is 15 W. According to Kavalchuk et al. (2015) the navigation system uses 15W. Window cleaners use approximately 60 W, and, in the model, it's assumed that they are always active during rainfall (Geringer and Tober, 2012; Kavalchuk et al., 2015).

Many small electronical features are added to modern vehicles. Their use depends on the type of vehicle and the driver's personal preferences. Some examples are the cigarette lighter, moving roof system, automated moving seats, multimedia screens, side windows and various sensors (Kavalchuk et al., 2015). It's hard to determine their energy use since this is dependent on the running time of each system. As this depends on the driver, the countries system standards, the intelligence of the systems and the outdoor conditions, an assumption has to be made. The model assumes that there is a constant power of 30W needed for these small features.

2.3 Microscopic traffic modelling

Traffic modelling is a method used by traffic scientists to try to understand driving behavior and traffic flows in real situations. The models are an approximate representation of reality. Since the 50s, engineers have been doing research on creating models which make predictions close to reality (Chandler et al., 1958). From this moment on, many traffic models have been developed, not only for cars, but also for pedestrians, bicycles, boats and other vehicles. Modelling traffic with simulation software instead of by making analytical models based on calculus has the advantage that it gives more insight in the traffic situation. Thanks to the rapid increase in computational power, it becomes easier to use these models (Burghout, 2004).

Developments in Intelligent Transport Systems (ITS) made the use of traffic models even more relevant. The traffic simulations are used to optimize traffic situations based on predictions. Examples are the introduction of advanced traffic management systems (Burghout, 2004) and smart traffic lights (Van der Bijl, 2018). Traffic models are also getting more attention from a climate change perspective, where simulation results are used to model amongst others GHG-emissions (Hofer et al., 2018; Jonkers et al., 2018).

2.3.1 Different traffic modelling scales

Three major directions in traffic modelling could be distinguished. First, macroscopic traffic modelling, which is often used to model large-scale situations, such as city or regional traffic flows. The model uses three macroscopic variables: traffic flow, traffic density and average speed. These variables are often calculated by using the geometric parameters of the road (such as the size of the road, the road type and the number of lanes) and the vehicle input. Vehicles have no individual characteristics since they aren't modeled individually (Burghout, 2004; Hamdar, 2012).

The second model is the microscopic model, which focusses on the individual characteristics of vehicles. Microscopic modelling is able to individually set parameters to different vehicle types. Flows are modeled by modelling the interactions between two individual vehicles, based on their parameters. Often, car-following models are implemented to simulate all the interactions between a leading vehicle and a following vehicle. Microscopic traffic modelling is often used at smaller scales, since it is more time-consuming to build these models due to the large number of parameters. Nevertheless, it is very relevant for scientific use, since it gives more possibilities to model driving behavior and other complex driver characteristics and car characteristics (Hamdar, 2012, Immers and Logghe, 2002, Fellendorf and Vortisch, 2010).

A third and rather new direction in traffic modelling is the mesoscopic traffic modelling approach. Mesoscopic is a hybrid of micro- and macroscopic modelling which combines characteristics from both modelling perspectives. Mesoscopic modelling still uses a very high level of detail for individual vehicles. However, the vehicle interaction models aren't as detailed as the microscopic modelling approach; they look more like macroscopic models. Mesoscopic models thus use both macroscopic as well as microscopic variables. Different mesoscopic simulation software packages exist, all with their own modelling approaches. Although these approaches all differ slightly, one similarity could often be found. Vehicles do have individual characteristics, but in the network, they'll behave as groups, having aggregated speeds (Burghout, 2004; Hamdar, 2012).

As this thesis focuses mainly on the individual vehicle behavior, microscopic models are preferred since they simulate the individual characteristics the best. The following subsections will discuss some fundamental models representing microscopic traffic behavior, after which several microscopic modelling tools are being discussed.

2.3.2 Car-following models

The first and most important element of microscopic behavior is the car-following model (Hamdar, 2012). Car-following models describe the behavior of a vehicle based on the behavior of the leading vehicle (Saifuzzaman and Zheng, 2014). In free flow, the effect of leading vehicles is assumed to be non-existing, thus vehicles will drive according to their desired speed. In congested situations, the distance between vehicles will reduce after which the behavior of the following vehicle will be mainly determined by the leading vehicle (Barth and Boriboonsomsin, 2009). The most researched model family is the Gazis-Herman-Rothery (GHR) family, which has been the base of many models (Olstam and Tapani, 2004). One of the GHR models is the GHP model by Gazis et al. (1959), where interactions are based on the speed difference between the leading vehicle and the following vehicle, changing the acceleration of the following vehicle. It enables different driving styles by changing the sensitivity of behavior adaptation. The Gipps model (Gipps, 1981) knows two driving modes, which are free-flow and car-following. Behavioral differences are modeled through changing the desired acceleration and deceleration rates of a vehicle. The Cellular Automaton model (Nagel and Schreckenberg, 1992) uses the same principle, though it has an extra randomness factor. It shows unrealistic deceleration rates, which has been solved in Krauss' S-K model (Krauss and Wagner, 1997). The maximum safety speed is set based on the maximum deceleration rate. The IDM and IDMM models (Treiber et al., 2006) model the behavior based on the velocity, the acceleration boundaries and the space headway. These models also assume imperfection in the estimation capabilities of drivers, simulating variation in the driving behavior. Wiedemann and Reiter proposed a model based on the differences in speed and distance between the leading car and the following car (PTV Group, 2016, Olstam and Tapani, 2004; Fellendorf and Vortisch, 2010). Yang and Koutsopoulos' (1996) MITSIM knows three driving states: free flow, car following and emergency decelerating.

Since the Wiedemann model used in VISSIM, it will be the most relevant model to discuss. The model assumes that the behavior of a car is always dependent on the behavior of the car in front of him (Fellendorf and Vortisch, 2010), based on the distance between the two vehicles. When the relative distance is large enough, the following vehicle will drive according to his desired speed. When the distance drops below a critical point, the vehicle reach the *reaction zone* (Figure 2.6, Saifuzzaman and Zheng, 2014) after which it changes its speed according to the speed of the leading vehicle. This phase is called the *unconscious reaction*, in which the speed of the following vehicle is determined based on the speed of the leading vehicle (Saifuzzaman and Zheng, 2014). The calculation of the vehicle speed it dependent on the state of the vehicle but in general has the following function:

$$\Delta v = \beta_1(\Delta x - ax) + \beta_2 \quad [14]$$

Where Δv is the speed difference from the following vehicles desired speed, Δx is the distance between the following and leading vehicle, a_x is the preferred minimal standstill distance and β_1 and β_2 are constants (Kim, 2006). Based on typical time headways for desired, risky and safe driving, the distances between the leading and following vehicle could be calculated for every phase by multiplying it by the driving speed. This approach suggests that at higher speeds, the time gap between two vehicles is bigger. This has been confirmed by Zhu et al. (2018).

Wiedemann's car-following model uses the parameters set in Table 2.5 (Fellendorf and Vortisch, 2010). Figure 2.6 shows a schematic representation of how a following driver approaches a slower vehicle and how the parameters have their effect on the following speed and distance.

Table 2.5 Wiedemann parameters

Quantity	Unit	Description
a_x	m	Desired minimal distance between two front bumpers during standstill
b_x	m	Desired minimal distance between two front bumpers during driving
s_{dv}		Point at which the driver reacts consciously to changes in front of him
c_{dv}		Additional safety line below the s_{dv} for extra braking
o_{pdv}		Point at which the following driver starts accelerating if he is slower
s_{dx}	m	Maximum following distance

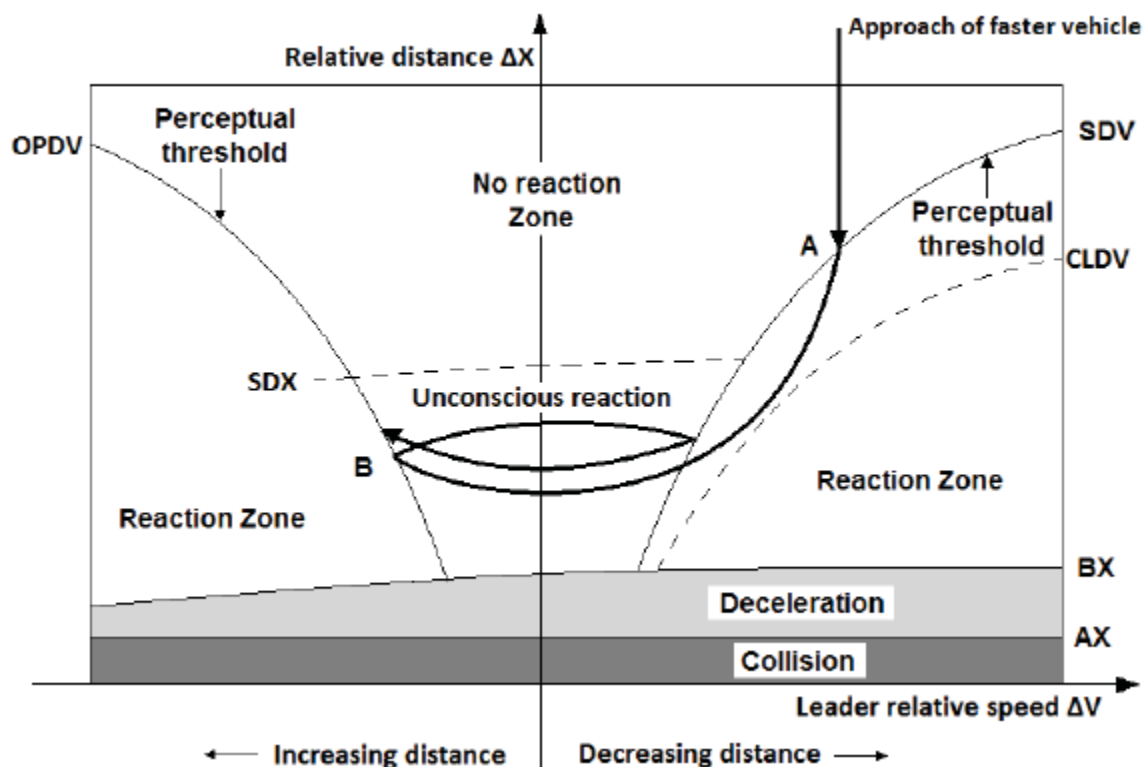


Figure 2.6 Wiedemann car-following model

2.3.3 Lane-changing models

Next to the car-following behavior, lane-changing models exist to simulate lateral movement of vehicles. Lateral movement is relevant in situations of road curvature, but also for lane-changing at multi-lane segments. Two different lane-changing situations could be distinguished: the mandatory (MLC) and discretionary lane change (DLC) (Ahmed, 1999). Mandatory lane

changes are required due to mostly infrastructural changes, such as on-ramp merging on highways. Discretionary lane changes are not required and are often performed to improve the driving conditions of an individual driver. Overtaking on highways is the most common example. An underlying model of the lane-changing model is always the gap-acceptance model. This latest model determines the gap a driver accepts between two vehicles on the target lane, before he makes a lane-changing move. This gap is often referred to as the safety distance (Fellendorf and Vortisch, 2010) and is assumed to have a linear relation with the desired speed. Lane discipline has been found to make models easier. A limitation of this method is that in highly congested situations, the minimum gap distance might never be reached, causing some cars to a standstill at the end of a lane segment. Ahmed (1999) tried to solve this with his forced merging model, where a certain understanding between the vehicles on the target lane and the lane-changing subject is reached. Different microsimulation software tools usually deal with these situations differently. While in VISSIM and ARTEMiS, vehicles disappear from the model after waiting too long to change lanes, in AIMSUN the vehicle will continue following the wrong route (Hidas, 2004). The acceptable gap has been determined by a base value for each behavioral scenario and a random term, which differs per driver and per situation.

$$G_n^{er}(t) = G_n + \epsilon_n^{er}(t) \quad [15]$$

Where G_n^{er} is the acceptable gap for driver n at situation er , G_n represents the gap component of the behavioral model of driver n while ϵ_n^{er} represents the random term, changing for every driver n and situation er .

Various researchers have tried to estimate lane-changing behavior. Gipps (1986) built the first lane change model for microsimulation (Toledo et al., 2003). It's a comprehensive model assessing whether it is necessary, desirable and safe to change lanes based on amongst others the infrastructural situation, speed, other (heavy) vehicles and driver behavior. Yang and Koutsopoulos (1996) and Yang et al. (1999) also differentiate between MLC and DLC. Once a car enters the MLC state, it stays there until it has changed its lane. The DLC state is constantly reconsidered based on the utility of the current lane and the target lane. Kesting et al. (2007) distinguished symmetric passing (as performed in the US) and asymmetric passing (with the 'keep-right' directive, as performed in Europe). Their model, MOBIL, contains a safety and incentive criteria and a politeness factor. Tang et al. (2018) proposed an estimation based on an Adapted Fuzzy Neural Network. Mahapatra and Maurya (2013) found a negative relationship between lateral acceleration and longitudinal speed, in other words vehicles tend to slow down when changing lanes.

Modelling software has different ways of modelling lane-changing behavior. VISSIM uses the MLC and DLC distinction. For MLC, the behavior is modeled based on a maximum deceleration of the target vehicle and the trailing vehicle on the target lane, as well as the distance to the emergency stop, which is often the end of the lane. For DLC, the behavior is based on minimum gap distance which is considered safe. The aggressiveness of changing lanes could only be modeled by decreasing the gap distance (PTV Group, n.d.).

2.3.4 Route choice models

Yang and Koutsopoulos (1996) distinguish informed and uninformed drivers. They use a multinomial logit model which minimizes travel time based on route information. A basic theory which is underlying in most route choice models is based on Kirchhoff's circuit laws, originating from electrical engineering theory (Lin et al., 2013). Kirchhoff's circuit law states that the sum of currents in a network node is always zero. In other words, the currents flowing in are equal to the currents flowing out, as in equation 16:

$$\sum_{k=1}^n i_k = 0 \quad [16]$$

If in a node all inflows are outflows, the following probability distribution based on the Kirchhoff laws could be made:

$$p(R_j) = \frac{U_j^k}{\sum_{i=1}^n U_i^k} = \frac{e^{k \cdot \log U_j}}{\sum_{i=1}^n e^{k \cdot \log U_i}} \quad [17]$$

Where $p(R_j)$ is the probability of choosing route j , U_j is the utility of route j and k is the sensitivity factor or *Kirchhoff factor*. The higher the sensitivity factor, the more sensitive the model is to differences in utility. A Kirchhoff factor of 0 would equally distribute all drivers over all routes, while a very high Kirchhoff factor will send all drivers to the best route (Fellendorf and Vortisch, 2010).

How the utility is being determined is model specific. Burghout (2004) describes a model in which the utility is based on the time-dependent travel time on a route. Fellendorf and Vortisch (2010) describe a utility function based on the generalized cost of each link. AIMSUN uses link cost/m for dynamic assignment, while VISSIM also uses surcharges to indicate extra costs on a link level (Bert et al., 2005; PTV Group, 2016b; PTV Group, n.d.)

These utilities are being calculated by using a shortest-path algorithm. A “path search problem involves finding the optimum path between the present location and the destination under given conditions” (Noto & Sato, 2000). Many shortest-path algorithms exist, all with their advantages and disadvantages. The Dijkstra algorithm (Dijkstra, 1959) is one of the most frequently applied methods for routing problems and calculates the shortest path with the minimum cost (Singal & Chhillar, 2014). It finds the shortest path from one node to all the other nodes after doing several iterations. The optimization computation time of the algorithm increases significantly at larger number of nodes which might be a limitation (Nazari et al., 2008; Noto & Sato, 2000). The Bellman-Ford algorithm is very similar to the Dijkstra algorithm, though it can solve problems with negative edges; something Dijkstra couldn't do (Ford, 1956; Bellman, 1958). A difficulty regarding these two algorithms was that they would only find the shortest path, also known as the all-or-nothing route choice. This would in no case represent reality, since in most situations people would also use other paths than the shortest, and usually one path cannot accommodate all vehicles (Burghout, 2004). By using a k -shortest path algorithm, this problem is solved. Next to the shortest path, the k -shortest path algorithm also finds $k-1$ other paths (Yen, 1971). By combining k -shortest path algorithms with the Kirchhoff distribution equation, vehicles will be distributed amongst all relevant paths. In traffic simulation software, C-logit models are often used (Ben-Akiva et al., 2004). C-logit models make use of a commonality factor which considers different paths with a lot of similarities.

$$p(R_j) = \frac{e^{U_j - CF_{jn}}}{\sum_{i=1}^n e^{U_i - CF_{in}}} \quad [18]$$

Where CF_{in} is the commonality factor of path i for person n , as calculated in the following equation:

$$CF_{jn} = \beta * \ln \sum_{i=1} \left(\frac{L_{ij}}{\sqrt{L_i L_j}} \right)^\gamma \quad [19]$$

Where L_{ij} is the length of all links common to path i and j , L_i and L_j are the path lengths of path i and j and β and γ are parameters. The C-logit model is part of a VISSIM extension, though the standard model (Kirchhoff distribution) is very similar (Fellendorf and Vortisch, 2010).

There are two ways of modelling demand. In the first method, the number of cars entering the network at each link is modeled. At each intersection, the turning percentages have to be set manually after which the cars will turn according to these rates. The destination of cars is thus determined by the turning percentages. The second method uses an OD-matrix for different time intervals (usually hourly or quarterly) to represent the demand. This second method proved to represent reality better than the first method (Burghout, 2004).

Some models provide en-route switching. En-route switching is the process of switching the desired route during driving, due to new information about the traffic situation which changes the utility functions of the routes (Burghout, 2004).

2.3.5 Additional models

The high amount of detail microsimulation software could give as an output nowadays resulted in the development of more models and plugins. The output is used to calculate other results than only time and cost, such as GHG-emissions, noise pollution and total economic loss (Immers and Logghe, 2002). An example is TNO's EnViVer, which couples TNO's emission database with VISSIM to calculate GHG-emissions and particulate matter (Scholten, 2010).

2.3.6 Microscopic modelling tools

Different computer tools to simulate microscopic traffic models have been created during the last decades. They differ in their functionalities and user-display, but mainly in the models used to predict individual driving behavior. Since the software tools use different car-following, lane-changing and route choice models, the individual driving behavior will be modeled with a different approach. Although this thesis will make use of VISSIM, some other relevant tools will also be assessed since they might give new insights in the modelling process. VISSIM has many tools to model individual driving behavior, which suits this research the best. Next to this, there are some practical considerations to use VISSIM.

2.3.6.1 VISSIM

VISSIM is a behaviour-based multi-purpose traffic flow simulator which outcome is determined by stochastic processes. It is a very common tool for traffic modelers and is able to model multiple traffic modes, such as private cars, pedestrian flows, public transport and mixed-traffic. Simulations are based on a wide variety of variables and use psycho-physical car-following models which are based both on psychological (behavioural) variables as well as physical variables. VISSIM reports different measures of effectiveness, such as speeds, acceleration, location, travel time along paths or at the entire networks and is therefore an effective tool for modelling the speed-profiles of a driver under various traffic intensity situations. VISSIM's system architecture is built upon three building blocks: the road infrastructure, the technical features of vehicles and traffic flows and the traffic control block. Together, these blocks generate the output data (Fellendorf and Vortisch, 2010).

2.3.6.2 PARAMICS

PARAMICS is a micro-simulation software tool which is able to model large networks (Olstam, 2004). PARAMICS is widely used due to its large number of tools (Gao, 2008). PARAMICS' car-following model is very similar to the models used in VISSIM, however, instead of using the Wiedemann models, it uses a Fritzsche model (Gao, 2008). An advantage of PARAMICS is the fact that users can override the software with API's (Gao, 2008), while a limitation is the fact that it cannot model oncoming traffic (Olstam, 2004).

2.3.6.3 AIMSUN

Similar to PARAMICS, AIMSUN enables users to override the software with API's (Gao, 2008). It can also not model oncoming traffic (Olstam, 2004). As well as VISSIM and PARAMICS, different measures of effectiveness could be used to evaluate micro-simulated traffic scenarios (Gao, 2008). AIMSUN uses the Gipps car-following model to simulate car-following behavior (Higgs et al., 2011).

2.3.7 Microscopic modelling principles

Different software packages deliver different microscopic modelling approaches. However, a certain uniformity in the structure of these models exists. The behavior of all individual vehicles is simulated by using analytical models. Based on a certain time step i , the vehicle output is generated for every $t + i \cdot \Delta t$, based on the output on t . Since their behavior can never be modeled with individual models, a model with certain parameter settings is used for every single vehicle type (Immers and Logghe, 2002; Hamdar, 2012). These vehicle types are modeled as follows:

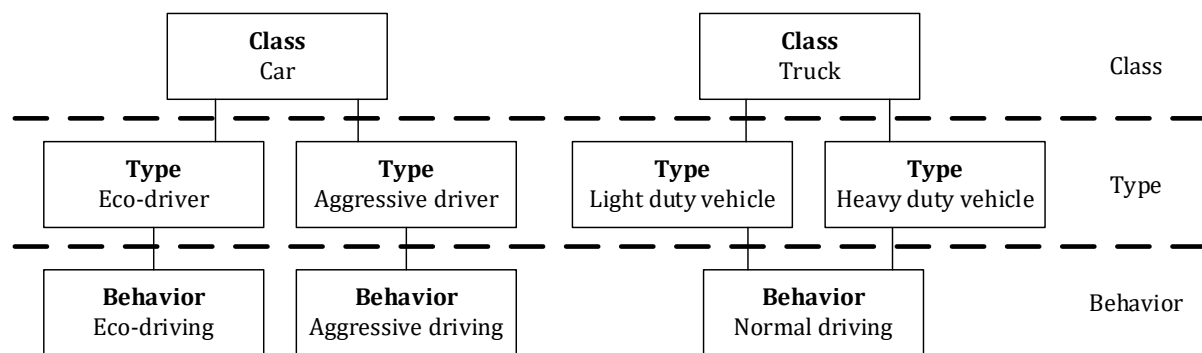


Figure 2.7 Vehicle type structure in VISSIM

As Figure 2.7 (PTV Group, 2016) shows, different types could be made for a single vehicle class. Different behaviors could be assigned to all types.

2.3.8 Limitations of microsimulation

In microsimulation, major limitations have a relation with the high amount of detail of the models. For daily practice, it might be too time-consuming and thus expensive to build microsimulation models, since little errors in the model could change the results dramatically. Especially in somewhat larger networks, human errors are easily made. Secondly, it's hard to model the demand. Microsimulation models are often very sensitive to calibrations which could dramatically influence the outcome of the model (Ge, 2016). Little variations in demand might lead to big variations in the traffic flow, causing congestions or stop-and-go traffic. Therefore, it's important that the vehicle input is as close as possible to reality, in example by doing measurements on-site. Again, this is very time-consuming.

Another limitation of the level of detail is that a lot of variables need to be calibrated. As no traffic situation is the same, there is no real standard for microsimulation parameters. Based on expert insights, trial and error seems to be the usual method to calibrate the model. It also means that once a model has been calibrated, these settings cannot be used for new projects. It requires a lot of expertise to calibrate these models. Most of the parameters are hard to measure, such as the deceleration rate. Therefore, estimations are used mostly to calibrate the model. By using measures of effectiveness (MOEs), often on link level, the calibrated model is compared to real situations. However, these MOEs don't give information on the individual parameter settings; they only assess the aggregated results (Burghout, 2004; PTV Group, 2016; Fellendorf and Vortisch, 2010).

2.4 Modelling the influence of driving style

The relevance of taking driving styles into account derives from the gained interest in the concept of eco-driving. Eco-driving is one of the concepts optimizing the energy-efficiency of EVs. Various definitions of eco-driving exist. Boriboonsomsin et al. (2012) defines eco-driving as a “fuel-efficient operation of a vehicle to achieve better fuel economy and lower tailpipe emissions while not compromising the safety of oneself and other road users”. Jimenez et al. (2014) defined the term as a “driving style followed by vehicle drivers to save fuel”. Feedback is a very important element of eco-driving and could double the savings potential (Barkenbus, 2010). A lot of attempts have been made, both in-car feedback systems as well as infrastructural elements such as the green wave.

Although many researchers have slightly different definitions, the following three parts are widely recognized:

- Informing the driver;
- Choosing the most energy-efficient route based on the available (real-time) data;
- Conforming with personal and societal preferences

Based on the literature, this thesis will define eco-driving as:

Eco-driving aims to inform the driver to choose the most energy-efficient route and driving style based on the available data, while not compromising personal and societal preferences.

It's good to mention that eco-driving is different from hypermiling (Barkenbus, 2010), which uses more extreme techniques to drive more energy efficient, often with increased safety risks.

Driving style is widely known to be an influencing factor on energy consumption and emissions for years (De Vlieger, 1997). Brundell-Freij and Ericsson (2005) found seven significant factors of driving style on fuel consumption. The results show a significant effect of stopping and accelerations on the fuel consumption and various GHG-emissions. The relative positive acceleration (RPA) is usually higher at local streets with a lot of traffic lights and stops and a high traffic volume. An interesting finding is that the RPA is also higher for double-lane streets than on single-lane streets, as the acceleration during overtaking costs energy (Gundana et al., 2018). Gundana et al. (2018) found that aggressive drivers use more energy than normal drivers when changing lanes. Ericsson (2001) found that the major fuel consumption of ICEVs is dependent on acceleration, the amount of stops and speed oscillations.

Many variables exist which could determine the driving style. Kedar-Dongarkar and Das (2012) conducted a Principal Component Analysis and a correlation analysis and found that acceleration and speed variables described 87% of the driving style, significantly increasing energy consumption and tailpipe emissions (Barth and Boriboonsomsin, 2009). Fonseca et al. (2010) found that aggressive drivers tend to accelerate more aggressively and more often. Wang et al. (2017) described the same for both acceleration and deceleration. Zhu et al. (2018) found that conservative (or 'eco-') drivers drive about 14% slower than aggressive drivers. Barth and Boriboonsomsin (2009) found that eco drivers were about 8% slower than non-eco drivers.

The acceleration rate is not measured by standard traffic management systems and therefore data is lacking (Boriboonsomsin et al., 2012). Nevertheless, a certain level of traffic intensity combined with a higher preferred acceleration and desired speed could be used to model a higher acceleration rate (Boriboonsomsin, 2009). Preferred lateral acceleration profiles have been created based on data from Wang et al. (2017) and Raymond et al. (2001). They are different for different driving styles and usually don't reach the technical maximum lateral acceleration of the vehicle. Figure 2.11 in subchapter 2.6.2 shows an explanation of the different profiles. The regenerative braking efficiency differs per driving style because the aggressive driver is thought to use his mechanical brakes more often (Walsh et al.; 2010, Gao et al, 2007)

and. Finally, Barth and Boriboonsomsin (2009) found that oscillations in the driving speed were higher for non-eco drivers than for eco-drivers. These oscillations are strongly related to the acceleration percentage rate and the aggressiveness of the acceleration itself.

The setup of different driving styles could be found in Table 2.6.

Table 2.6 Model settings for driving styles

	Eco-driving	Normal driving	Aggressive driving
Speed relative to desired speed	95%	100%	105%
Acceleration*	2 m/s ²	3 m/s ²	4 m/s ²
Deceleration*	-1,5 m/s ²	-2 m/s ²	-3 m/s ²
Acceleration percentage rate	n.a.	n.a.	n.a.
Lateral acceleration (v=0 m/s)	4,5	6,5	8,5
Regeneration efficiency**	90%	40%	15%

* Based on Wang et al. (2017).

** Based on Walsh et al. (2010).

2.5 Modelling the influence of environmental variables

Environmental effects, such as wind, air density and temperature, have an influence on the energy consumption (Hollweck et al., 2018). Wind and air density have an influence on the aerodynamic forces acting on the vehicle, especially for high driving speeds (Evtimov et al., 2017). Temperature mainly influences the need for auxiliary energy through the climate system (Evtimov et al., 2017). The influence of temperature could therefore best being described per time interval, since the climate system uses more energy when it's turned on for a longer period of time. The influence of wind and air density on their turns, differs for different routes and driving styles, based on the driving speed.

Table 2.7 Weather scenarios

Variable description	Scenario 1 Winter	Scenario 2 Average
Ambient temperature (daily average)	0 °C	12,0 °C
Air pressure	1011,3 hPa	1011,3 hPa
Relative humidity	79%	79%
Air density	1,2877 kg/m ³	1,2306 kg/m ³
Wind speed	-	-
Wind direction	-	-
Minimal sight distance*	-	-

* The minimal sight distance of 3 km at December 21 (KNMI, 2018) is assumed to have no influence on the driving behavior and is thus taken out of consideration. Though, data shows that the sight distance is significantly lower during rainy or foggy days. Future research is needed to find the effect of heavy rainfall and fog on sight and driving behavior.

To generate a baseline situation for the predictions, data has been collected representing the average situation in the Netherlands (Table 2.7). Weather data is being gathered by using KNMI weather statistics of 2018 (KNMI, 2018). The average weather scenario in the Netherlands has been determined by taking the average namely winter solstice (or midwinter, at December 21) and summer solstice (midsummer, at June 21) and will be used in the calculations in this research without further note. In order to assess the boundaries of the weather on the energy

consumption, another imaginary scenario has been taken into consideration: a very cold winter day.

Air density has been calculated by using equation 20:

$$\rho_{\text{humid air}} = \frac{p_d M_d + p_v M_v}{RT} \quad [20]$$

With p_d and p_v being the partial pressure of dry air and the partial pressure of water vapor (in Pa), M_d being molar mass of dry air which is 0,028964 kg/mol and M_v being the molar mass of water vapor which is 0,018016 kg/mol. R is the universal gas constant (8,314 J/(K*mol)) (Omni calculator, n.d.).

Urban wind could be either measured or calculated using Computational Fluid Dynamics (CFD). Measuring wind (real-time) would require measurement tools at a large quantity of streets, which has practical and financial implications. By using CFD, in theory it would be possible to calculate the wind on a microscale. Research showed that the accuracy of CFD simulations is close to real measurements. However, creating such models to predict wind is very time consuming and would require a lot of computational power (Blocken, 2014).

As wind in urban situations is coming from all directions due to the presence of buildings, Bert Blocken (full professor in urban physics and wind engineering at the Eindhoven University of Technology) advised to consider wind speed in these situations to be 0 m/s. The effect of wind will be calculated in the individual calculations though, for eventual future use. Further research is needed to completely cover the effect of wind in real situations.

2.6 Modelling the influence of infrastructural design elements

The infrastructural design of a road and its posted speed limits influence the speed profile of a vehicle and thus the energy consumption, according to equation 9. By modelling individual infrastructural elements, their influence on the energy consumption could be measured. The following subchapters describe how infrastructural design could possibly influence the energy consumption through various design elements.

2.6.1 Road type and rolling resistance

The road surface and its material strongly influence the rolling resistance of a vehicle while driving. Different road types and surface materials have different rolling resistance coefficients. Next to this, amongst others the size, structure and material of the tires also influence the rolling resistance, as well as weather influences. Michelin (2003) researched the effect of changing black tires with green tires and found a decrease in rolling resistance of about 30%, resulting in 4% lower total fuel consumption. To lower extent, even the driving speed reduces the rolling resistance. Finally, the more cars pass a certain road link, the more the road wears down and the profile loses height, reducing the rolling resistance of older asphalt (Goubert and Sandberg, 2016). Good to mention is the fact that most cars also perform better on noise reduction when having a lower rolling resistance (Goubert and Sandberg, 2016; Ejsmont et al., 2016). Wang et al. (2017) found rolling resistance coefficients for different roads under different temperatures through coasting down tests (Figure 2.8, Wang et al., 2017). These tests have been conducted by using an adapted Volkswagen Lupo 3L.

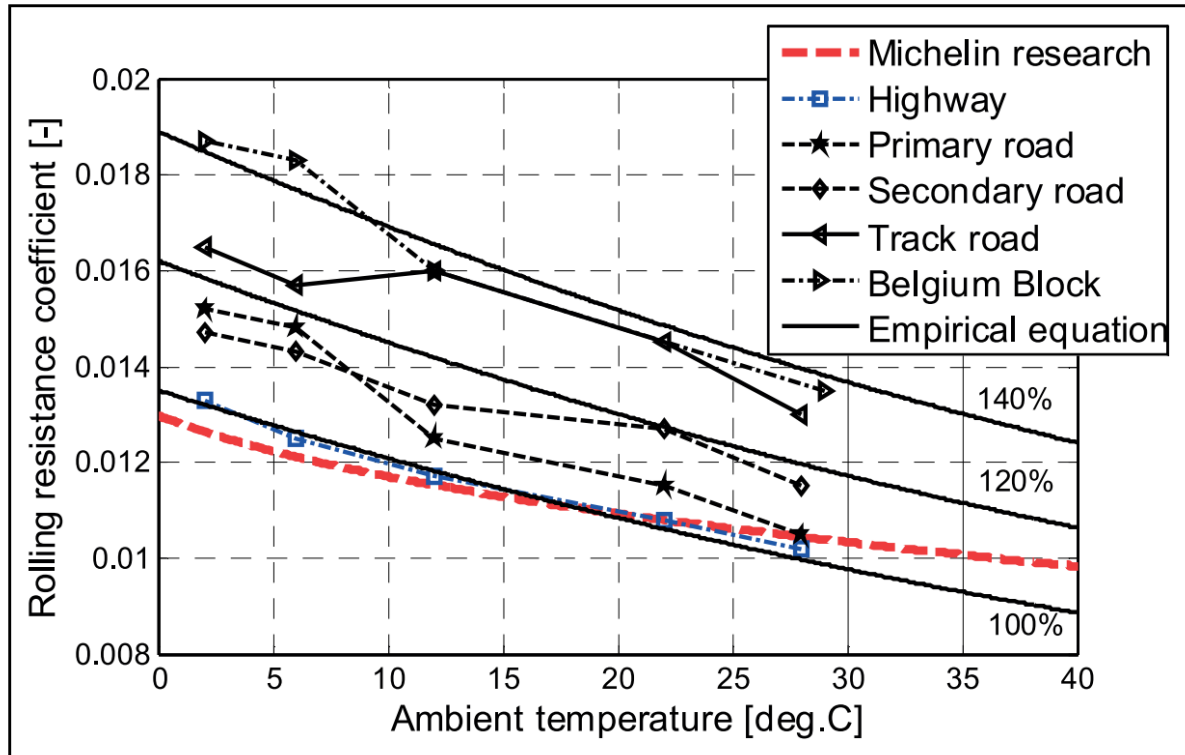


Figure 2.8 Rolling resistance coefficient for different temperatures and road types

Different research has been done into tire rolling resistance. Many research projects are done in the PERSUADE project. Together, different researchers conducted a very extensive research project in various European countries on rolling resistance of tires, comparing many different tires on different road types (Ejsmont et al., 2015; Ejsmont et al., 2016; Ejsmont et al., 2017; Goubert and Sandberg, 2016; Sandberg et al., 2013 and Bendtsen, 2015). They found similar results to the Michelin (2003) research. Many drum tests with different drum profiles have been done, as well as real road tests. According to Groenendijk (2010) and Ejsmont et al. (2015), the DAC and PERS drum profiles are the most similar to pervious concrete, the material most often used for Dutch highways (Rijkswaterstaat, n.d.). When combining the results from previous research, the rolling resistance of a BMW i3 on pervious concrete would follow the following equation:

$$f_{r,pervious\ concrete} = 0,0118 - 0,00013 * T \quad [21]$$

Where $f_{r,pervious\ concrete}$ is the rolling resistance coefficient on pervious concrete and T is the temperature in °C. The equation assumes that the vehicle uses ECOPIA EP500 tires, the standard tires for the BMW i3 (BMW, 2018).

Although it is hard to define an exact formula for the rolling resistance on all different roads in the Netherlands, Wang et al. (2017) made an estimation for different road types based on coasting down tests. When adapting this estimation to the situation in this thesis, the rolling resistance coefficient for all different road types in the Netherlands could be estimated (Figure 2.9).

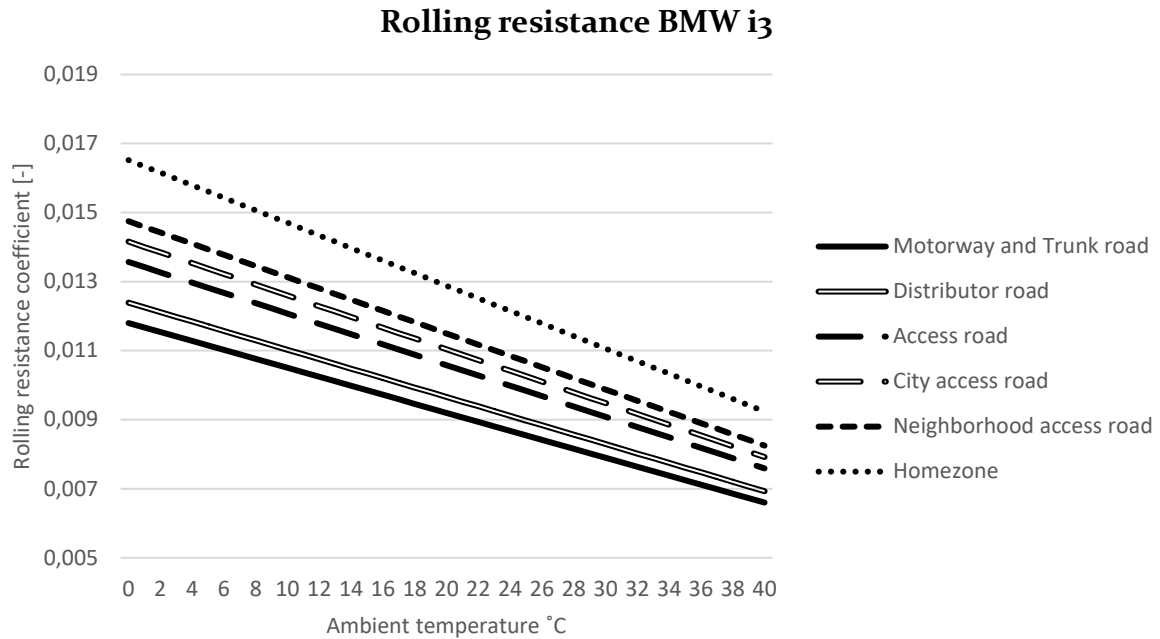


Figure 2.9 Rolling resistance coefficient of the BMW i3 for different road types and temperatures

2.6.2 Road curvature

In curved road sections, the maximum driving speed of a car is limited by the lateral acceleration. The lateral acceleration of a vehicle is being calculated by using the following formula (Wang et al., 2017):

$$a_y = \frac{v^2}{R} \quad [22]$$

Where a_y is the lateral acceleration, v is the maximum speed which could be driven on the curved road segment, and R is the radius of the curve. The lateral acceleration of vehicles could usually reach 8 m/s^2 , though strongly reduces when the driving speed increases. According to driving tests by Raymond et al. (2001) the lateral acceleration would not surpass 7 m/s^2 and drop to almost 1 m/s^2 for highway driving (Figure 2.10).

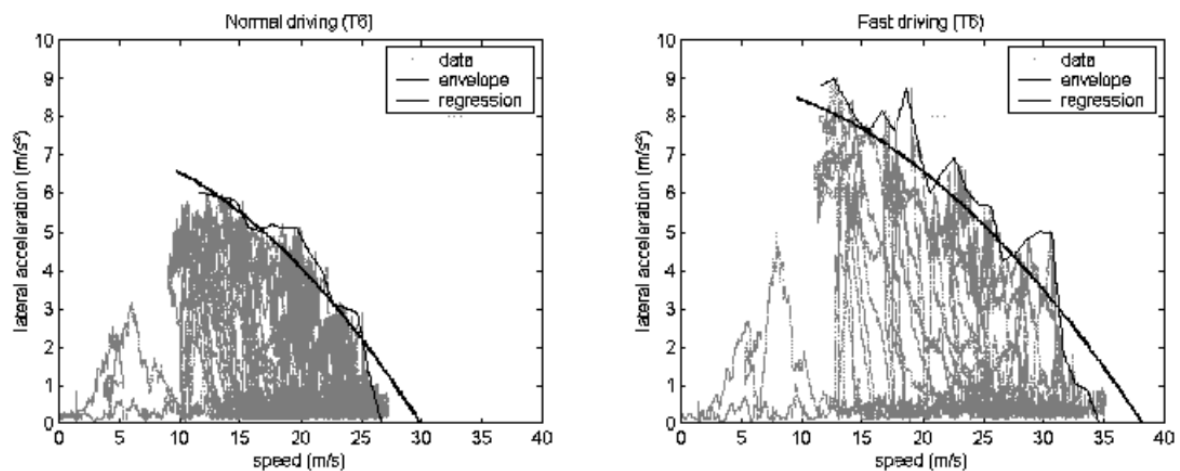


Figure 2.10 Lateral acceleration for different driving speeds

Based on the data given by Wang et al. (2017) and Reymond et al. (2001), a lateral acceleration profile has been conducted for all driving styles. The lateral acceleration does usually not reach the technical maximum of the vehicle; often drivers choose taking turns with a lower acceleration due to comfort reasons (Reymond et al., 2001). Figure 2.11 implies that the more aggressive the driving style, the faster a driver would drive through curved road sections. The different reductions in a curved road section relate to the higher energy consumption due to the required deceleration and acceleration.

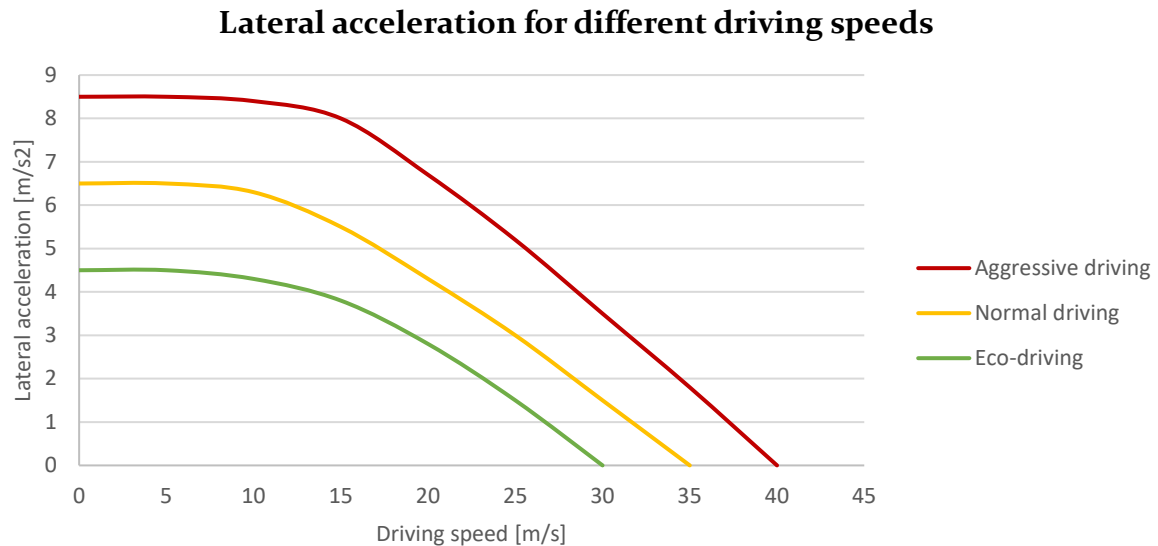


Figure 2.11 Assumed lateral acceleration for different driving speeds and styles

2.6.3 Road slopes and hilly driving

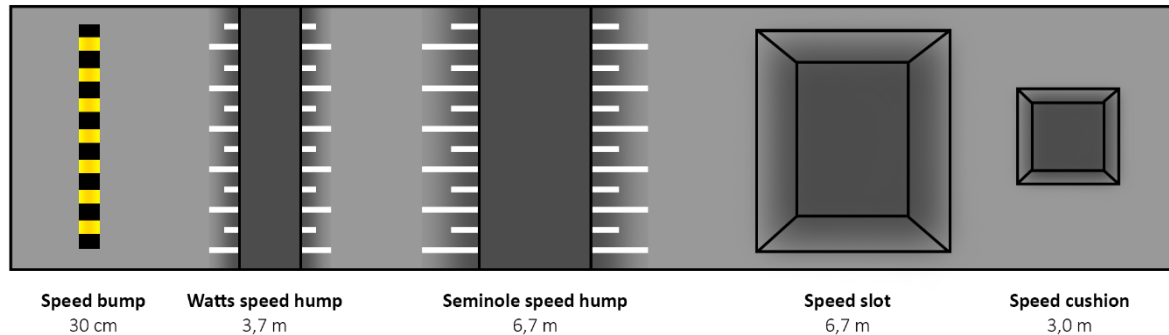
Slopes influence the energy consumption via the rolling resistance and the gravitational forces (equation 2 and 4). A higher slope leads to an increase of these gravitational forces, while the rolling resistance decreases. Liu et al. (2017) did an extensive research to the influence of road slopes on electric vehicle's energy efficiency based on driving tests in Japan. One of the results found was that 75% of the total traveled distance had a grade of -1% to 1%, while 98% of the trips were in the range of -5% to 5%. The logarithmic regression models used by Liu et al. (2017) had a goodness of fit ranging from 0,616 to 0,726. Instead of modelling each individual slope, it assigned percentages of the trip distance to their matching road gradient categories.

2.6.4 Traffic calming measures

The speed profile for crossing a road bump depends not only on the driving style, but also on the type of road bump. Johnson and Nedzesky (2004) gathered data for the crossing speeds at different types of speed bumps. Although this thesis only considers passenger cars, it's good to notice that the speed reduction of buses and service vans is significantly higher, thus having a larger influence on the energy consumption (Johnson and Nedzesky, 2004). Ahn and Rahka (2009) collected speed profiles for different speed humps and bumps as well based on GPS data. Gupta (2014) measured the effect of height of speed humps on speed reduction. Table 2.8 and Figure 2.12 show the different types of bumps concerned, and their estimated speed reduction. The selected speed bumps match the guidelines the Dutch CROW set up for traffic calming measures (Struyk Verwo Infra, n.d.). Struyk Verwo Infra (n.d.) also mentions that the speed reduction of speed bumps increases when the distance between multiple speed bumps decreases.

Table 2.8 *Types of traffic calming measures*

Type	Length	Speed reduction
Speed bump	30 cm	80%
Watts speed hump (75 mm)	3,7 m	50%
Watts speed hump (100 mm)	3,7 m	60%
Seminole speed hump	6,7 m	40%
Speed slot	6,7 m	20%
Speed cushion	3,0 m	60%

**Figure 2.12** *Different types of traffic calming measures*

Two ways of speed bump modelling have been distinguished. The first model used a speed profile which is as close to reality as possible, where a car should reach the desired speed reduction before the bump and starts accelerating after the bump. The second model is a simplification of this process, where only the centerline of the bump is considered the point where a speed reduction should be finished. Right after this speed reduction, the cars accelerate. A schematic overview of the two models is shown in Figure 2.13. An advantage of the second model is that it simplifies defining speed bumps in a larger network, because only one point for speed reduction is enough to calculate the energy consumption. Also, this second model doesn't require the exact length of the bump, reducing the amount of data which is necessary for the prediction. Test runs resulted in very small differences between the models. Calculations starting right at the beginning of the bump and ending at the end of the bump showed differences under 3% in extreme conditions. Measurements by Gupta (2014) also showed similar speed profiles to the second modeling method. Due to the higher efficiency of the second model, this is considered the best model to use when predicting larger networks.

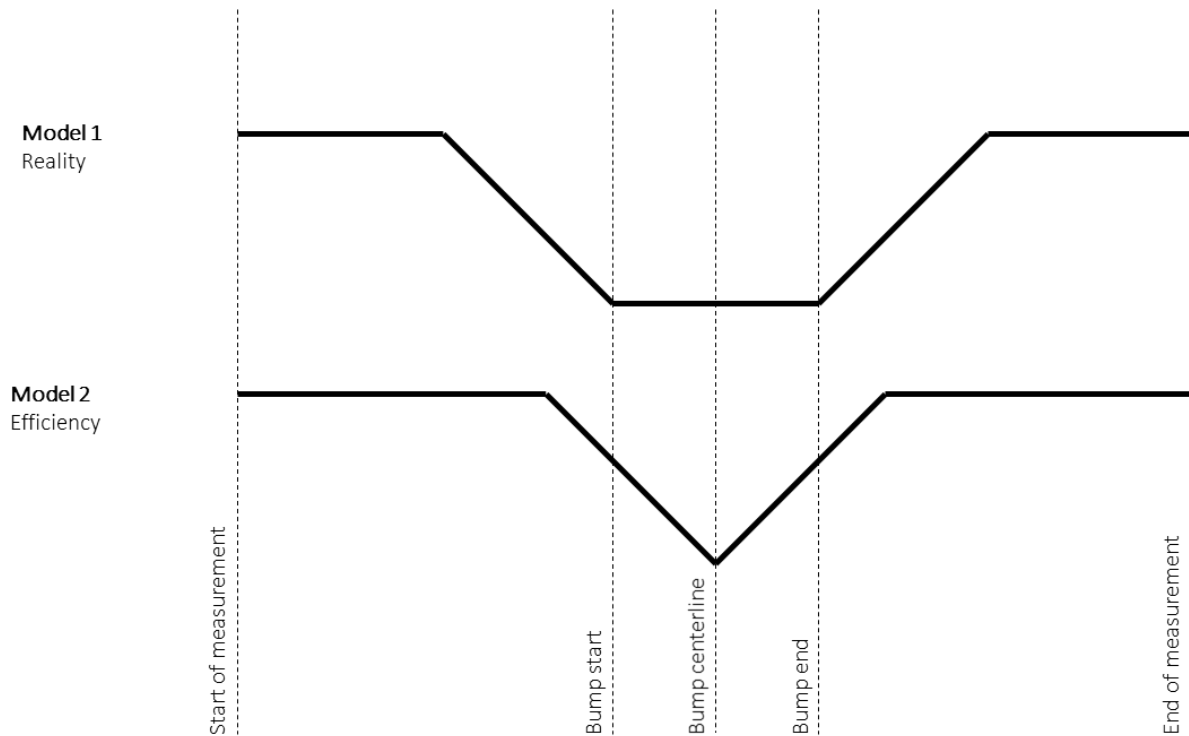


Figure 2.13 Schematic representation of the two used traffic calming measure models

2.6.5 Signalized intersections

Signalized intersections could be considered as stop-and-go situations, similar to the traffic calming measures. A difference is the speed reduction, which could be expressed in percentage of the original speed for traffic calming measures, whereas the speed reduction at traffic lights will be 100%. Another difference is the probability of this speed reduction. For traffic calming measures, one always needs to reduce its speed, while for signalized intersections this depends on the state of the traffic light. For green lights, the influence of traffic lights is considered to be zero since a driver doesn't need to change its behavior. For amber and red lights, the vehicle is considered to stop and decelerate to 0 km/h. How this deceleration affects the energy consumption has been calculated. Next to this, the waiting time also has an influence on the energy consumption, since auxiliary systems such as the climate system will keep on running. The influence of this waiting time is therefore strongly related to the ambient temperature. To cover this effect, different scenarios have been calculated.

2.7 Modelling the influence of traffic intensity

Congestion has many negative externalities. Smeed (1949) proposed his Smeed's law stating that traffic fatalities increase when traffic congestion increases. Barth and Boriboonsomsin (2009) mention that traffic instability could occur at high traffic intensities, resulting in significant speed variations of individual vehicles. As this traffic instability might increase the energy consumption of the individual vehicles, it's interesting to measure the influence of different traffic intensities on individual vehicles' energy consumptions. The following subchapters will discuss the relevant literature to do so.

2.7.1 Measuring traffic flow

A common means to measure the amount of traffic is by measuring the traffic flow (Immers and Logghe, 2002). Traffic flow is a macroscopic traffic variable, however it has its influence on the microscopic behavior of vehicles (Barth and Boriboonsomsin, 2009). Its equation is:

$$\text{Traffic flow} = \frac{n_{\text{vehicles}}}{t_1 - t_0} \quad [23]$$

Where $t_1 - t_0$ is representing a time interval (usually in hours) and n_{vehicles} is the counted number of vehicles between t_0 and t_1 .

Another method which is noteworthy to mention is calculating the traffic density.

$$\text{Traffic density} = \frac{n_{\text{vehicles}}}{d_1 - d_0} \quad [24]$$

Where $d_1 - d_0$ is representing a road segment length in km and n_{vehicles} is the counted number of vehicles between d_0 and d_1 (Immers and Logghe, 2002).

2.7.2 Level of Service

One common way to categorize traffic flow is by using the level of service (LOS) (C/CAG of San Mateo County, 2005). The level of service describes the operational conditions of a road segment. It enables traffic engineers to compare different traffic scenarios based on the traffic intensity, which will give insight in the traffic situation (Mathew and Rao, 2007; C/CAG of San Mateo County, 2005). The traffic intensity could be calculated by dividing the traffic flow by the capacity of a road segment.

$$\text{Traffic intensity} = \frac{\text{Traffic flow}}{\text{Capacity}} \quad [25]$$

Typical traffic intensity values for different levels of service are given in Table 2.9 (C/CAG of San Mateo County, 2005). Barth and Boriboonsomsin (2009) state that the higher a LOS, the higher the influence of driving style on the energy efficiency.

Table 2.9 Typical traffic intensity values for different levels of service

LOS	A	B	C	D	E	F
Traffic intensity	<0,6	0,6-0,7	0,7-0,8	0,8-0,9	0,9-1	1>

The capacity depends on the type of road, the number of lanes, the speed and other infrastructural elements. While it's hard to calculate the capacity for each road segment in the entire country, standardized values have been set up (Rijkswaterstaat, 2018). The LOS of a road increases with an increasing traffic intensity, though typical traffic intensity values for each LOS level differ per road type and situation.

A typical behavior in the speed flow curves for different traffic intensities, is that multilane streets can handle higher intensities way better than single lane streets (Figure 2.14). Speeds at multilane streets generally stay almost constant until traffic intensity values of 0,65 and higher, while single lane streets drop in average speed right after the intensity increases (Rijkswaterstaat, 2018). Fellendorf and Vortisch (2010) found that aggressive drivers tend to drive with faster average speeds in high traffic intensities than eco-drivers. Though Barth and Boriboonsomsin (2009) state that for single lane streets, the aggressive driver adapts his speed to the slower eco-driver.

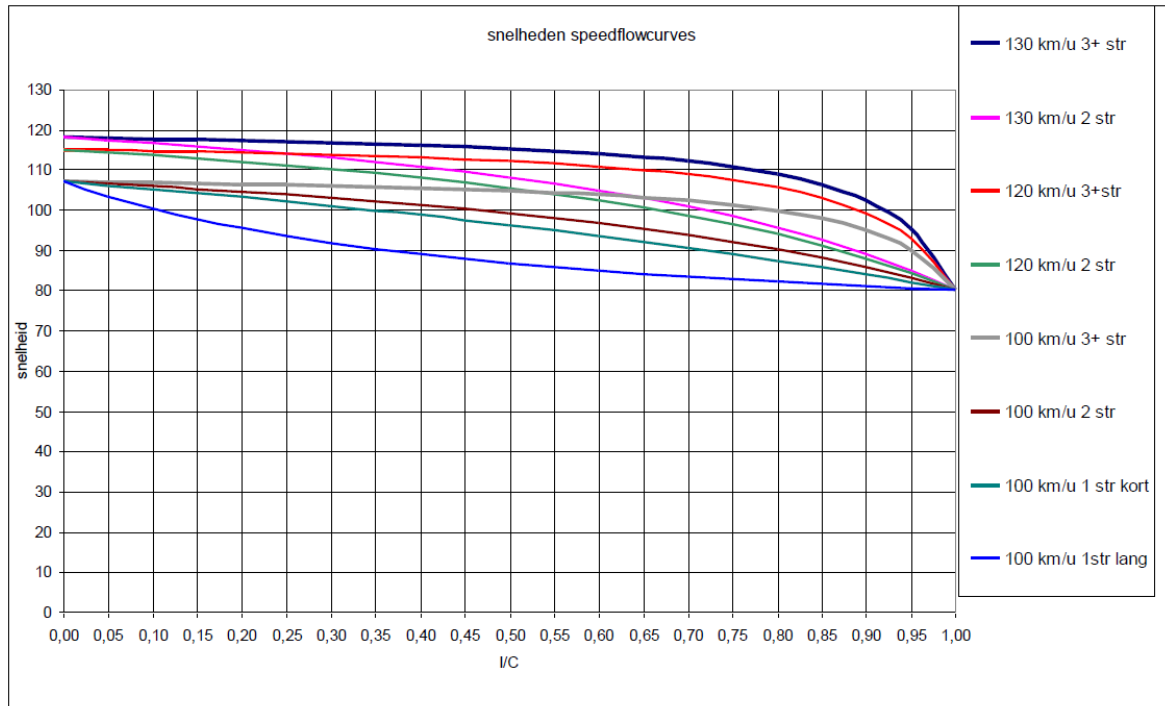


Figure 2.14 Speed flow curve of a motorway for different intensities and road layouts

2.7.3 Implications of traffic flow on energy consumption

Immers and Logghe (2002) describe the acceleration behavior in real traffic conditions as follows:

$$a_a(t + T_r) = Sens * \frac{\Delta v_a(t)}{s_a(t)^2} \quad [26]$$

Where the acceleration of the following car is dependent on the reaction time of the vehicle (T_r) and the sensitivity to react to the driver in front ($Sens$). The acceleration is calculated by dividing the difference in speed between the driver and the driver in front of him by the squared distance between the driver and the driver in front. Therefore, the closer two cars are to each other, the larger the acceleration. Considering the traffic density equation, which shows the amount of traffic per distance, the higher the traffic density, the lower the distances between cars and thus the higher the accelerations on a road segment. Higher accelerations would increase the tractive forces of cars significantly and therefore, the traffic flow is ought to have an impact on the energy consumption of cars.

The effect is well visible in congested roads, in phenomena called shockwave traffic jams (Sugiyama et al., 2008). Measurements could be seen in Figure 2.15 (Sugiyama et al., 2008). The results show the sudden loss in speed on a circular circuit due to the shockwave effect. What's also visible is that all cars have a different behavior regarding their braking behavior. Some tend to slow down more aggressively than others.

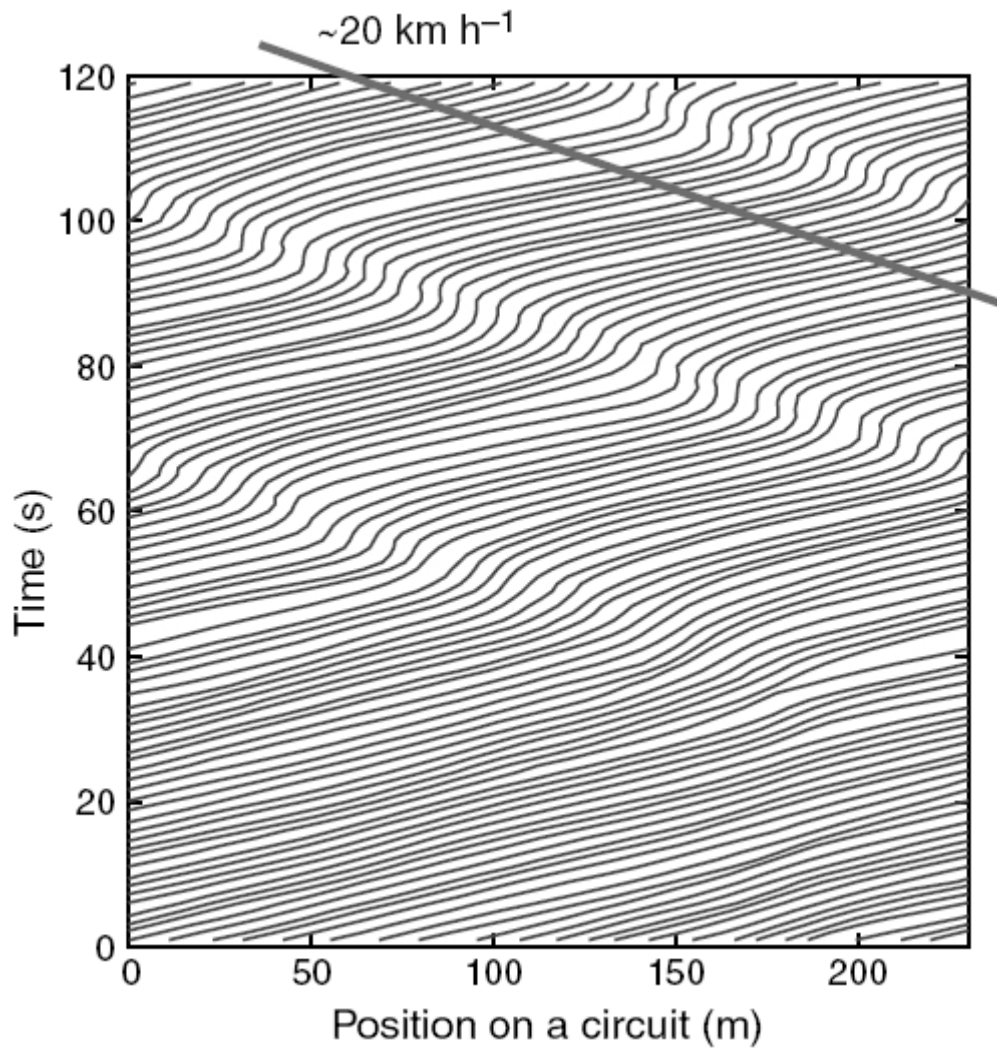


Figure 2.15 Individual vehicle traces

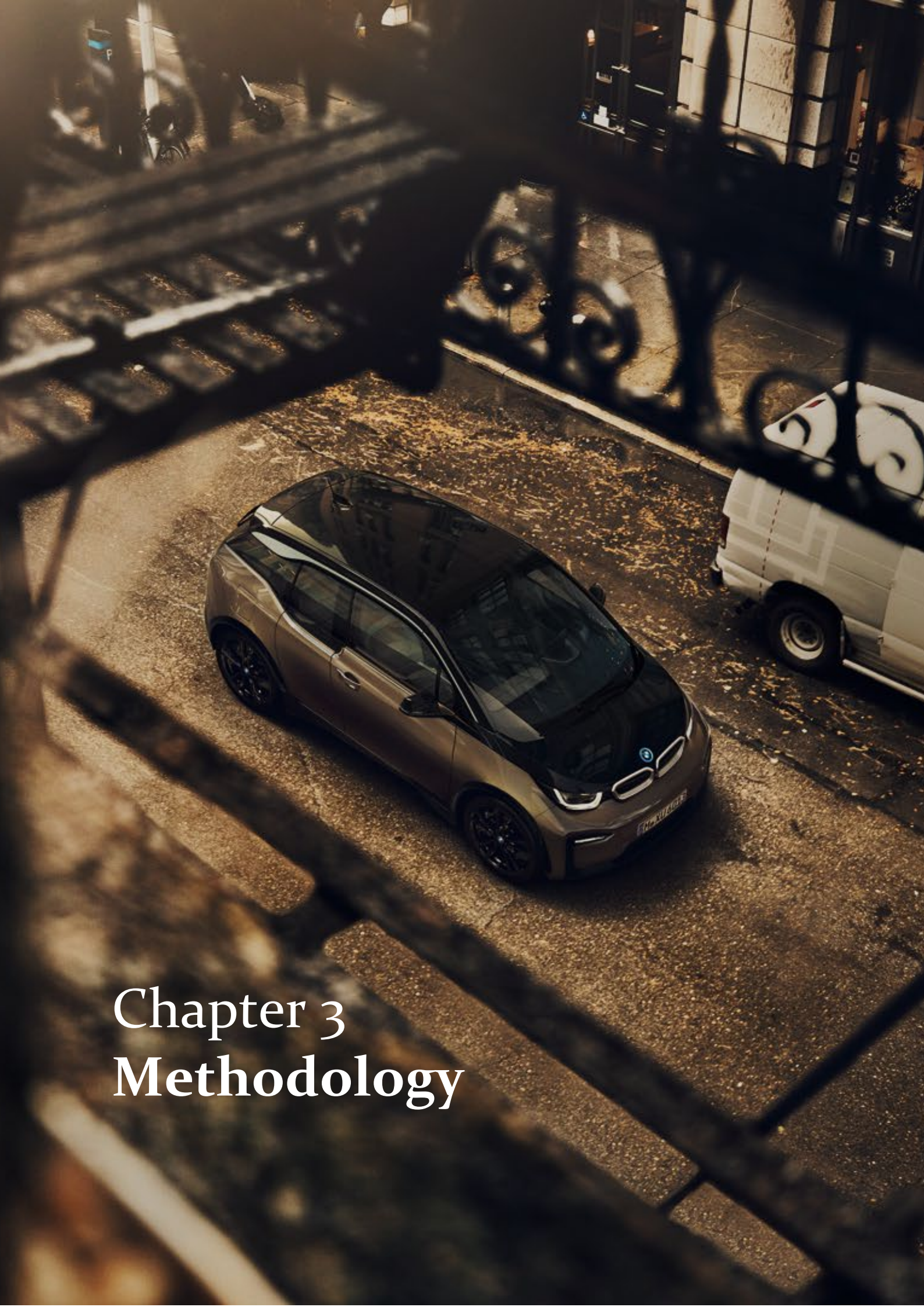
2.7.4 Decreasing time headway and platoons

Velocity oscillations proved to affect the energy consumptions within cars significantly. One trend in automotive industry is creating higher traffic flows by creating platoons to reduce congestion and thus velocity oscillations (Hoogendoorn and Knoop, 2013). The traffic flow could be calculated by using equation 27:

$$Q = \frac{v}{l + THW \cdot v} \quad [27]$$

where Q is the vehicle flow (in s^{-1}), v is the velocity (in m/s), l is the length of the vehicle (in m) and THW is the time headway (in s).

As Schoenmakers (2018) states, the THW of vehicles will likely decrease with an increasing number of vehicle automation (such as platoon management) and in future situations fully automated vehicles. Another advantage of platoon driving is that it enables vehicles to drive in each other's slip stream, resulting in lower aerodynamic forces. In highway situations, this might reduce the energy consumption significantly (Heijne, 2014).

An aerial, high-angle photograph of a dark-colored BMW i3 electric car parked on a city street. The car is positioned diagonally, facing towards the bottom right. The street is paved with cobblestones and has some fallen leaves scattered on it. To the right of the car, a white van is partially visible. In the foreground, a dark, ornate metal railing with circular patterns is out of focus, creating a frame around the car. The background shows a city street with buildings and a few people walking. The lighting is warm, suggesting late afternoon or early morning.

Chapter 3 Methodology

Chapter 3. Methodology

Chapter 3 will emphasize the methods which have been used to answer the research question and sub-questions. The question this research aimed to answer was:

To what extent do driving style, environmental variables, infrastructural design and traffic intensity have an effect on the energy efficiency of electric vehicles and how could route optimization reduce the energy consumption within a driver's time constraints?

With its sub-questions:

What is the effect of different driving styles on the energy efficiency of electric vehicles?

Which environmental variables do have an effect on the energy efficiency of electric vehicles and to what extent?

What is the influence of different infrastructural elements on the energy efficiency of electric vehicles?

What is the effect of traffic intensity (intensity/capacity) on the energy efficiency of electric vehicles?

Can route optimization and style optimization make more energy efficient routes within a driver's time constraints, and if yes, to what extent?

To what extent does this predicted efficiency correspond to reality?

3.1 Research methodology

The research started with a theoretical literature review. This review aimed to lay a foundation of fundamental knowledge in electric driving, traffic modelling and energy prediction. As the University of Alabama (n.d.) states: "Often [a theoretical review] is used to help establish a lack of appropriate theories or reveal that current theories are inadequate for explaining new or emerging research problems". The theoretical review is therefore perfect to create a fundamental base from which new solutions could be built, which fits this research seamlessly. Different existing theories have been reviewed, after which the relationships between theories about electric driving, energy prediction and traffic modelling have been found.

After the theoretical review, a systematic review has been conducted. Systematic reviews focus on causal research questions in the form "to what extent does x contribute to y ". According to the University of Alabama (n.d.), "[the systematic review] consists of an overview of existing evidence pertinent to a clearly formulated research question, which uses pre-specified and standardized methods to identify and critically appraise relevant research, and to collect, report, and analyse data from the studies that are included in the review". The method is therefore able to partially answer sub-questions 1, 2 and 3.

In order to add strength to the results from the systematic literature review, the influences of individual elements related to the first three sub-questions have been calculated. This has been done by using an adapted CMEM model, mentioned to as energy consumption model in this research. This model has been based upon many researches and has a proven efficiency with an error smaller than 5% (Wang et al., 2017). The individual calculations have been made by using two techniques. First, each individual element has been set up manually and calculated manually, by manually creating the speed profiles and use these as an input for the physical model. Secondly, the individual elements have been modeled in VISSIM. Speed profiles have been taken as an output of the simulations, which again are used as input for the energy consumption model. All the parameters which form the input of each VISSIM model are

modeled based upon theoretical and systematic literature review to create a microsimulation which accurately represents reality. The combination of these two calculations will result in an overview of the influence of different individual elements on the energy consumption and therefore answer the first sub questions. A limitation of this method is that some influences, such as temperature and wind, couldn't be modeled in VISSIM due to software limitations, which is why they are only researched using manual calculations.

After calculating the individual influences, a case study has been performed in Nieuwegein, Utrecht (the Netherlands). A traffic model of the south-western part of Nieuwegein has been created by using VISSIM. The model has an area of about 10 km² and contains all individual elements, such as different road types, traffic calming measures and slopes. By performing this case study, the sequence of different elements could be tested. Different scenarios have been created. After performing a baseline study, different traffic intensities, weather scenarios and driving style compositions have been tested. By doing so, the answer to sub-questions 1 and 2 got more accurate and complete, while simultaneously answering sub-question 3.

Sub-question 4 has been tackled by creating a generalized cost model. Generalized cost is a common tool to evaluate different economic options (Langbroek et al., 2016) and is also used a lot in travel research (Wang et al., 2019; Long et al., 2019; Tang et al., 2018). Route optimization in VISSIM is also done by using generalized cost models. The model is created by using the most recent data about wages, charging costs, CO₂-emissions and CO₂-emission allowances and uses theory from other models in travel research as a foundation. The different scenarios calculated in the Nieuwegein case have been optimized based on different trip purposes and income levels. Next to this, the influence of future CO₂-emission allowance prices has been reviewed. The generalized cost model shows how different routes and driving styles are considered to be optimal for different scenarios, and therefore answers sub-question 4.

To validate the model, three validation methods have been used. First, dynamometer measurements have been used to validate the physical model. The dynamometer research made use of the same vehicle type and has results for different driving cycles and weather conditions. Secondly, 30 driving tests in Nieuwegein have been conducted. The tests are conducted under average Dutch circumstances and are therefore a valid way to validate the calculations. Finally, the calculations are validated against the technical specifications of BMW itself, to compare the outcome of real driving tests with the information BMW provides. The threefold validation answered sub-question 5.

The research closes with a conclusion and a critical discussion, reflecting on the results and their relevance for both science, enterprises and society. The limitations of this research have been discussed and recommendations for follow-up research have been made.

3.2 Data collection

As this research aims to provide insight in the influence of different urban characteristics on the energy consumption, urban data has been collected which is as close to reality as possible. Since the validation will be done in the Netherlands, a strong preference for Dutch data was present. Finally, as the research should be reproducible, open data had the preference over private data sources. The data collected could be categorized in four categories:

1. Vehicle data
2. Data to calculate the influence of individual characteristics
3. Data to model the Nieuwegein case study
4. Data to validate the model

First, vehicle data has been collected by using technical data provided by BMW (BMW, 2018). In depth data about the vehicles which are being used for the driving tests has been gathered

by using internal Sweco information about their vehicles, such as the size of the tires and the range of the vehicles. By using information of Argonne National Laboratory (2015), the powertrain efficiency has been determined.

Secondly, data has been gathered to calculate the influence of individual characteristics. This data consists of weather data and infrastructural data. Weather data is gathered from the KNMI (2018). They cover the necessary weather data for this research. Infrastructure data is gathered by using many sources. First, rolling resistance has been researched by reviewing results from coasting down tests. Wang et al. (2018) found rolling resistance coefficients for various road types at ambient temperatures between 0 and 40 degrees Celsius. Wang et al. (2017) also specified minimum, maximum and nominal speeds for these road types. Ejsmont et al. (2016) tested multiple car tires in laboratories and on the road, amongst which the Bridgestone ECOPIA EP500 which are used at the BMW i3. These results have been combined with data from Rijkswaterstaat (2018) about the Dutch road categories. Road curvature has been calculated by using satellite photos from Google Maps. The slope of each road segment has been calculated by using data from the Actueel Hoogtebestand Nederland, which is a map showing the altitude of the Netherlands. The data, which is openly available via a digital map, contains the altitude for every square meter. The most recent altitude data for Nieuwegein is available through the AHN3 dataset and originates from 2014 (Actueel Hoogtebestand Nederland, n.d.). The layout of traffic calming measures and signalized intersections has been based upon the literature review.

To create a realistic traffic model of Nieuwegein, data has been gathered about the infrastructure and the traffic intensity. Data about the road network has been collected by both using satellite data as well as doing a site visit. Input for the traffic lights has been gathered from an internal Sweco file in VISVAP and manually edited in Notepad++. Data for creating public transport lines is openly available. For this area, the public transport map of Syntus Utrecht (2018) has been used. To create realistic traffic volumes, traffic count data has been used. Both internal counts by Sweco, as well as data from VRU2015 (Huisman, 2018).

Finally, different sources are consulted to be able to validate the results. As the validation is done in threefold, three data sources have been used. First, the dynamometer results from the D3 database of Argonne National Laboratory (2015) are used to validate the model against standard driving cycles. Secondly, BMW data is used to compare the results to the information provided by BMW. This data is originated from the same dataset as the data in category 1. Finally, own measurements are done by using two BMW i3 94Ah's from 2017 and 2018. Speed measurements have been performed by using a Transystem GL-770 GPS data logger. The logger can log data on a 5 Hz output rate, and measures amongst others speed, distance, elevation, latitude and longitude.

3.3 VISSIM modelling methodology

After predicting the energy consumption during different situations based on mathematical and physical formulas, the different scenarios are modeled in the microscopic traffic simulator VISSIM. This subchapter will elaborate on the modelling work done in this simulator. First, different settings will be discussed. By manually editing these settings, an attempt is made to simulate realistic traffic behavior based on the earlier findings of this research. Apart from the individual driving behavior, these settings also include the way different infrastructural situations are modeled, as well as how peak hour traffic is being simulated.

3.3.1 Driving behavior modelling

As discussed earlier, driving styles in VISSIM are modeled through a system of vehicle classes (e.g. ‘truck’), vehicle types (e.g. ‘heavy truck’) and driving behavior (e.g. ‘heavy truck behavior’). For this research, the following structure is being used:

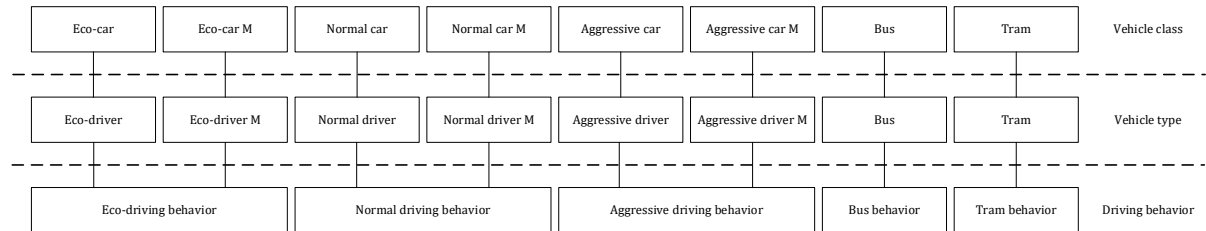


Figure 3.1 Structure of vehicle classes, types and behaviors

The structure contains the three driving behaviors, as well as a bus and tram behavior. For public transport, the standard VISSIM behavior for bus and tram has been used, because the little details in microscopic driving behavior of those few public transport vehicles is not expected to have a significant influence on the energy consumption of other vehicles. The other three driving behaviors are all related to two vehicle types and classes. The ‘eco-driver’ and the ‘eco-driver M’ both have exactly the same settings, except for their color in the visualization. Though, the ‘eco-driver M’ class relates to the cars which follow a static, predefined route in the model (and thus could be used for the measurements), while the ‘eco-driver’ follows a dynamic route and could not be used for measurements. This method largely decreases the size of the data output of VISSIM and is therefore preferred over using a single vehicle type and class to model a driving style.

The driving behavior consists of multiple settings, of which the most relevant ones will be discussed in the next subchapters.

3.3.1.1 Desired speed

One of the biggest differences of the three different driving styles is the difference in driving speed. This could be best modeled by using different desired speed profiles for each driving style. In VISSIM, each individual has a specific desired speed, around which the real driving speed will oscillate. The oscillations could happen due to the influence of other traffic, or due to its own speed oscillations. Desired speed distributions are connected to a link (street) and are often related to the design speed of a road. For a single vehicle type, one desired speed distribution is made, which is a distribution of different possible desired speeds on a certain road. These curves are very close to normal distributions with the lowest value slightly below the design speed and its highest value somewhat higher (Figure 3.2). The distribution implies that even when using only a single driving style, the software could still simulate small differences in driving behavior in order to create a more realistic scenario. To create different driving behaviors, three different desired speed distributions have been made for each situation. An example of the desired speed distributions for different driving styles could be found in Figure 3.2. The lowest and highest value of the normal driving behavior are extracted from VISSIM, and the lowest and highest value of the eco-driver and the aggressive driver are the same values, plus or minus five percent. On average, the desired driving speed is 5 percent higher than the design speed, which is the legal driving speed in the Netherlands. Each vehicle chooses a value for its desired speed based on the distribution of its driving style this position is the same for the entire simulation and is also used for the desired speed distributions at other streets. Thanks to this, the fastest car of the normal driving group will be the fastest car on all 50 km/h roads, but also on all 30 km/h roads.

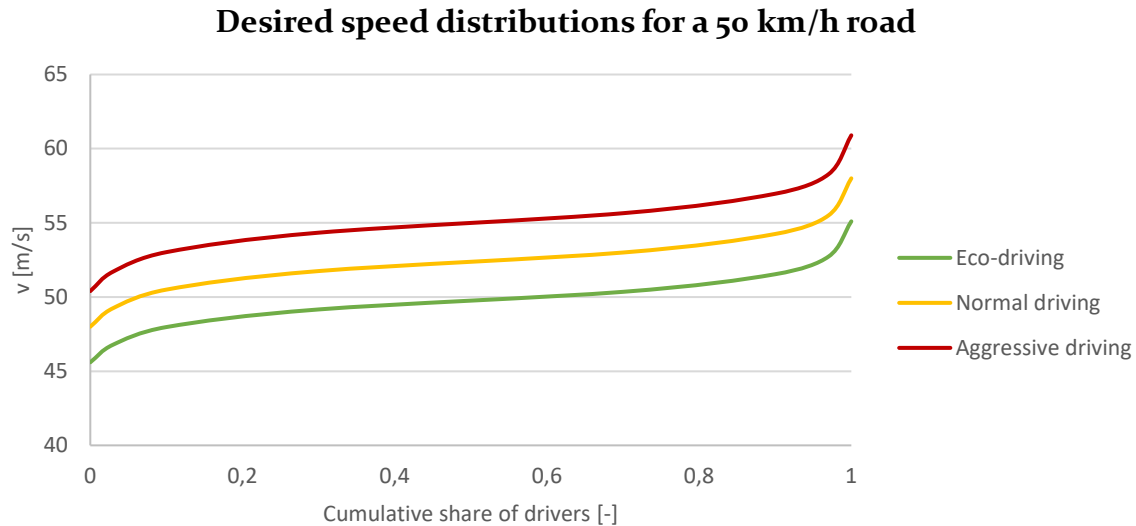


Figure 3.2 Desired speed distributions for a 50 km/h road

3.3.1.2 Acceleration and deceleration

A second measure to define driving behavior is the acceleration and deceleration behavior. Earlier in this thesis, different values for acceleration and deceleration were given for the different driving styles. Based on these values, the acceleration and deceleration profile of other vehicles, such as the TU/e's Lupo EL (Wang et al., 2017) and the maximum acceleration of a BMW i3 based on its 0-100 km/h time (Automobile Catalog, n.d.), maximum and desired acceleration and deceleration profiles have been created for the three driving styles (Figure 3.4). These profiles have an average, a maximum and a minimum value for each driving speed (Figure 3.3). The shape of the profile is extracted from VISSIM. As could be seen from the graph, the acceleration is higher for lower driving speeds. This corresponds to measurements done with the TU/e's Lupo EL. The vehicle's powertrain limits the acceleration and deceleration at higher speeds (Wang et al., 2017).

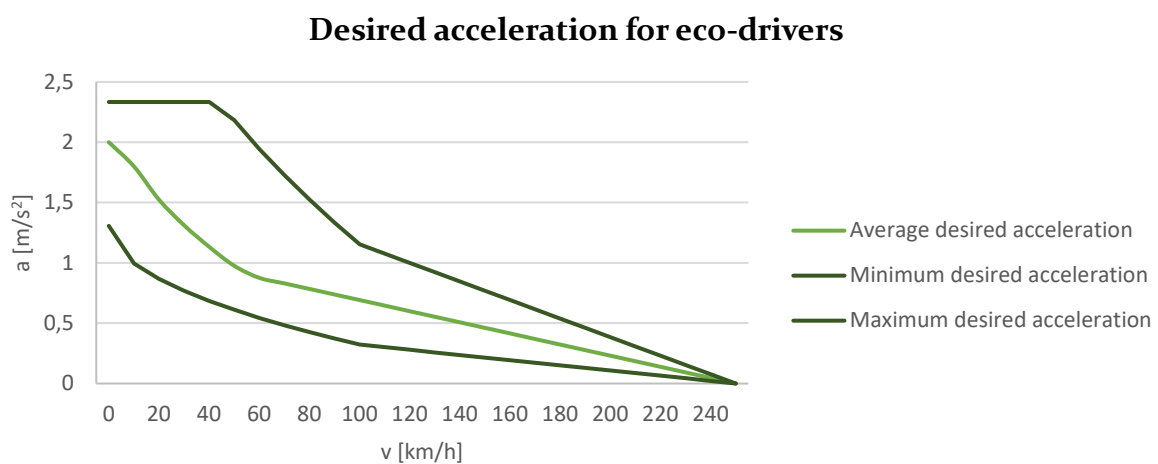


Figure 3.3 Desired acceleration for eco-drivers

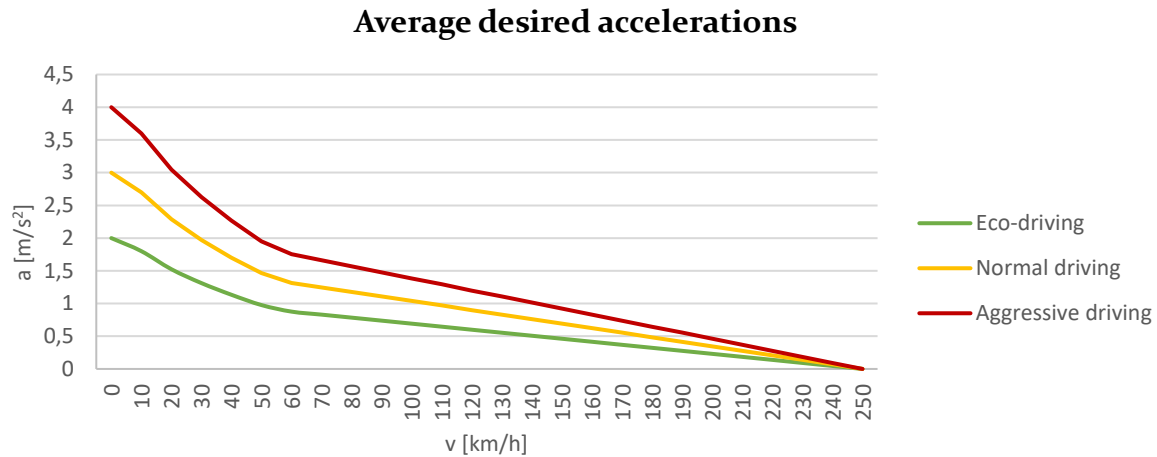


Figure 3.4 Average desired acceleration for different driving styles

3.3.2 Infrastructure modelling

Infrastructure in VISSIM is modeled by mainly using links and connectors, which represent the basic street network. However, for some infrastructural elements, such as signaled intersections, other additional VISSIM tools have to be used. Some infrastructural elements and their effects, such as the reduced speed at traffic calming measures or when driving on a curved road segment have no standard VISSIM tool and are modeled in a different way. The next subchapters discuss the modelling process of these elements.

3.3.2.1 Signalized intersections

The signalized intersections, or traffic lights, are being modeled by using different VISSIM tools. For both three-legged and four-legged crossings, signal heads and detectors are being used for each separate lane. Fixed numbers for the signal heads and detectors are used, which relate to turning right, left or going straight. Each traffic light is controlled by using a primary, secondary and tertiary detection loop. By using VISVAP 2.16, the traffic controls have been created. A standard control file setup by Sweco has been used as a base file, after which some of the control has been manually adapted based on expert judgement.

Some intersections contain bus or tram lanes and have bus and tram priority in the traffic light controls. Again, this has been controlled by using VISVAP 2.16. For busses, the same three detection loops are places similarly to the ones at normal lanes. When a bus enters a junction with bus priority, simply all other signals will turn red for a fixed time period after the bus have left the third detector. For trams, only two detectors have been used. The first detector is placed 30m before the tram's signal head and will turn the signal head green when triggered. The second one is placed after the intersection and will detect when the tram completely crossed the intersection. After this, the standard signal control will continue. The detector layout is visualized in Figure 3.5 and Figure 3.6. It goes without saying that there's no difference in settings for the different driving behaviors.

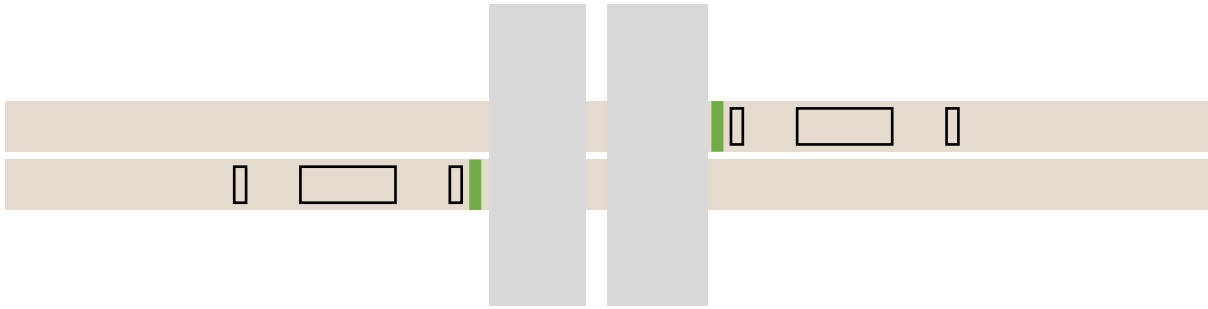


Figure 3.5 Detector layout for cars, busses and trucks

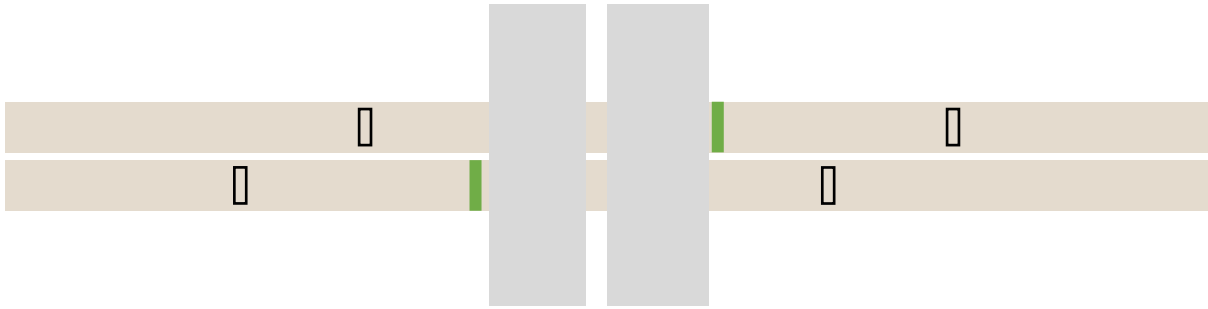


Figure 3.6 Detector layout for trams

3.3.2.2 Traffic calming measures

The different traffic calming measures, which have been discussed earlier in this thesis, have no specific tool in VISSIM. Therefore, reduced speed areas are used. A reduced speed area is an area in which a different desired speed profile could be used, to create a temporary area of reduced speed. The vehicles decide when they start decelerating based on their own speed, the speed at the reduced speed area and their desired deceleration, but always reach the reduced speed at the exact start of the reduced speed area. Each vehicle will keep this reduced speed when driving in the reduced speed area and start accelerating after the reduced speed area. This way of modelling traffic calming measures is similar to model 1, as being discussed Figure 2.13 in subchapter 2.6.4. When creating very short reduced speed areas (in order to approach model 2 of Figure 2.13), most cars skip the speed reduction. This is caused due to the fact that time in VISSIM is a discrete variable, with a minimum interval of 0,1 s. For this reason, all traffic calming measures in the Nieuwegein model have been modeled with their real length, with a minimum of 1 m.

Three different desired speed profiles have been created for each traffic calming measure, related to the three driving styles. The values of these speed profiles are calculated as follows:

$$v.\text{desired}_{\min,\text{speed bump}} = v.\text{desired}_{\min,\text{original}} * (1 - \text{speed reduction}) \quad [28]$$

$$v.\text{desired}_{\max,\text{speed bump}} = v.\text{desired}_{\max,\text{original}} * (1 - \text{speed reduction}) \quad [29]$$

3.3.2.3 Curved road sections

For curved road sections, the reduced speed depends on the curve radius and diameter. As it would be time consuming to create different speed profiles for every single turn, some general profiles have been created based on the most occurring situations. The individual influence of these profiles on the energy consumption has been calculated in subchapter 4.3.2. These profiles are based on the radius and diameter of the curved road section. The length of the reduced speed area has been determined based on expert judgement. In general, shorter curves have shorter reduced speed areas.

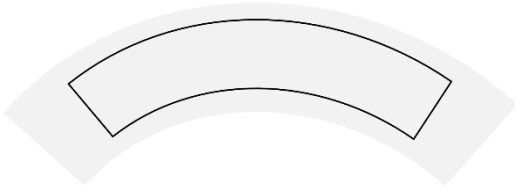


Figure 3.7 Reduced speed area on a curved road segment

3.3.2.4 Public transport

Two types of public transport are being used in this research; bus and tram. Both are modeled by using public transport lines and public transport stops. They are used in the model to create random delays to the other traffic. In the Nieuwegein model, the tram track is completely separated from the normal road, though it crosses the road sometimes. The bus stops are sometimes placed on the normal road itself, or on separate bus lanes, as being visualized in Figure 3.8. Since the entire model is within the built-up area of Nieuwegein, all buses go first when leaving their bus stops. This causes the vehicles on the normal road to reduce their speed.

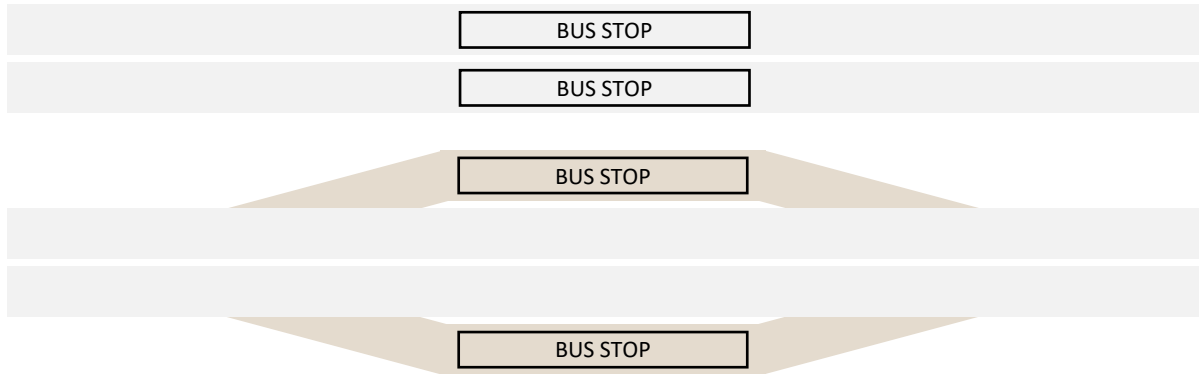


Figure 3.8 Different bus stop configurations

3.3.3 Excel model

The energy consumption model has been implemented in an Excel script to quickly perform the energy prediction calculations. The excel file contains some sheets covering the different variables related to the environmental influence, auxiliary energy consumption, road types, rolling resistance and car performance. For the manual calculations of individual scenarios, such as a speed bump, different sheets have been created which could quickly simulate speed profiles of these elements.

The major input of the model will be the speed profile, either created manually or extracted from VISSIM. The speed input is first corrected to exclude negative speeds (which sometimes occurred during standstill due to measurement inaccuracies). Afterwards, the acceleration at each timestep is calculated using:

$$a_t = \frac{v_{t+1} - v_{t-1}}{(t+1) - (t-1)} = \frac{v_{t+1} - v_{t-1}}{2} \quad [30]$$

where t represents a timestep.

An average speed is calculated at every timestep using:

$$v_{average,t} = v_t + 0,5 * a_t \quad [31]$$

The driven distance is calculated using:

$$d_t = d_{t-1} + v_{average,t} * (t - (t - 1)) = d_{t-1} + v_{average,t} \quad [32]$$

Since the model is instantaneous, for every t , the forces are being calculated using the average speed at every time interval t . The tractive and regenerative powers are being calculated using the driving speed. To calculate the energy discharged and charged by the tractive power and regenerated power, these powers are multiplied by the powertrain efficiency and the regenerative braking efficiency first. The last efficiency is related to the different driving styles.



Chapter 4

Individual elements

Chapter 4. Individual elements

The influence of the individual elements on an EVs energy consumption has been tested extensively. Chapter 4 highlights these influences. Results are shown both qualitatively and quantitatively. By both performing manual calculations and using VISSIM, the influence of driving style, environmental variables and infrastructure has been calculated. This chapter covers these influences in this respective order.

4.1 Influence of elements related to driving style

In the following subsections the influence of elements related to driving style will be emphasized. As discussed in the literature review, speed differences, preferences for acceleration and deceleration and speed oscillations typify one's driving style. Therefore, the influence of each of these individual characteristics will be discussed.

4.1.1 Speed differences

First, speed differences have been researched. The speed a driver drives on a road segment is often being regulated by law, defined as the posted speed limit. Different standardized posted speed limits occur in the Netherlands, often related to the design of a road (design speed). As could be seen in Table 4.1, the most efficient driving speed is 30 km/h. The higher the speed, the higher the energy consumption and the bigger the differences between the different driving styles (Figure 4.1). This is caused by the dominant aerodynamic drag force at high speeds. Interesting is the fact that at very low speeds, the energy consumption rises, and that eco-driving is less efficient as aggressive driving. The cause of this phenomena is the use of climate control (which uses energy every second). At very slow driving speeds, the time it takes a vehicle to drive 500 m is so high that the influence of the climate control is dominant. As the eco-driver – with his lower speed – takes longer to drive 500 m than the aggressive driver, the eco-driver will use more energy. Since most of the roads in the Netherlands has a design speed of 30-km/h or faster, one could state that for most design speeds, eco-driving is the most energy-efficient driving style.

Figure 4.2 shows the percentual differences per driving style. For desired speeds of about 30 km/h, the energy consumption is not influenced by the driving style anymore. This is the speed where the auxiliary power and the driving style differences extinguish each other's effects. Though, one should notice that this point is strongly influenced by the auxiliary power consumption, meaning that during extremely cold conditions (and thus a high auxiliary power consumption), the point would occur at higher speeds. In strong Dutch winter conditions, this point would only be reached at 50 km/h.

Table 4.1 Energy consumption after driving 500 m

Desired speed [km/h]	Eco-driving	Normal driving	Aggressive driving
15	0,0563 kWh 102,7%	0,0548 kWh 100%	0,0535 kWh 97,6%
30	0,0437 kWh 100,9%	0,0433 kWh 100%	0,0431 kWh 99,5%
50	0,0451 kWh 98,3%	0,0459 kWh 100%	0,0469 kWh 102,2%

60	0,0489 kWh 97,0%	0,0504 kWh 100%	0,0520 kWh 103,2%
80	0,0605 kWh 95,1%	0,0636 kWh 100%	0,0668 kWh 105,0%
100	0,0768 kWh 93,8%	0,0819 kWh 100%	0,0872 kWh 106,5%
130	0,109 kWh 92,3%	0,118 kWh 100%	0,127 kWh 107,6%

Energy consumption for different desired speeds

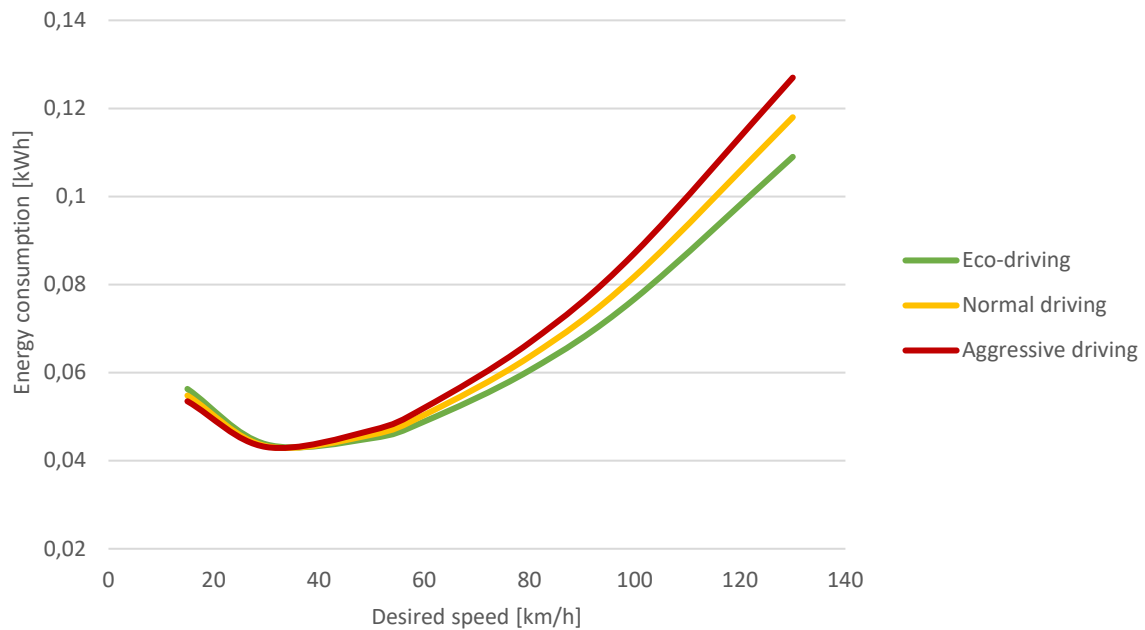


Figure 4.1 Energy consumption for different desired speeds

Percentual differences in energy consumption for different desired speeds

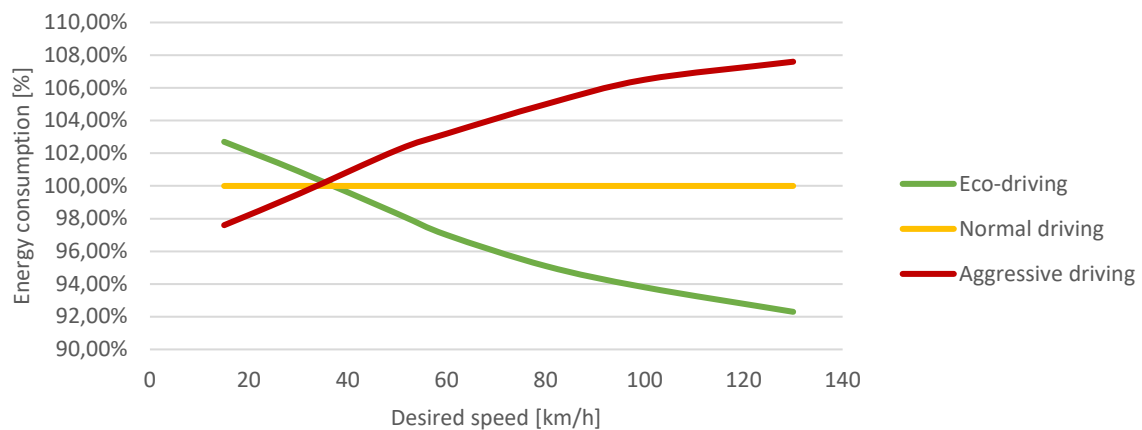


Figure 4.2 Percentual differences in energy consumption for different desired speeds

4.1.2 Acceleration and deceleration

Table 4.2 shows the energy consumption during acceleration for different levels of aggressiveness of acceleration. The measurement starts at the moment the acceleration process starts and ends immediately when the desired speed is reached. It shows that for the full acceleration process, the most aggressive acceleration is more energy efficient than the eco-acceleration. Especially at high speeds, the more aggressive the acceleration, the lower the energy consumption. Though, the driven distance of the eco-acceleration is way bigger than the aggressive acceleration, since the process took longer. At high speeds, the driven distance of the eco-acceleration could be 100% higher than the aggressive one. Therefore, a second way of measuring the energy consumption during acceleration has been proposed, as could be seen in Figure 4.3. The results of this second model could be found in Table 4.3.

Table 4.2 Energy consumption during different accelerations, model 1

Speed [km/h]	E for $a = 2 \text{ m/s}^2$	E for $a = 3 \text{ m/s}^2$	E for $a = 4 \text{ m/s}^2$
0-15	0,0522 kWh 103,2%	0,0506 kWh 100%	0,0505 kWh 99,8%
15-30	0,0134 kWh 101,5%	0,0132 kWh 100%	0,0134 kWh 101,5%
30-50	0,0329 kWh 103,1%	0,0319 kWh 100%	0,0313 kWh 98,1%
50-60	0,0224 kWh 104,2%	0,0215 kWh 100%	0,0208 kWh 96,7%
60-80	0,0587 kWh 104,1%	0,0564 kWh 100%	0,0550 kWh 97,5%
80-100	0,0776 kWh 105,0%	0,0739 kWh 100%	0,0717 kWh 97,0%
100-130	0,157 kWh 106,8%	0,147 kWh 100%	0,142 kWh 96,6%

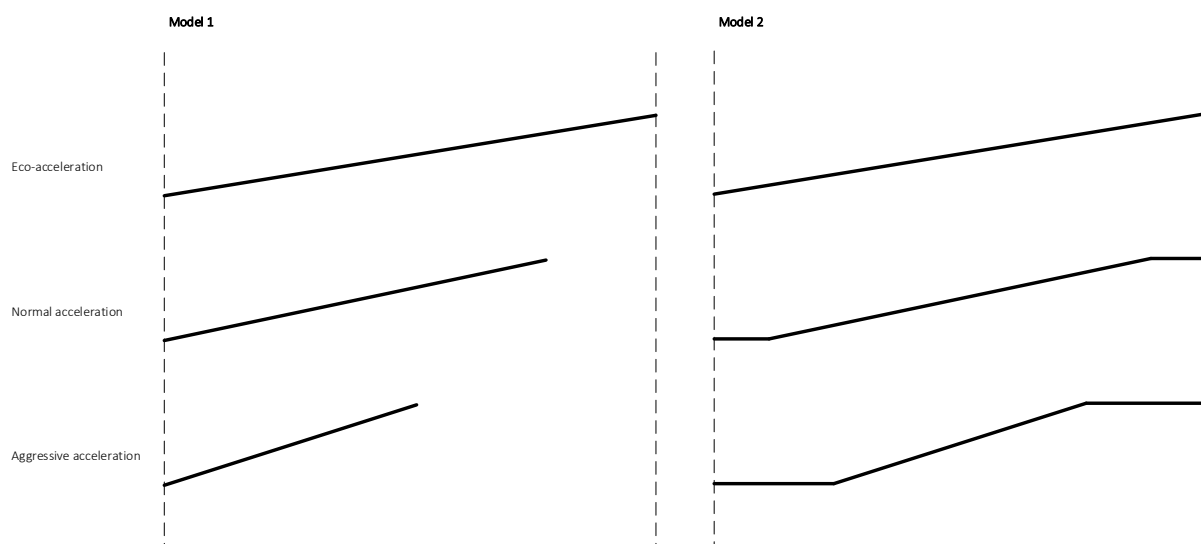


Figure 4.3 Two ways of measuring the energy consumption during acceleration

Table 4.3 Energy consumption during different accelerations, model 2

Speed [km/h]	a = 2 m/s ²	a = 3 m/s ²	a = 4 m/s ²
0-15	0,00522 kWh 97,9%	0,00533 kWh 100%	0,00514 kWh 96,4%
15-30	0,0140 kWh 97,9%	0,0143 kWh 100%	0,0145 kWh 101,4%
30-50	0,0329 kWh 98,5%	0,0334 kWh 100%	0,0336 kWh 100,6%
50-60	0,0224 kWh 97,0%	0,0231 kWh 100%	0,0232 kWh 100,4%
60-80	0,0587 kWh 98,3%	0,0597 kWh 100%	0,0599 kWh 100,3%
80-100	0,0776 kWh 98,2%	0,0790 kWh 100%	0,0792 kWh 100,3%
100-130	0,157 kWh 98,7%	0,159 kWh 100%	0,159 kWh 100%

Although the eco-acceleration is slightly more efficient overall, the difference is still very small. This is logical. On the one hand, higher acceleration means higher acceleration forces. Though if the acceleration is multiplied by two, the acceleration time (so also the time these acceleration forces are active) is divided by two. Therefore, the acceleration itself has no effect. Though, these calculations are still based on a fixed speed acceleration. In practice, the aggressive driver will be driving a bit faster than the average, while the eco-driver will be driving a bit slower. If we consider this effect, and thus combine the influence of slight speed differences and acceleration differences, the results show more varied results. Table 4.4 shows an overall improvement of over 10% for eco-drivers compared to normal drivers, while aggressive drivers overall use 10% more energy for accelerating at all design speed levels. In Figure 4.4, these results are visualized.

Table 4.4 Energy consumption during acceleration for different driving styles

Desired speed [km/h]	Eco-driving	Normal driving	Aggressive driving
0-15	0,0121 kWh 85,2%	0,0142 kWh 100%	0,0157 kWh 110,6%
15-30	0,0202 kWh 87,4%	0,0231 kWh 100%	0,0255 kWh 110,4%
30-50	0,0297 kWh 88,9%	0,0334 kWh 100%	0,0368 kWh 110,2%
50-60	0,0202 kWh 91,4%	0,0221 kWh 100%	0,0266 kWh 120,4%
60-80	0,0523 kWh 87,9%	0,0595 kWh 100%	0,0657 kWh 110,4%
80-100	0,0696 kWh 88,7%	0,0785 kWh 100%	0,0870 kWh 110,8%
100-130	0,140 kWh 89,2%	0,157 kWh 100%	0,174 kWh 110,8%

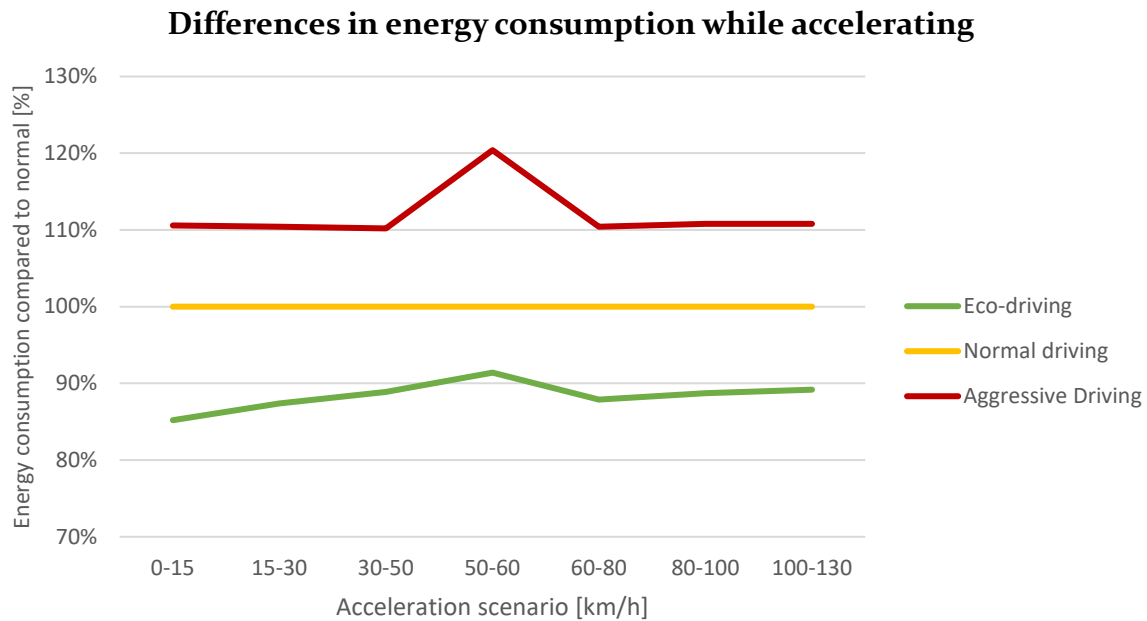


Figure 4.4 Differences in energy consumption while accelerating

Apart from differences in acceleration, aggressive drivers also tend to have a more aggressive decelerations style, as found in the literature review. The deceleration results (Table 4.5 and Figure 4.5) show the total energy consumption during deceleration for the different driving styles. The results show an incredible increase in regen efficiency for eco-driving compared to aggressive driving. The difference grows at higher speeds, due to the higher influence of aerodynamic drag force on the aggressive driver at these speeds. At very low speeds, the absolute difference is lower, due to the high influence of the auxiliary energy.

Table 4.5 Energy consumption during deceleration for $P_{aux} = 906\text{ W}$

Desired speed [km/h]	Eco-driving	Normal driving	Aggressive driving
15-0	-0,00143 kWh 397,2%	-0,00036 kWh 100%	0,000404 kWh -112,2%
30-15	-0,00591 kWh 233,6%	-0,00253 kWh 100%	-0,00027 kWh 10,7%
50-30	-0,0147 kWh 222,7%	-0,0066 kWh 100%	-0,0012 kWh 18,2%
60-50	-0,00985 kWh 220,9%	-0,00446 kWh 100%	-0,00076 kWh 17,0%
80-60	-0,0251 kWh 226,1%	-0,0111 kWh 100%	-0,0014 kWh 12,6%
100-80	-0,0308 kWh 233,3%	-0,0132 kWh 100%	-0,00028 kWh 21,2%
130-100	-0,0550 kWh 364,2%	-0,0151 kWh 100%	0,0039 kWh -25,8%

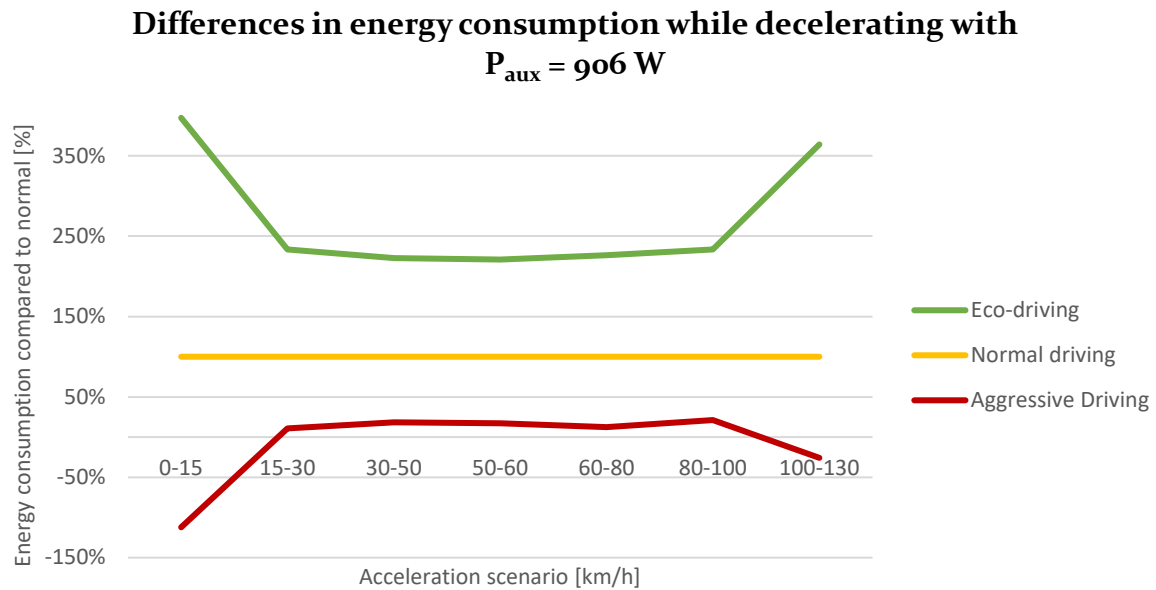


Figure 4.5 Differences in energy consumption while decelerating with $P_{aux}=960 \text{ W}$

Table 4.6 and Figure 4.6 shows the energy consumption during deceleration for lower auxiliary energy consumptions. The results show that the differences, especially for slow speeds, are more stable.

Table 4.6 Energy consumption during deceleration for $P_{aux} = 350 \text{ W}$

Desired speed [km/h]	Eco-driving	Normal driving	Aggressive driving
15-0	-0,00163 kWh 171,6%	-0,00095 kWh 100%	-0,00025 kWh 26,3%
30-15	-0,00545 kWh 172,5%	-0,00316 kWh 100%	-0,00102 kWh 32,3%
50-30	-0,0131 kWh 174,7%	-0,0075 kWh 100%	-0,0023 kWh 30,7%
60-50	-0,00867 kWh 173,4%	-0,00500 kWh 100%	-0,00148 kWh 29,6%
80-60	-0,0220 kWh 178,9%	-0,0123 kWh 100%	-0,0032 kWh 26,0%
100-80	-0,0268 kWh 182,3%	-0,0147 kWh 100%	-0,0028 kWh 19,0%
130-100	-0,0476 kWh 191,2%	-0,0249 kWh 100%	-0,0016 kWh 6,4%

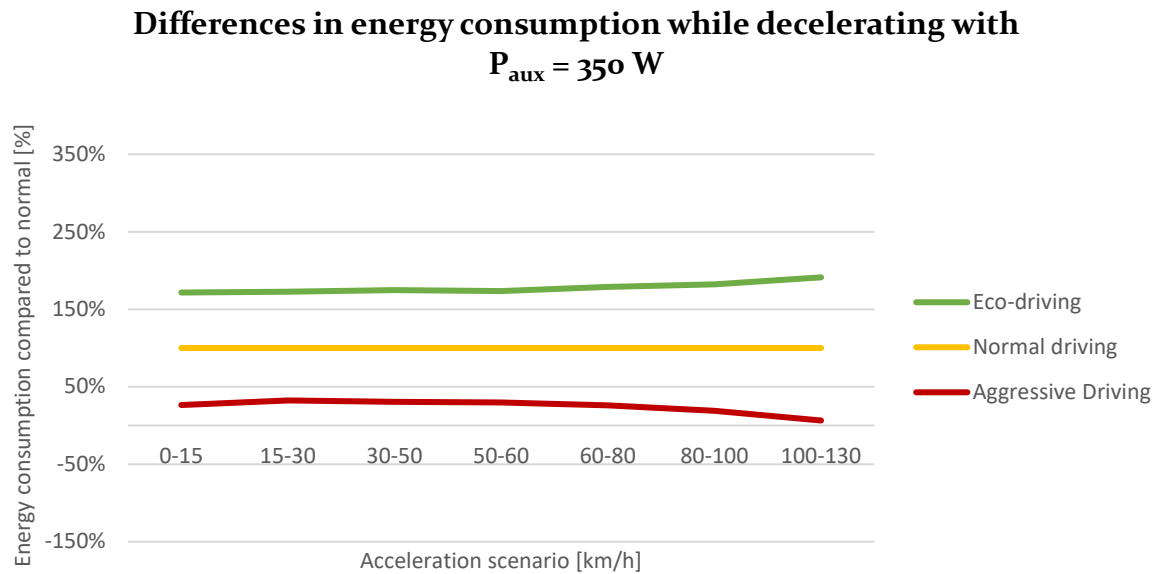


Figure 4.6 Differences in energy consumption while decelerating with $P_{aux}=350 \text{ W}$

4.1.3 Speed oscillations

VISSIM's Wiedemann 74 model uses random accelerations and decelerations to create oscillations in the driving speed. With this behavior, the software tries to simulate realistic driving behavior, as the real driving speed would normally also oscillates a bit. The model chooses a random acceleration by multiplying a random value of an $N(0,5; 0,15)$ -distribution by 0,4. This leads to accelerations and decelerations of approximately $0,2 \text{ m/s}^2$ (W. Moerland, personal communication, April 12, 2019). The effect of these oscillations has been calculated in Table 4.7. It shows energy consumptions for the measured speeds of 60 vehicles, compared to the energy consumption without oscillations of these vehicles (by using the average speed as driving speed). The results are an indication of the positive influence technological developments, such as cruise control, might have on the energy consumption.

First, manual calculations have been performed (Table 4.7), based on the speed profiles shown in Figure 4.7, Figure 4.8 and Figure 4.9. As could be seen in Figure 4.10, the speed oscillations don't influence the eco-driver very much, while they do have a huge influence on the aggressive driver. The combination of a slightly higher speed with some small speed oscillations results in a fair increase in energy consumption.

Table 4.7 Influence of speed oscillations on the energy consumption for different driving styles

Oscillation	Eco-driving	Normal driving	Aggressive driving
Baseline, V=30 km/h, d=500 m	0,0437 kWh 100,9%	0,0433 kWh 100%	0,0431 kWh 99,5%
0,1 m/s ²	0,0427 kWh 98,6%	0,0434 kWh 100,2%	0,0444 kWh 102,5%
0,2 m/s ²	0,0456 kWh 105,3%	0,0506 kWh 116,9%	0,0549 kWh 126,8%
0,3 m/s ²	0,0492 kWh 113,6%	0,0592 kWh 136,7%	0,0663 kWh 153,1%

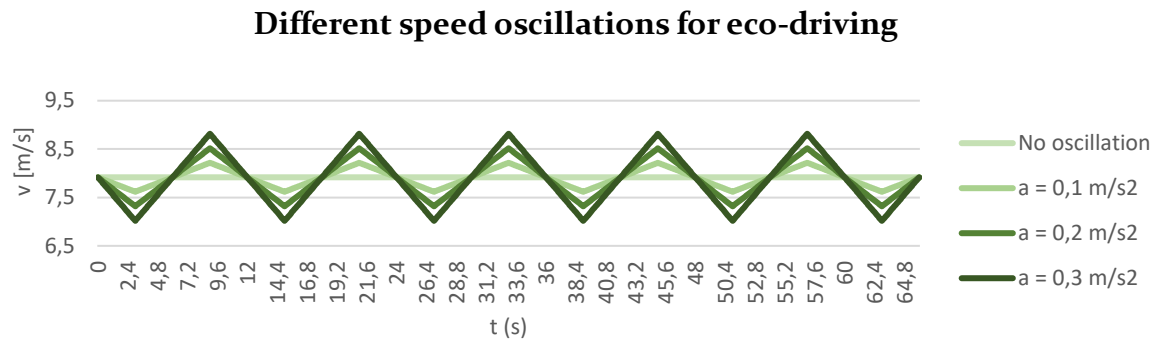


Figure 4.7 Different speed oscillations for eco-driving

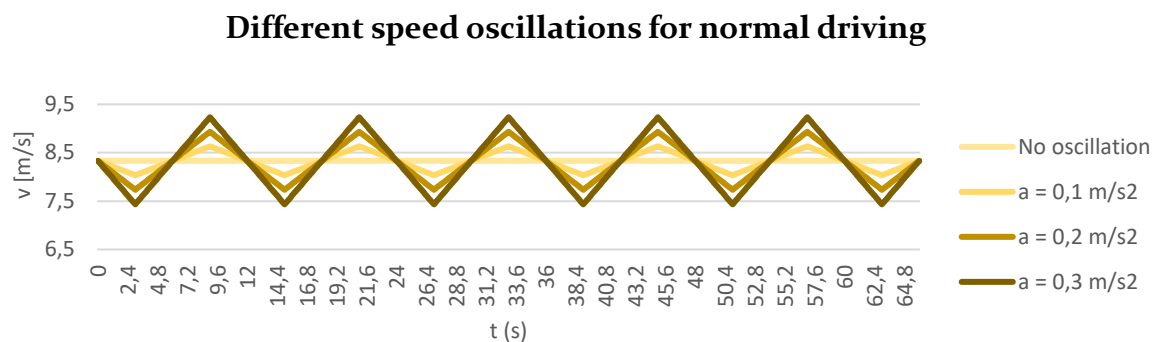


Figure 4.8 Different speed oscillations for normal driving

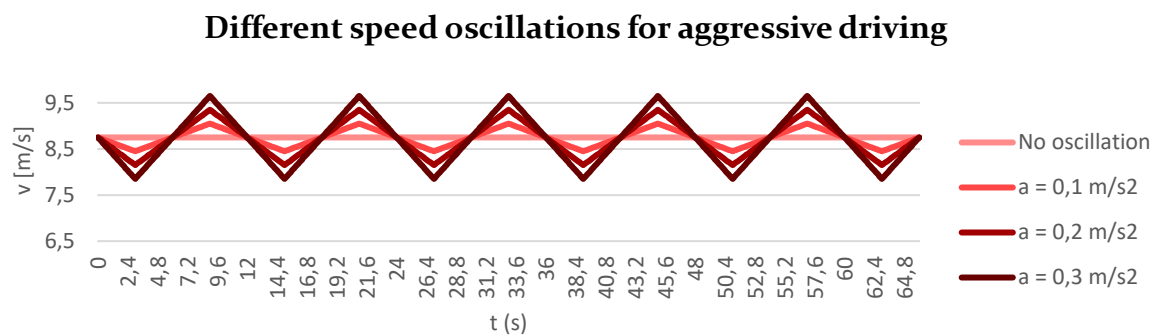


Figure 4.9 Different speed oscillations for aggressive driving

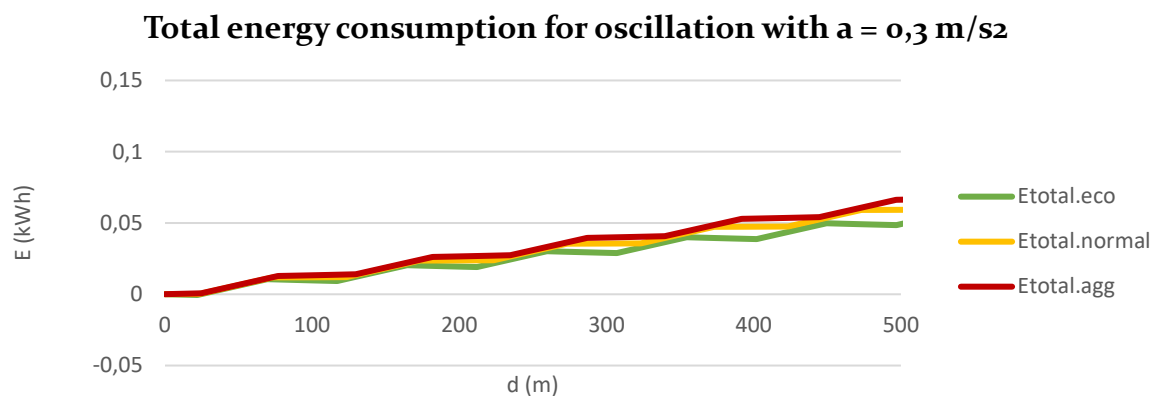


Figure 4.10 Total energy consumption per driving style for high speed oscillations

After the manual calculations, the oscillations have been tested in VISSIM by using the Wiedemann 74 model (Table 4.8 and Figure 4.11). The output shows an average acceleration and deceleration of approximately $0,2 \text{ m/s}^2$ and shows similar results to the manual calculations. The oscillations again have significant effects on the energy consumption of aggressive drivers. This proves the efficiency of cruise control and other driving assistance technologies in terms of energy savings. Another interesting result is the deviation in energy consumption within each driving style (Figure 4.12). For each of the three driving styles, cars are found that use over $0,0075 \text{ kWh}$ (although this refers to only one eco-driver compared to 9 aggressive drivers) and under $0,0015 \text{ kWh}$.

The Wiedemann 99 model doesn't include these random speed oscillations. This model only contains speed oscillations in the car-following model, so that they only occur after a certain traffic intensity.

Table 4.8 Effect of speed oscillations on energy consumption, VISSIM results

Scenario	Eco-driving	Normal driving	Aggressive driving
- 50 m			
Average desired speed	8,510 m/s	8,897 m/s	9,388 m/s
Average speed	8,465 m/s	8,853 m/s	9,458 m/s
Lowest speed measured	7,558 m/s	7,603 m/s	8,428 m/s
Highest speed measured	9,428 m/s	10,003 m/s	10,722 m/s
Average acceleration	0,192 m/s ²	0,208 m/s ²	0,202 m/s ²
Average deceleration	-0,205 m/s ²	-0,191 m/s ²	-0,179 m/s ²
Without oscillations	0,00439 kWh	0,00438 kWh	0,00438 kWh
	100,2%	100%	100%
With oscillations	0,004438 kWh	0,005186 kWh	0,005340
	101,3 %	118,4 %	121,9%

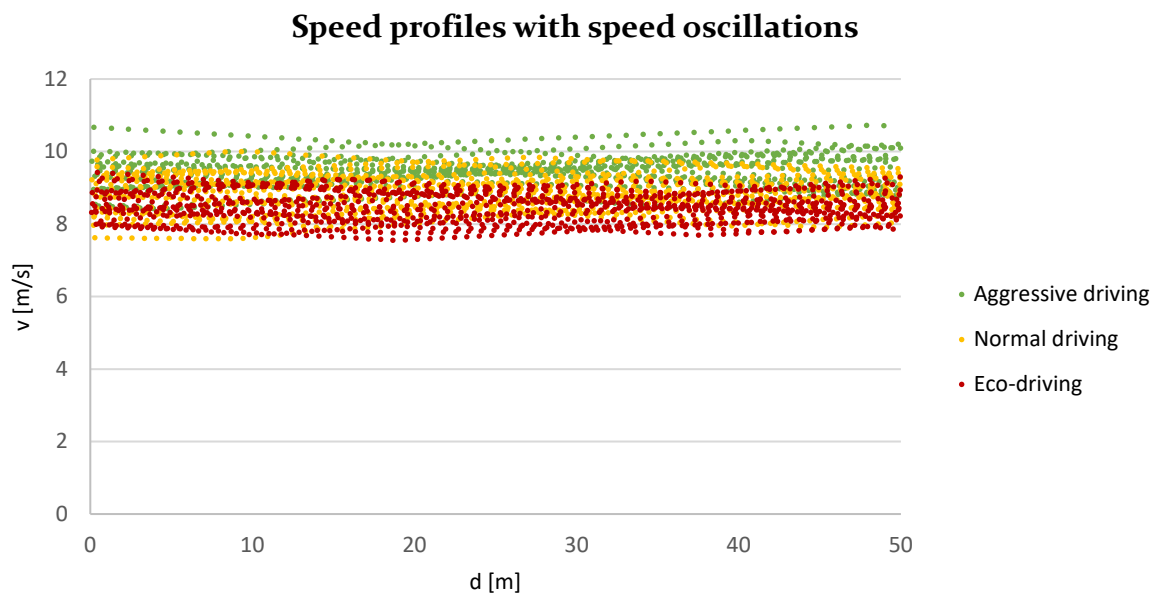


Figure 4.11 Speed distribution for different driving styles with speed oscillations

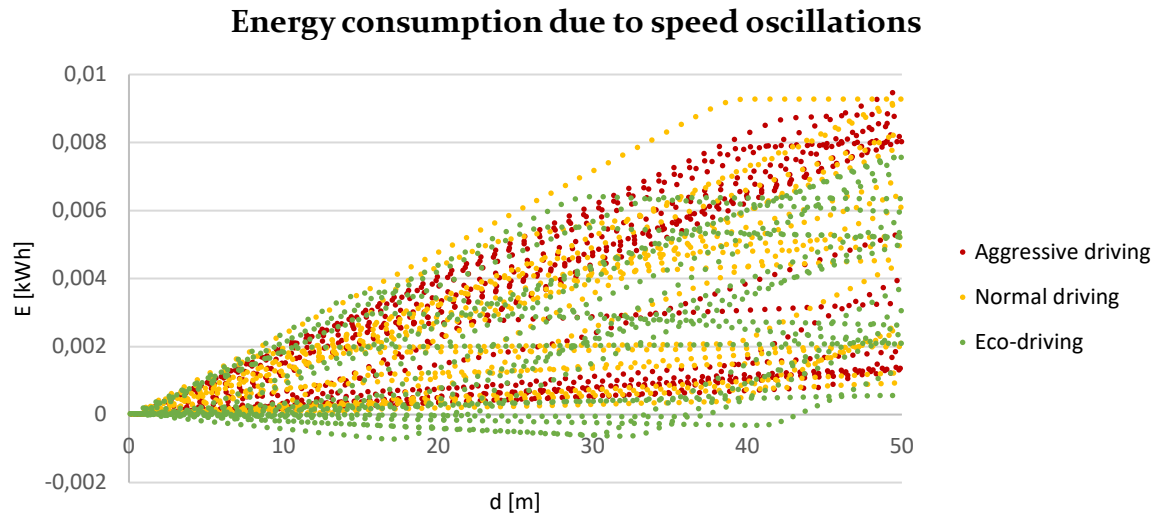


Figure 4.12 Energy consumption for different driving styles due to speed oscillations

4.2 Influence of elements related to environmental variables

The second part of this chapter is dedicated to the influence of environmental variables on the energy efficiency of electric vehicles. Although many environmental variables exist and likely influence the energy consumption, three variables have been researched. First, the influence of temperature will be discussed, after which the influence of head- and tailwind will be analyzed. Finally, the increase in auxiliary energy due to the use of the lighting system on different moments of the day has been quantified.

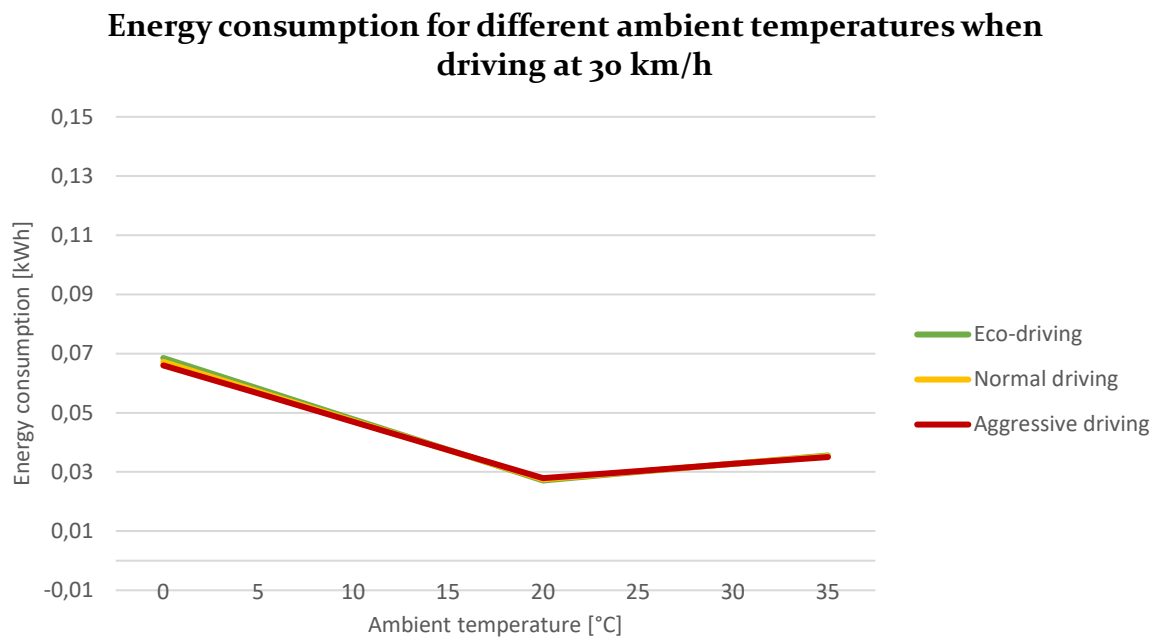
4.2.1 Temperature

To measure the influence of temperature on the energy consumption, a single trip has been calculated in excel for different temperature scenarios, ranging from 0 °C to 35 °C. This has been done for driving 30 km/h and driving 130 km/h to compare the influence for slow and fast traffic. The calculations consider the use of the climate system, the influence of the temperature on the aerodynamic forces through the changing air density and the influence of the temperature on the rolling resistance. Although temperature might influence the efficiency of a vehicle through more variables, these three are likely to give a good insight, especially because the energy consumption of the climate system is so large. Further research is necessary to define the influence of these other factors.

Table 4.9 and Figure 4.13 show the results of the 30 km/h calculations. The influence of temperature is significant, doubling the energy consumption at very low temperatures compared to the 20 °C scenario. The energy consumption at 20 degrees and at 0 degrees Celsius differ so much that the range is strongly related to the ambient temperature.

Table 4.9 Influence of ambient temperature on the energy consumption while driving at 30 km/h

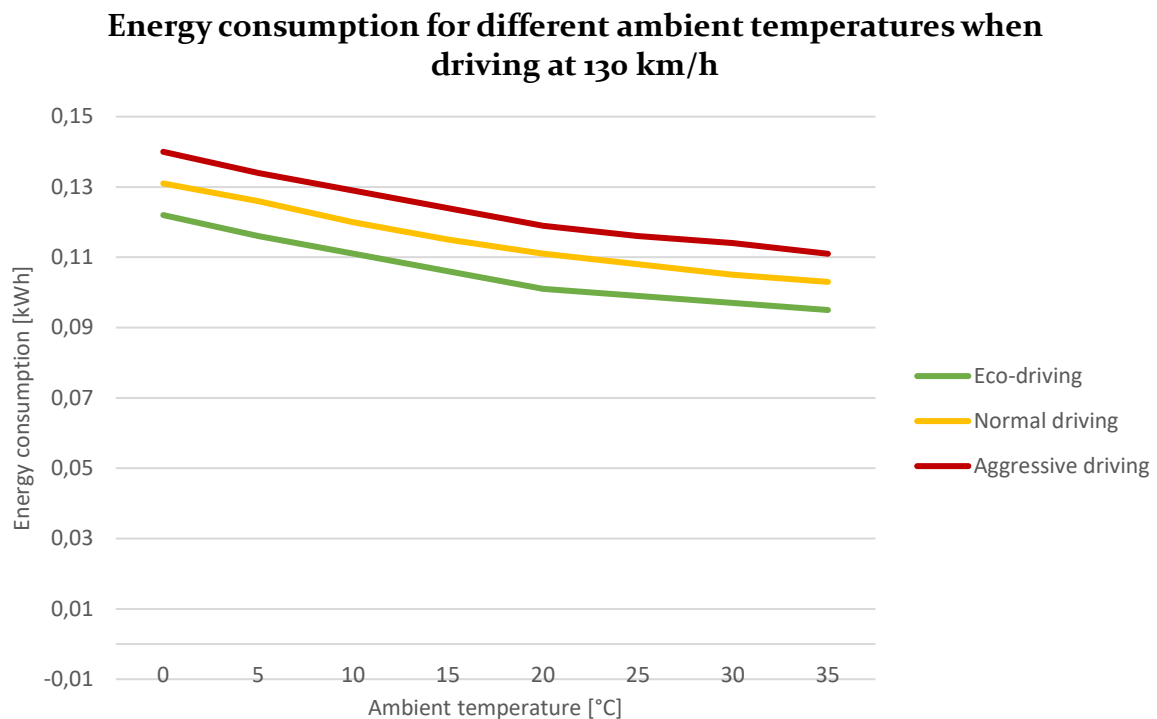
Scenario	Eco-driving	Normal driving	Aggressive driving
Baseline	0,0437 kWh	0,0433 kWh	0,0431 kWh
- V = 30 km/h	100,9%	100%	99,5%
- T = 12 °C			
- $\rho = 1,230599$			
T = 0 °C	0,0685 kWh 158,2%	0,0672 kWh 155,2%	0,0660 kWh 152,4%
T = 5 °C	0,0582 kWh 134,4%	0,0572 kWh 132,1%	0,0565 kWh 130,5%
T = 10 °C	0,0478 kWh 110,4%	0,0473 kWh 109,2%	0,0469 kWh 108,3%
T = 15 °C	0,0375 kWh 86,6%	0,0374 kWh 86,4%	0,0374 kWh 86,4%
T = 20 °C	0,0271 kWh 62,6%	0,0275 kWh 63,5%	0,0279 kWh 64,4%
T = 25 °C	0,0300 kWh 69,3%	0,0301 kWh 69,5%	0,0303 kWh 70,0%
T = 30 °C	0,0328 kWh 75,8%	0,0327 kWh 75,5%	0,0327 kWh 75,5%
T = 35 °C	0,0356 kWh 82,2%	0,0353 kWh 81,5%	0,0350 kWh 80,8%

**Figure 4.13** Energy consumption for different ambient temperatures when driving at 30 km/h

The effect of temperature is lower for higher speeds, as could be seen in Table 4.10 and Figure 4.14. Due to the high speeds, the time a vehicle is on a road segment is lower. Therefore, the climate system (which uses energy every second) has less time to consume energy. An interesting result, as this implies that different seasons might have different optimal routes. In heavy winters, these optimal routes are likely to be related to the fastest route, while in summer this might differ.

Table 4.10 Influence of ambient temperature on the energy consumption while driving at 130 km/h

Scenario	Eco-driving	Normal driving	Aggressive driving
Baseline	0,109 kWh	0,118 kWh	0,127 kWh
- V = 130 km/h	92,3%	100%	107,6%
- T = 12 °C			
- $\rho = 1,230599$			
T = 0 °C	0,122 kWh 103,4%	0,131 kWh 111,0%	0,140 kWh 118,6%
T = 5 °C	0,116 kWh 98,3%	0,126 kWh 106,8%	0,134 kWh 113,6%
T = 10 °C	0,111 kWh 94,1%	0,120 kWh 101,7%	0,129 kWh 109,3%
T = 15 °C	0,106 kWh 89,8%	0,115 kWh 97,5%	0,124 kWh 105,1%
T = 20 °C	0,101 kWh 85,6%	0,111 kWh 94,1%	0,119 kWh 100,8%
T = 25 °C	0,099 kWh 83,9%	0,108 kWh 91,5%	0,116 kWh 98,3%
T = 30 °C	0,097 kWh 82,2%	0,105 kWh 89,0%	0,114 kWh 96,6%
T = 35 °C	0,095 kWh 80,5%	0,103 kWh 87,3%	0,111 kWh 94,1%

**Figure 4.14** Energy consumption for different ambient temperatures when driving at 130 km/h

4.2.2 Wind

Wind has an influence on the aerodynamic drag force and is therefore influencing the energy consumption. Although wind won't be taken into account in the Nieuwegein case study, it's interesting to quantify the influence of different wind speeds in individual scenarios. Comparable to the temperature calculations, a 30 km/h (Table 4.11 and Figure 4.15) and a 130 km/h (Table 4.12 and Figure 4.16) scenario have been tested. As could be seen for both scenarios, the relation between wind and energy consumption is non-linear. This could be explained by the quadratic relationship between wind speed and aerodynamic drag force. This also explains the enormous influence of high wind speeds on the energy consumption. In absolute terms, the influence of wind is higher for high speeds than for low speeds, though relatively the graphs are very similar. When the wind speed is the same as the driving speed and the wind is coming from the tailwind direction, the aerodynamic drag force will be 0N and therefore no influence of wind on the energy consumption will be present.

Table 4.11 Influence of head- and tailwind on the energy consumption when driving at 30 km/h

Scenario	Eco-driving	Normal driving	Aggressive driving
Baseline	0,0437 kWh	0,0433 kWh	0,0431 kWh
- v = 30 km/h	100,9%	100%	99,5%
- no wind			
Headwind, 100 km/h	0,128 kWh 295,6%	0,129 kWh 297,9%	0,131 kWh 302,5%
Headwind, 50 km/h	0,0723 kWh 167,0%	0,0728 kWh 168,1%	0,0734 kWh 169,5%
Headwind, 10 km/h	0,047 kWh 108,5%	0,0471 kWh 108,8%	0,0470 kWh 108,5%
Tailwind, 10 km/h	0,0411 kWh 94,9%	0,0407 kWh 94,0%	0,0403 kWh 93,1%
Tailwind, 30 km/h	0,0393 kWh 90,8%	0,0385 kWh 88,9%	0,0378 kWh 87,3%

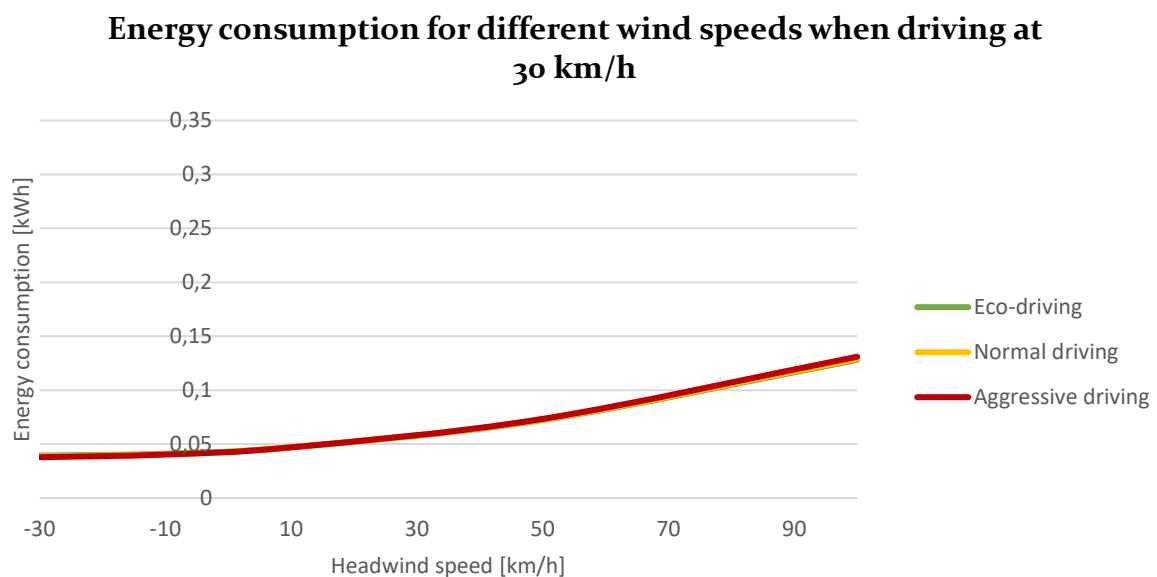
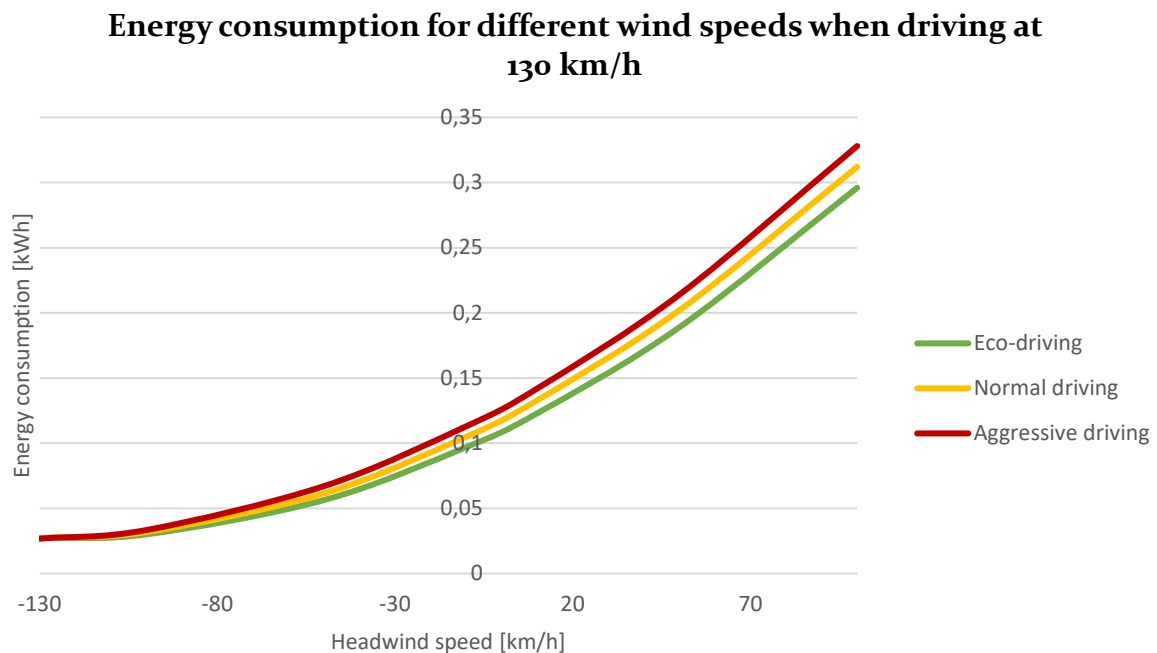


Figure 4.15 Energy consumption for different wind speeds when driving at 30 km/h

Table 4.12 Influence of head- and tailwind on the energy consumption when driving at 130 km/h

Scenario	Eco-driving	Normal driving	Aggressive driving
Baseline	0,109 kWh	0,118 kWh	0,127 kWh
- v = 30 km/h	92,3%	100%	107,6%
- no wind			
Headwind, 100 km/h	0,296 kWh 250,8%	0,312 kWh 264,4%	0,328 kWh 278,0%
Headwind, 50 km/h	0,189 kWh 160,2%	0,202 kWh 171,2%	0,214 kWh 181,4%
Headwind, 10 km/h	0,123 kWh 104,2%	0,133 kWh 112,7%	0,142 kWh 120,3%
Tailwind, 10 km/h	0,097 kWh 82,2%	0,105 kWh 89,0%	0,113 kWh 95,8%
Tailwind, 50 km/h	0,0564 kWh 47,8%	0,0615 kWh 52,1%	0,0671 kWh 56,9%
Tailwind, 100 km/h	0,0301 kWh 25,5%	0,0319 kWh 27,0%	0,0334 kWh 28,3%
Tailwind, 130 km/h	0,0273 kWh 23,1%	0,0270 kWh 22,9%	0,0268 kWh 22,7%

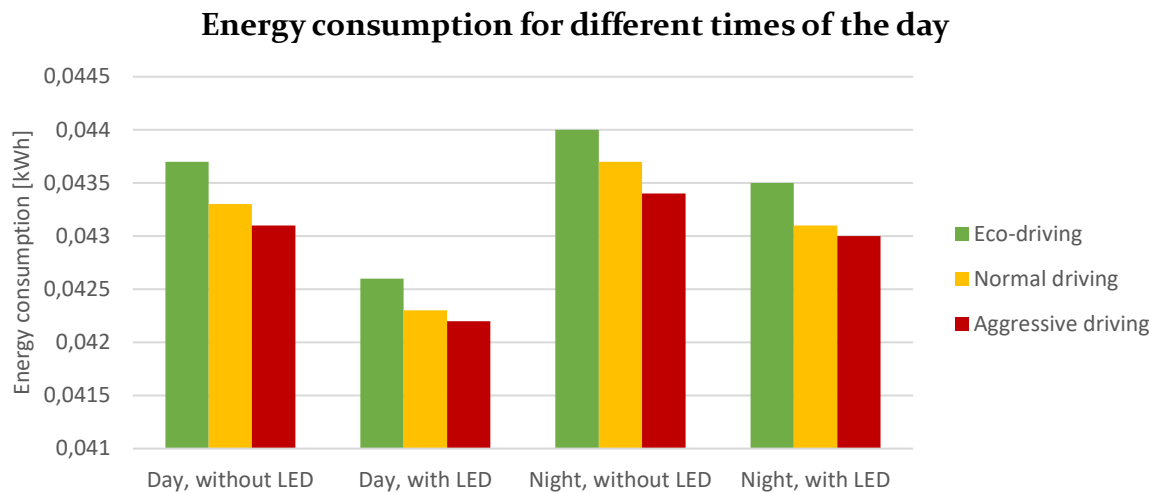
**Figure 4.16** Energy consumption for different wind speeds when driving at 130 km/h

4.2.3 Daytime and nighttime driving

A final environmental influence is the difference of daytime and nighttime driving. Four scenarios have been tested, differentiating in day and night and in LED and conventional lighting systems. The results are shown in Table 4.13 and Figure 4.17. Although both the absolute and relative effects show very little difference, it is visible that LED lighting could potentially save 1-2% of energy. For an average driver, driving 13.000 km/year, this would save about 20 kWh yearly, based on BMW i3 average consumption data (BMW, 2018).

Table 4.13 Influence of daytime and nighttime driving and LED lighting on the energy consumption

Scenario	Eco-driving	Normal driving	Aggressive driving
Day, without LED	0,0437 kWh 100,9%	0,0433 kWh 100%	0,0431 kWh 99,5%
Day, with LED	0,0426 kWh 98,4%	0,0423 kWh 97,7%	0,0422 kWh 97,5%
Night, without LED	0,0440 kWh 101,6%	0,0437 kWh 100,9%	0,0434 kWh 100,2%
Night, with LED	0,0435 kWh 100,5%	0,0431 kWh 99,5%	0,0430 kWh 99,3%

**Figure 4.17** Influence of daytime and nighttime driving and LED lighting on the energy consumption

4.3 Influence of elements related to infrastructural design

After quantifying the influence of driving style and environmental variables, chapter 4.3 quantifies the influence of infrastructural design elements. The influence of a broad set of elements has been calculated. First, the road type has been dealt with, which influences the energy consumption through a changing rolling resistance. After this, road curvature has been emphasized. Different turns require vehicles to decelerate and accelerate causing the vehicle to use more energy than on straight road elements. The influence of road slopes has been calculated for single slopes, as well as for some hilly driving scenarios. Finally, typical stop-and-go traffic elements, such as traffic calming measures and signalized intersections, influence the energy consumption through the deceleration and acceleration caused by these elements. These effects are quantified in the last two subchapters.

4.3.1 Road type

The effect of road types has been calculated based on their different rolling resistances. Table 4.14 and Figure 4.18 show the calculations of the energy consumption on different road types based on the same driving speed. One could see that the lower the rolling resistance, the lower the energy consumption. An increase of 40% rolling resistance results in an increase of about 20% in energy consumption in this scenario. The relative influence on energy consumption is

highly dependent on other factors. Apart from this, driving 30 km/h on a motorway is an unlikely scenario. Therefore, Table 4.15 and Figure 4.19 show the influence of rolling resistance on the energy consumption for realistic driving speeds on these different road types. They show how eco-driving gets more efficient at higher speeds, compared to aggressive driving. Comparing these results to the influence of speed differences in chapter 4.1.1, also shows that a 20% higher rolling resistance increases the energy consumption with about 10%. Again, one should notice that these percentages highly depend on other factors, such as the use of auxiliary energy use. However, in absolute numbers, the influence of rolling resistance shows very stable results. For all driving styles, the influence of adding 1% to the rolling resistance results in an increased energy consumption of 0,00047 kWh/km. Although this little increase in rolling resistance would only add 0,35% to the total energy consumption of a trip (according to an average consumption of 0,131 kWh/km. BMW, 2018), the influence is significant when comparing two road types, since the relative differences in rolling resistance are quite big.

Table 4.14 Rolling resistance scenario for different road types, road segments of 500 m

Road type	Desired speed [km/h]	Desired speed [m/s]	Rolling resistance scaling [-]	Rolling resistance	Result [kWh] and [%]		
					Eco- driving	Normal driving	Aggressive driving
Motorway	30	8,333	1,00	0,01215	0,0437 100,9%	0,0433 100%	0,0431 99,5%
Trunk road	30	8,333	1,00	0,01215	0,0437 100,9%	0,0433 100%	0,0431 99,5%
Distributor road	30	8,333	1,05	0,0127575	0,0447 103,2%	0,0445 102,8%	0,0443 102,3%
Access road	30	8,333	1,15	0,0139725	0,0472 109,0%	0,0469 108,3%	0,0466 107,6%
City access road	30	8,333	1,20	0,01458	0,0483 111,5%	0,0480 110,9%	0,0478 110,4%
Neighborhood access road	30	8,333	1,25	0,0151875	0,0495 114,3%	0,0492 113,6%	0,0490 113,1%
Homezone*	30	8,333	1,40	0,01701	0,0530 122,4%	0,0527 121,7%	0,0525 121,5%

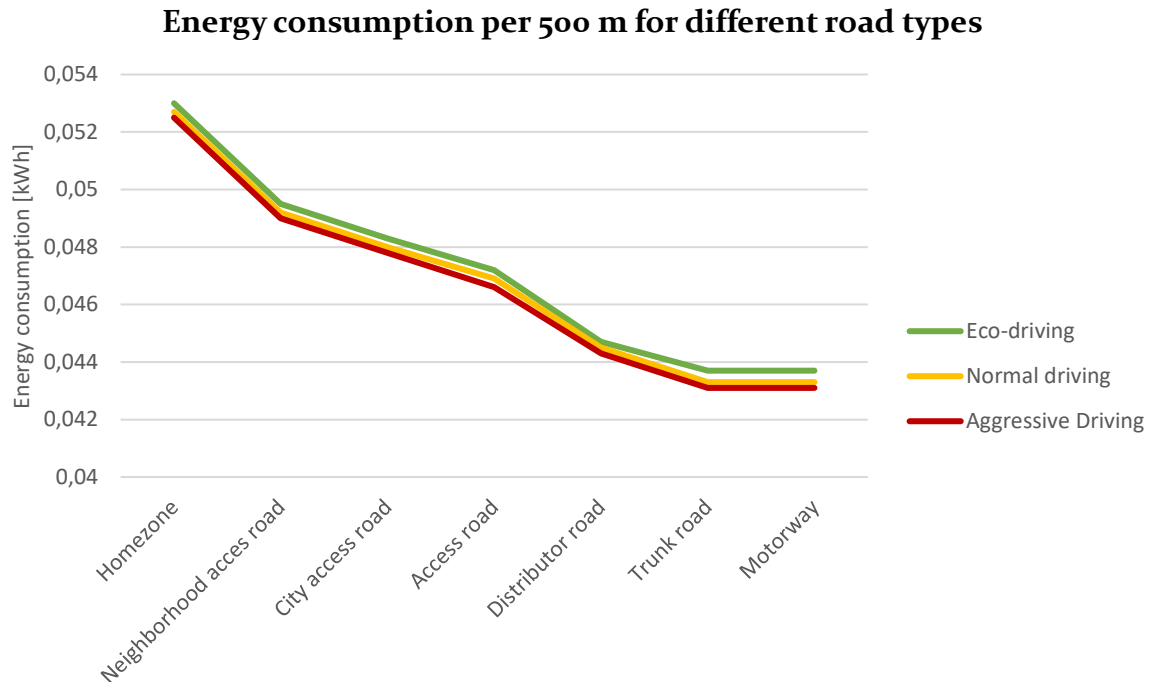


Figure 4.18 Energy consumption per 500 m for different road types

Table 4.15 Rolling resistance scenario for different road types and speeds, road segments of 500 m

Road type	Desired speed [km/h]	Desired speed [m/s]	Rolling resistance scaling [-]	Rolling resistance	Result [kWh] and [%]		
					Eco-driving	Normal driving	Aggressive driving
Motorway	130	36,111	1,00	0,01215	0,109	0,118	0,127
					92,4%	100%	107,6%
Trunk road	100	27,778	1,00	0,01215	0,0769	0,0819	0,0872
					93,9%	100%	106,4%
Distributor road	80	22,222	1,05	0,0127575	0,0617	0,0647	0,0680
					95,3%	100%	105,1%
Access road	60	16,667	1,15	0,0139725	0,0524	0,0539	0,0555
					97,2%	100%	103,0%
City access road	50	13,889	1,20	0,01458	0,0498	0,0506	0,0516
					98,4%	100%	102,0%
Neighborhood access road	30	8,333	1,25	0,0151875	0,0495	0,0492	0,0490
					100,6%	100%	99,6%
Homezone*	15	4,167	1,40	0,01701	0,0656	0,0642	0,0629
					102,2%	100%	98,0%

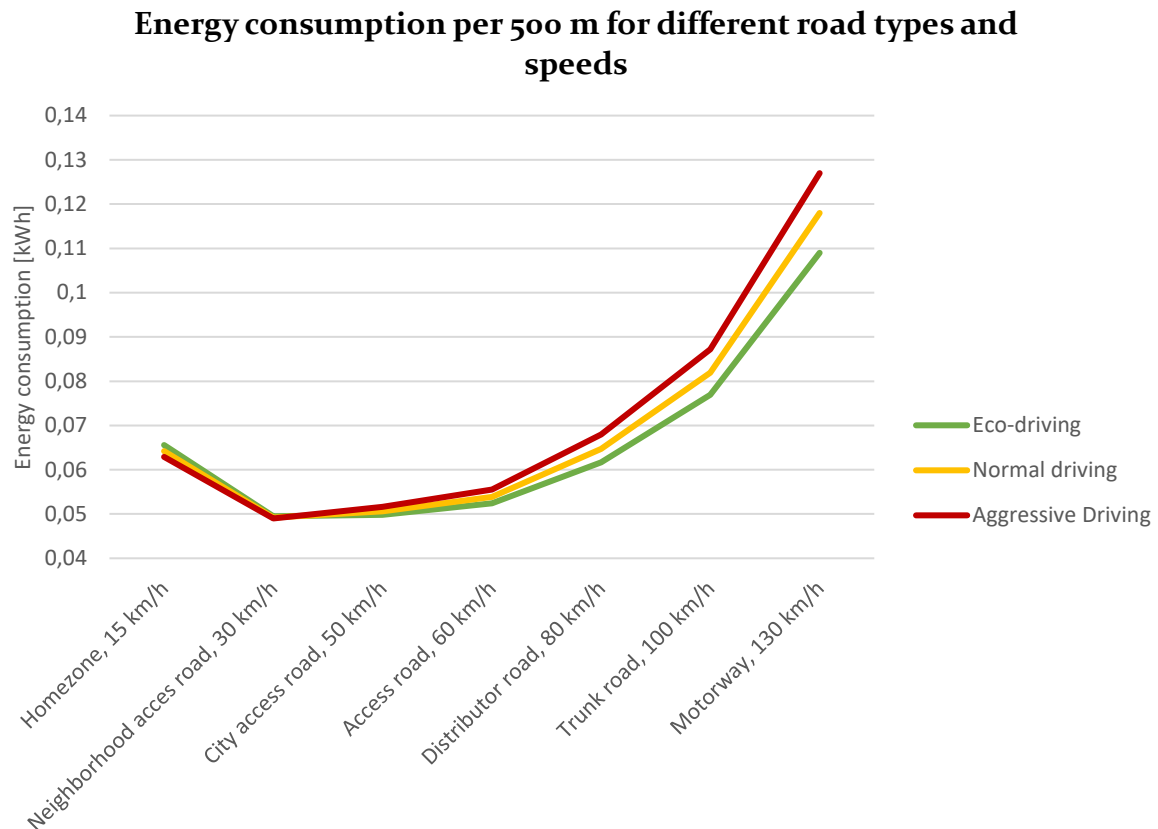


Figure 4.19 Energy consumption per 500 m for different road types and speeds

4.3.2 Road curvature

Different curved road profiles have been analyzed. The rise in energy consumption is caused by the deceleration and acceleration during the turn. The maximum speed in these curves is dependent on the radius of the curve and the preferred lateral acceleration of a driver. Figure 4.20 shows the influence of radius on the maximum driving speed for different lateral accelerations. The lateral accelerations used for the calculations (eco-driving, normal driving and aggressive driving at 50 km/h) have been shown in green, yellow and red. What could be seen is that a turn with a radius of 24 m, the aggressive car can take this turn with 50 km/h, while the eco-driver needs double the radius to take the turn with the same speed. Although the eco-driver is less affected by acceleration and deceleration, he is more likely to be influenced by curves than the aggressive driver once the curve's radius is big enough.

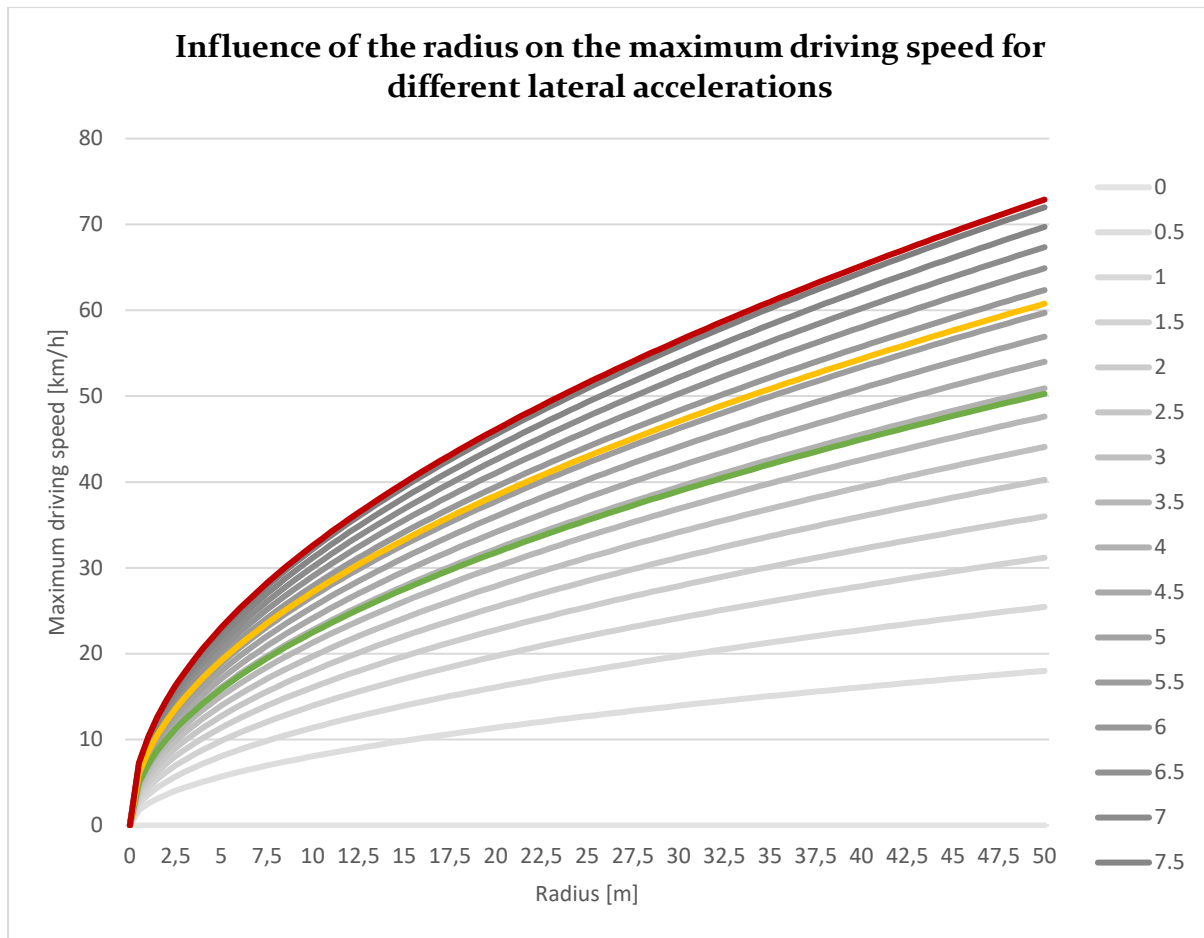


Figure 4.20 Influence of radius on maximum driving speed for different lateral accelerations

Two common curve types with a different radius have been compared to a baseline scenario of a straight 50 km/h road of 130 m (Table 4.16). A significant influence of the radius has been found. As could be seen in Figure 4.23, curved road sections with a high radius don't influence the speed of most aggressive drivers. Therefore, the energy consumption of all driving styles is comparable (Figure 4.24). For sharper turns, aggressive drivers and normal drivers also need to slow down (Figure 4.21). This results in a higher energy consumption for the normal and aggressive drivers (Figure 4.22). Because the aggressive driver still takes the sharper turn with a relatively high speed ($v=46,1$ km/h compared to $v=38,4$ km/h for the normal driver), the energy consumption is comparable with the normal driver. For even sharper turns, the gap between the normal driver and aggressive driver is likely to increase. Figure 4.25 shows an overview of the influence of the radius and shows the significant influence the radius of curved road sections has on the energy consumption, especially for non-eco drivers.

Table 4.16 Energy consumption for different curved road segments

Scenario	Eco-driving	Normal driving	Aggressive driving
Baseline	$E = 0,012$ kWh	$E = 0,012$ kWh	$E = 0,012$ kWh
130 m, straight road			
R=30m	$a_y = 3,9$ m/s ²	$a_y = 5,7$ m/s ²	$a_y = 8,2$ m/s ²
$\alpha=90^\circ$	$v_{\text{curve}} = 38,9$ km/h	$v_{\text{curve}} = 47,1$ km/h	$v_{\text{curve}} = 52,5$ km/h
Single curve	$E = 0,014$ kWh	$E = 0,016$ kWh	$E = 0,016$ kWh
R=20m	$a_y = 3,9$ m/s ²	$a_y = 5,7$ m/s ²	$a_y = 8,2$ m/s ²
$\alpha=90^\circ$	$v_{\text{curve}} = 31,8$ km/h	$v_{\text{curve}} = 38,4$ km/h	$v_{\text{curve}} = 46,1$ km/h
Single curve	$E = 0,017$ kWh	$E = 0,027$ kWh	$E = 0,029$ kWh

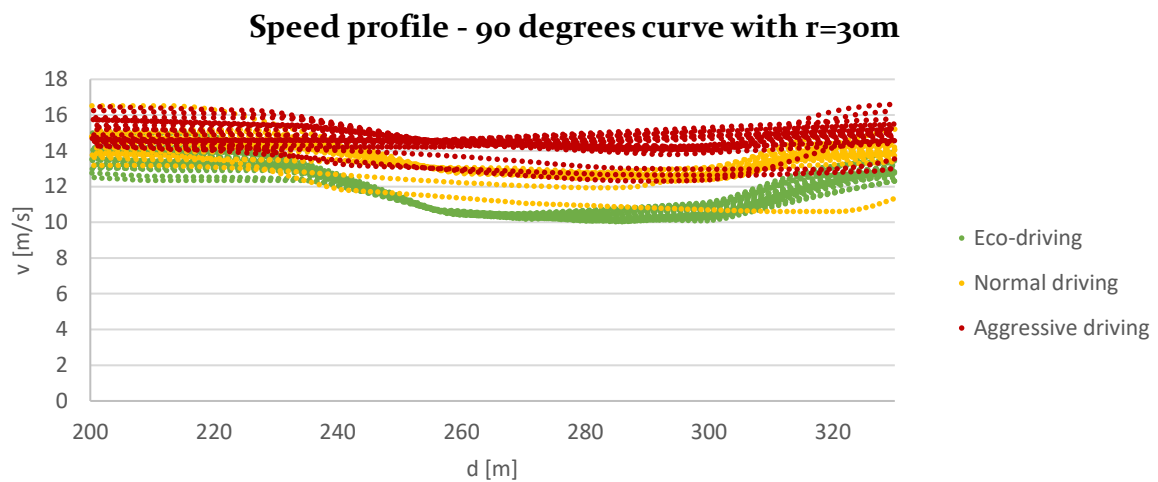


Figure 4.21 Speed profile for a 90 degrees curve with a radius of 30 meter

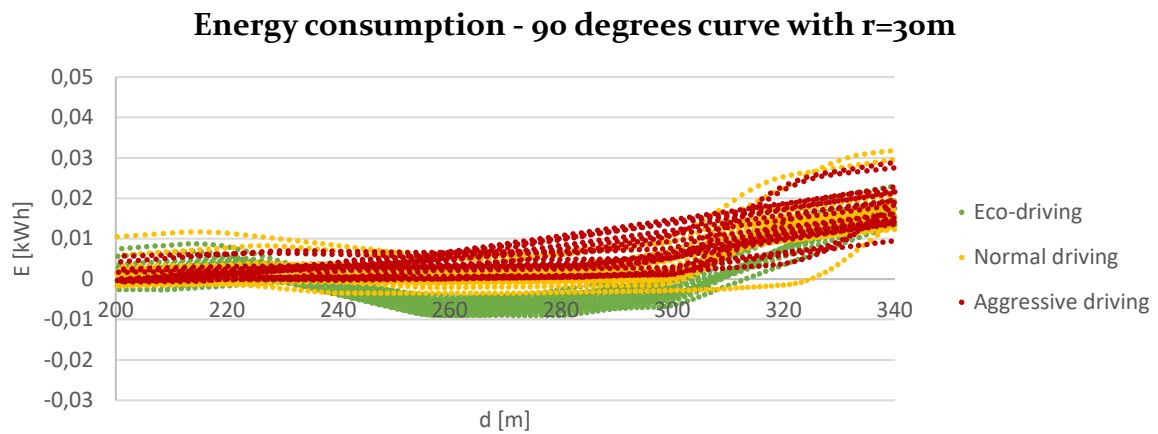


Figure 4.22 Energy consumption for a 90 degrees curve with a radius of 30 meter

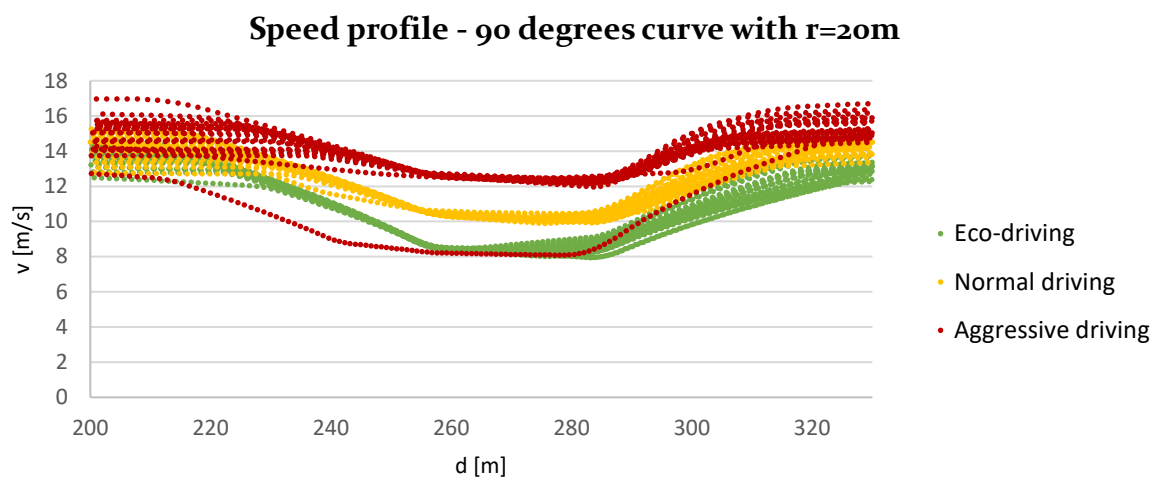


Figure 4.23 Speed profile for a 90 degrees curve with a radius of 20 meter

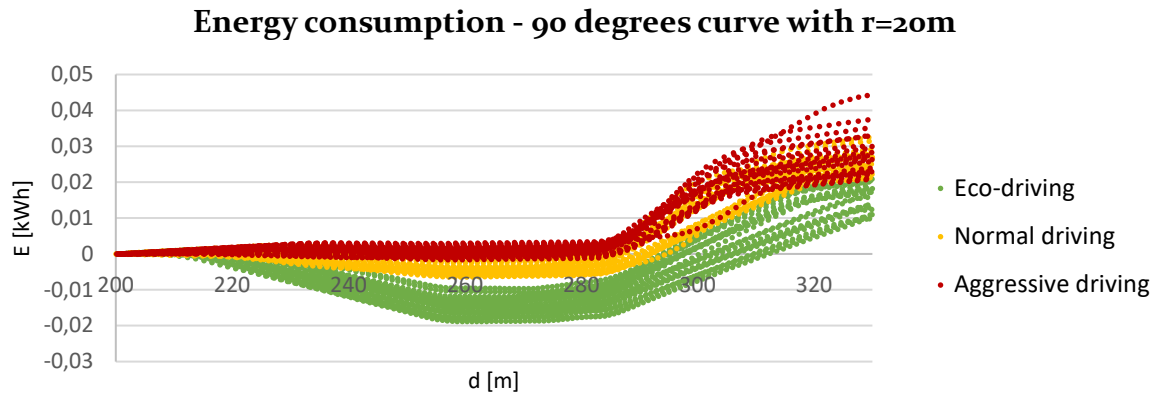


Figure 4.24 Energy consumption for a 90 degrees curve with a radius of 20 meter

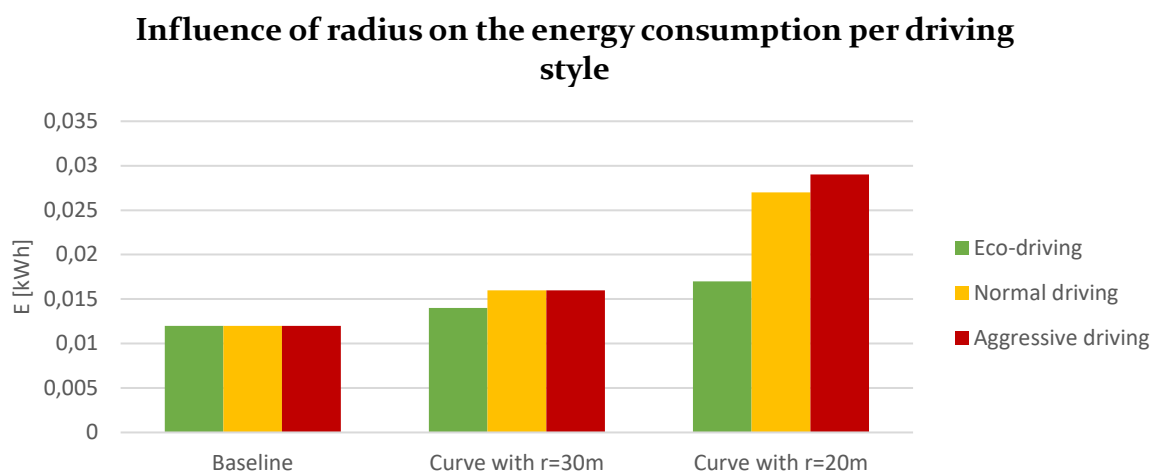


Figure 4.25 Influence of radius on the energy consumption per driving style

4.3.3 Hilly driving

The quantitative influence of slopes has been calculated for different downward and upward slopes, both for slow driving (30 km/h, Table 4.17 and Figure 4.26) and fast driving (130 km/h, Table 4.18 and Figure 4.27). For the uphill scenarios, there seems to be no difference between the driving styles. This is caused by the fact that driving style doesn't influence the gravitational and rolling resistance forces. Therefore, relative differences between the driving styles degrade with higher uphill slopes. For downhill slopes, the influence of driving style is very big, caused by the differences in the efficiency of creating regenerative energy as well as the differences in driving speed. The higher the slope, the bigger the absolute and relative differences are.

Interesting is the fact that the absolute difference between uphill driving is not only equal for different driving styles, but also for different driving speeds. The increase in energy consumption is about 0,08 kWh/km for every added degree in gradient. Based on an average consumption of 0,131 kWh/km (BMW, 2018), a constant slope of 1° would increase the energy consumption by 61%. The relative difference is lower for fast driving than for slow driving, simply because the baseline energy consumption is higher.

Table 4.17 Influence of up- and downhill driving on the energy consumption when driving 30 km/h

Scenario	Height difference	Eco-driving	Normal driving	Aggressive driving
Baseline, 30 km/h	0	0,0437 kWh	0,0433 kWh	0,0431 kWh
- 500 m		100,9%	100%	99,5%
Downwards, slope 10°	88,2-0	-0,224 kWh	-0,09 kWh	-0,02 kWh
		-517,3%	-208,9%	-46,2%
Downwards, slope 5°	43,7-0	-0,095 kWh	-0,034 kWh	-0,002 kWh
		-219,4%	-78,5%	-4,6%
Downwards, slope 2°	17,5-0	-0,018 kWh	0,0002 kWh	0,0101 kWh
		-41,6%	4,6%	23,3%
Downwards, slope 1°	8,7-0	0,008 kWh	0,0118 kWh	0,0144 kWh
		18,5%	27,3%	33,3%
Upwards, slope 1°	0-8,7	0,0835 kWh	0,0832 kWh	0,0830 kWh
		192,8%	192,1%	191,7%
Upwards, slope 2°	0-17,5	0,123 kWh	0,123 kWh	0,123 kWh
		284,1%	284,1%	284,1%
Upwards, slope 5°	0-43,7	0,243 kWh	0,242 kWh	0,242 kWh
		561,2%	561,2%	561,2%
Upwards, slope 10°	0-88,2	0,440 kWh	0,440 kWh	0,440 kWh
		1016,1%	1016,1%	1016,1%

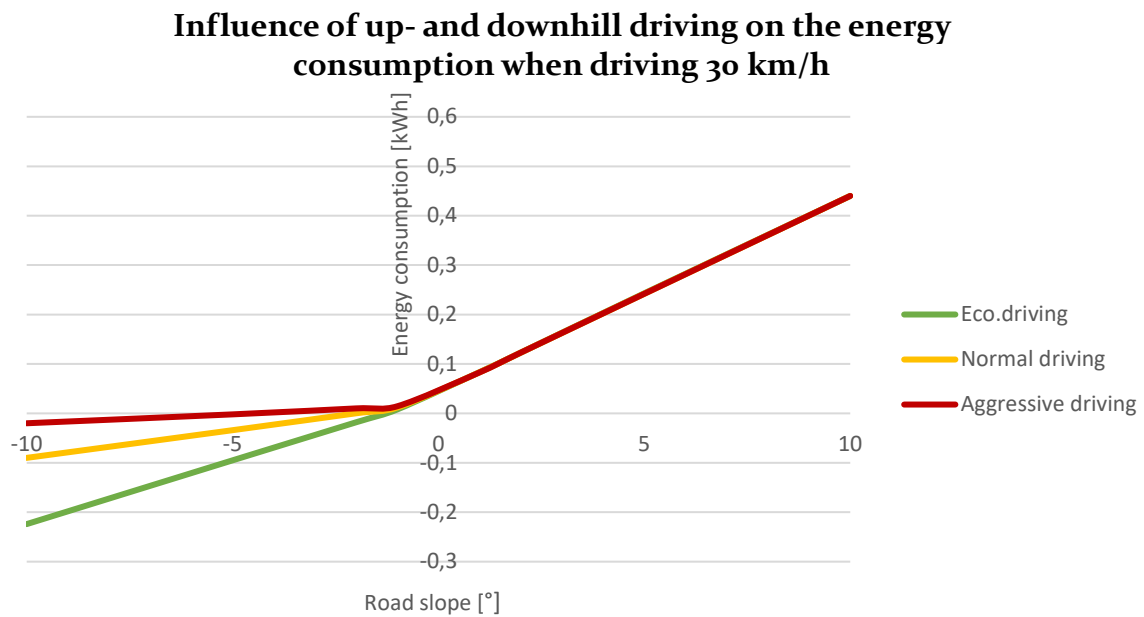
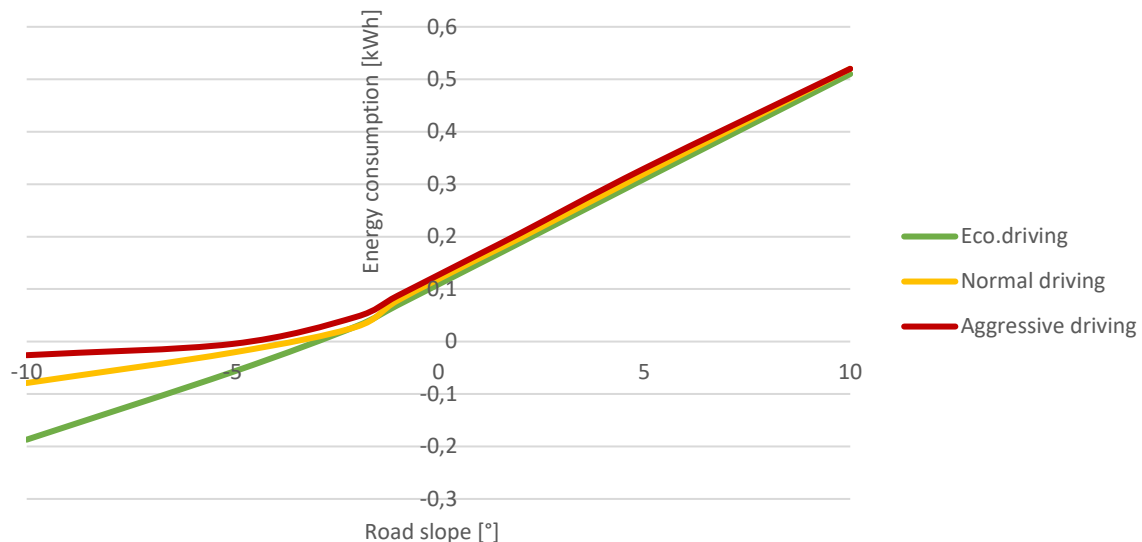
**Figure 4.26** Influence of up- and downhill driving on the energy consumption when driving 30 km/h

Table 4.18 Influence of up- and downhill driving on the energy consumption when driving 130 km/h

Scenario	Height difference	Eco-driving	Normal driving	Aggressive driving
Baseline, 130 km/h	0	0,109 kWh	0,118 kWh	0,127 kWh
- 500 m		92,3%	100%	107,6%
Downwards, slope 10°	88,2-0	-0,187 kWh	-0,079 kWh	-0,026 kWh
		-158,4%	-66,9%	-22,0%
Downwards, slope 5°	43,7-0	-0,058 kWh	-0,021 kWh	-0,0045 kWh
		-49,2%	-17,8%	-3,8%
Downwards, slope 2°	17,5-0	0,029 kWh	0,028 kWh	0,047 kWh
		24,6%	23,7%	39,8%
Downwards, slope 1°	8,7-0	0,069 kWh	0,078 kWh	0,087 kWh
		58,5%	66,1%	73,7%
Upwards, slope 1°	0-8,7	0,149 kWh	0,159 kWh	0,167 kWh
		126,3%	134,7%	141,5%
Upwards, slope 2°	0-17,5	0,189 kWh	0,198 kWh	0,207 kWh
		160,2%	167,8%	175,4%
Upwards, slope 5°	0-43,7	0,31 kWh	0,32 kWh	0,33 kWh
		262,7%	271,2%	279,7%
Upwards, slope 10°	0-88,2	0,51 kWh	0,52 kWh	0,52 kWh
		432,2%	440,7%	440,7%

Influence of up- and downhill driving on the energy consumption when driving at 130 km/h**Figure 4.27** Influence of up- and downhill driving on the energy consumption when driving 130 km/h

After calculating the effect of individual slopes, four scenarios have been tested, as could be seen in Table 4.19 and Figure 4.28, Figure 4.29, Figure 4.30 and Figure 4.31. An interesting result is that the order of uphill and downhill driving makes no difference in energy consumption. This has been calculated for slopes of 1° and 10°. It implies that it's possible to calculate the energy consumption for any height profile by simply knowing all the slopes and

the driving distances at each slope. The approach created by Liu et al. (2017), which assigns percentages of a trip to their matching road gradient categories, seems valid.

The graphs also show the steeper the downhill slope, the bigger the differences in energy consumption for the different driving styles. There's almost no difference between the driving styles when driving uphill. The most interesting is the fact that for low gradients, such as the slope of 1° , the difference between the baseline scenario and the scenario with slope is relatively low compared to the difference at high slopes. However, the energy consumption would still increase about 5-10% for low slope scenarios, which still makes them relevant when they occur often.

Table 4.19 *Hilly driving scenarios*

Scenario	Height difference [m]	Eco-driving	Normal driving	Aggressive driving
Baseline	0	0,0437 kWh	0,0433 kWh	0,0431 kWh
- 500 m		100,9%	100%	99,5%
Uphill-downhill slope 1°	0 \rightarrow 8,7 \rightarrow 0	0,0458 kWh	0,0469 kWh	0,0477 kWh
		105,8%	108,3%	110,2%
Downhill-uphill slope 1°	0 \rightarrow -8,7 \rightarrow 0	0,0458 kWh	0,0471 kWh	0,0477 kWh
		105,8%	108,8%	110,2%
Uphill-downhill slope 10°	0 \rightarrow 88,2 \rightarrow 0	0,108 kWh	0,173 kWh	0,208 kWh
		249,2%	399,5%	480,4%
Downhill-uphill slope 10°	0 \rightarrow -88,2 \rightarrow 0	0,108 kWh	0,175 kWh	0,208 kWh
		249,2%	404,2%	480,4%

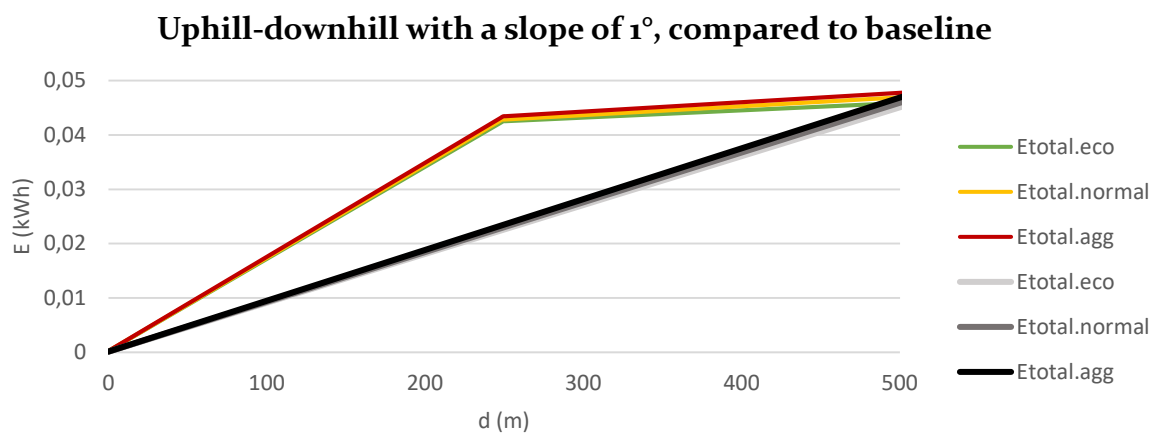


Figure 4.28 *Uphill-downhill with a slope of 1° , compared to baseline*

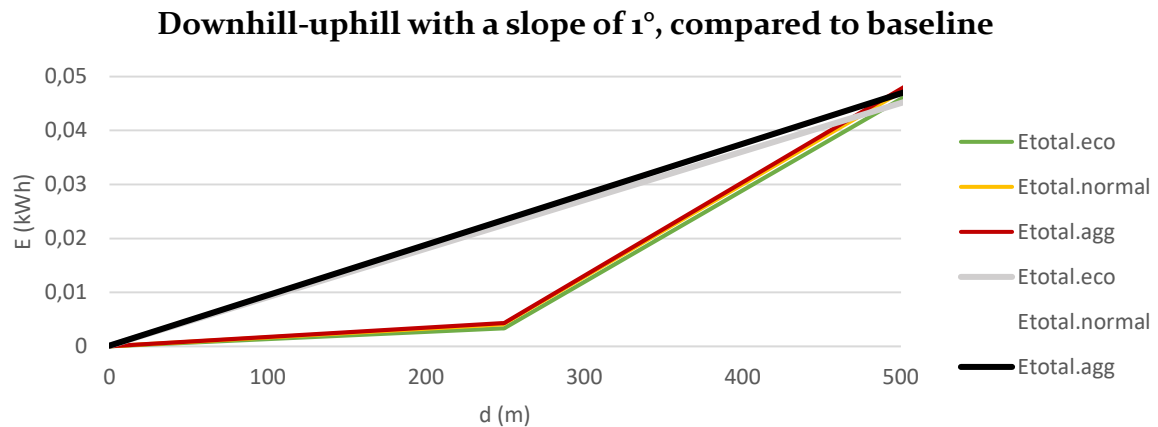


Figure 4.29 Downhill-uphill with a slope of 1°, compared to baseline

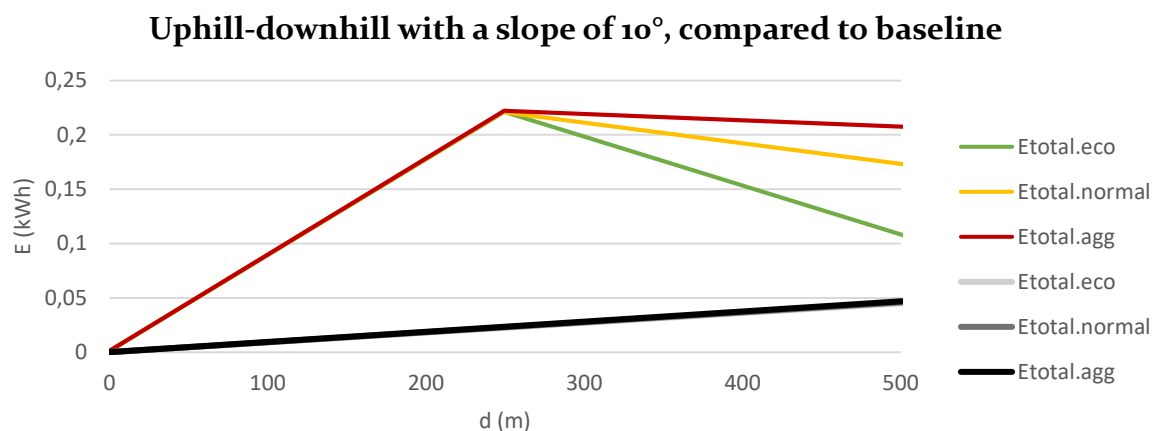


Figure 4.30 Uphill-downhill with a slope of 10°, compared to baseline

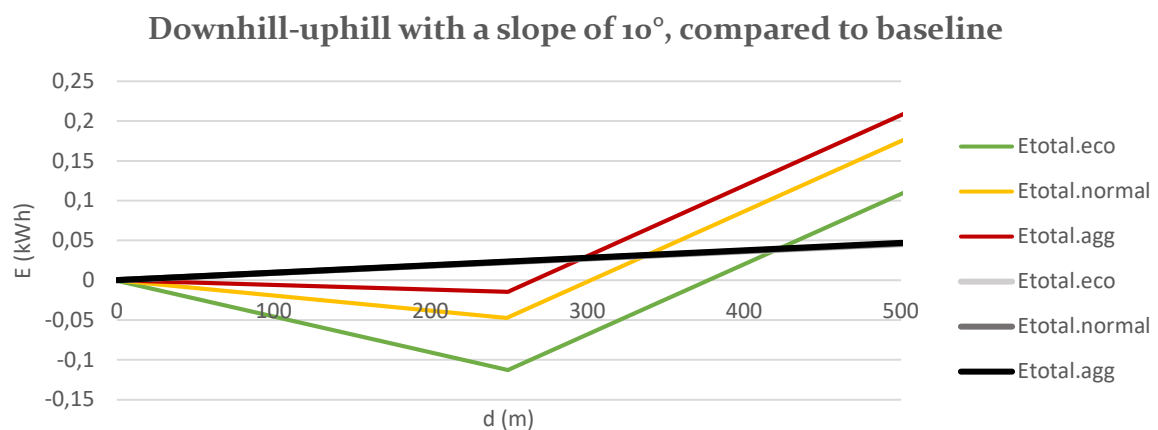


Figure 4.31 Downhill-uphill with a slope of 10°, compared to baseline

4.3.4 Traffic calming measures

The influence of traffic calming measures on the energy consumption could be explained by the fact that a vehicle needs to slow down before and accelerate after the traffic calming measure. This results in high acceleration forces. Five traffic calming measures have been manually calculated. Table 4.20 and Figure 4.32 show the huge differences between the three driving

styles. The aggressive driver uses about two times the amount of energy an eco-driver needs to do the same maneuver. At the speed bump, the toughest traffic calming measure, an eco-driver would use over two times the amount of energy compared to the baseline, while the aggressive driver almost uses five times the amount of energy. Figure 4.33 shows the relation between the speed reduction of a traffic calming measure and the extra energy consumption.

Table 4.20 Results of the individual calculations

Scenario	Eco-driving	Normal driving	Aggressive driving
Baseline	0,00443 kWh 100,9%	0,00440 kWh 100%	0,00438 kWh 99,5%
Speed bump	0,0102 kWh 231,8%	0,0163 kWh 370,5%	0,0207 kWh 470,5%
Watts speed bump	0,00857 kWh 194,8%	0,0133 kWh 302,3%	0,0167 kWh 379,5%
Seminole speed bump	0,00788 kWh 179,1%	0,0118 kWh 427,3%	0,0147 kWh 334,1%
Speed slot	0,00626 kWh 142,3%	0,00838 kWh 190,5%	0,00987 kWh 224,3%
Speed cushion	0,00920 kWh 209,1%	0,0145 kWh 329,5%	0,0184 kWh 418,2%

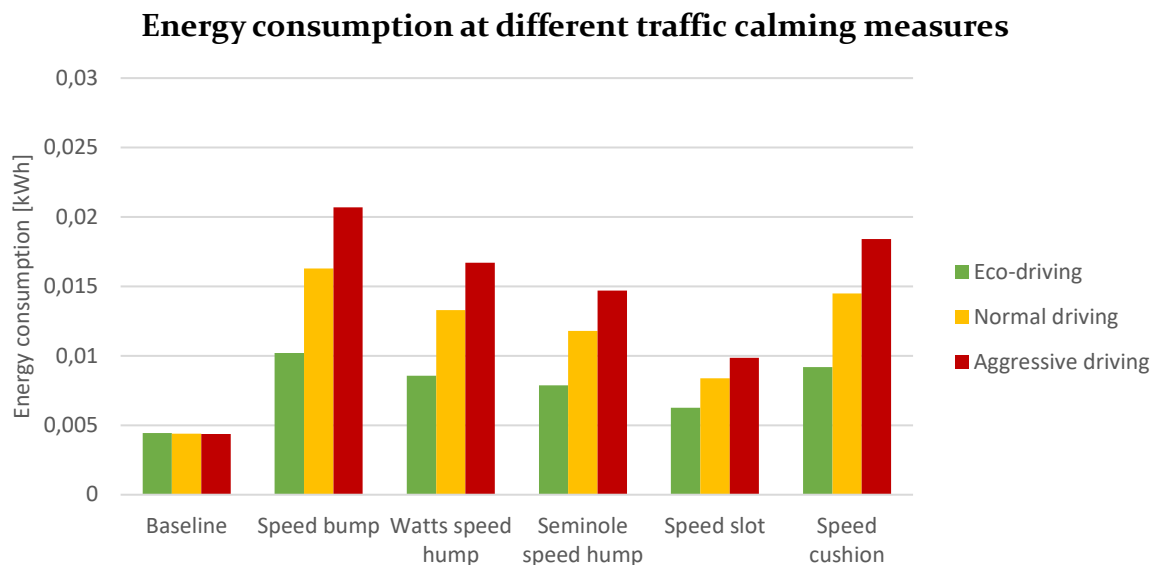


Figure 4.32 Energy consumption at different traffic calming measures

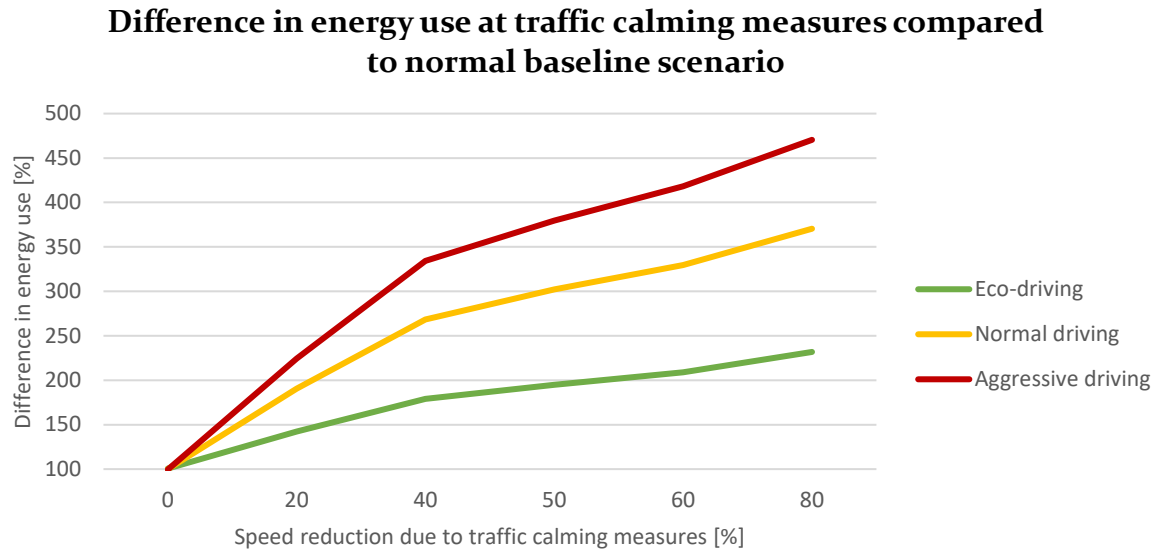


Figure 4.33 Relation between speed reduction and increase in energy consumption

Apart from the manual calculations, all traffic calming measures have been individually modeled in VISSIM (Table 4.21). The influence of traffic calming measures has been slightly underestimated in the manual calculations. However, the VISSIM calculations already include the speed oscillations caused by the Wiedemann 74 model, causing this higher influence on the energy consumption.

Table 4.21 Results of the VISSIM simulations

Scenario	Eco-driving	Normal driving	Aggressive driving
Baseline	0,004438 kWh 85,6%	0,005186 kWh 100%	0,005340 kWh 103,0%
Speed bump	0,0115 kWh 221,8%	0,0182 kWh 350,9%	0,0240 kWh 462,8%
Watts	0,00799 kWh 154,1%	0,0146 kWh 281,5%	0,0194 kWh 374,1%
Seminole	0,00690 kWh 133,1%	0,0130 kWh 250,7%	0,0176 kWh 339,4%
Speed slot	0,00502 kWh 96,8%	0,00902 kWh 173,9%	0,0117 kWh 225,6%
Speed cushion	0,00953 kWh 183,8%	0,0160 kWh 208,5%	0,0221 kWh 426,1%

4.3.4.1 Speed bump

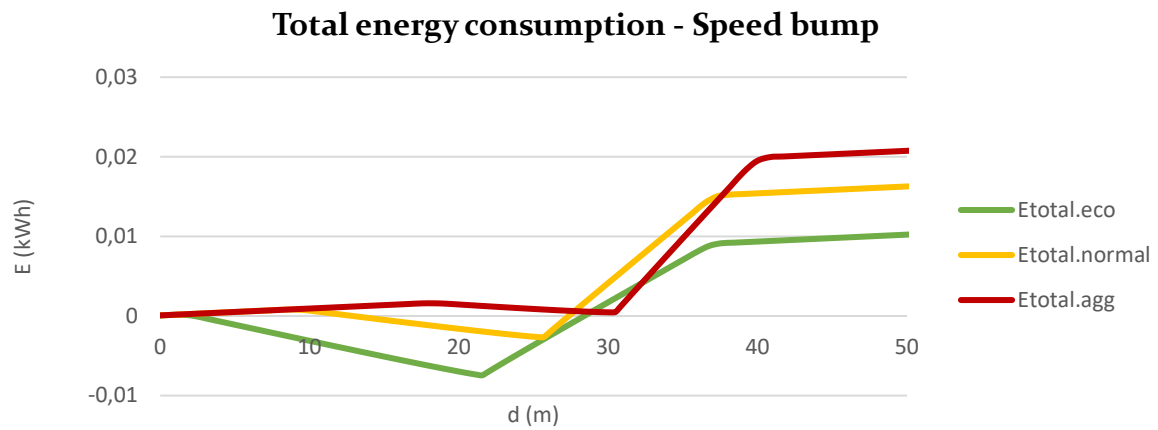


Figure 4.34 Energy consumption at the speed bump

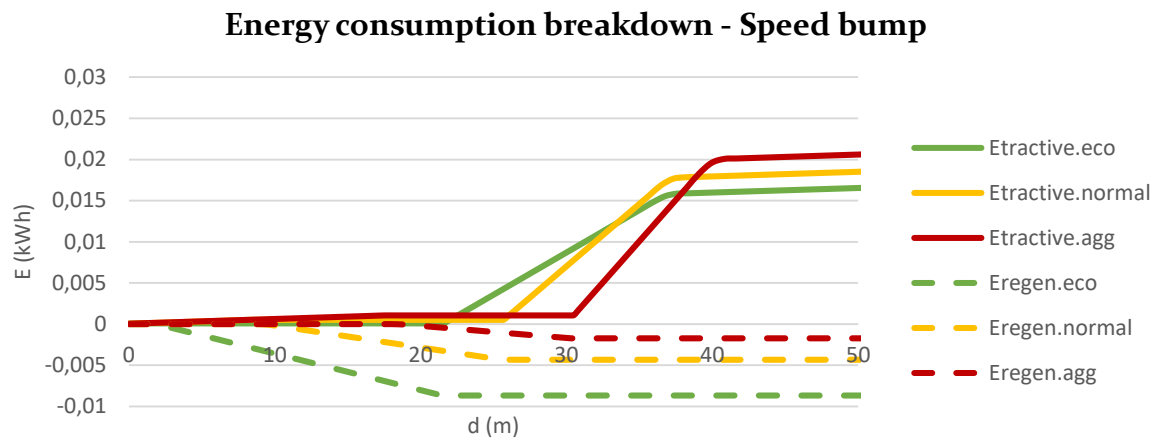


Figure 4.35 Energy consumption breakdown at the speed bump

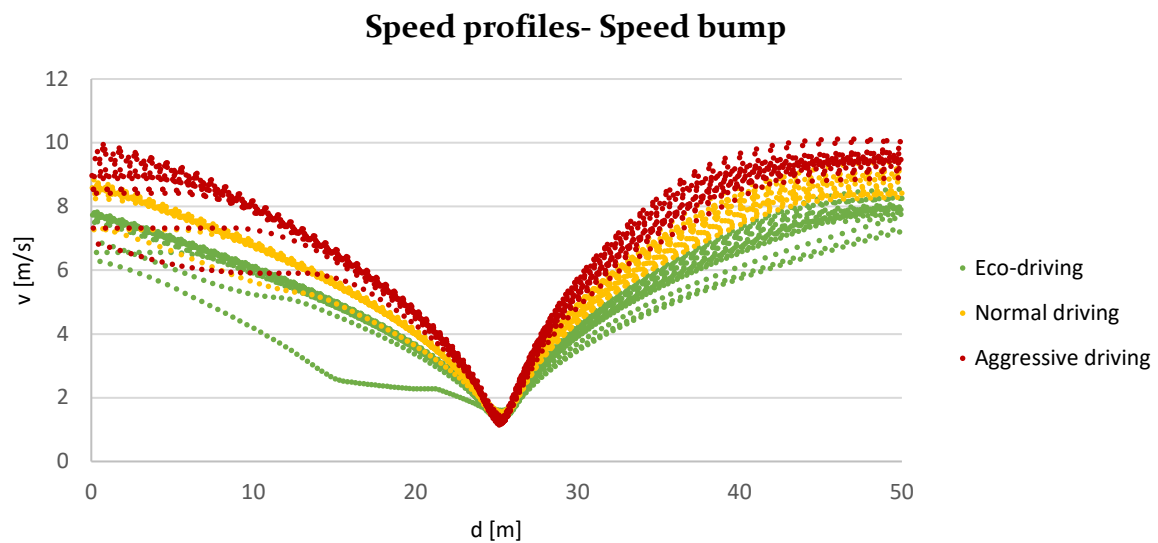


Figure 4.36 Speed profiles at the speed bump

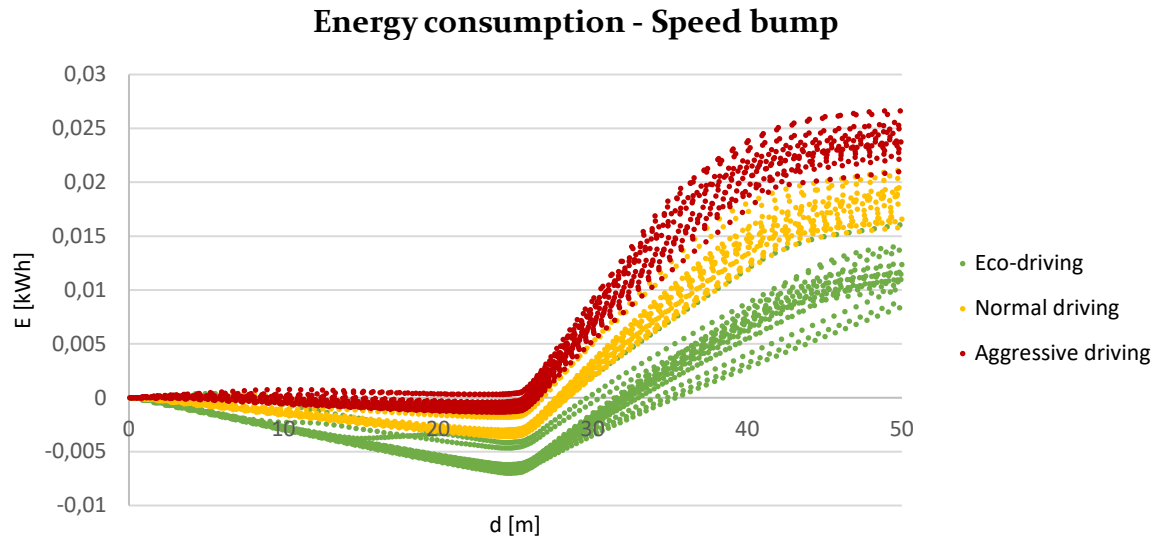


Figure 4.37 Energy consumption at the speed bump

4.3.4.2 Watts speed bump

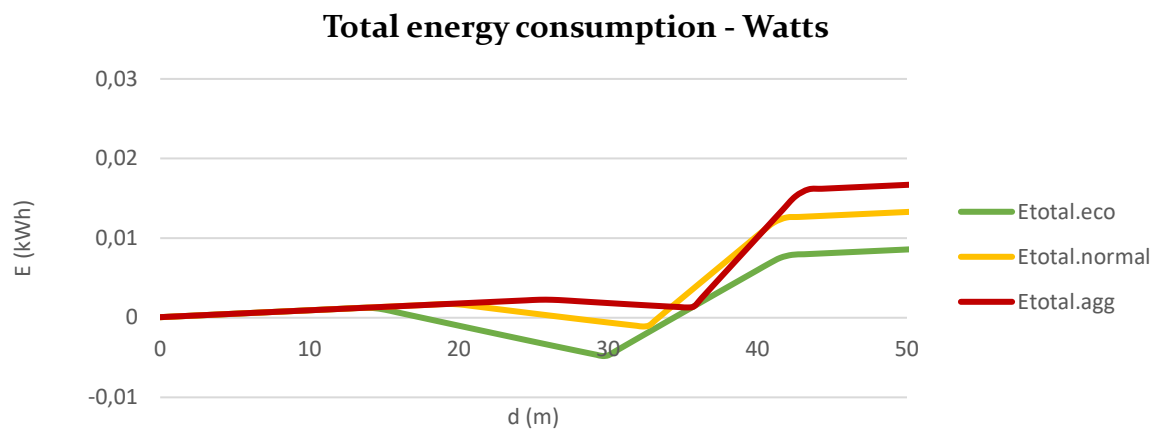


Figure 4.38 Energy consumption at the Watts speed bump

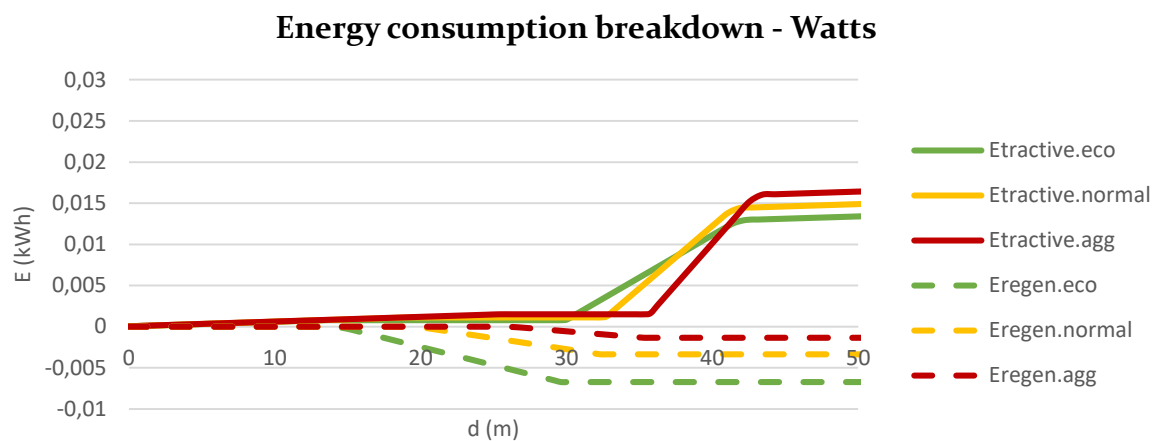


Figure 4.39 Energy consumption breakdown at the Watts speedbump

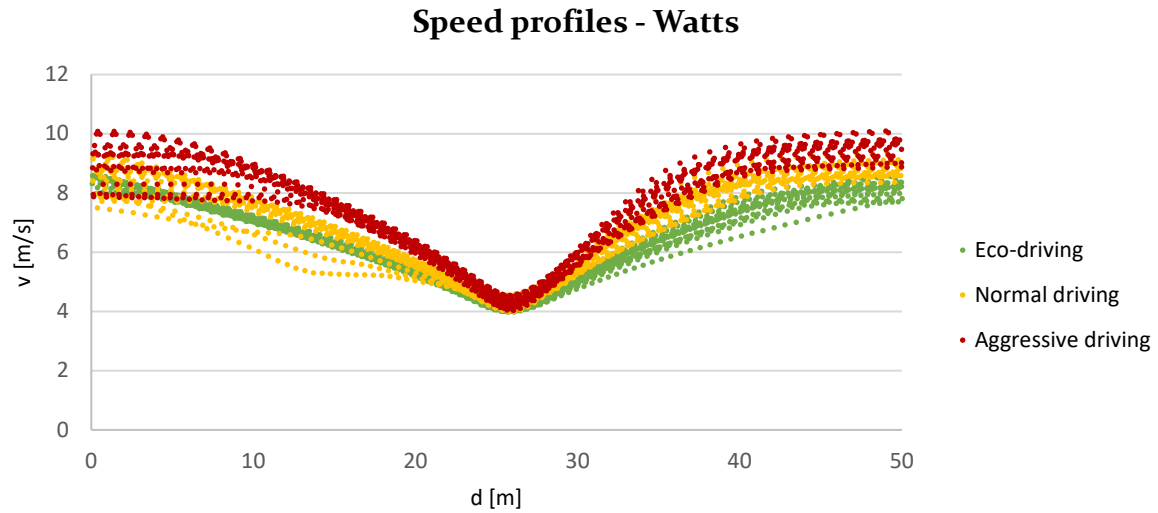


Figure 4.40 Speed profiles at the Watts speed bump

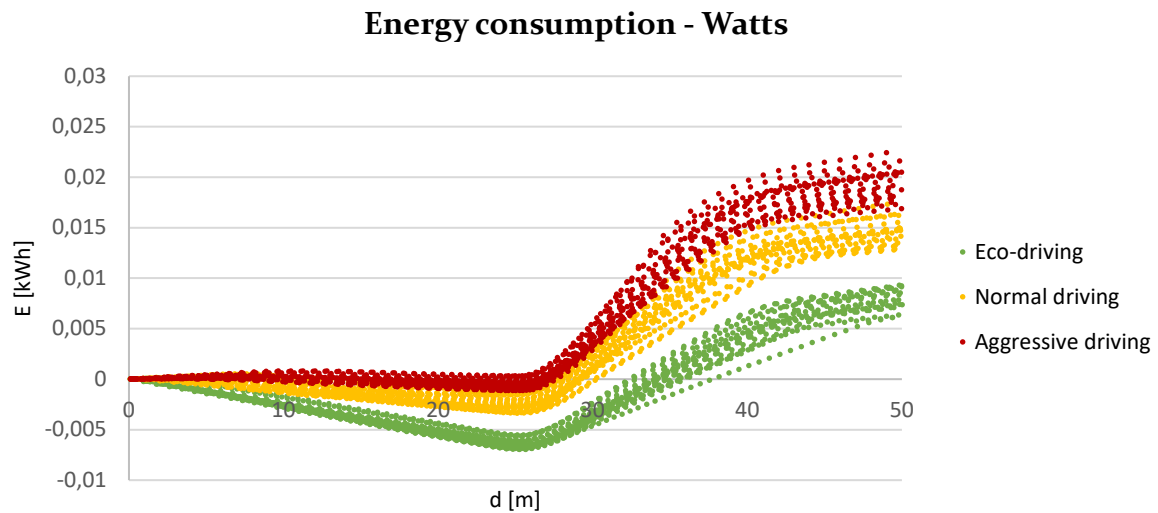


Figure 4.41 Energy consumption at the Watts speed bump

4.3.4.3 Seminole speed bump

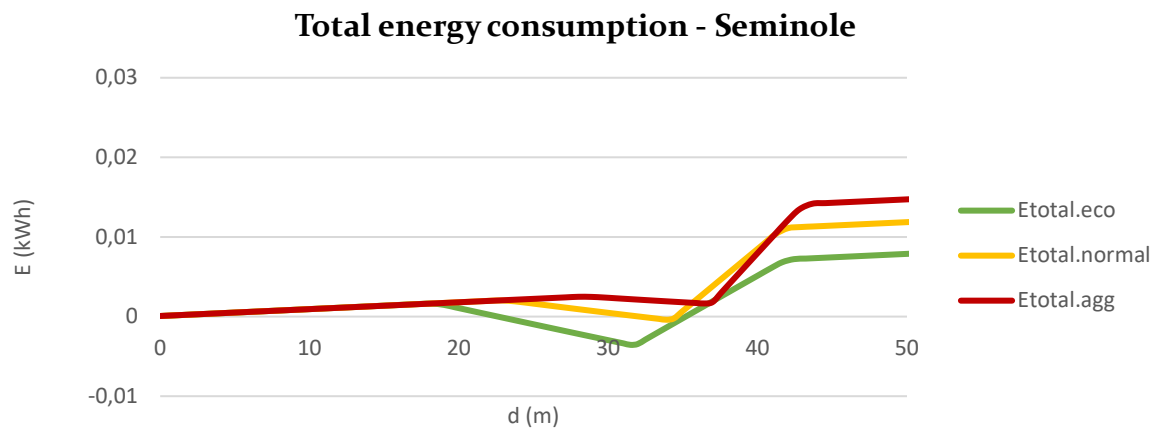


Figure 4.42 Energy consumption at the Seminole speed bump

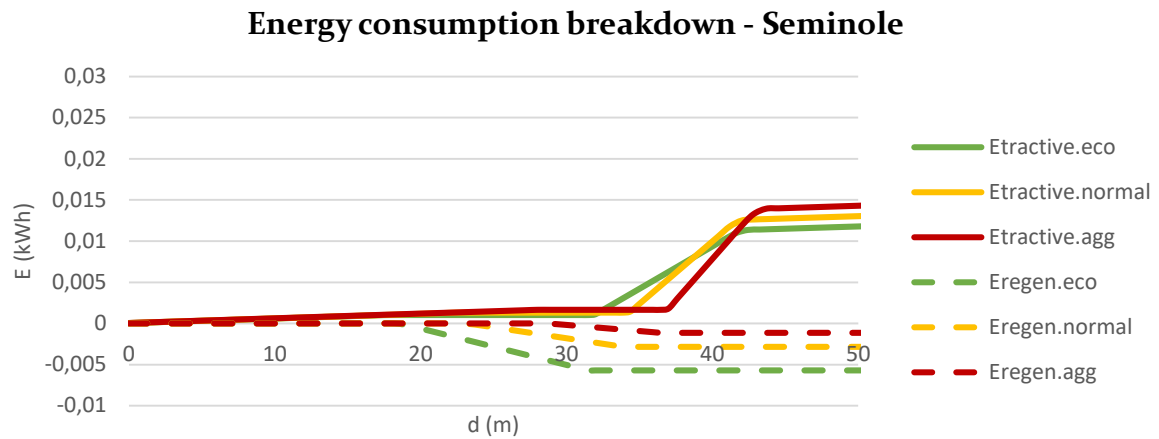


Figure 4.43 Energy consumption breakdown at the Seminole speed bump

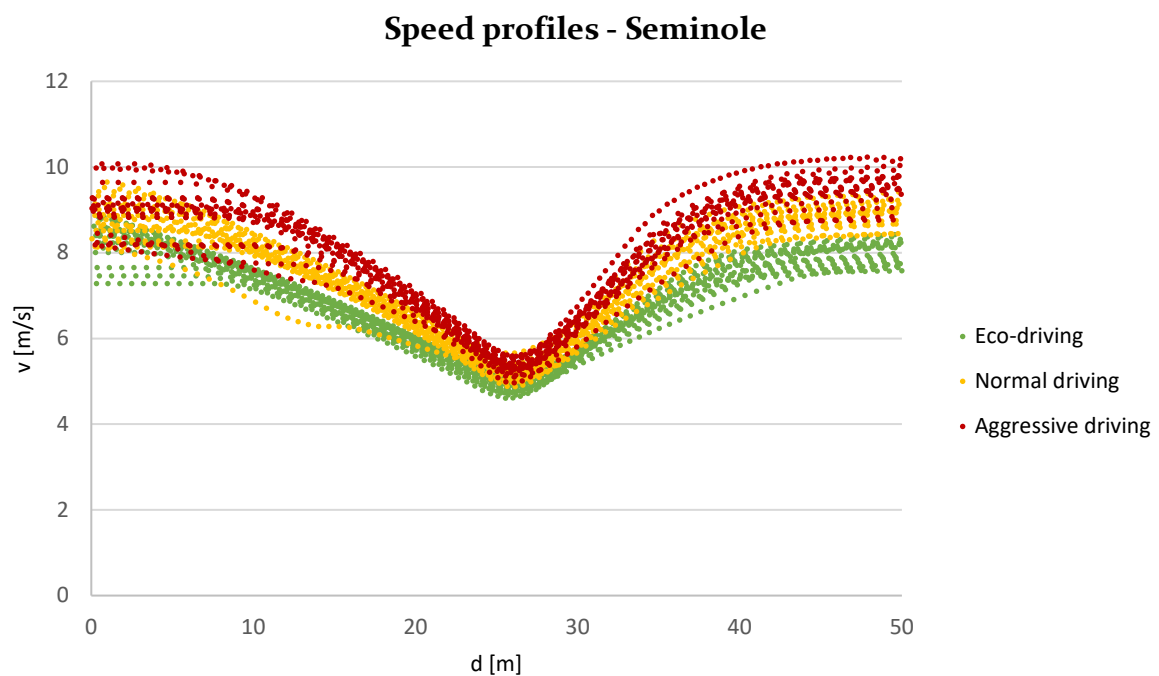


Figure 4.44 Speed profiles at the Seminole speed bump

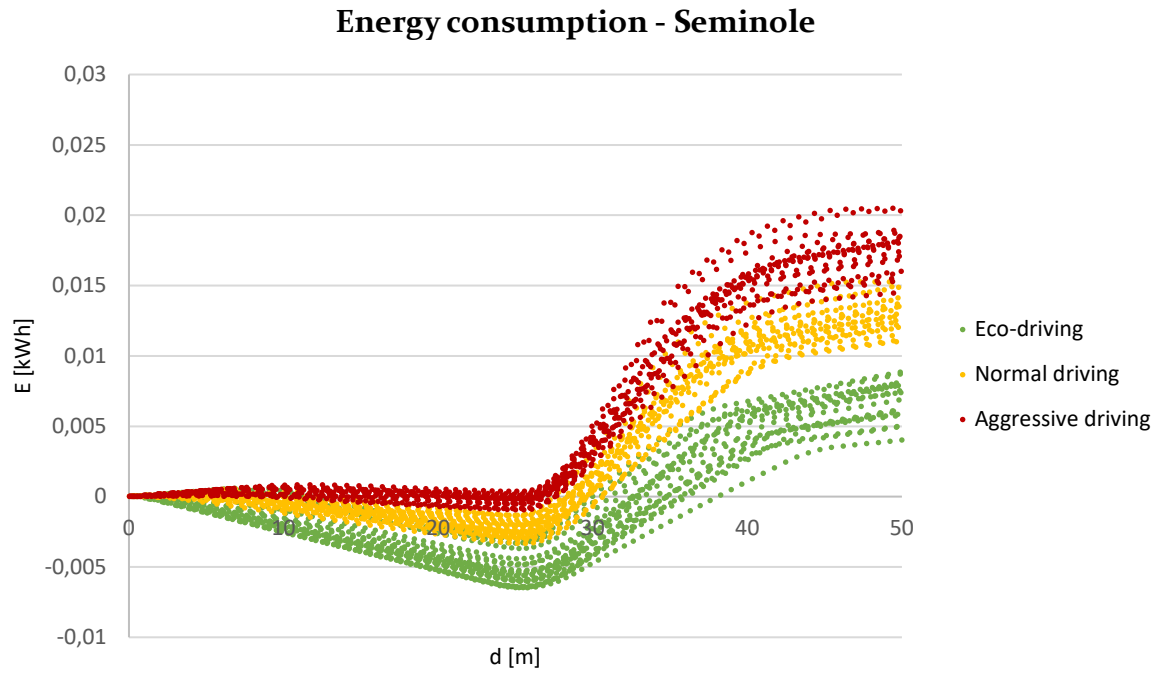


Figure 4.45 Energy consumption at the Seminole speed bump

4.3.4.4 Speed slot

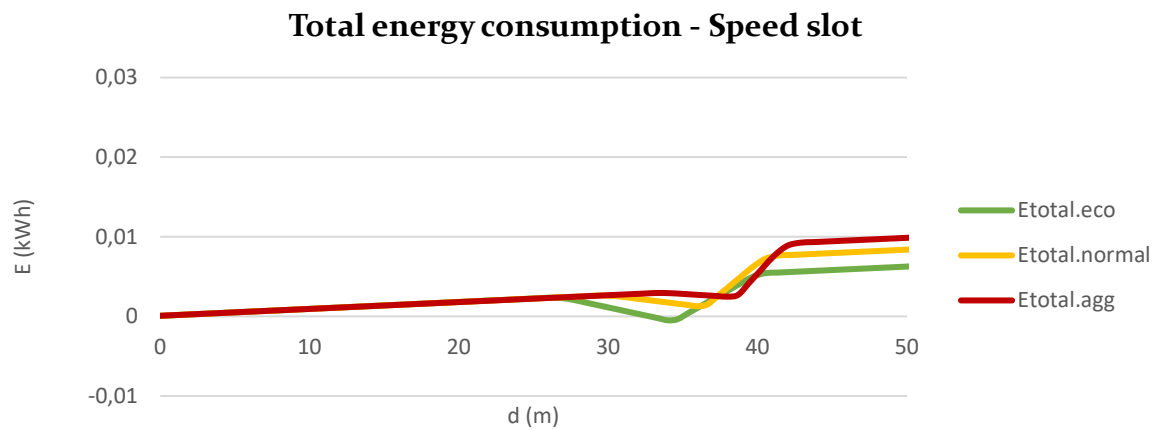


Figure 4.46 Energy consumption at the speed slot

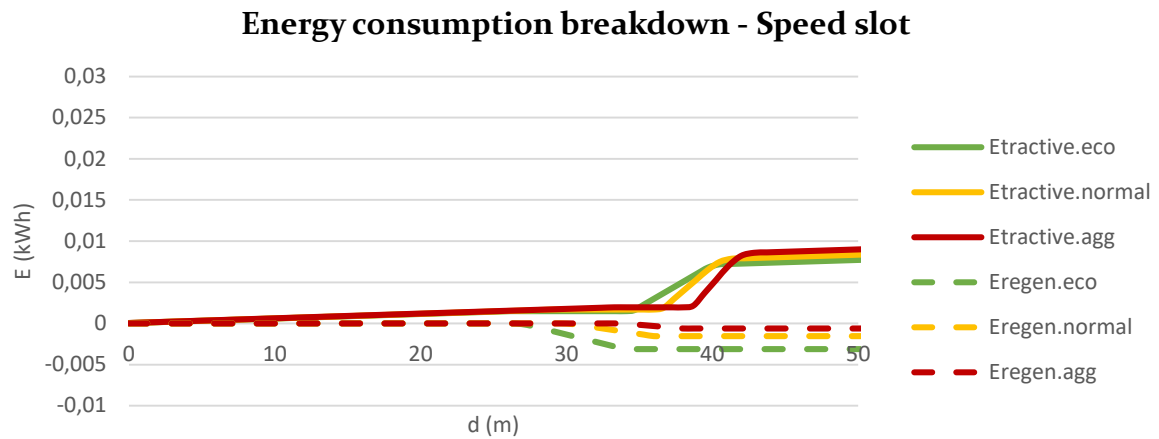


Figure 4.47 Energy consumption breakdown at the speed slot

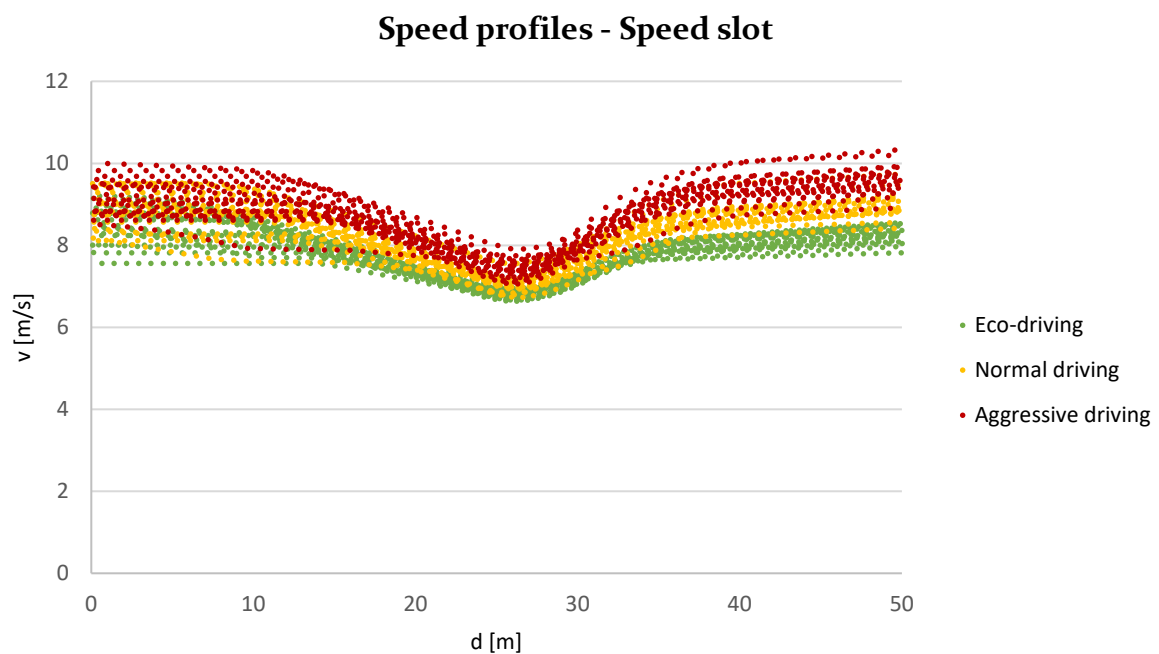


Figure 4.48 Speed profiles at the speed slot

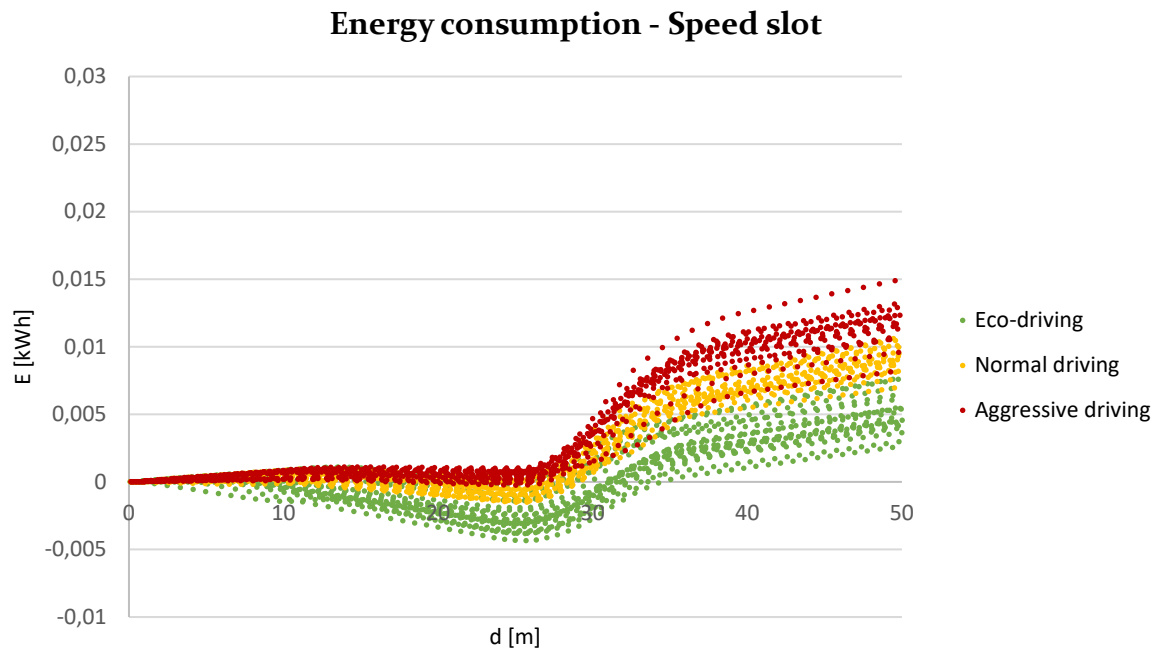


Figure 4.49 Energy consumption at the speed slot

4.3.4.5 Speed cushion

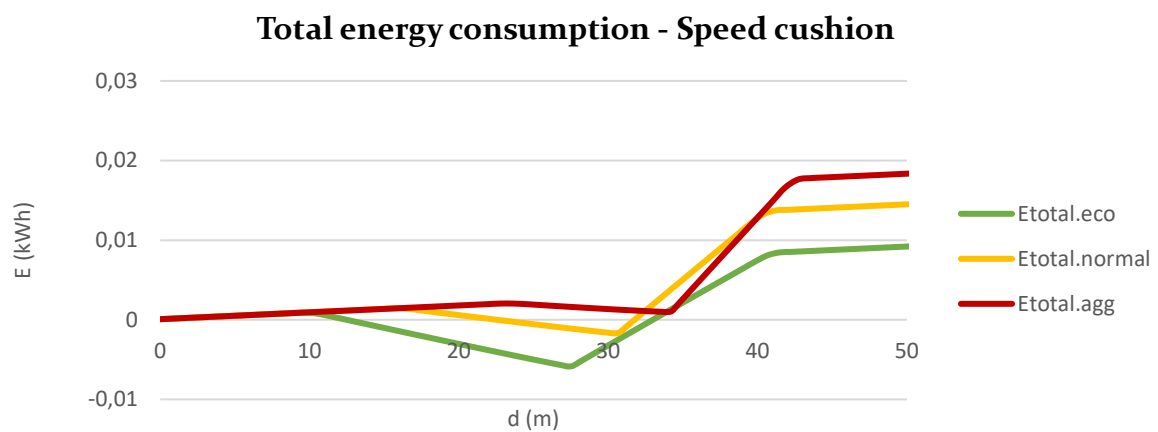


Figure 4.50 Energy consumption at the speed cushion

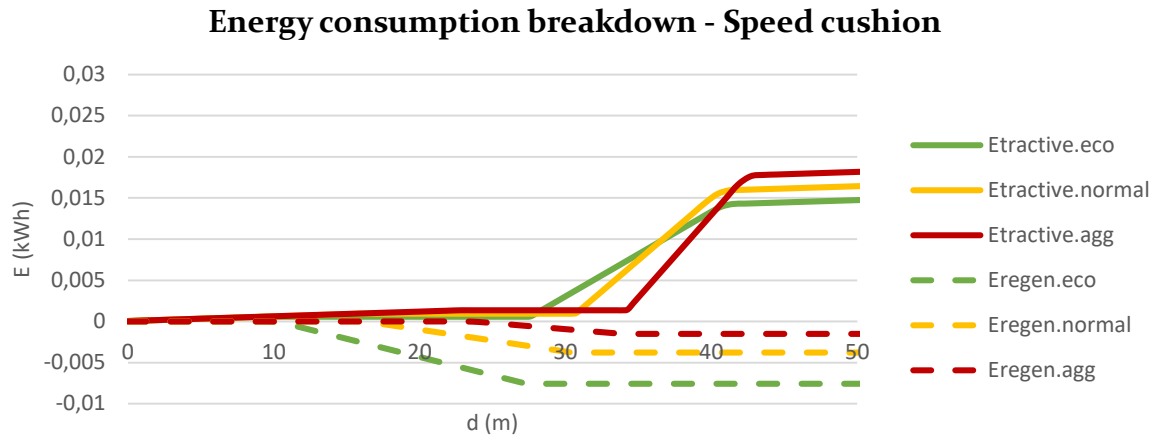


Figure 4.51 Energy consumption breakdown at the speed cushion

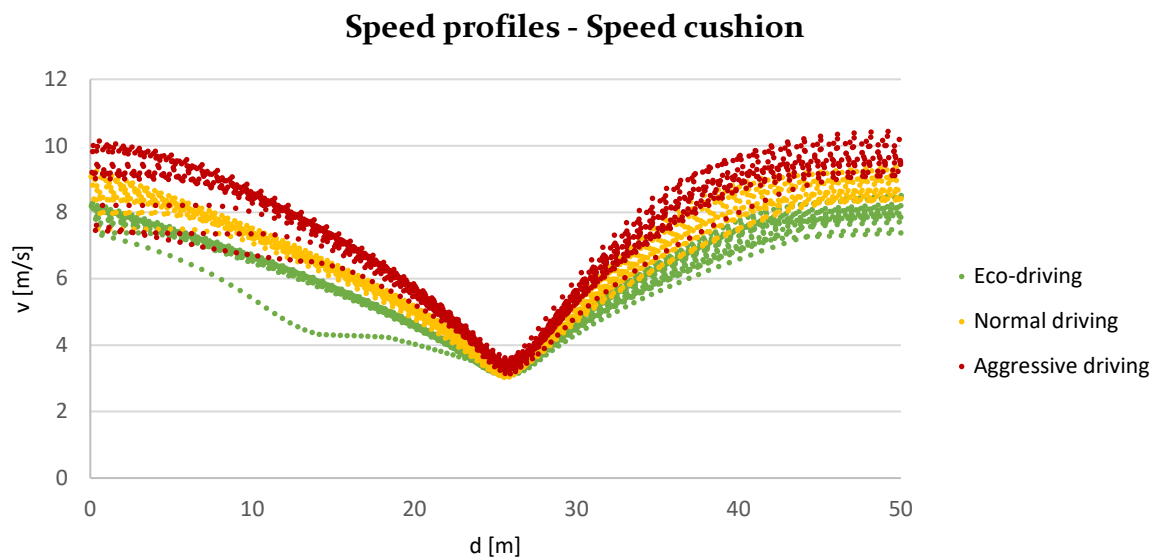


Figure 4.52 Speed profiles at the speed cushion

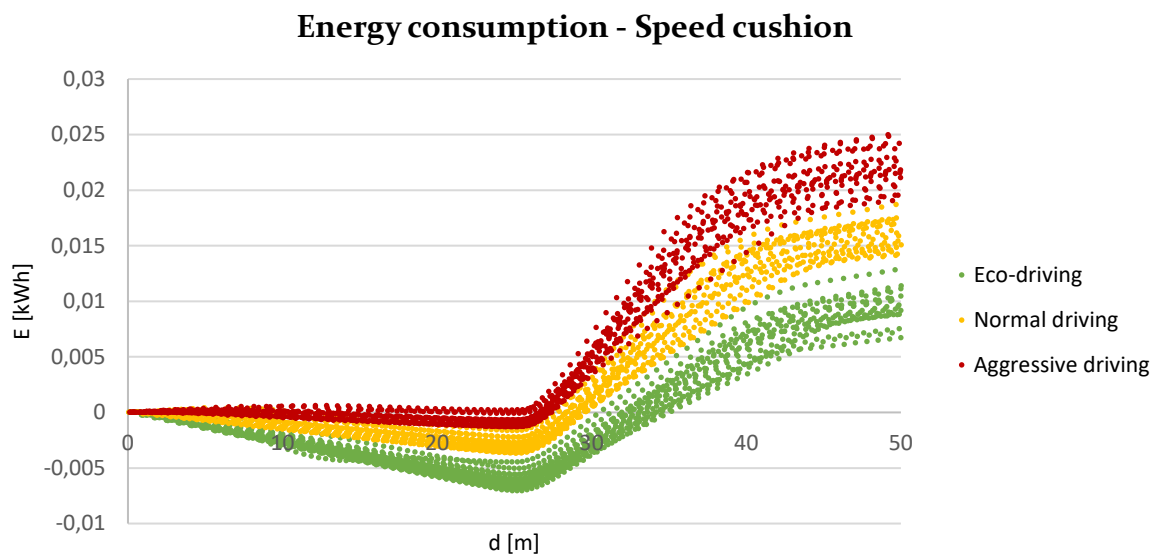


Figure 4.53 Energy consumption at the speed cushion

4.3.4.6 Sequence of speed bumps

In some traffic situations, it might happen that speed bumps follow up on each other very quickly. Apart from measuring the influence of a speed bump, it might also be interesting to measure the influence of a sequence of speed bumps. When the distance between two speed bumps is large enough, theoretically cars will accelerate to the desired speed and start decelerating afterwards for the next speed bump. For these situations, knowing the influence of a single speed bump is sufficient. However, two other situations could occur:

1. The speed bumps are so close to each other that the distance a car needs to accelerate to the desired speed and decelerate afterwards is too short. In this case, the vehicle will accelerate towards the maximum possible speed for this situation.
2. The distance between the speed bumps is far enough to accelerate to the desired speed, but the driver chooses not to for environmental or comfort reasons.

Figure 4.54 shows a schematic representation of the speed profile of these alternative situations. The effect on the energy consumption depends on the distance between the two speed bumps, which is different for different speeds and bump types. Every situation has a different critical point for which the normal situation doesn't apply anymore and alternative situation 1 (Figure 4.54) should be calculated. These distances could be calculated by calculating the distance it requires a vehicle to accelerate to the desired speed and the distance which is required to decelerate again. Differences in driving styles will occur due to their different preferred accelerations and decelerations, while differences for different traffic calming measures occur due to the difference in speed reduction. Table 4.22 shows the distance between two traffic calming measures for which this critical point applies. As could be seen, the minimum distances between two traffic calming measures when driving 30 km/h is so small that in reality the 'alternative situation 1' will not often apply on these roads. Though, as the minimum distance to reach this critical point when driving 50 km/h is way higher, 'alternative situation 1' might occur in these situations.

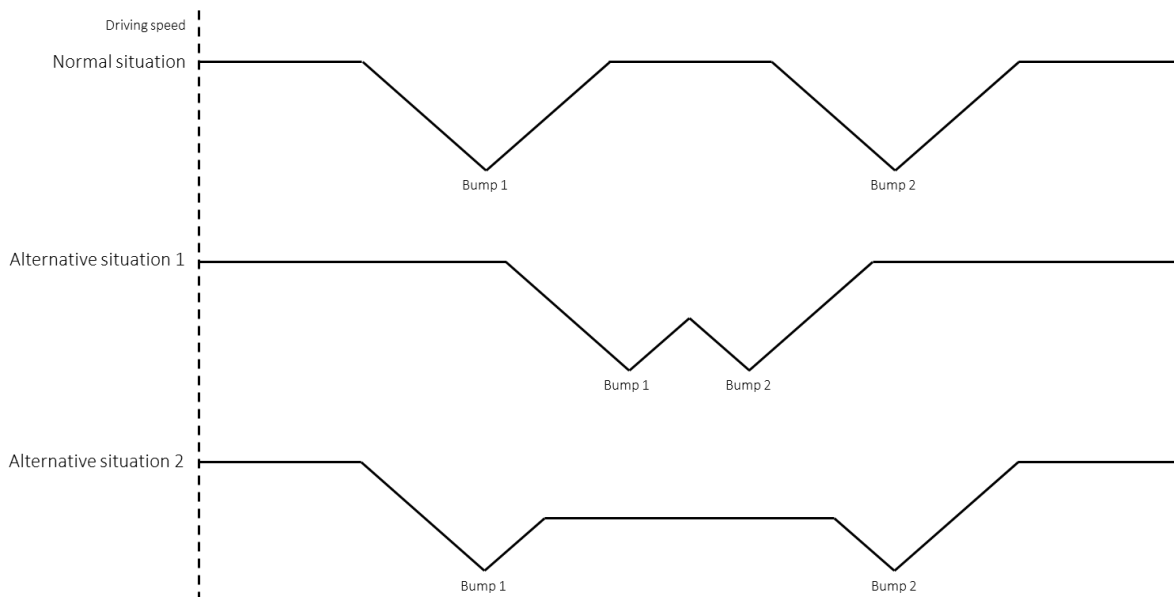


Figure 4.54 Three scenarios for driving at a sequence of traffic calming measures

Table 4.22 Different distances between two traffic calming measures before the critical point

Desired speed	Traffic calming measure	Eco-driving	Normal driving	Aggressive driving
30	Speed bump	35,1 m	27,8 m	21,4 m
30	Watts	27,4 m	21,7 m	16,7 m
30	Seminole	23,4 m	18,5 m	14,3 m
30	Speed slot	13,2 m	10,4 m	8,0 m
30	Speed cushion	30,7 m	24,3 m	18,8 m
50	Speed bump	97,5 m	77,2 m	59,5 m
50	Watts	76,2 m	60,3 m	46,5 m
50	Seminole	65,0 m	51,4 m	39,7 m
50	Speed slot	36,6 m	28,9 m	22,3 m
50	Speed cushion	85,3 m	67,5 m	52,1 m

Table 4.23 Energy consumption for different scenarios of 'alternative scenario 1'

Distance between two speed bumps	Eco-driving	Normal driving	Aggressive driving
Baseline	0,0451 kWh	0,0459 kWh	0,0469 kWh
- v=50km/h	98,3%	100%	102,2%
- d=500m			
- No bumps			
50 m	0,0663 kWh* 144,4%	0,0967 kWh* 210,7%	0,1248 kWh* 271,9%
70 m	0,0690 kWh* 150,3%	0,1042 kWh* 227,0%	0,1339 kWh 291,7%
90 m	0,0717 kWh* 156,2%	0,1078 kWh 234,9%	0,1339 kWh 291,7%
110 m	0,0729 kWh* 158,8%	0,1078 kWh 234,9%	0,1339 kWh 291,7%

* distance is below critical point

The calculated energy consumptions (Table 4.23) could be explained by using the speed profiles of the different driving styles for every situation. Figure 4.55, Figure 4.56 and Figure 4.57 represent the speed profiles of the three driving styles for the four different situations when driving 50 km/h. They show that whether a driver can reach the desired speed in between two speed bumps depends on the acceleration of the driver. Therefore, the aggressive driver can reach his desired speed when the spacing between the bumps is only 70 meters, while the eco-driver needs a larger spacing. As could also be seen in Table 4.23, when the distance between two speed bumps is above the critical point for that situation and driving style, it doesn't influence the vehicle's energy consumption any more.

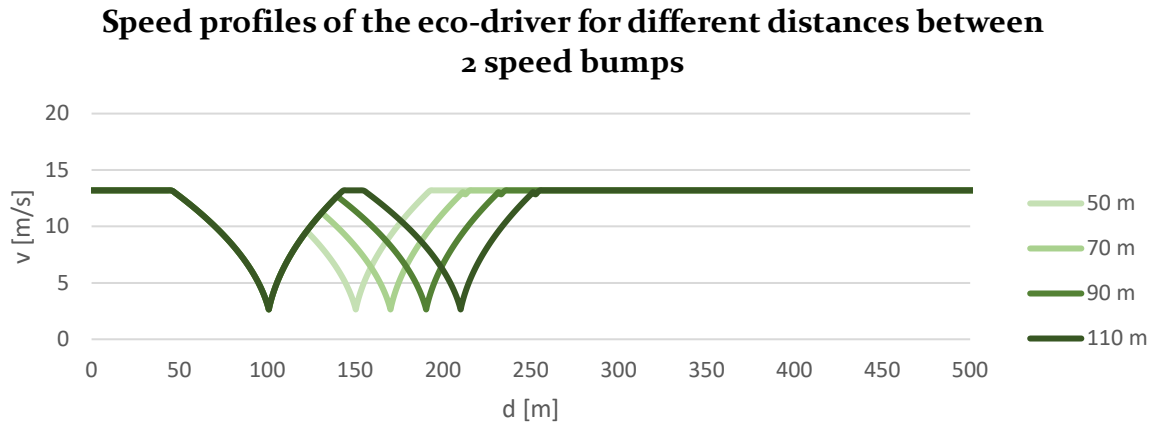


Figure 4.55 Speed profiles of the eco-driver for different distances between two speed bumps

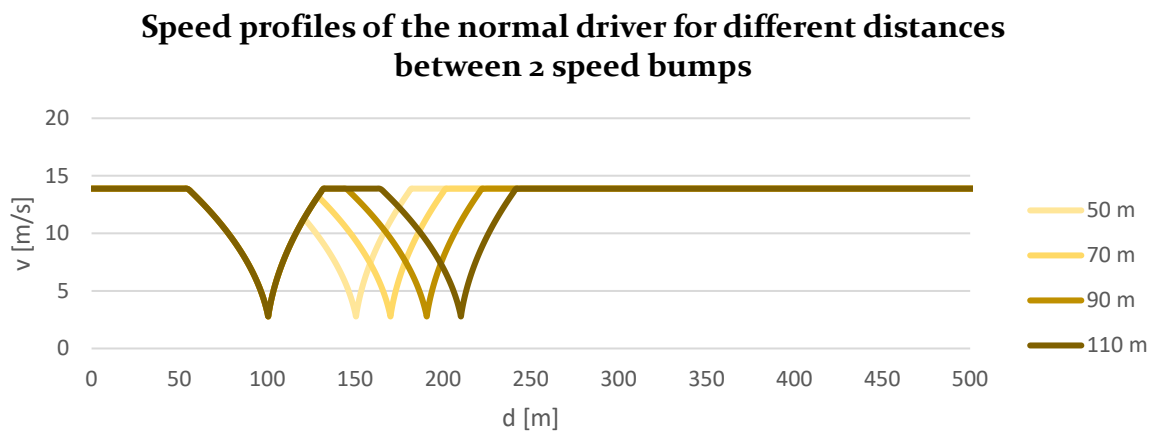


Figure 4.56 Speed profiles of the normal driver for different distances between two speed bumps

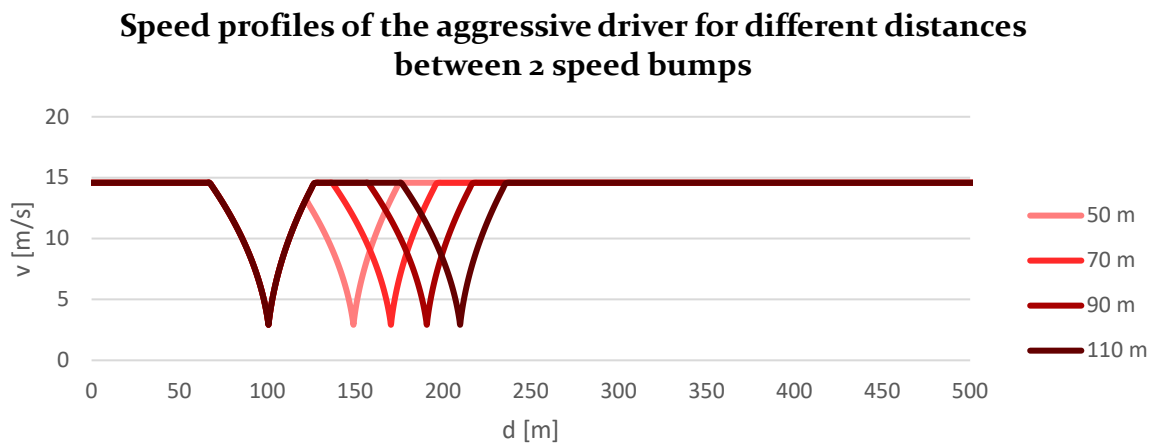


Figure 4.57 Speed profiles of the aggressive driver for different distances between two speed bumps

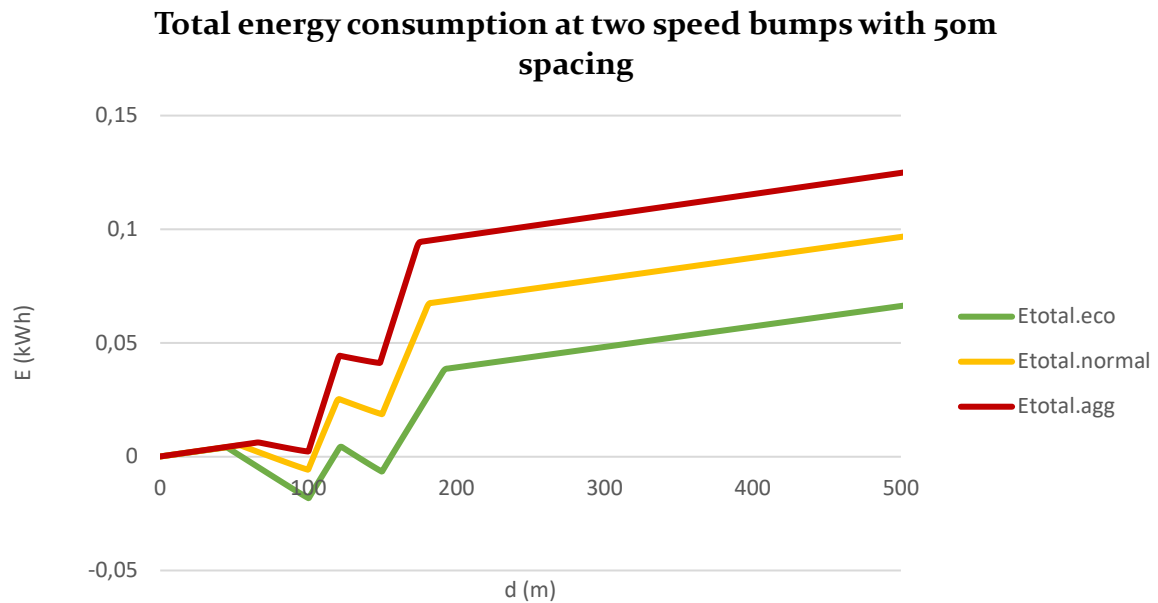


Figure 4.58 Total energy consumption with two speed bumps with 50 m spacing

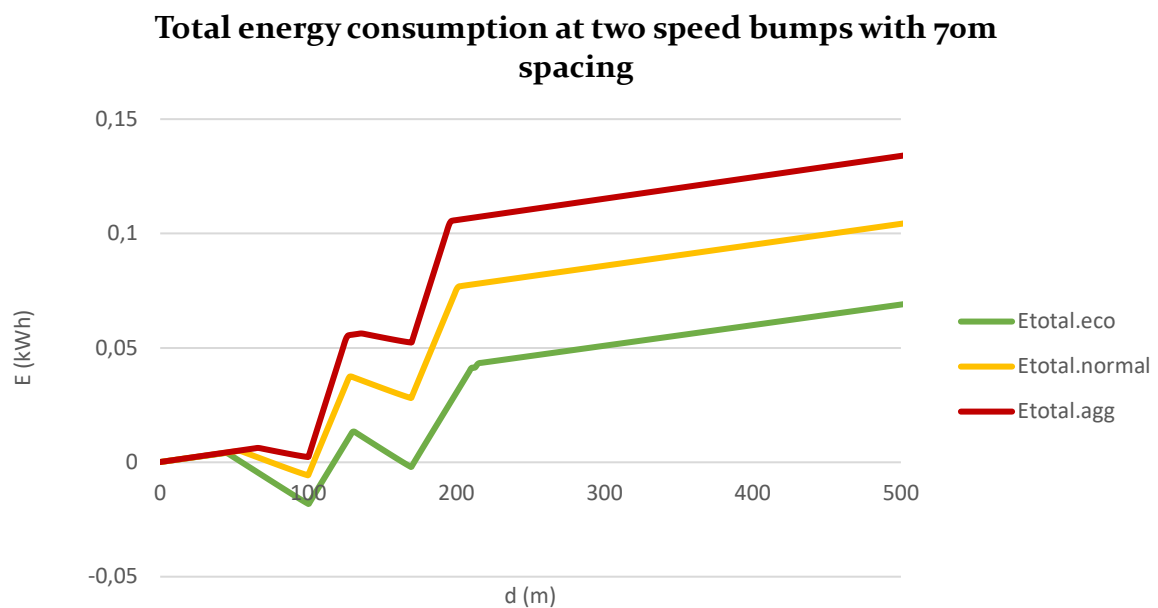


Figure 4.59 Total energy consumption at two speed bumps with 70 m spacing

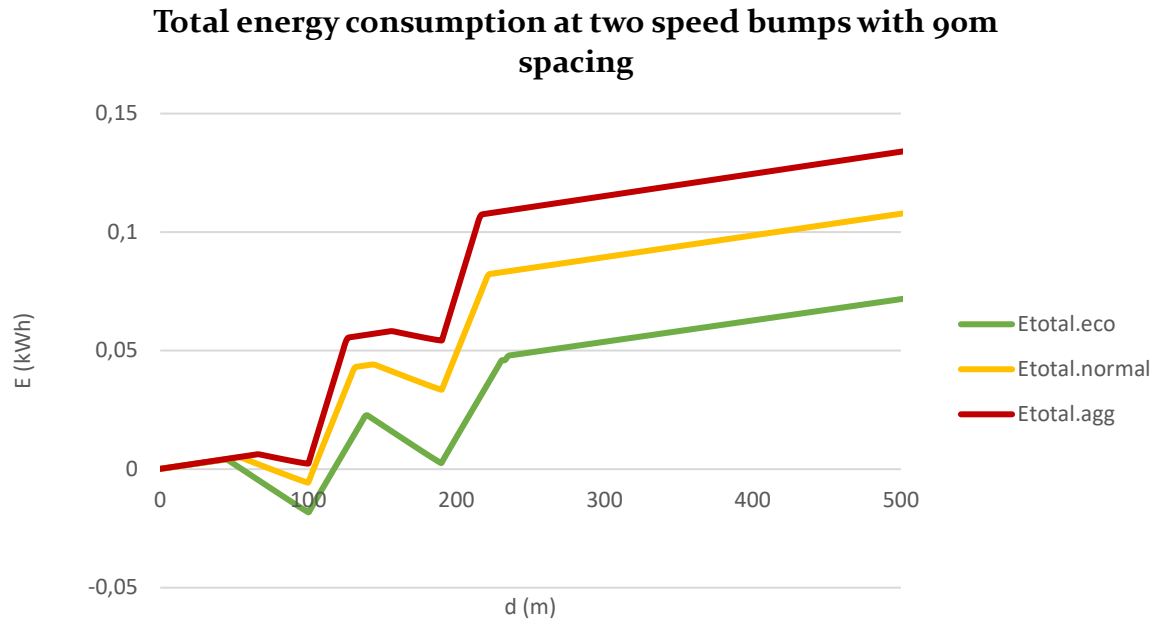


Figure 4.60 Total energy consumption at two speed bumps with 90 m spacing

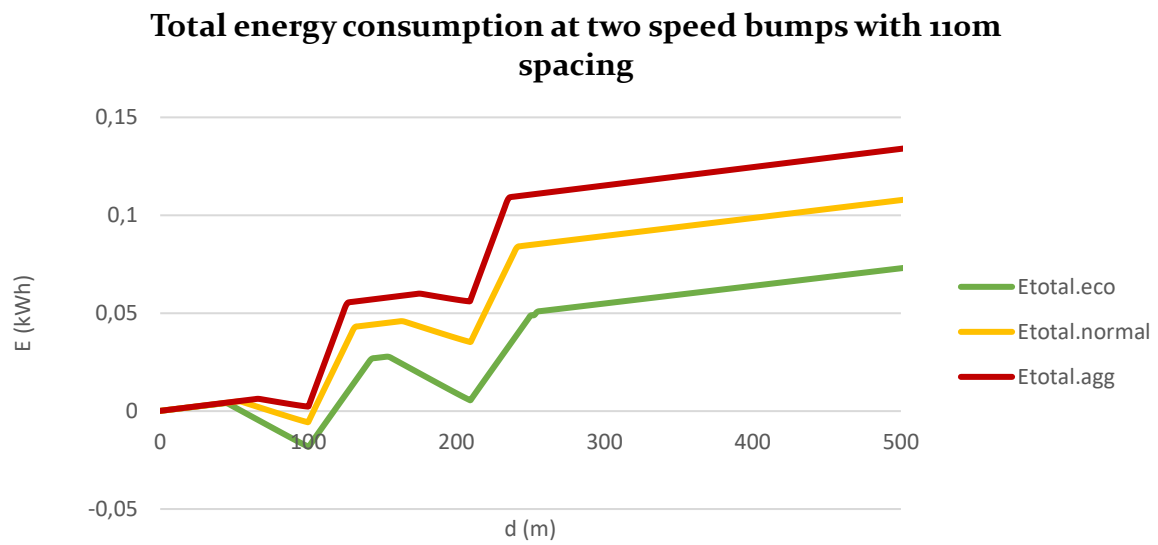


Figure 4.61 Total energy consumption at two speed bumps with 110 m spacing

In order to reduce the energy consumption between two speed bumps, a driver could choose to not fully accelerate to the desired speed in between two bumps. 'Alternative scenario 2' in Figure 4.54 show a schematic representation of this strategy. The amount of energy this strategy saves has been calculated in Table 4.24. As is shows, energy consumption between the two speed bumps reduces significantly when not accelerating to the full desired speed in between the two bumps. When performing this strategy, the travel time would obviously increase. As the table shows, the payoff for eco-driving with higher speeds in between the bumps seems to be better than aggressive driving with low speeds in between the bumps. It could be concluded that the driving style has a higher influence than the speed in between the bumps and that before performing this last strategy, an aggressive or normal driver should first consider changing driving behavior.

Table 4.24 Energy consumption for different scenarios of 'alternative scenario 2'

Distance between two speed bumps	Eco-driving	Normal driving	Aggressive driving
Baseline	0,0729 kWh*	0,1078 kWh	0,1339 kWh
- v=50km/h	67,7%	100%	124,2%
- d=500m			
- two bumps, 110m spacing	$\Delta t = 47,8 \text{ s}$ 110,1%	$\Delta t = 43,4 \text{ s}$ 100%	$\Delta t = 39,7 \text{ s}$ 91,5%
- accelerating to full desired speed			
Accelerating to 75% of speed difference	0,0678 kWh 62,9%	0,0961 kWh 89,1%	0,1173 kWh 108,8%
	$\Delta t = 48,4 \text{ s}$ 111,5%	$\Delta t = 44,3 \text{ s}$ 102,1%	$\Delta t = 40,8$ 94,0%
Accelerating to 50% of speed difference	0,0639 kWh 59,3%	0,0871 kWh 80,8%	0,1045 kWh 96,9%
	$\Delta t = 50,4 \text{ s}$ 116,1%	$\Delta t = 46,6 \text{ s}$ 107,4%	$\Delta t = 43,2 \text{ s}$ 99,5%
Accelerating to 25% of speed difference	0,0619 kWh 57,4%	0,0814 kWh 75,5%	0,0961 kWh 89,1%
	$\Delta t = 56 \text{ s}$ 129,0%	$\Delta t = 52,1 \text{ s}$ 120,0%	$\Delta t = 48,7 \text{ s}$ 112,2%
No acceleration	0,0648 kWh 60,1%	0,0821 kWh 76,2%	0,0951 kWh 88,2%
	$\Delta t = 75,9 \text{ s}$ 174,9%	$\Delta t = 71,3 \text{ s}$ 164,3%	$\Delta t = 67 \text{ s}$ 154,4%

4.3.5 Signalized intersections

Different scenarios have been calculated to cover the influence of signalized intersections on the energy consumption. As mentioned before, the scenarios consider a vehicle to decelerate to 0 km/h at a traffic light. As it's interesting to quantify the different effects of traffic lights for different driving speeds, scenarios for a vehicle driving 30 km/h (Table 4.25) and one driving 80 km/h (Table 4.26) have been calculated. For both cases, a traffic light with 30s waiting time and one without waiting time are compared to a baseline scenario. Since the influence of waiting time for different weather scenarios is also relevant, these scenarios are covered in Table 4.27 and Table 4.28. The difference between an ambient temperature of 12 °C and 0 °C has been quantified per second waiting time.

Table 4.25, Table 4.26 and Figure 4.62 show the energy consumption at one traffic light for speeds of 30 and 80 km/h. One could observe that the influence of a traffic light on the energy consumption becomes bigger when driving at higher speeds, both relatively as well as in absolute numbers. This could be explained by the longer period of acceleration, which consumes a lot of energy. Next to this fact, the results also show an increasing influence of the driving style on the energy consumption for driving at higher speeds. This could be explained both by the more aggressive acceleration of the aggressive driver (which consumes more energy) as well as by the higher efficiency of the regenerative braking for the eco-driver.

Table 4.25 Influence of a traffic light when driving 30 km/h

Scenario	Eco-driving	Normal driving	Aggressive driving
Baseline	0,0437 kWh	0,0433 kWh	0,0431 kWh
- V = 30 km/h	100,9%	100%	99,5%
- D = 500 m			
- T = 12 °C			
1 traffic light	0,0502 kWh	0,0562 kWh	0,0607 kWh
- 200m	115,9%	129,8%	140,2%
- No waiting time			
1 traffic light	0,0578 kWh	0,0638 kWh	0,0683 kWh
- 200m	133,5%	147,3%	157,7%
- Waiting time at traffic light = 30s			

Table 4.26 Influence of a traffic light when driving 80 km/h

Scenario	Eco-driving	Normal driving	Aggressive driving
Baseline	0,0605 kWh	0,0636 kWh	0,0668 kWh
- V = 80 km/h	95,1%	100%	105,0%
- D = 500 m			
- T = 12 °C			
1 traffic light	0,0911 kWh	0,1393 kWh	0,1770 kWh
- 200m	143,2%	219,0%	278,3%
- No waiting time			
1 traffic light	0,0987 kWh	0,1469 kWh	0,1846 kWh
- 200m	155,2%	231,0%	290,3%
- Waiting time at traffic light = 30s			

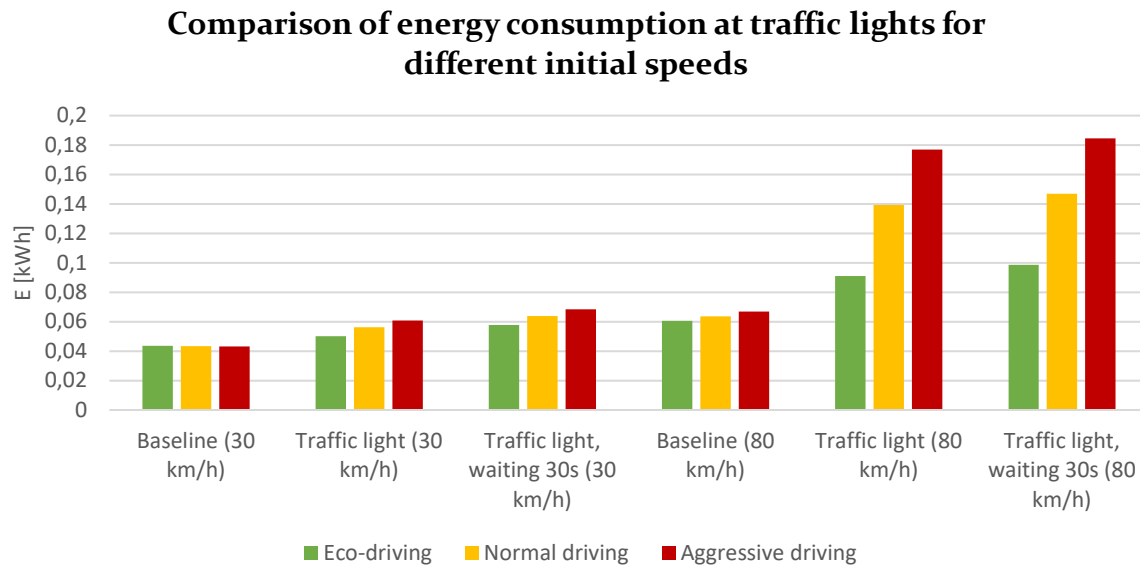


Figure 4.62 Comparison of energy consumption at traffic lights for different initial speeds

Table 4.27, Table 4.28 and Figure 4.63 show the influence of waiting time for different weather scenarios. Figure 4.64 shows a typical speed profile for two stops at traffic lights. The energy consumption during the standstill period at a traffic light has a significant effect on the total energy consumption and is the same for all vehicles (Figure 4.65 and Figure 4.66). In normal situations (when the outdoor temperature is 12 degrees Celsius), each car consumes 0,252 Wh for every second it's waiting for a traffic light to turn green. For longer periods of waiting, this could reduce the range significantly. This result directly couples the traffic flow and average waiting time of a traffic light to the energy consumption.

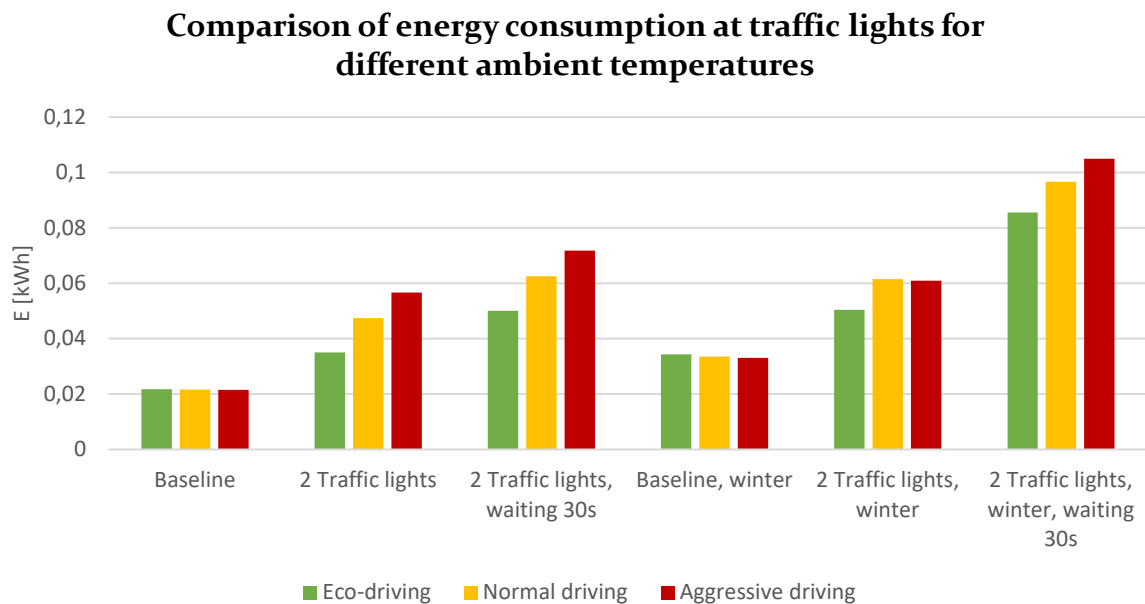
Figure 4.67 and Figure 4.68 show how the total energy consumption at the traffic lights increases during more extreme weather conditions. When calculating the same situation, but with an ambient temperature of 0 degrees Celsius, a significant rise could be seen in the energy consumption during the waiting period. About 0,585 Wh is used by an idling car every second during these circumstances.

Table 4.27 Influence of traffic lights on the energy consumption

Scenario	Eco-driving	Normal driving	Aggressive driving
Baseline	0,0218 kWh	0,0216 kWh	0,0215 kWh
- V = 30 km/h	100,9%	100%	99,5%
- D = 250 m			
- T = 12 °C			
2 traffic lights	0,0350 kWh	0,0474 kWh	0,0567 kWh
- 100 m	162,0%	219,4%	262,5%
- 200 m			
- No waiting time			
2 traffic lights	0,0501 kWh	0,0625 kWh	0,0718 kWh
- 100 m	231,9%	289,4%	332,4%
- 200 m			
- Waiting time per traffic light = 30s			

Table 4.28 Influence of traffic lights on the energy consumption during winter

Scenario	Eco-driving	Normal driving	Aggressive driving
Winter baseline	0,0343 kWh	0,0336 kWh	0,0331 kWh
- V = 30 km/h	102,3%	100%	98,5%
- D = 250 m			
- T = 0 °C			
2 traffic lights	0,0504 kWh	0,0615 kWh	0,0699 kWh
- 100 m	150,0%	183,0%	208,0%
- 200 m			
- No waiting time			
2 traffic lights	0,0855 kWh	0,0966 kWh	0,1050 kWh
- 100 m	254,5%	287,5%	312,5%
- 200 m			
- Waiting time per traffic light = 30s			

**Figure 4.63** Comparison of energy consumption at traffic lights for different ambient temperatures

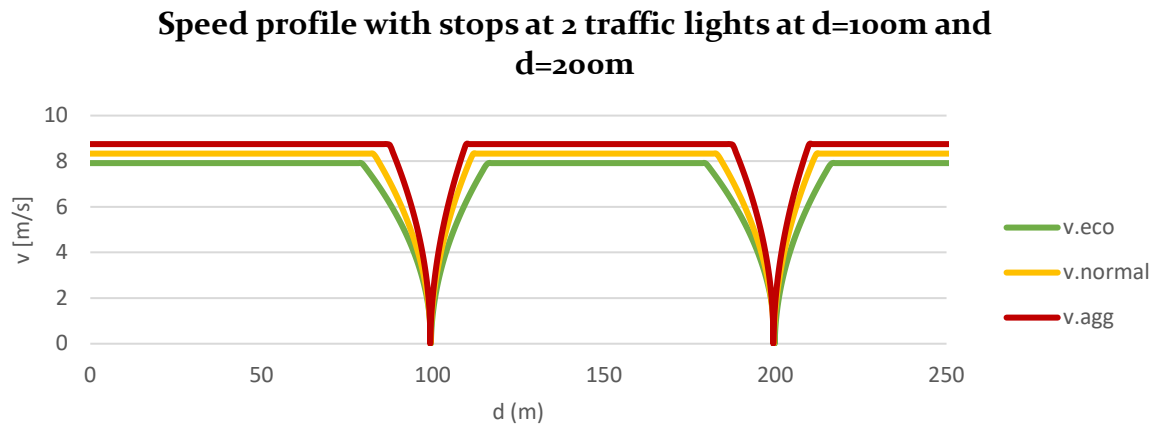


Figure 4.64 Speed profile with stops at two traffic lights at $d=100\text{m}$ and $d=200\text{m}$

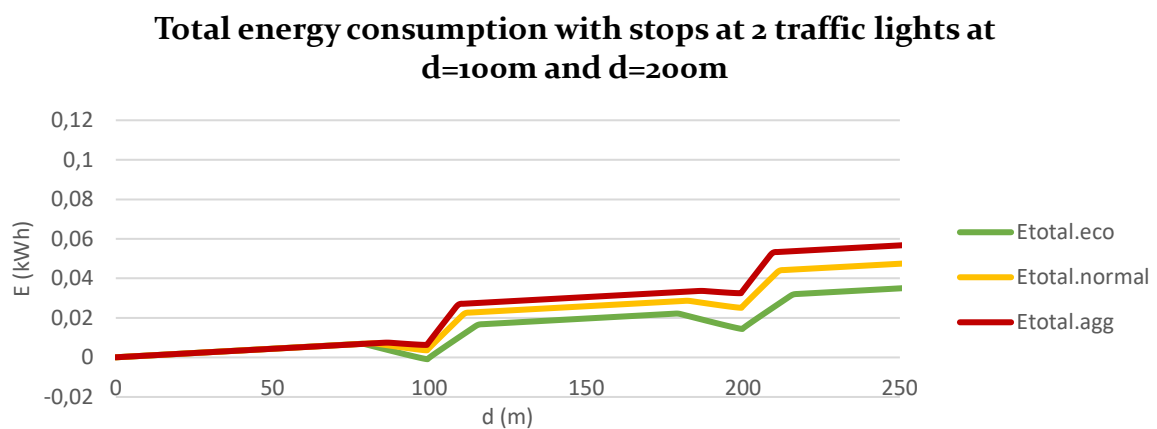


Figure 4.65 Total energy consumption with stops at two traffic lights at $d=100\text{m}$ and $d=200\text{m}$

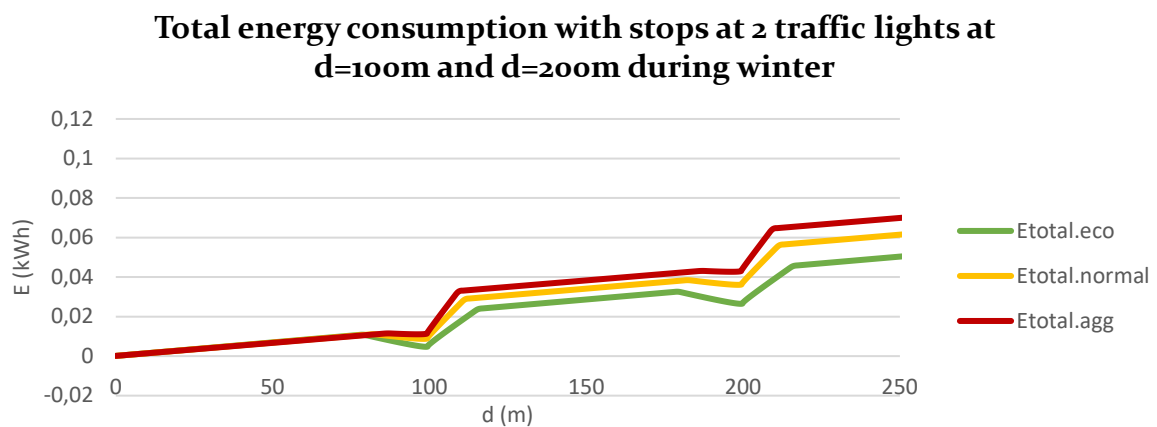


Figure 4.66 Total energy consumption with stops at two traffic lights at $d=100\text{m}$ and $d=200\text{m}$ during winter

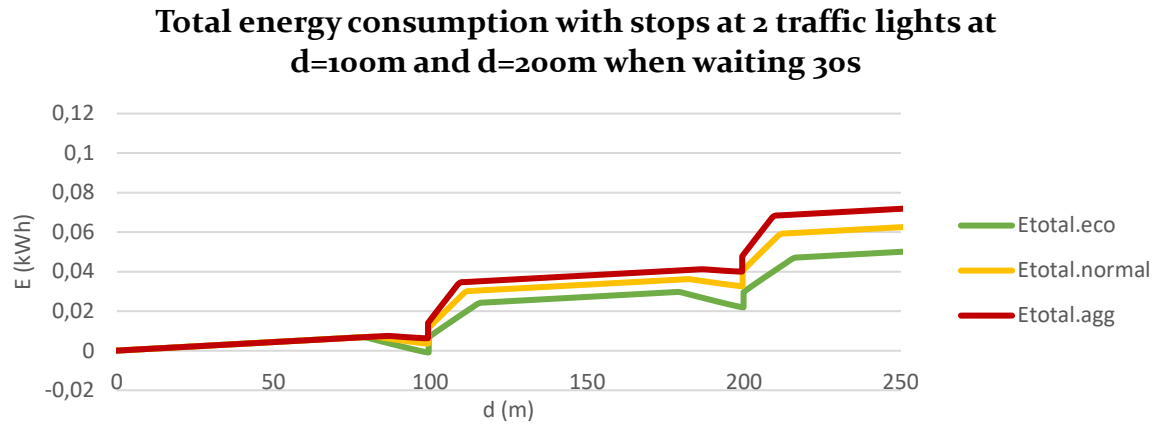


Figure 4.67 Total energy consumption with stops at two traffic lights at $d=100\text{m}$ and $d=200\text{m}$ when waiting 30s

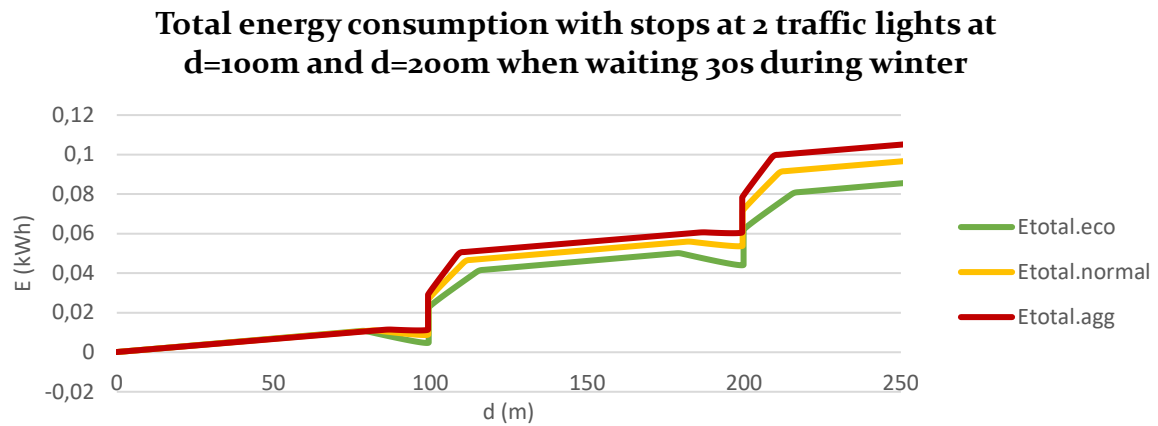


Figure 4.68 Total energy consumption with stops at two traffic lights at $d=100\text{m}$ and $d=200\text{m}$ when waiting 30s during winter



Chapter 5

Nieuwegein case study

Chapter 5. Nieuwegein case study

After quantifying the influences of individual elements on the energy consumption, it's valuable to qualitatively and quantitatively describe the interconnection of these individual elements. This interconnection has been found by predicting the energy consumption for different routes and scenarios in the city of Nieuwegein. This chapter describes the VISSIM model and its configurations, the different scenarios tested and their results. Afterwards, a route optimization model has been used to find the best route for different scenarios, based on travel time, cost and CO₂-emissions. Will the optimal route be the shortest route or the fastest route? And will the optimal route change for different scenarios and personal preferences? Finally, a validation study has been performed to validate the results.

5.1 Model and methodology

In order to test the effect of different variables on the energy consumption of EVs in real scenarios, a microscopic traffic model has been made of the southern part of Nieuwegein. A section with three competitive routes has been chosen. Table 5.1 shows the comparison of travel distance and travel times at different moments of the day. Apart from their competitive nature, the three routes have been chosen because they contain numerous infrastructural elements, amongst others different traffic calming measures, traffic lights, several bus and tram lines, slopes, different design speeds and different levels of urbanization. First, the routes will be discussed, after which the different scenarios which have been predicted will be elaborated.

5.1.1 Routes

The residential route leads drivers through the middle of the area. It contains both 30- and 50-km/h roads and crosses two residential areas and a park. Due to the proximity of multiple sport associations and schools, the street houses many speed bumps. The entire route consists of one-lane streets, making it almost impossible to overtake other vehicles. As could be seen in Table 5.1, the route is the shortest one in distance, and its travel time fluctuates the least.

The second route could be typified by its complex signalized intersections. The route, which leads vehicles to Nieuwegein's largest shopping mall, contains 50-roads with multiple lanes. Furthermore, the route contains separate bus-lanes and is crossed by four tram-lanes. The route also serves as a connection between a residential area and different larger roads, resulting in many commuters during peak hours. Travel times on this route fluctuate more during peak hours, due to the uncertainty of the traffic lights.

The last route, which is the route with the longest travel distance, leads drivers around the area via the A2, a large national motorway connecting Amsterdam and Maastricht. Although it is the longest route, the travel times are likely to be comparable to the other two routes, since higher driving speeds are possible on this route. About two-third of the route contains motorway driving, while the first part of the route serves as a thoroughfare between two residential neighborhoods.

Table 5.1 Comparison of routes based on Google Maps data

Route	Distance [km]	Travel time [min] Tuesday, 03:00	Travel time [min] Tuesday, 08:00	Travel time [min] Tuesday, 17:00
Residential	3,1	6	5-8	5-7
City center	3,7	6	5-12	6-12
Motorway	4,5	5	5-9	5-9

5.1.2 Scenarios

To create the most realistic results, four scenarios have been tested (Table 5.2). They differ in time of the day, the mix of driving styles and the outdoor temperature. The other traffic is modeled with a dynamic assignment based on morning or evening hour OD-matrices, while the measured traffic drives a static route. The first scenario is tested to measure the energy consumption without any other traffic on the road. It is used as a baseline scenario, while simultaneously showing the effect of a sequence of different individual infrastructural elements. The second scenario is used to measure the influence of peak hour traffic on the energy consumption and travel time. Barth and Boriboonsomsin (2009) found that for high traffic intensities, the overall energy consumption would drop with a higher share of eco-drivers. The third scenario is therefore used to see what will happen if all cars – even the non-measured ones – would switch to an eco-driving strategy. Finally, the last scenario measures the influence of a low outdoor temperature on the total energy consumption in a real-life scenario. To reduce the influence of randomness, 180 measurements have been done for each scenario, consisting of 20 measurements per driving style per route. Since for the third scenario, the influence of the moment entering the network was very large, more simulations have been performed. A full analysis of the influence of eco-driving on the travel times and energy consumption has been made by performing 450 simulations with different entering times; 50 of each driving style for every route.

Table 5.2 Tested scenarios in Nieuwegein

Scenario	Time of the day	Other traffic	Outdoor temperature [°C]
1	-	None	12
2	07:00-09:00	Mix	12
3	07:00-09:00	All eco-driving	12
4	07:00-09:00	Mix	0

5.1.3 Traffic intensity

The traffic intensity is being modeled by using OD-matrices. Real traffic counts have been performed at the N210, the motorway through the modeled area. By using OmniTRANS, these traffic counts have been exported to OD-matrices. A limitation of this method is that the OD-matrix will never be exactly the same as the traffic counts, however, a reasonable estimation will be the outcome. Since for this research, the traffic intensity will mainly be used to create slower traffic and more interactions between vehicles, this estimation is assumed to be sufficient. OmniTrans has been used to predict the traffic volumes for the N210 and the roads next to it (Figure 5.1). Some intersections of the city center route had to be calculated manually. The incoming and outgoing traffic volumes of each road has been estimated based on the predicted traffic volumes of the left part of the model, some older traffic counts on the north side of the model and the sociodemographic data of this neighborhood, named Fokkesteeg (AlleCijfers.nl, 2019). The working population is about 4000, of which half of the population is expected to drive through the modeled network during morning and evening peak hours, which is divided

over the Graaf Florisweg, the Muiderschans, the Zwolsveste and the Henri Dunantlaan. The other traffic is expected to leave the area via the eastern part of the neighborhood or via the route alongside the water, directly connected to a major road. Some people will use other means to go to their work, such as public transport or their bicycles) and others won't leave the area at all (as they are working for one of the 285 companies in the neighborhood) or outside the peak hours.

The distribution of the traffic inside the city center area is done based on the outgoing traffic of each street. If street x has a lot of outgoing traffic compared to the other streets, more cars from street y are expected to leave at street x . The exact amounts are calculated as follows:

$$Traffic_{from\ x\ to\ y} = Traffic_{from\ x} * \frac{Traffic_{to\ y}}{Traffic_{total\ in\ network}} \quad [33]$$

The traffic from the city center going to the left part of the network is distributed with the same relative distribution as the distribution from OmniTRANS.

The traffic volumes from four VISSIM simulations have been measured at five measurement locations for the full morning peak and compared to the VRU2015 measurements. The measurements at the motorway gave realistic results. The number of vehicles leaving the residential area has been overestimated. Although the accuracy at some individual points is low, in absolute numbers the traffic is relatively representative compared to the VRU2015 in the total network. In absolute terms, the total of all measurements shows an accuracy of 95%. Individually, the measurement locations show a relative accuracy of 80% compared to the individual VRU2015 measurements. As the OD-matrix' major function is to add a representation of the traffic in the total network, the volumes are representative enough for this research. The traffic volumes are also being compared with the typical traffic at Tuesday morning during peak hours by using Google Maps. These volumes also show similar results to the VISSIM measurements.

The measured vehicles are modeled by using a static route. They are being distributed by using a Poisson distribution which determines the time gap between two successive vehicle departures (Fellendorf & Vortisch, 2010). After selecting the total amount of vehicles λ , the Poisson distribution creates a distribution with a mean of λt while the time gaps are calculated with an exponential distribution with a mean of $1/\lambda$. The probability of the time gap is calculated by using the following equation:

$$p(x, \lambda) = \lambda e^{-\lambda x} \quad [34]$$

With p being the probability, x being the time gap and λ being the total amount of vehicles.

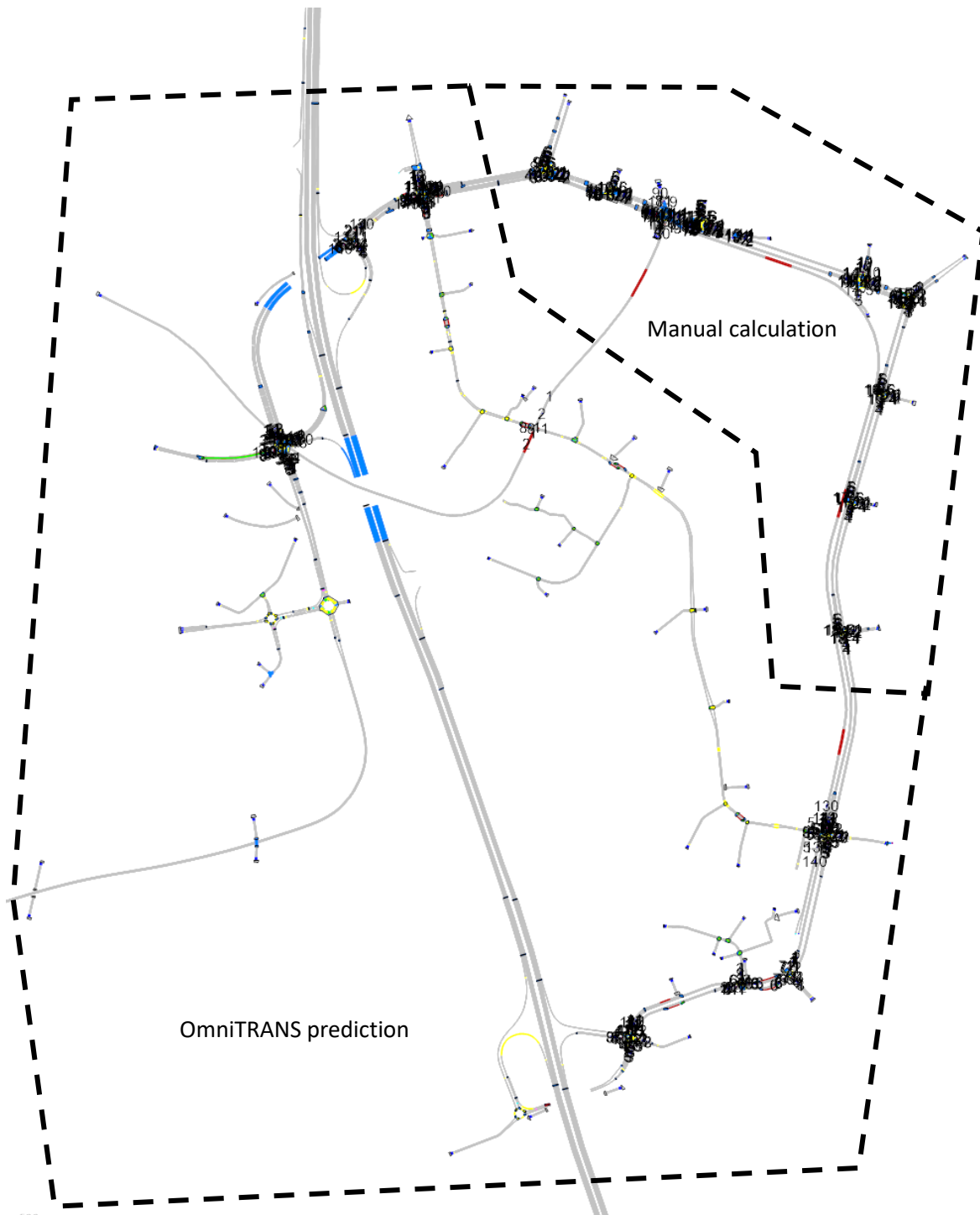


Figure 5.1 Schematic representation of zones calculated manually and by using OmniTRANS

5.1.4 Slope

As the area of Nieuwegein is relatively flat, only eight significant slopes have been identified. The first two are up- and downhill near the entrance of the A2 at the height of the Zandveldseweg, the third and fourth slope are the up- and downhill slopes when the A2 crosses the Hollandsche IJssel, the fifth and sixth could be found at the exit of the A2 at the height of Weg naar de Poort, while finally the last two slopes could be found at the point where the Zuidstedeweg crosses the Doorslag. Table 5.3 and Figure 5.2 show an overview of the slopes.

Table 5.3 Slopes in the Nieuwegein model

Number	Location	Length [m]	Δ Height [m]	Slope [°]
1	Entrance A2	600	3,5	0,29
2	Entrance A2	600	-3,5	-0,29
3	A2-Hollandsche IJssel	400	4,5	0,64
4	A2-Hollandsche IJssel	400	-4,5	-0,64
5	Exit A2	400	4,5	0,64
6	Exit A2	400	-4,5	-0,64
7	Zuidstedeweg-Doorslag	250	5,5	1,26
8	Zuidstedeweg-Doorslag	250	-5,5	-1,26

**Figure 5.2** Locations of the slopes in the Nieuwegein model

5.2 Results

The results of the Nieuwegein case study are presented following the same order as the scenarios. First, the simulations in the empty network are analyzed, after which morning peak simulations are being discussed. The third scenario presented analyzes what would happen with the energy consumption and travel times if everybody would choose for the eco-driving style. Finally, the fourth scenario emphasized the influence of cold weather on the energy consumption.

5.2.1 Scenario 1: Driving on an empty network

In the first scenario, vehicles have been simulated individually while no other vehicle was present at the network. This scenario shows the effect on the energy consumption when combining multiple individual elements into a network. It shows how three typical different streets compare in terms of energy efficiency and travel time. As expected, the eco-driving outperforms the normal and aggressive driving styles in energy efficiency on all routes. On

average, the eco driver uses about 25% less energy than the normal driver and 35% less than the aggressive driver. The consequence is an increase in travel time of 6% compared to the normal driver and 11% compared to aggressive drivers.

Calculations also show a huge difference between the different routes (Figure 5.3). Drivers on the residential route use about 25% less energy than drivers on the city center route, while using about 50% less energy than motorway drivers. However, this does come with a significant increase in travel time. The residential route is 10-15% slower than the city center route and 25-30% slower than the motorway route. When combining the different routes and driving styles, the most ecological route only uses 35% of the energy the worst ecological route uses, while increasing the travel time with 42%. With these energy savings on a route of 3 km, one could charge an iPhone for almost a year (Helman, 2013).

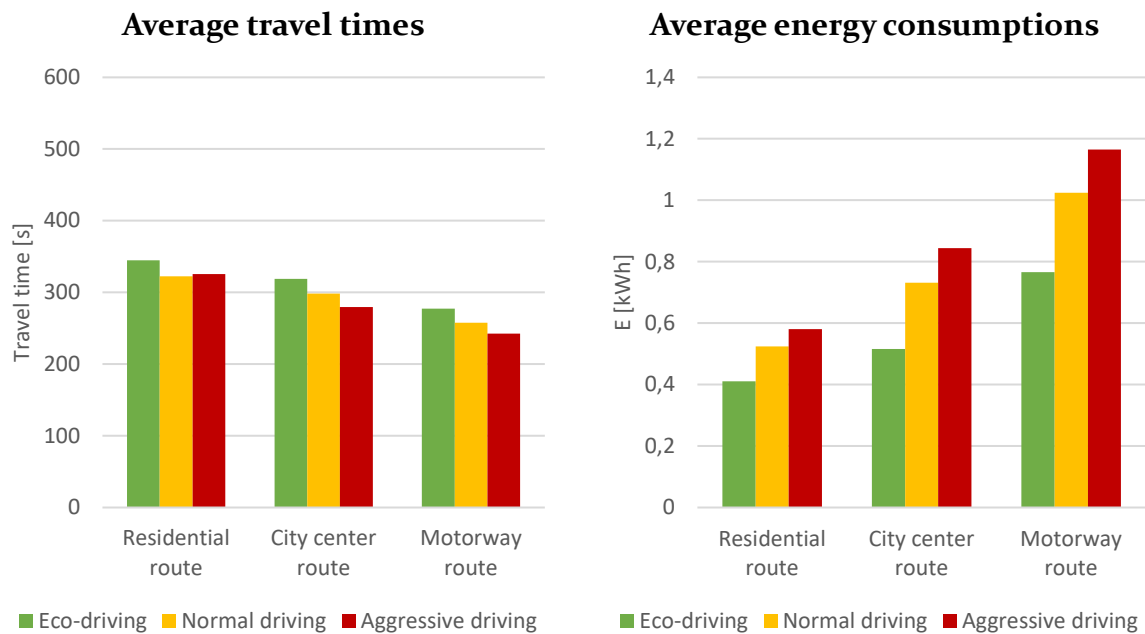


Figure 5.3 Average travel times and energy consumptions for scenario 1

An analysis in the graphical representations clearly shows the repetition of individual infrastructural elements. The residential route in example, shows gains in the energy consumption every time a speed bump occurs, while these increases also occur at every traffic light at the city center route. The energy profiles at these specific elements in the case study are similar to the individual energy profiles calculated in chapter 4. They also show the influence of the driving speed through the steepness of the curve as well as the high efficiency of regenerative braking of the eco-driver compared to the other driving styles.

5.2.2 Scenario 2: Driving during the morning peak hour

The second scenario measures the influence of traffic intensity. By adding a realistic amount of morning peak hour traffic to the simulation, the influence of this traffic on the energy consumption could be measured by comparing the results with the first scenario. A significant increase in travel times has been measured for all driving styles on all routes. While in relative terms the difference between the gain in travel times for the different driving styles is very small, the difference between the routes is very big. The travel times on the residential route increased with approximately 20% and the travel times on the motorway increased with about 35%. However, the travel times on the city center route increased with a stunning 55%, making the

route the worst in travel time. The gain in travel times has a leveling effect, decreasing the relative difference between the routes and the driving styles.

The energy profiles show interesting results (Figure 5.4). A first observation is that the effect of the traffic intensity on the energy consumption is way smaller than the influence on the travel times. The energy consumptions on the residential route and city center route increase with about 5%. However, the energy consumption on the motorway slightly decreases. The slower driving speeds due to the large amount of traffic largely decrease the aerodynamic drag, resulting in a lower energy consumption.

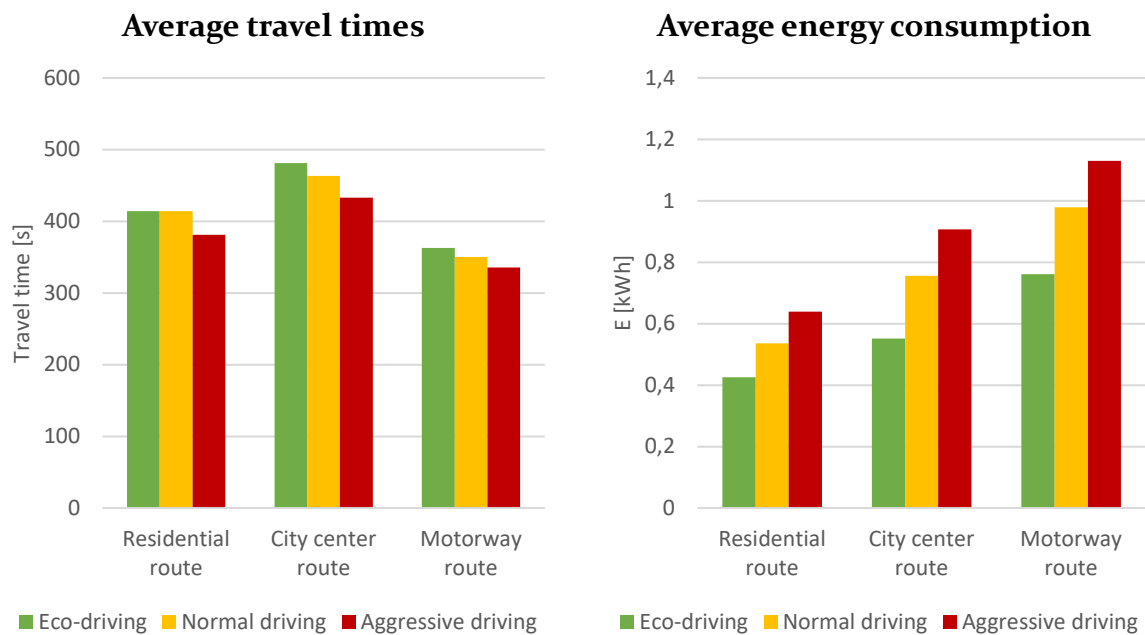


Figure 5.4 Average travel times and energy consumptions for scenario 2

When analyzing the energy consumption profiles, the most interesting results occur in the city center route. As this route contains a lot of signalized junctions, the increase in traffic directly influences the traffic flow through these traffic lights. These traffic lights have a divergent effect on the energy profiles, resulting in a bigger spread of energy consumptions. The higher amount of traffic mainly increased the randomness on this road, as some cars are 'lucky' and are not affected by the traffic lights, while some vehicles have to wait longer and thus consume more energy. One could conclude that the higher the amount of traffic, the higher the randomness in energy consumption, and therefore the harder it is to predict the energy profile. Interesting is that the divergent effect is weaker for eco-drivers since they are less affected by the stop-and-go situations.

5.2.3 Scenario 3: Driving in an all-eco scenario

The first two scenarios clearly showed that eco-driving is more energy efficient in all scenarios. Though, the travel times of the eco-driver are longer, their acceleration and deceleration take longer, and thus eco-drivers are more likely to cause delays in the network. What would happen if all cars switch to an eco-driving style? This has been researched in scenario 3.

As could be seen in Figure 5.5, there is an incredible gain in travel times at the motorway route (18%), causing traffic on this route to drive almost with the same speed as traffic on the residential route. This makes the residential route favorable for all driving styles, which could lead to undesirable effects such as noise disturbance, safety concerns and a higher local emission of fine particles.

The energy consumption doesn't seem to be affected by this scenario compared to scenario 2. Therefore, it could be concluded that in terms of energy consumption, it would be favorable to have an all-eco scenario, however, the traffic flow on certain roads should be closely monitored as huge delays could occur. Some roads would possibly need an increase in capacity to prevent shortage traffic.

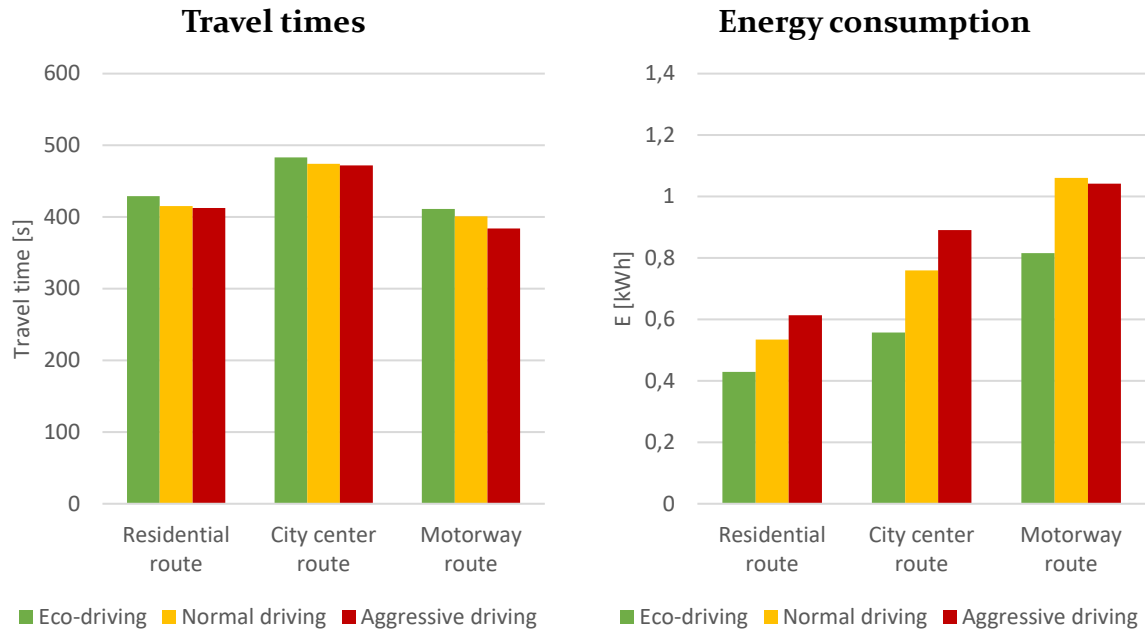


Figure 5.5 Average travel times and energy consumptions for scenario 3

5.2.3.1 Influence of the morning peak on travel times in an all-eco scenario

The all-eco scenario influences the traffic flow so badly that congestions occur. This subchapter dives into the influence of applying an all-eco strategy to the travel times and energy consumption. It tries to find out whether there is a relationship between those.

The morning peak – which lasts from 07:00 till 09:00 – is hugely affected by the all-eco scenario. Figure 5.6, Figure 5.8 and Figure 5.10 show the relationship between the moment a car enters the network and its travel time. As could be seen, the effect is different for the different routes. The residential route is so affected by the traffic that the influence of driving style on the travel time is completely faded away (Figure 5.6). Small effects of congestion on the travel time start to occur after 40 minutes, while the travel times rise to 1800 seconds in the end of the simulations. The energy consumption follows the travel times, with increasing energy consumptions later in the simulations (Figure 5.7). The conclusion would be that the higher energy consumption is not caused by the higher travel times, but by other effects of the congestion.

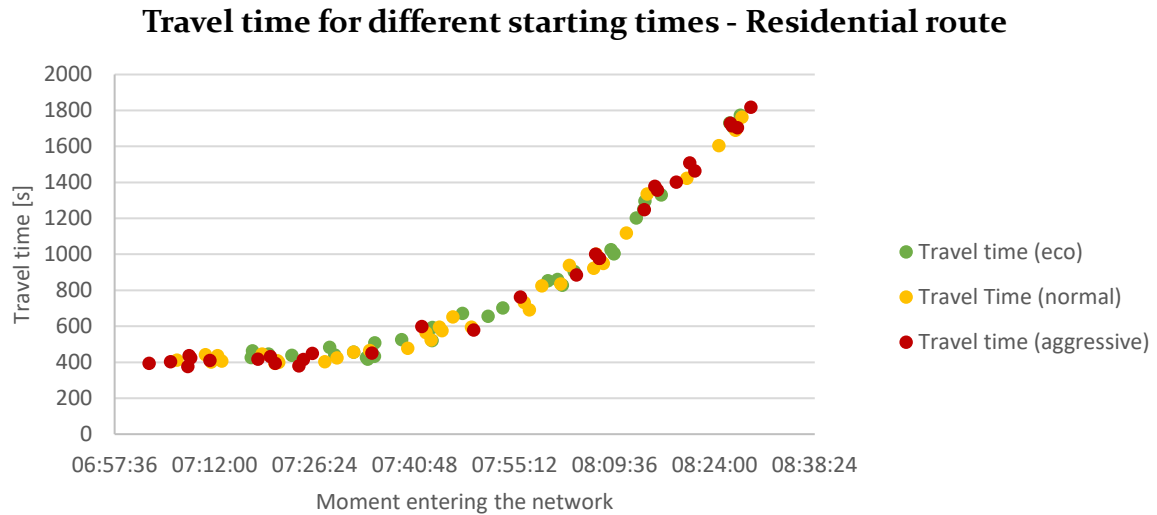


Figure 5.6 Travel time for different starting times when driving the residential route

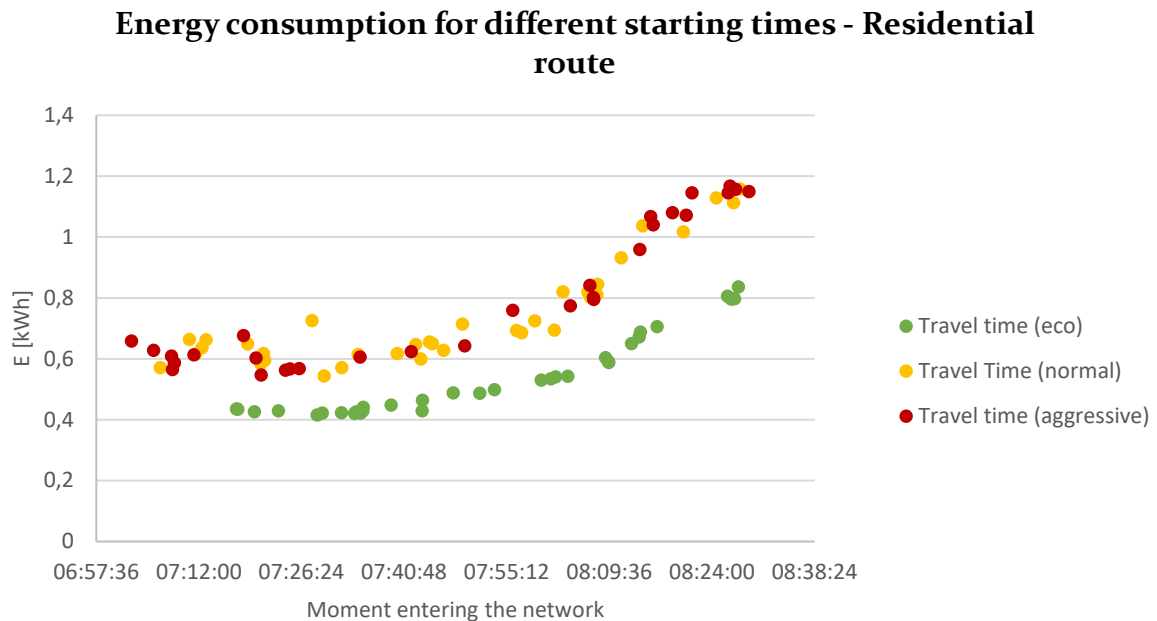


Figure 5.7 Energy consumption for different starting times when driving the residential route

The city center route shows different effects. The spread in travel times is way bigger than at the residential route, though there seems to be no relation between the travel times and the driving style (Figure 5.8). Variations in travel time are likely caused by the randomness of the signalized junctions. In the end of the network, congestion does occur, causing the travel times to boom. The energy consumption shows rational results, with all eco-drivers consuming the least amount of energy, followed by the normal drivers and finally the aggressive drivers consuming the most (Figure 5.9). There seems to be no significant relation between the moment entering the network and the energy consumption.

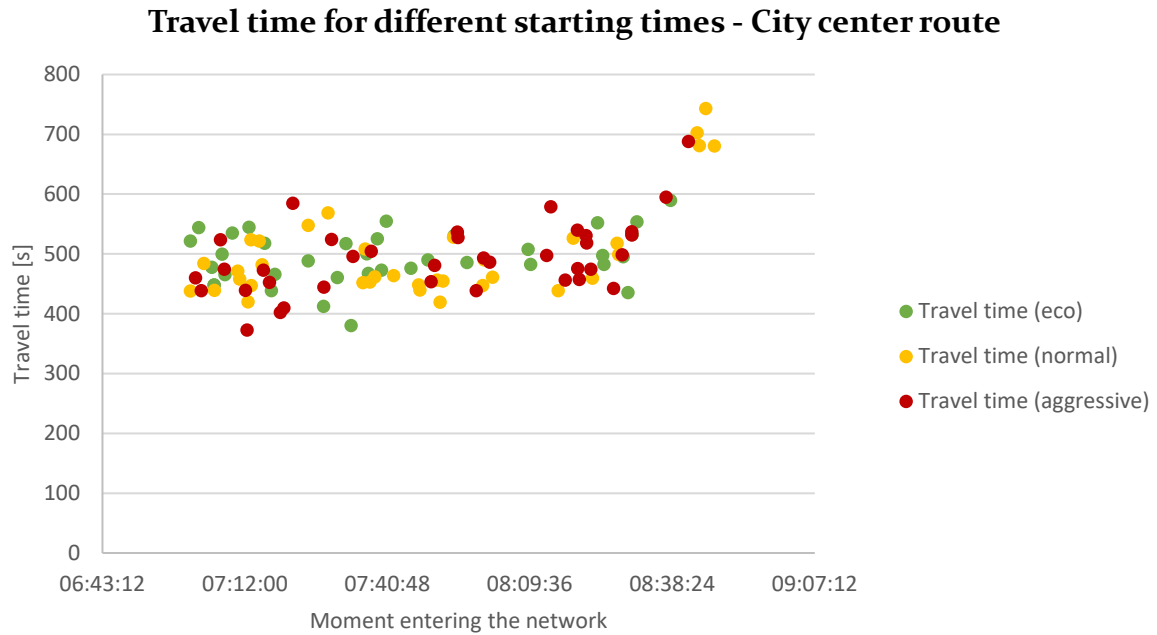


Figure 5.8 Travel time for different starting times when driving the city center route

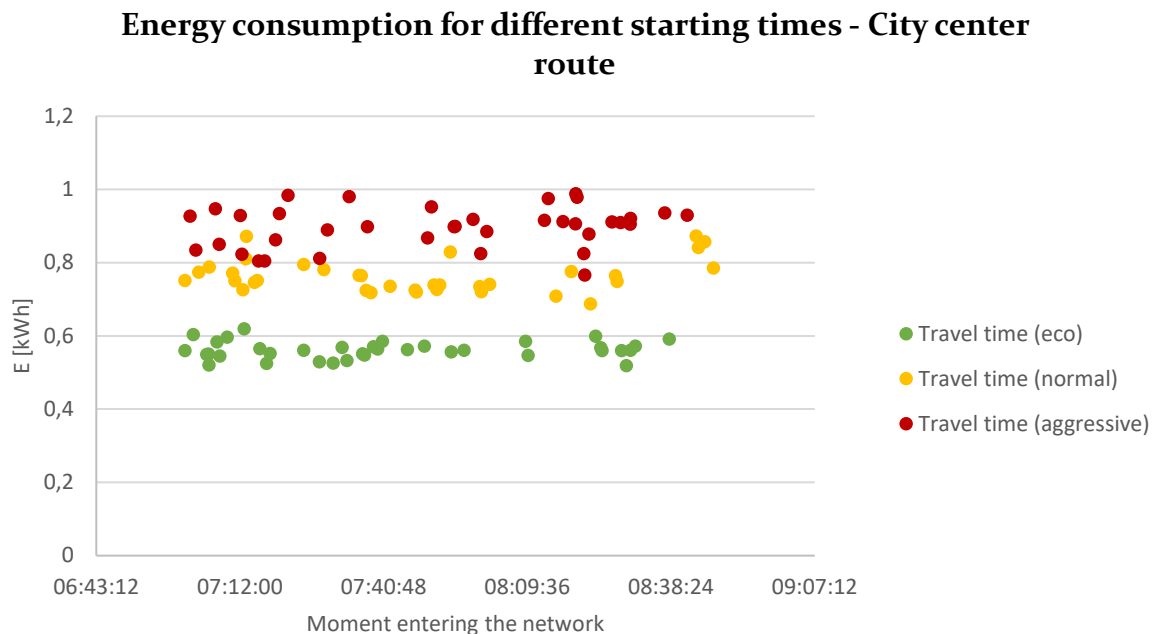


Figure 5.9 Energy consumption for different starting times when driving the city center route

At the motorway route, there seems to be a slight relationship between the driving style and the travel times, while the moment entering the network doesn't seem to affect the travel times (Figure 5.10). The 4-lane motorway simply has such a high capacity that no congestion occurs during peak hours. The energy consumption shows similar results as the city center route, as results are completely rational (Figure 5.11).

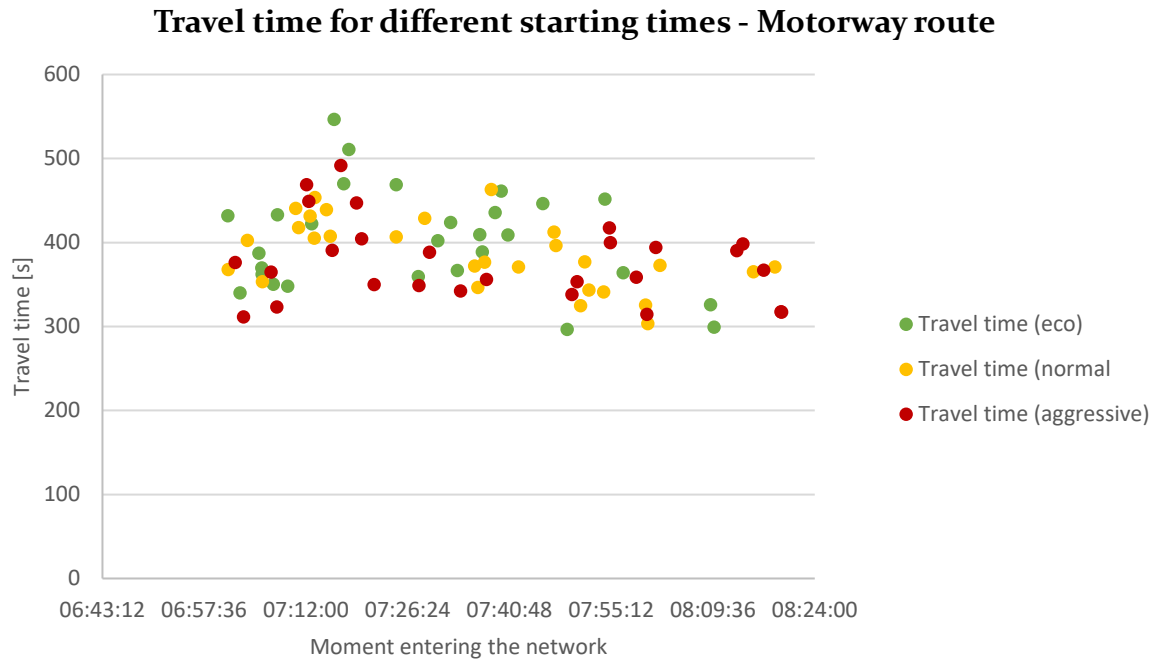


Figure 5.10 Travel time for different starting times when driving the motorway route

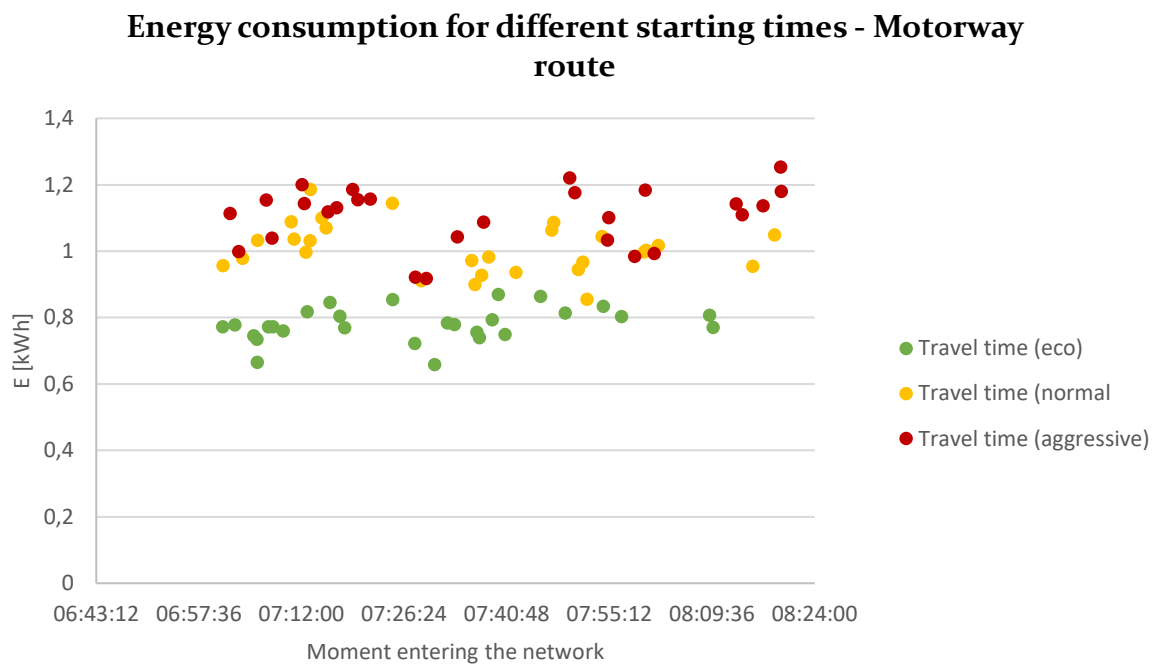


Figure 5.11 Energy consumption for different starting times when driving the motorway route

5.2.4 Scenario 4: Driving during a winter morning peak hour

Chapter 4 showed that a temperature of 0 °C could increase the energy consumption with 50-60%. However, these calculations were based on a straight road section of 500 meter without the influence of other traffic or infrastructural elements. The increase in energy consumption in real driving situations has been modeled in scenario 4.

As Figure 5.12 shows, the travel times are the same. VISSIM contains no weather variables and therefore the influence of temperature on the energy consumption has been

calculated outside the VISSIM environment. The energy consumption results are interesting though, since the increase in energy consumption is way higher for the eco-drivers than for the aggressive drivers, reducing the influence of driving style on the energy consumption. This result could be linked to the fact that the eco-drivers spend more time in the network and therefore their climate systems are running for a longer time. The eco-driver's energy consumption increases with 32%, while the normal and aggressive driver respectively consume 23% and 18% more energy.

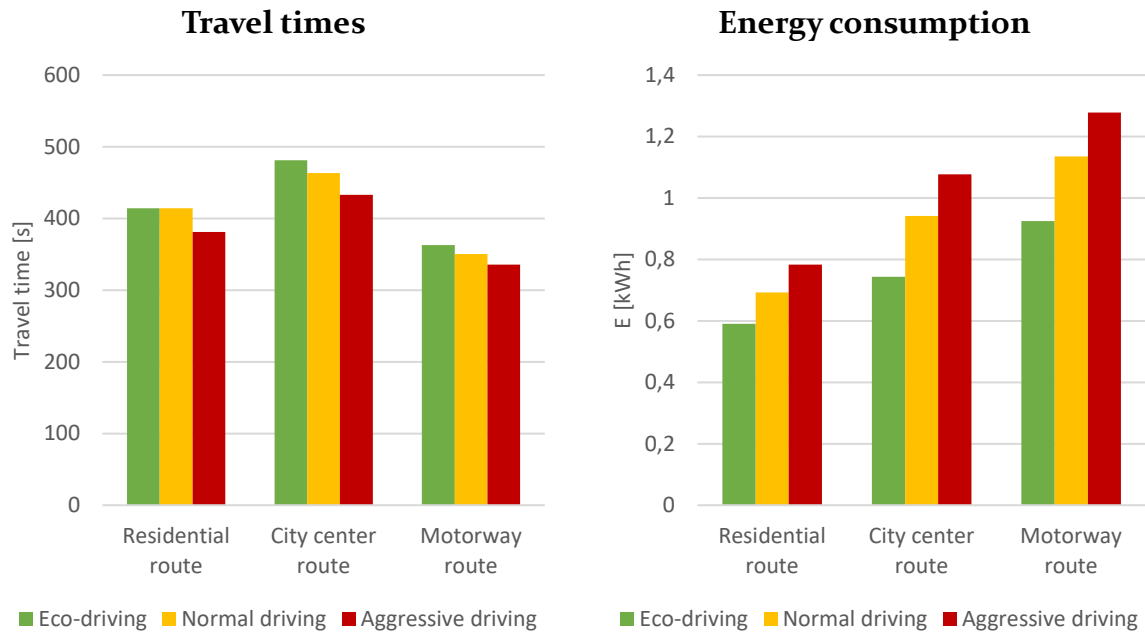


Figure 5.12 Average travel times and energy consumptions for scenario 4

5.3 Power breakdown

After analyzing the energy consumption and travel times at different routes, it's interesting to find how these energy consumptions are built up. To research this, power breakdowns have been made of all the routes, which show the different powers working on the vehicle during the trip. The results of this analysis could be used to find strategies to make parts of the road network more sustainable, based on the dominant forces in that segment. First, power breakdowns have been created based on scenario 1. They show the power consumed by a vehicle based on the infrastructural design of a road. After this, power breakdowns have been made of scenario 2 and 4, to show how other traffic and cold weather influence the power breakdowns and ultimately, the strategical decisions which should be made to make a road network or a driving style more sustainable.

5.3.1 Power breakdown when driving in an empty network

Figure 5.13 shows the comparison between the share of different powers working on a vehicle for the three different routes. As could be seen, there's a big variation in dominant forces for every route, indicating that it takes different strategies to improve the energy efficiency on these routes. On the residential route, the rolling resistance is dominant, closely followed by the acceleration power. Compared to the other routes, the auxiliary power is relatively high. The city center route is dominated by acceleration forces. This could be explained by the high frequency of signalized junctions, requiring vehicles to decelerate and accelerate very often. The

power consumption by aerodynamic drag forces is very high on the motorway route compared to the other routes.

Power breakdown - Route comparison

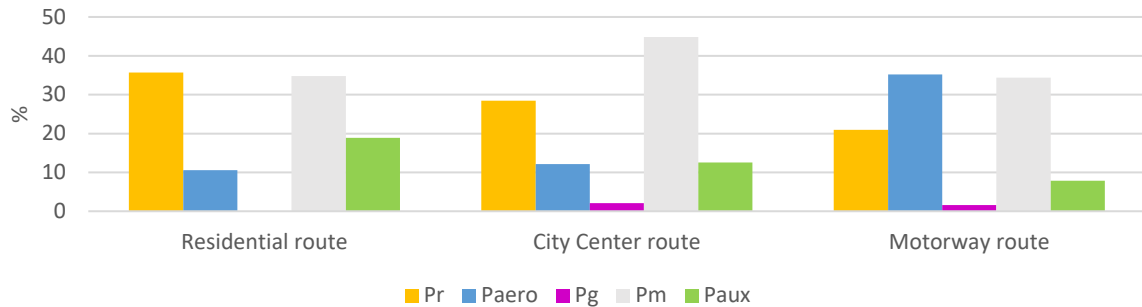


Figure 5.13 Power breakdown of the three different routes when driving in an empty network

Figure 5.14, Figure 5.15 and Figure 5.16 show the individual power breakdown profiles of each different route. As could be seen, the rolling resistance power follows the speed profile, while a quadratic relationship between the aerodynamic drag and the speed exist. Therefore, the power to overcome these forces rises significantly while driving on the motorway.

Power breakdown - Normal driver on the residential route

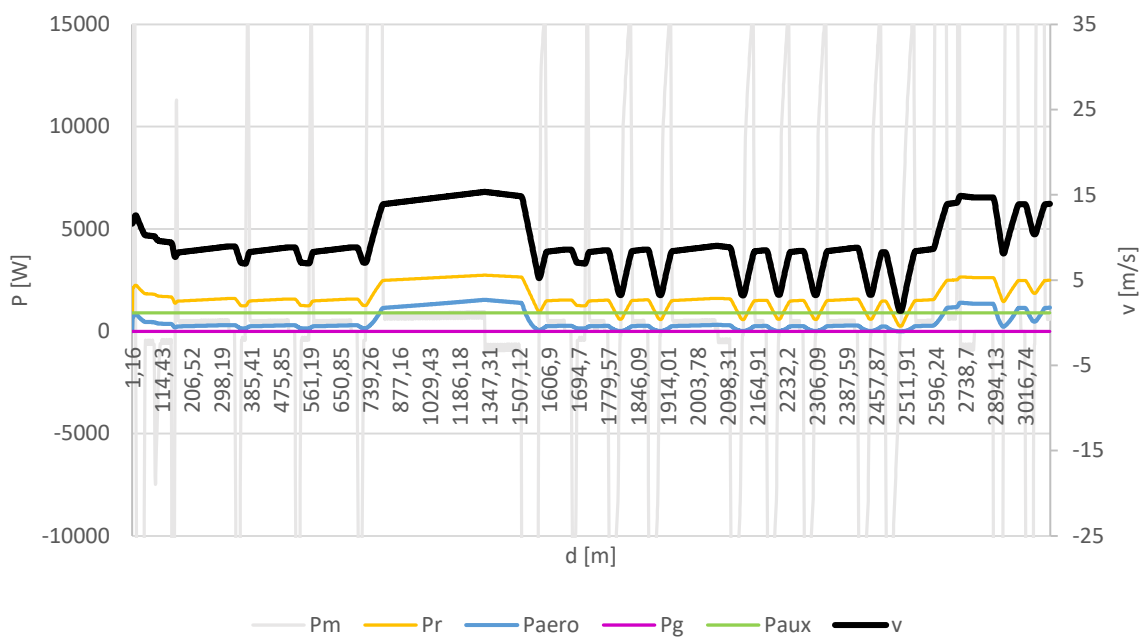


Figure 5.14 Power breakdown of a normal driver on the residential route

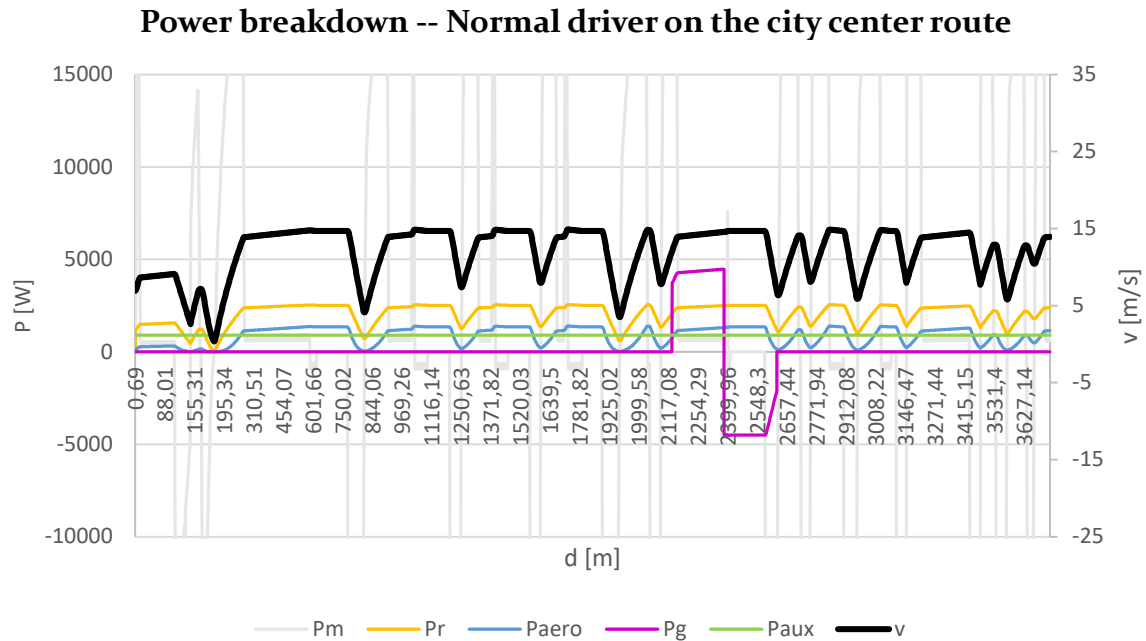


Figure 5.15 Power breakdown of a normal driver on the city center route

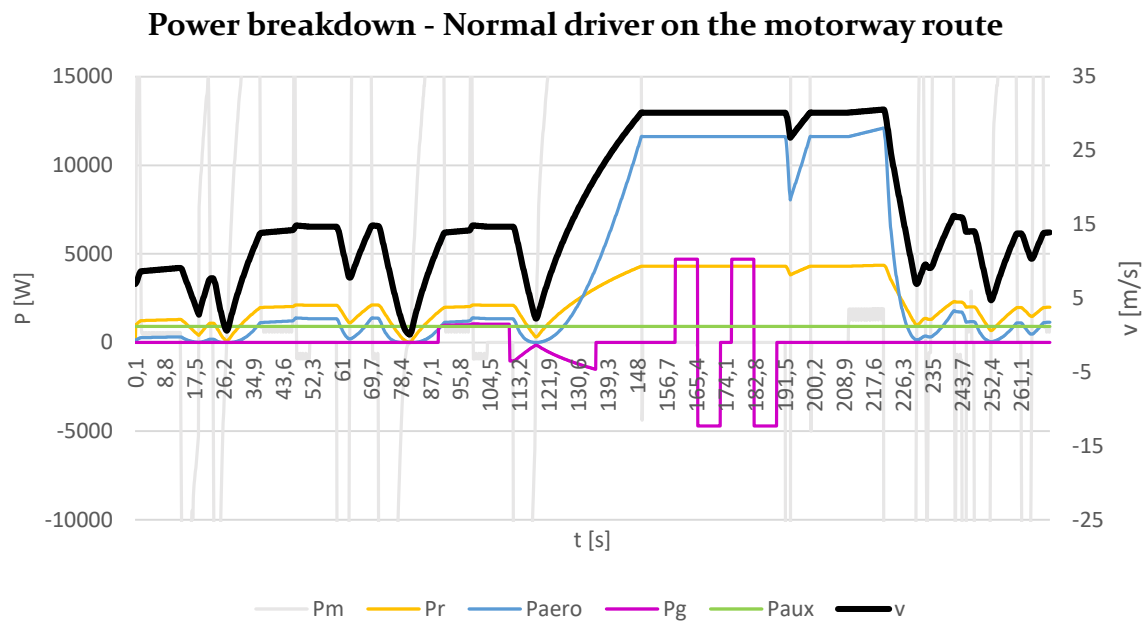


Figure 5.16 Power breakdown of a normal driver on the motorway route

5.3.2 Power breakdown when driving during a morning peak hour

Figure 5.17 shows the route comparison for normal drivers driving in a morning peak. The morning peak increased the share of auxiliary energy for all routes, since the travel times have gone up. Interesting is the decrease in aerodynamic drag on the motorway. Since the power of aerodynamic drag has a quadratic relationship with the driving speed, small decreases in speed result in a large drop in aerodynamic drag. Therefore, the shares of other powers have risen. The share of forces for other routes is almost similar to the empty network, which shows that the traffic intensity may influence travel times and energy consumption but doesn't really influence the share of powers.

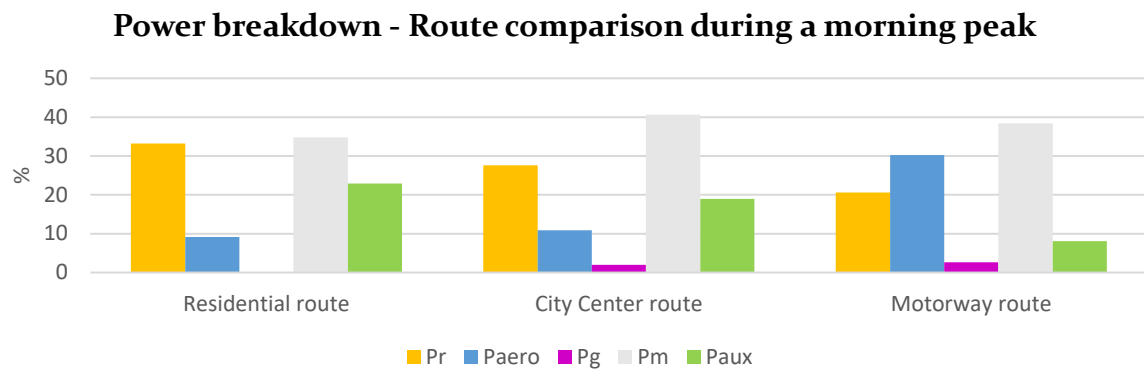


Figure 5.17 Power breakdown of the three different routes when driving in a morning peak

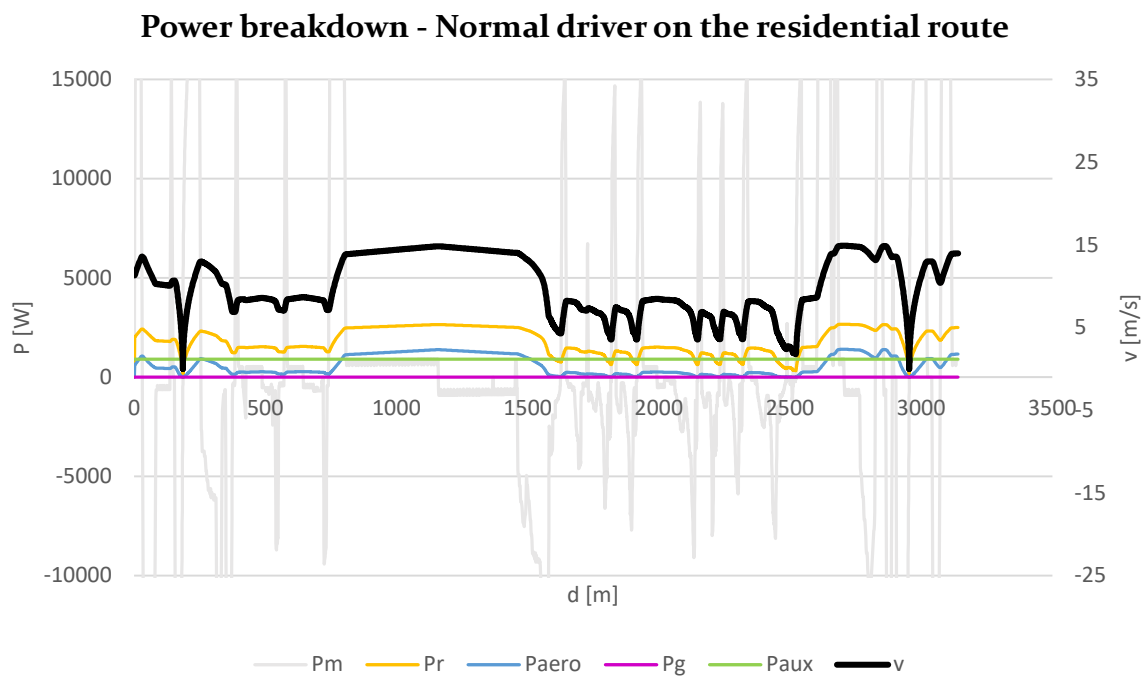


Figure 5.18 Power breakdown of a normal driver on the residential route

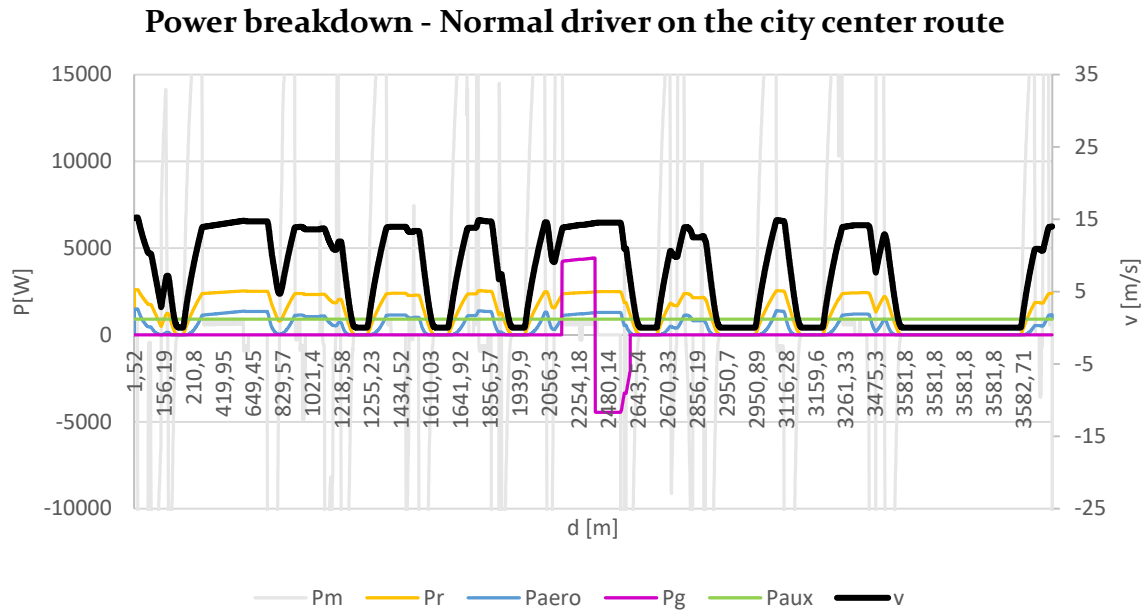


Figure 5.19 Power breakdown of a normal driver on the motorway route

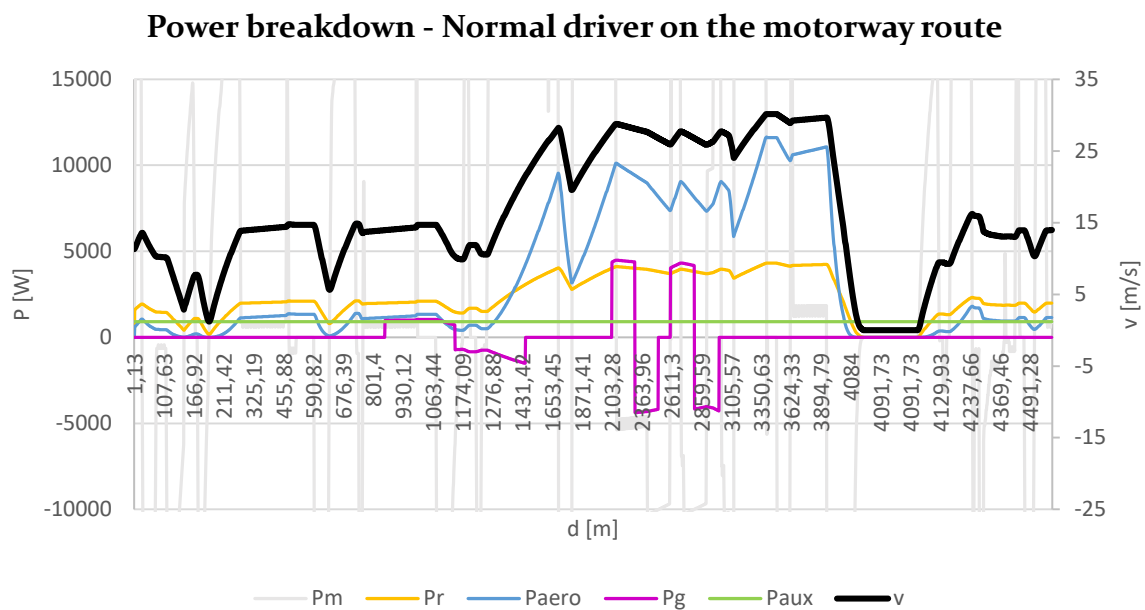


Figure 5.20 Power breakdown of a normal driver on the motorway route

5.3.3 Power breakdown when driving during a winter morning peak hour

Power breakdown profiles of the winter scenario show the impact of the temperature on the auxiliary energy. Figure 5.21 shows that the auxiliary power consumption with an ambient temperature of 0°C rises significantly to 16% of the power consumption on the motorway route to 40% of the energy consumption on the residential route. Technological improvements in the climate system are urgent to sustain a commercially attractive range in the winter period.

The ambient temperature also influences the rolling resistance and the aerodynamic drag. The rolling resistance coefficient of a road would increase 18% in the winter, directly affecting the rolling resistance forces. Simultaneously the aerodynamic drag forces increase with 4% due to a higher air density. Figure 5.21 clearly shows that the share of rolling resistance stayed

the same on the motorway, thus rising significantly in absolute terms. Though, the shares of power consumed by aerodynamic drag and acceleration force dropped a bit. Most interesting is that 70% of the power consumed on the residential route during winter morning peaks is caused by the rolling resistance and the auxiliary energy, which makes strategies to decrease those powers extremely effective. Figure 5.22, Figure 5.23 and Figure 5.24 show the high constant share of auxiliary energy during all routes, while also showing a massive increase in rolling resistance power consumption while driving at high speeds.

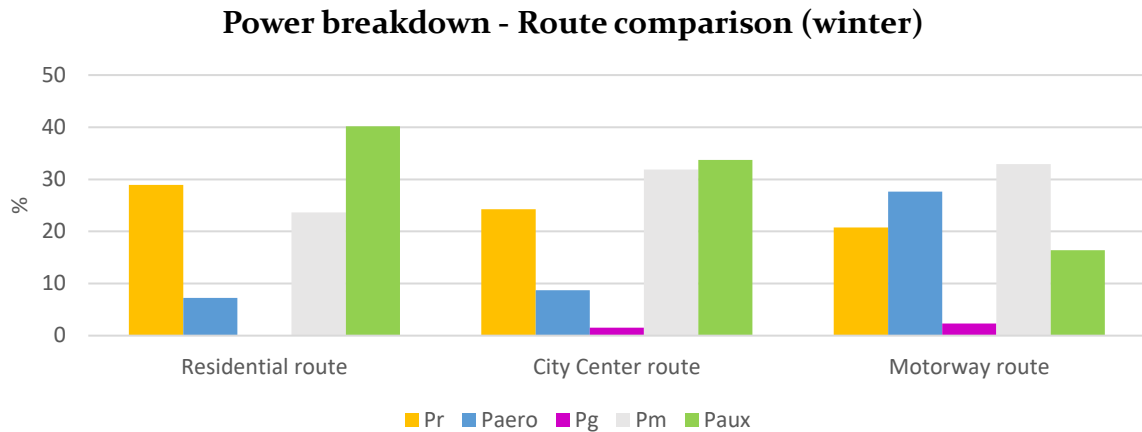


Figure 5.21 Power breakdown of the three different routes when driving in a winter morning peak

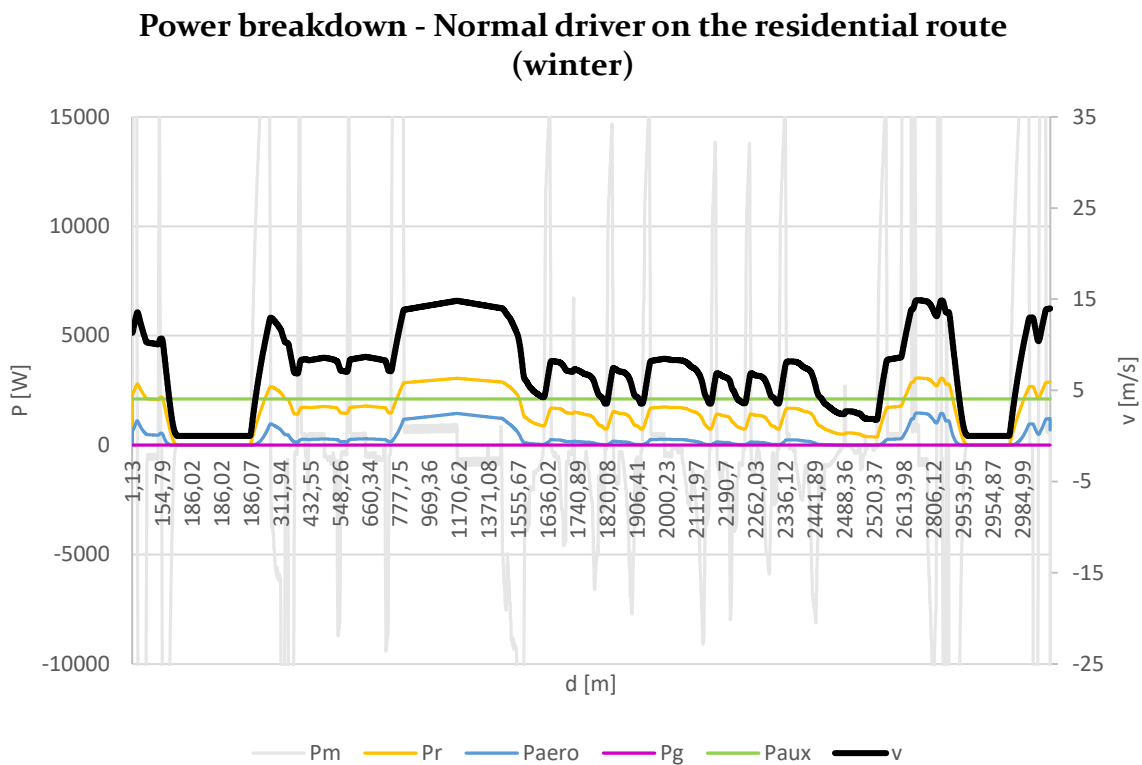


Figure 5.22 Power breakdown of a normal driver on the residential route in a winter morning peak

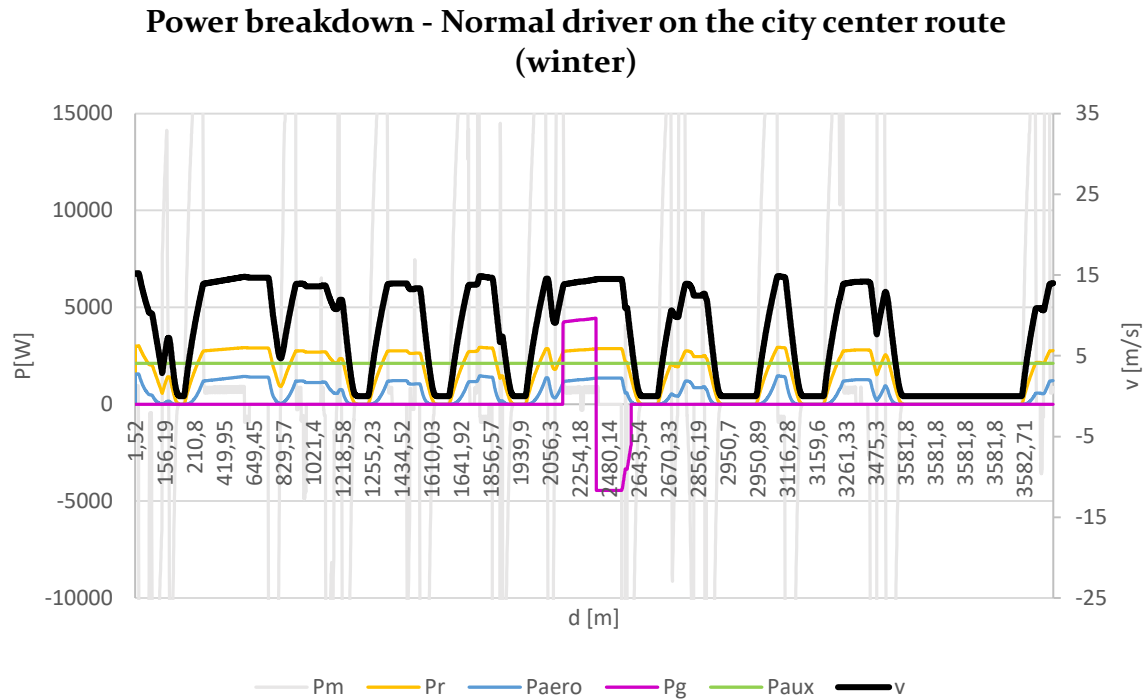


Figure 5.23 Power breakdown of a normal driver on the city center route in a winter morning peak

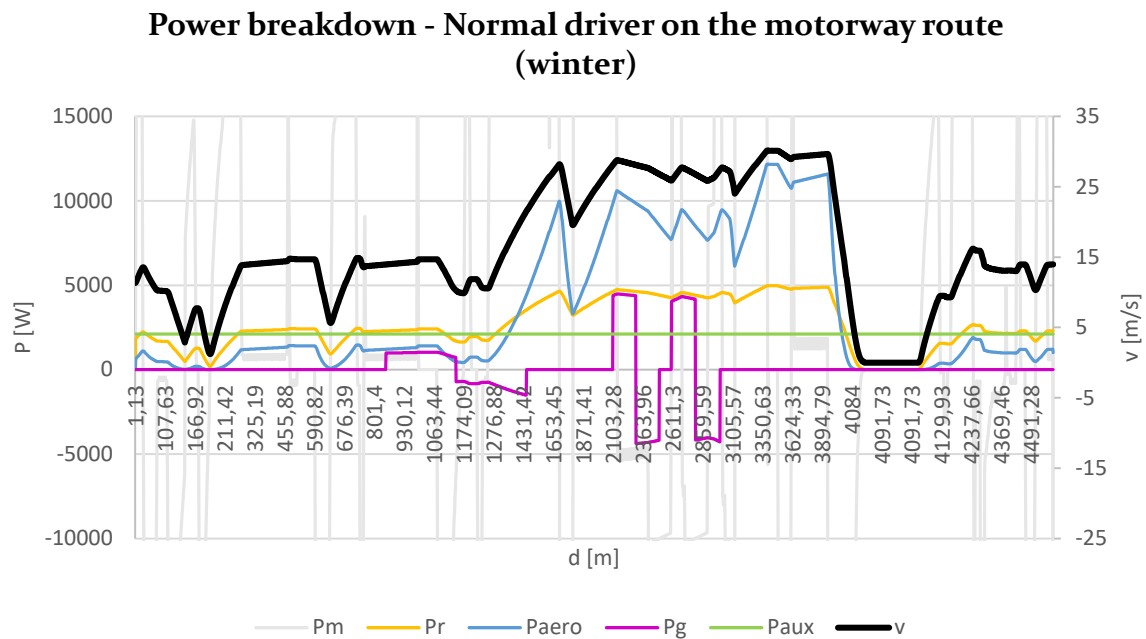


Figure 5.24 Power breakdown of a normal driver on the motorway route in a winter morning peak

5.4 Route optimization

The simulations in Nieuwegein showed that a driver has different options concerning driving style and route. They also show that different scenarios have different influences on the energy consumption and the travel time. A route optimization model has been created to predict the optimal route based on charging costs, travel time valuation and CO₂-pricing. The model tries to find if the optimal route is similar to the fastest or shortest route. Next to this, it also analyzes whether the optimal route changes for different scenarios and personal preferences. First, the principles of the model are explained after which the generalized costs 12 scenarios have been calculated.

5.4.1 Charging costs

The first and most concrete costs are the costs for charging the vehicle. Based on the different routes and driving styles, different amounts of energy are required, and thus different costs are charged for charging the vehicle. As there are many different providers and regulations, the charging costs per kWh differ significantly in the Netherlands. First, there are two options for charging at home. Conventional energy has a price of approximately €0,22/kWh and could be directly used to charge EVs. Houses with solar panels could also use the energy generated by these panels to charge their vehicle. Although the energy is free, one misses the change to set this energy off to the grid. As energy suppliers pay about €0,11/kWh (GreenChoice, n.d.), the costs of charging an EV with solar energy is set to this €0,11/kWh.

Public charging is more expensive, and according to Westeneng (2019), one would pay €0,34/kWh on average at public charging points. As these providers might use a dynamic pricing system based on energy supply and demand, prices might fluctuate. Fast charging is usually the most expensive and is on average set on €0,65/kWh. Though, as the market is new, providers sometimes dramatically decrease their prices (Fastned, n.d.; Business Insider, 2019). Finally, some companies are also offering charging opportunities. Charging at these charging points is usually cheaper than charging at home and will cost about €0,11/kWh (Klut, 2016).

As only 5% of the charging events occurs at public charging points (Mathieu, 2018), this research uses the price of home charging (€0,22/kWh) to calculate the charging costs.

5.4.2 Travel time

A different valuation of travel time is usually made based on trip purpose and income level. McEvoy, Prince and Ferreira (1995) found that there is a strong correlation between income and value of time (VoT). Litman (2009) describes the VoT of business travel as a direct function of the hourly income. He also sketches a difference VoT based on trip purpose, estimating the VoT per person in Europe of business travel to be €21/h, of commuting to be €6/h and of leisure travelling to be €4/h. Wardman and Toner (2018) used a bit higher numbers based on UK recommendations, though the differences between the trip purposes are similar.

Based on the literature, it is reasonable to value business trips based on the labor costs. These labor costs are approximately 130% of the gross salary (Persoon Advies, 2017; Tentoo, n.d.), which is €22/h in the Netherlands, according to CBS (2016). This results in average labor costs of €28,60/h. According to the research of Litman (2009) and Wardman and Toner (2018), the costs for non-work-related trips are approximately 0,3 times the gross salary, resulting in a VoT of €6,60/h. Raijmakers (2019) confirmed the higher valuation of travel time for business trips.

5.4.3 CO₂-emissions

The European Union created a trading system for CO₂ emission allowances. Companies could buy and sell these allowances, which represent a ton of emitted CO₂. If a company exceeds its cap of CO₂-emissions, it could buy these allowances to compensate for their emissions. On the other hand, if a company stays under its cap, it could sell allowances (Carbon Expert, n.d.). The price of these allowances varies over time but has been rising steadily since 2017 (Figure 5.21, *Markets Insider*, 2019) and has a closing price of about €25/tCO₂eq.

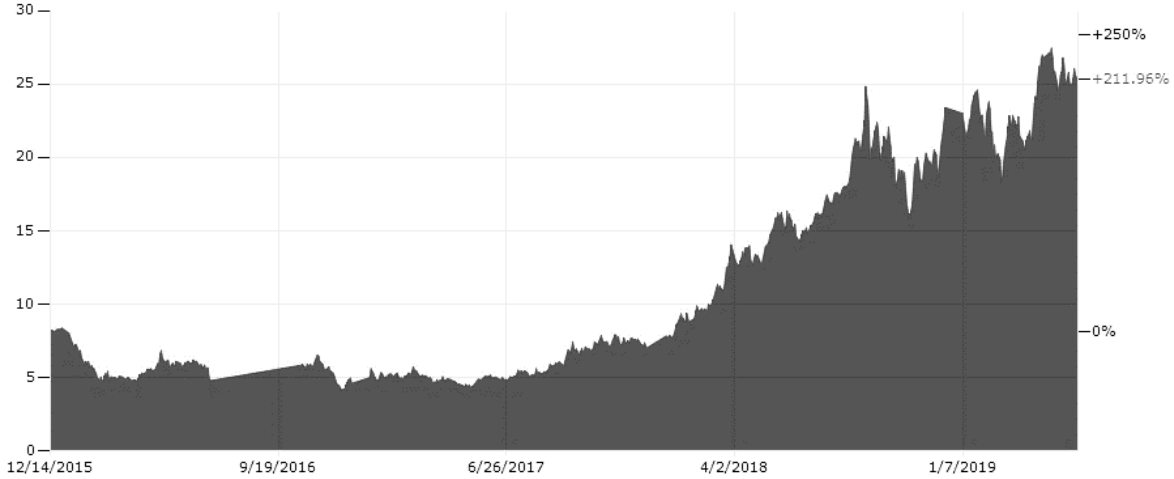


Figure 5.25 Price development of CO₂ emission allowances since the Paris Agreement

The CO₂-emissions of electric vehicles could be calculated by using the carbon intensity of the current energy mix. In the Netherlands, this energy mix has a carbon intensity of 459 gCO₂eq/kWh (ElectricityMap, 2019). Considering the current price of CO₂ allowances, the price for one kWh of energy in the Netherlands would cost €0,011475. The significance of this number, compared to the actual price of charging one kWh, is very low. With an average travel distance of 13.000 km/year (CBS, 2017), the average person would be charged with approximately €25 per year. Though, it is not unimaginable that, under pressure of policy makers and climate organizations, the price of allowances will rise. Economists calculated that the pricing of CO₂ allowances should at least increase with about 200-300% to achieve the Paris temperature target (Stern and Stiglitz 2017). Stanford scientists Moore and Diaz concluded that the social cost of a ton CO₂ should be €200/tCO₂eq (Than, 2015).

5.4.4 Generalized cost model

Combining the cost for charging, the value of travel time and the price for CO₂ would result in a generalized cost function:

$$\text{Generalized cost} = t * VoT + E * (C_{\text{charging}} + C_{\text{CO}_2}) \quad [35]$$

with t being the travel time in hours, VoT being the value of time in €/h, E being the energy consumption of the trip in kWh and C_{charging} and C_{CO_2} are the costs for charging and emitting CO₂ in €/kWh.

5.4.5 Route optimization results

Table 5.4 shows the results of the generalized cost model. Interesting is the fact that an increased traffic intensity affects the city center the most considering generalized cost. The normal driving style never seems to be the best; according to the model, one should either drive

sustainable or fast. Whether one should drive with an aggressive or eco-driving style and which route one should take, largely depends on the trip purpose and the income.

Table 5.4 Output of the generalized cost model for different scenarios and driving styles

Scenario	Time of the day	Other traffic	Outdoor temperature	Trip purpose	Income [€]	Residential GC [€]	City center GC [€]	Motorway GC [%]
1	-	None	12	Business	22	Eco: 2,84 Normal: 2,68 Aggr.: 2,72	Eco: 2,65 Normal: 2,54 Aggr.: 2,42	Eco: 2,38 Normal: 2,28 Aggr.: 2,20
2	-	None	12	Business	12	Eco: 1,59 Normal: 1,52 Aggr.: 1,54	Eco: 1,50 Normal: 1,46 Aggr.: 1,41	Eco: 1,38 Normal: 1,35 Aggr.: 1,32
3	-	None	12	Leisure	22	Eco: 0,92 Normal: 0,89 Aggr.: 0,91	Eco: 0,88 Normal: 0,88 Aggr.: 0,86	Eco: 0,84 Normal: 0,85 Aggr.: 0,85
4	-	None	12	Leisure	12	Eco: 0,54 Normal: 0,54 Aggr.: 0,56	Eco: 0,53 Normal: 0,56 Aggr.: 0,56	Eco: 0,54 Normal: 0,57 Aggr.: 0,59
5	07:00-09:00	Mix	12	Business	22	Eco: 3,39 Normal: 3,42 Aggr.: 3,18	Eco: 3,95 Normal: 3,86 Aggr.: 3,65	Eco: 3,06 Normal: 3,01 Aggr.: 2,93
6	07:00-09:00	Mix	12	Business	12	Eco: 1,89 Normal: 1,92 Aggr.: 1,80	Eco: 2,21 Normal: 2,18 Aggr.: 2,09	Eco: 1,75 Normal: 1,74 Aggr.: 1,72
7	07:00-09:00	Mix	12	Leisure	22	Eco: 1,09 Normal: 1,11 Aggr.: 1,06	Eco: 1,27 Normal: 1,28 Aggr.: 1,24	Eco: 1,04 Normal: 1,06 Aggr.: 1,06
8	07:00-09:00	Mix	12	Leisure	12	Eco: 0,64 Normal: 0,66 Aggr.: 0,64	Eco: 0,75 Normal: 0,78 Aggr.: 0,77	Eco: 0,65 Normal: 0,68 Aggr.: 0,70
9	07:00-09:00	Mix	0	Business	22	Eco: 3,43 Normal: 3,45 Aggr.: 3,21	Eco: 3,99 Normal: 3,90 Aggr.: 3,69	Eco: 3,10 Normal: 3,04 Aggr.: 2,96
10	07:00-09:00	Mix	0	Business	12	Eco: 1,93 Normal: 1,96 Aggr.: 1,83	Eco: 2,26 Normal: 2,23 Aggr.: 2,12	Eco: 1,79 Normal: 1,78 Aggr.: 1,75
11	07:00-09:00	Mix	0	Leisure	22	Eco: 1,12 Normal: 1,15 Aggr.: 1,09	Eco: 1,32 Normal: 1,32 Aggr.: 1,28	Eco: 1,08 Normal: 1,10 Aggr.: 1,10
12	07:00-09:00	Mix	0	Leisure	12	Eco: 0,68 Normal: 0,70 Aggr.: 0,68	Eco: 0,80 Normal: 0,82 Aggr.: 0,81	Eco: 0,69 Normal: 0,72 Aggr.: 0,73

Liu et al. (2017) found that privately used EVs use less energy than commercially used EVs. This matches the generalized cost model outcome, where business travelers tend to use the aggressive driving style on the motorway route more often than leisure travelers.

5.5 Validation

5.5.1 Validation against laboratory measurements

Argonne National Laboratory (ANL) shares a large publicly available dataset, the Downloadable Dynamometer Database, generated at the Advanced Mobility Technology Laboratory (AMTL) at Argonne National Laboratory under the funding and guidance of the U.S. Department of Energy (DOE). The mission of the research conducted by ANL and DOE was to “enable petroleum displacement through technology assessment & data dissemination” (Stutenberg, 2014). The database consists of dynamometer data from research performed in a research facility with a controlled environment. The data from tests with a 2014 BMW i3 are used to compare this research with the ANL results. The i3 has been tested under different circumstances, amongst others with different ambient temperatures and with different preferred indoor temperatures. The dynamometer had a fixed route installed, based on multiple standard driving cycles. The route started with an UDDS cycle of 12 km followed by a Hwy cycle of 16,5 km. After the Hwy cycle, another UDDS cycle was driven, to finish the test with an USo6 cycle of 12,8 km. Figure 5.22 shows the speed profile of the ANL tests. This combination of driving cycles shows a rich variety of different driving scenarios, with the UDDS being a typical urban driving cycle and the USo6 and Hwy cycles being more similar to highway driving.

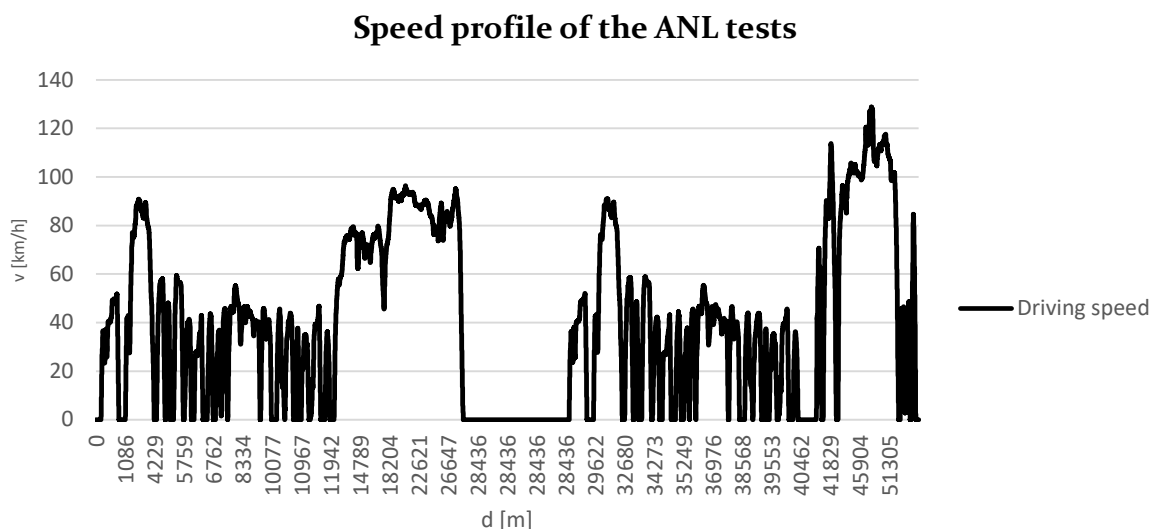


Figure 5.26 Speed profile of the ANL tests

Table 5.5 Validating the results against the ANL measurements

ID	T _{ambient} [°C]	T _{target} [°C]	Cycle length [km]	E _{measured} [kWh]	E _{predicted} [kWh]	Prediction/ measurement [%]
61505028	3,14	22,22	53,46	9,47279	9,51517	100,4
61505019	23,65	23,65	53,29	6,280	6,12275	97,5
61505024	36,43	22,22	53,46	6,957	6,51796	93,7

Table 5.5 shows the validation of three predictions against three different ANL measurements. As could be seen, the model is very accurate (within 2,5% difference of the measurements) for temperatures between 3 and 24 °C. For extremely high temperatures (over 35 °C), the difference becomes bigger than 6%. It's reasonable to believe that the climate system's energy consumption has been underestimated in the model for these extreme

temperature differences. Further research, preferably in a controlled research facility such as the ANL facility, is needed to quantify the influence of auxiliary systems more accurate.

5.5.2 Validation against driving test measurements

The ANL measurements show very precise measurements of the energy consumption of the BMW i3. A limitation of the ANL measurements – and many dynamometer tests in general – is that they don't cover some real driving circumstances. The dynamometer cannot cover traffic intensity and since the speed profile is fixed, it also doesn't cover different driving styles. The research performed at the ANL dynamometer only made use of a single drum, resulting in the fact that also different road types are not covered by these tests. To create a more realistic validation, 30 driving tests have been performed in Nieuwegein. All tests have been made in the same week. They include driving with and without the climate system running. All routes are being tested on all different timeslots to reduce the influence of the day. Different days of the week, as well as timeslots, are chosen to cover possible differences. June is considered one of the best periods for performing driving tests, as the average amount of days raining and the amount of rain are close to the yearly average. Furthermore, the average temperature within the measurement period ranges between a minimum of 10,8 °C and a maximum of 19,2 °C which is also representative for the Netherlands during morning driving tests (KNMI, 2019; MeteoGroup, n.d.).

The aggregated results of the measurements could be found in Table 5.6. The table shows the measured efficiency, which has been acquired by measuring dashboard data during the driving tests. Secondly, the table shows the predicted energy, which has been predicted by using the GPS speed measurements of the different routes. The table contains aggregated trip results of each route per testing day. The prediction error is calculated using the Mean Absolute Percentage Error (MAPE), which is frequently used to evaluate forecasting studies (De Myttenaere et al., 2017) and has also been used by other energy prediction studies (Wang et al., 2017). The MAPE is calculated with the following equation:

$$MAPE = \frac{100\%}{n} \sum_{t=1}^n \left| \frac{E_{measured} - E_{predicted}}{E_{measured}} \right| \quad [36]$$

Table 5.6 Driving test results

Date (dd-mm-yyyy)	Timeslot	Climate system on	Measured efficiency (kWh/100km)	Predicted efficiency (kWh/100km)	Average MAPE per trip [%]	MAPE of total daypart [%]
11-06-2019	12:30-16:00	No	R: 12,42 C: 12,96 M: 13,20	R: 12,06 C: 12,86 M: 14,05	7,6% 8,3% 3,1%	2,9% 0,8% 6,7%
12-06-2019	09:30-13:00	No	R: 10,25 C: 11,57 M: 12,90	R: 10,60 C: 12,07 M: 12,55	12,7% 7,3% 7,9%	3,5% 4,4% 2,7%
12-06-2019	09:30-13:00	Yes, ΔT = 7,5 °C	R: 18,15 C: 20,45 M: 21,45	R: 19,03 C: 20,76 M: 14,91	4,4% 13,8% 30,0%	4,8% 1,5% 30,5%
Average					10,57%	6,42%
Average without the last motorway measurement					7,82%	3,41%

The MAPE has been calculated per trip (to represent the accuracy of short distance trips), and for the total daypart (aggregating all individual trips in that daypart, representing long distance trips). The MAPE per trip shows an average MAPE of 10%, meaning that there's a significant error rate in the short individual measurements. However, a large part of this is caused by the measurements with the climate system on. The last measurement at the motorway is a significant outlier, since the model predicted a way too low energy consumption. This could be explained by the fast driving speed of the vehicle, especially on the motorway route and partially on the city center route. Shitzer (2005) found that at higher speeds, the heat transfer coefficient rises almost linearly with the driving speed. Since a higher heat transfer coefficient requires more thermal power to heat up an object, the climate system would need more power at higher driving speeds. This effect isn't considered in the energy model. Further research should determine how to model the power consumption of the climate systems at high driving speeds, since the energy consumption rises significantly. If the last measurement isn't considered, the MAPE per trip is 7,82%. The last column of Table 5.6 shows the MAPE of the total daypart, consisting of the sum of all trips on a certain route. It represents the accuracy of the prediction for longer trips (5-20 km) and shows a significant increase in accuracy, resulting in an average MAPE of 3,41% when not taking the last motorway measurement into account. Wang et al. (2017) concluded the MAPE of other papers is around 10% and therefore a significant gain in efficiency has been realized for trips of 5 km and higher.

The prediction error of all individual trips (representing short trips) and the daypart averages (representing long trips) could be found in Figure 5.27.

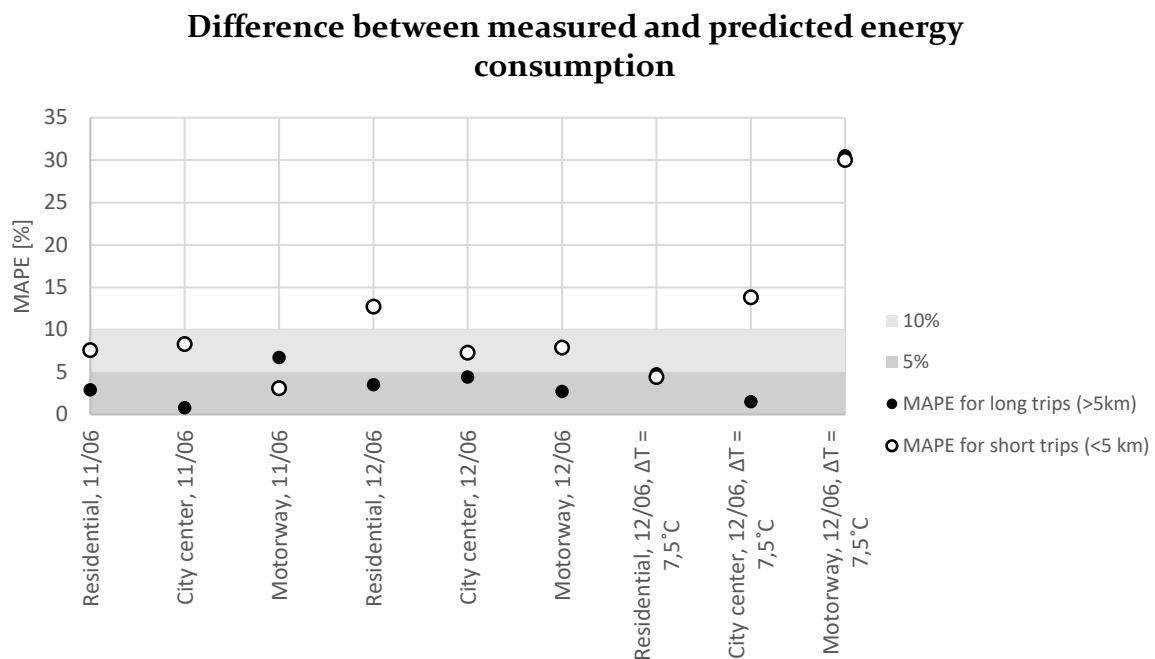


Figure 5.27 Difference between measured and predicted energy consumption

The influence of the climate system on the measured energy consumption has been visualized by Figure 5.23. Measurements done with the climate system off show a peak at 10-12 kWh/100km, with an average efficiency of 12,3 kWh/100km. Simultaneously, the measurements performed with the climate system on have an average efficiency of 20,0 kWh/100km.

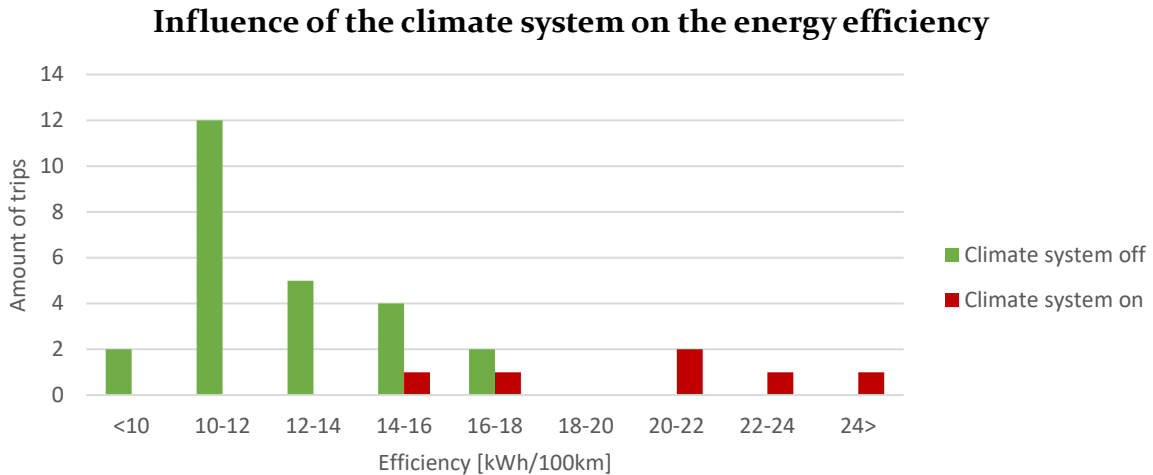


Figure 5.28 Influence of the climate system on the energy efficiency

These test measurements match with the real driving tests which have been performed by members of Spritmonitor (n.d.). Measurements have been performed by using 59 different BMW i3's with in total 5445 fuelings. The results could be found in Table 5.6.

Table 5.7 Electricity consumption of 59 BMW i3's

Count (-)	Fuelings (-)	Min (kWh/100km)	Max (kWh/100km)	Mean (kWh/100km)	Median (kWh/100km)
59	5445	8,18	22,88	16,31	15,11

5.5.3 Validation against BMW measurements

BMW (2018) also did measurements with the i3 based on the Worldwide Harmonised Light Vehicle Test Procedure (WLTP) in order to compare the i3 with other vehicles. The WLTP replaces the former NEDC-driving cycle test and is aimed to be a more realistic simulation of real driving circumstances (Pavlovic et al., 2018). The WLTP has a speed profile which is very similar to the profile used in the ANL test, with about 50% of the cycle being an urban cycle, and the other 50% being outside the city (e.g. motorway driving). Figure 5.24 shows the WLTP driving cycle:

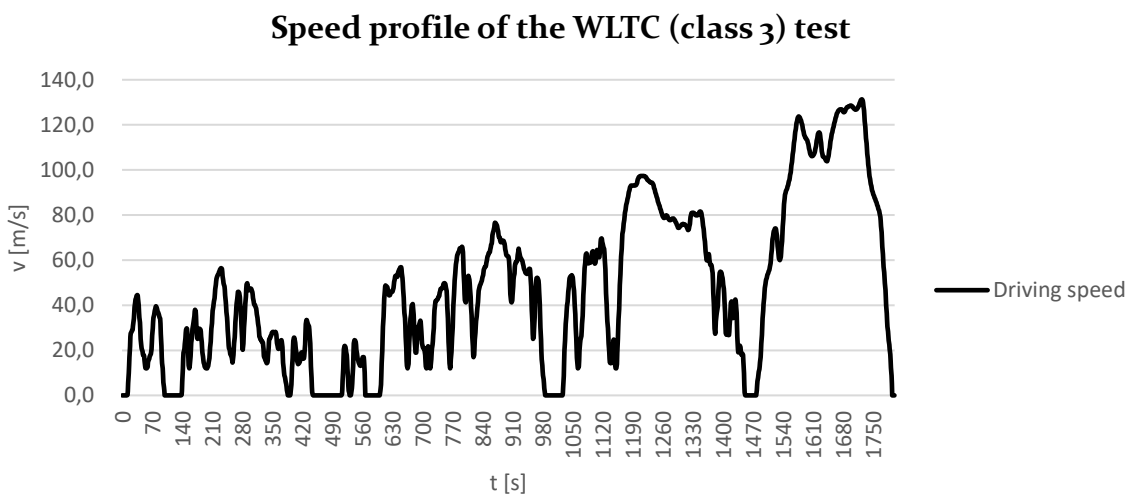


Figure 5.29 Speed profile of the WLTC (class 3) driving cycle

BMW predicts an average energy consumption of 13,1 kWh/100 km. When predicting a standard WLTC driving cycle with the energy prediction model in, the outcome is 13,4 kWh/100 km. As the difference is very small, one would say that the prediction made by BMW (which based on EU legislations) is very close to reality. However, a critical note has to be made here. To reach 13,4 kWh/100 km, the model needed to be calibrated in the most extreme Eco-settings. No wind or slopes were used in the prediction, as well as no auxiliary energy (meaning that the climate system, navigation system, radio and lighting were all turned off).

Comparing the BMW prediction to the Nieuwegein results would give more realistic results. In scenario 1, the Nieuwegein model indeed shows 13,1 kWh/100 km, although this is on the most sustainable route with the most sustainable driving style. When considering different scenarios, the results get worse. The winter scenario, in the middle of the morning peak, shows an energy consumption of 28,8 kWh/100 km for the aggressive driving style on the city center route. Also, highway driving reaches 28,0 kWh/100 km there, meaning that the range would be less than 50% of the range promoted by BMW.

A critical review of the system has been made by shifting from testing with NEDC-cycles towards WLTC-cycles, which created more realistic results in terms of CO₂ (Pavlovic et al., 2018). However, to be able to inform drivers about the possibilities of electric vehicles, the industry should be fair about the variations in driving range. Legislation could be a means to stimulate the industry towards better provision of information.



Chapter 6

Conclusion and discussion

Chapter 6. Conclusion and discussion

6.1 Conclusion

This thesis aimed to quantify the effects of various environmental variables, traffic intensities and driving styles on the efficiency of electric vehicles, in order to provide the car with optimized route information based on the most energy efficient route and travel time preferences. The desire to gain more insight in this underdeveloped field of research led to the following research question: *To what extent do driving style, environmental variables, infrastructural design and traffic intensity have an effect on the energy efficiency of electric vehicles and how could route optimization reduce the energy consumption within a driver's time constraints?* Major changes in the mobility sector are necessary to reduce the influence of the greenhouse effect, of which shifting from combustion engines to electric vehicles is one of the major developments. However, the persistent consumer constraints regarding range anxiety have a negative influence on the market penetration of EVs. Creating new quantitative insights in the relation between weather, infrastructural design, driving style and traffic intensity and the energy consumption of these vehicles might lead to an acceleration of sustainability strategies and could reduce range anxiety.

One's driving style has a significant influence on the way a vehicle is used and propels on the road network. To measure the influence of the driving style on the energy consumption, the following sub-question has been answered: *What is the effect of different driving styles on the energy efficiency of electric vehicles?* Combinations of a higher driving speed and a higher acceleration resulted in a significant increase in energy consumption for the aggressive drivers, confirming the findings of Wang et al. (2017). However, individually, these elements are found to have a very low effect on the energy consumption. This leaves an interesting research gap: determining the optimal eco-driving style considering both energy efficiency and travel time. Ericsson (2001) found that speed oscillations influence the energy consumption. This thesis extended this knowledge, finding that speed oscillations have a higher impact on aggressive drivers compared to eco-drivers. Using cruise-control turned out to be the most efficient for all driving styles.

Based on a literature review, many weather variables have been found to influence the energy consumption. To quantify these influences, the following sub-question has been answered: *Which environmental variables do have an effect on the energy efficiency of electric vehicles and to what extent?* Temperatures of 0°C have been found to have a significant impact on the energy consumption, mainly due to the use of the climate system, and could increase the energy consumption with 50% compared to average Dutch temperatures, confirming the findings of Hollweck et al. (2018) and Evtimov et al. (2017). Hollweck et al. (2018) also found a higher influence of temperature on urban driving cycles, which has also been found in this thesis. However, this thesis gives new insights by taking an increasing aerodynamic drag (5%) and an increasing rolling resistance (18%) into account. A quadratic relationship between wind speed and the energy consumption has been found, resulting in extreme aerodynamic drag forces for high wind speeds. This explains findings of Evtimov et al. (2017) who found that wind mainly influences motorway driving. The influence of the lighting system is found to be very small compared to other forces, as also found by Evtimov et al. (2017).

A road's infrastructural design is the main determinant of the speed profile on that road. Typical infrastructural elements, such as curves, road slopes, road types, traffic calming measures and signalized junctions have been researched to answer the following research question: *What is the influence of different infrastructural elements on the energy efficiency of electric vehicles?* Rolling resistance has been found to have a relatively high effect on low driving

speeds. As Michelin (2003) mentions, the main reason is that these roads surfaces typically have a higher resistance. Road curves are found to have an influence on the energy consumption if the lateral acceleration of a vehicle requires the vehicle to slow down during the curve. The lower the radius of the curve and the higher the initial driving speed of the vehicle, the higher the influence on the energy consumption. Since aggressive drivers tend to take turns with a higher lateral acceleration, they slow down less during some curves, resulting in a lower influence compared to less aggressive driving styles. This extends the knowledge of recent models (Wang et al., 2017) which didn't consider different lateral accelerations for different driving styles. Hilly driving influences the energy consumption through the increased gravitational forces. For very steep hills, the influence of the gravitational force is so large that differences between driving styles disappear. Another finding is that the order of hills doesn't matter: uphill-downhill scenarios resulted in the same energy consumption as downhill-uphill scenarios. These insights help to explain findings by Liu et al. (2017), however more research to create practical hilly driving predictions is necessary. Traffic calming measures influence the energy consumption through the acceleration forces and are typical elements in stop-and-go traffic scenarios. The elements cause cars to decelerate and accelerate, resulting in higher energy consumptions. A linear relation has been found between the speed reduction on a speed bump and the increase in energy consumption. This influence is about twice as much for the normal driver compared to the eco-driver, while the influence is three times as much for aggressive drivers. Calculations also showed that in a sequence of speed bumps, a significant improvement in energy efficiency could be achieved if a driver chooses to keep his speed lower in between the speed bumps. The influence of a signalized intersection depends on the waiting time and the ambient temperature. During normal weather, the deceleration and acceleration itself have a higher influence than a waiting time of 30 seconds. However, during winter, the climate system causes a significant increase in energy consumption during the waiting time. While the influence of traffic calming measures is weather independent, the temperature does have a significant influence on signalized intersections. To the best of my knowledge, this is the most extensive research into the microscopic influence of traffic calming elements on a vehicle's energy consumption.

Roads have a maximal capacity, and traffic is found to be influenced by the traffic intensity if this intensity reaches the capacity. The influence this intensity has on the energy efficiency has been researched in the following sub-question: *What is the effect of traffic intensity (intensity/capacity) on the energy efficiency of electric vehicles?* The morning peak traffic only had a little influence on the energy consumption, however travel times rose significantly. The city center route, which contains a lot of signalized junctions, is affected the most by a gain in traffic due to the longer waiting times at the traffic lights. In a winter scenario, the long waiting times at the traffic lights negatively influence the energy consumption. Calculations have shown that the city center is affected the worst by the winter scenario. Due to their longer travel times, eco-drivers are also more heavily affected by cold weather than aggressive drivers, reducing the gap in energy efficiency between the different driving styles. If all drivers in the network would switch to an eco-driving strategy, the traffic intensity has huge implications for the travel times. The low driving speed and calm acceleration and deceleration cause the network to collapse during peak hours, as the intensity outreaches the capacity. Concluding, eco-driving is positive for the energy efficiency of vehicles, though the network capacity should be closely monitored from a macro-perspective. Most researched microscopic models lack in taking traffic intensity into account and therefore don't give a full overview of the energy efficiency and travel times.

Strategies to create a higher energy efficiency and thus reduce range anxiety could be performed on an individual level as well as on larger scale levels. To get insights in the larger scale, power breakdowns have been created for the different routes, to get new insights in the relation between different routes and scenarios and the different power consumptions of a

vehicle. Individual strategies relate to the decision-making process of the individual, based on the extended knowledge of travel time and energy consumption. These two methods aim to answer the following sub-question: *Can route optimization and style optimization make more energy efficient routes within a driver's time constraints, and if yes, to what extent?* The power breakdown profiles give insights in the power consumption and could be used to create more sustainable infrastructure and vehicles on the longer run. Different powers turned out to be dominant for different routes. In the residential route, the rolling resistance was the dominant power. Acceleration forces caused the high energy consumption at the city center, while aerodynamic drag dominated the power consumption on the motorway route, confirming findings of Evtimov et al. (2017). The immense share of the auxiliary power consumption during winter driving has been quantified by running winter simulations, resulting in a share of 30-40% of the total power consumption. Individual strategies relate to the decision-making process of route and driving style decisions. A generalized cost model based on charging costs, travel time valuation and CO₂-emission pricing has been created. The model showed that the preferences have a significant influence in the preferred route and driving style. Business travel, cold weather and a high income turned drivers towards aggressive driving on the motorway, as the travel time has a huge influence on these drivers. Drivers which perform leisure trips in average weather conditions and have a lower income tend to switch towards more sustainable driving styles and routes. The results extend findings of Litman (2009), who found that business travelers have a higher travel time valuation and Liu et al. (2017), who found that business travelers consume more energy per driven kilometer. Calculations found that shifting to a more sustainable driving style has more effect on the energy efficiency than shifting to a more sustainable route. The research proved that different optimal routes exist for different scenarios and different personal preferences. These routes have different dominant energy sources, resulting in different strategic choices to make these routes more sustainable.

To validate the accuracy of the model, the last sub-question which has been answered was: *To what extent does this predicted efficiency correspond to reality?* The accuracy has been validated in threefold. First, the results have been compared to laboratory measurements. The model showed an accuracy of 99% compared to the lab measurements for Dutch driving conditions. Secondly, the model has been validated against real driving tests performed in Nieuwegein with a BMW i3. The measurements show similar energy efficiency values as modeled in chapter 5 and show the differences between the different routes. They also prove the influence of the climate system on the energy efficiency. These measurements have been compared to data from 5445 fuelings by 59 BMW i3's gathered from Spritmonitor, showing similar minimum and maximum efficiencies. Finally, the efficiency given in the technical specifications of BMW itself have been compared to the model, resulting in some critical notes to BMW.

When combining the answers to the sub-questions, an answer on the main research question could be formulated. *To what extent do environmental variables, traffic intensity and driving style have an effect on the energy efficiency of electric vehicles and how could route optimization reduce the energy consumption within a driver's time constraints?* Environmental variables, traffic intensity, driving style and the infrastructural design all have an influence on the energy consumption. Combining these variables into a network creates complex scenarios, resulting in different optimal routes in terms of energy efficiency and travel time for each scenario. Combined with different personal preferences, personalized route and driving style information could be provided based on the available urban data.

6.2 Discussion

This thesis adds knowledge to a fundamental basic understanding of electric vehicles and their use in cities and is therefore relevant for both scientific and societal purposes. Simultaneously, the findings of this thesis could be used by numerous professionals. Subchapter 6.2.1, 6.2.2 and 6.2.3 emphasize the most important findings for different practical applications and suggest further research in these fields.

Academic understanding has been created by quantifying the relationship between built environment variables and the energy consumption of electric vehicles. A fundamental understanding of our cities and their influence on vehicles is scientifically relevant as research in electric driving is emerging. A gap in knowledge has been filled by not only quantifying the energetic influence of individual elements, but also combining these to create insight in the interconnection of these elements.

A refreshing method has been used, by using methods from multiple research fields. Combining knowledge from electrical engineering, automotive, traffic engineering and the built environment resulted in new insights. The combination of physical calculations, traffic modelling, energy modelling and driving tests created a better understanding at the interfaces of the different research directions. It also led to many new questions being raised. The method has the potential to perform many more research with.

Likewise, the findings are obviously also societally relevant, as any research that accelerates the transition towards electric driving brings society closer to the UN's Sustainable Development Goals. The findings in this research give new insight in the energy consumption of electric vehicles and thus contributes to reducing range anxiety.

Further research topics should focus on the further development and implementation of the energy prediction model. Eboli et al. (2017) mention the underdevelopment of the influence of e.g. socioeconomic and behavioral differences, as well as mood, on the driving style and energy consumption of electric vehicles. Further developing this knowledge would also create more accurate driving style profiles. Another interesting topic is the emergence of automated vehicles and MaaS. The rising amount of interest for these research topics is promising. Yet, still more research is needed in how automated vehicles could positively influence energy consumption on roads, and how the energy prediction models could be game changers for MaaS business models. As this research has created a basic understanding of the energetic influence of basic driving style parameters, further research could determine an optimal driving style for AVs, both individually as well as in a network (such as the positive influence of platoons). Incorporating the model activity-based travel research would be interesting to research how mobility decisions relate to people's activity planning and how route optimization could lead to a more sustainable mobility decision making process. A current limitation of eco-driving is that it assumes that the driver has knowledge about a route. Jimenez (2014) created some first insights in how to inform eco-drivers, however, more research is necessary. Finally, research should be done towards a practical implementation of this thesis. What data is necessary, how to link all this data and how to create traffic management systems which (centralized or decentralized) manage the vehicles. A mesoscopic approach would be interesting as it allows estimations at a larger scale.

6.2.1 Application for navigation companies

This thesis has proven that optimal routes are dependent on many variables. It showed that the shortest route is not always the most sustainable. The generalized cost model proved that the most attractive route also differs for personal preferences. Research and development could be performed to create better navigation systems which could better inform the driver. Not only the calculations in the system, but also the way information is shared through the navigation system and the driver is nudged towards a better driving style and route deserves more research.

6.2.2 Application for car manufacturers

This thesis gives insight in the changing dominant powers working on a vehicle at different routes. It proves that different sustainability strategies to reduce energy consumption on a route work the best for different scenarios. This research could help car manufacturers in making design choices based on the energetic consequences of these choices. Especially on motorways, better aerodynamic performance would save a significant amount of energy. The efficiency of the motor and the regenerative braking also have a big effect on the energy consumption. As bidirectional charging systems are emerging (Hoelen, 2019), reaching a destination with as much energy as possible could make some profit with the remaining energy in the vehicle. Therefore, knowledge about eco-driving and eco-routing combined with vehicle to grid technologies is a promising research field which is currently underdeveloped.

6.2.3 Application for traffic engineers

The thesis gives qualitative insight in the energetic consequences of a road design. It shows that relatively, the road type has a big influence on the energy consumption, especially in winter and on residential roads. Stop-and-go traffic situations (such as speed bumps) should be avoided if possible, as they significantly increase the energy consumption. Other ways of slowing down traffic more constantly, such as different linings or smaller roads, would increase a vehicles energy efficiency. Furthermore, focusing on lower delay times at signalized junctions is proven to be a sustainable measure, especially in winter. Focusing on the vehicle flow on a macro-scale would significantly reduce travel times but has not found to be a very effective sustainability strategy. However, when all cars shift to an eco-driving strategy, traffic flow is affected badly. Therefore, monitoring the traffic flow on a macroscopic level and improving it where necessary is a requirement for improving the energy efficiency of the total network.

6.2.4 Data

Finally, this thesis gives insight in how different datasets could be used to create an energy prediction model, and how much of an influence the variables are on the energy consumption. It gives insights in how different types of data could be used in the models. Very important is correct vehicle data about the rolling resistance of the tires, the aerodynamic drag coefficient and the energetic performance of the vehicle (both discharge as regenerative). Concerning the weather, the outdoor temperature should be used to determine the air density and rolling resistance. Wind has a significant influence, though more research is needed to create a good wind model for cities to properly determine the wind speed and it's direction. The influence of day- and night should not necessarily be modelled, as the energy consumption by the lighting system could be measured by the vehicle itself. The same goes for the climate system. Road slopes also have an effect on the energy consumption, but this effect turned out to be very minor in the Nieuwegein case study, especially if the regenerative braking efficiency is high. Therefore, the advice is to only model significant slopes. Road curvature influences the energy efficiency but is hard to model manually. More research is needed to create faster and more consequent ways of determining the energy consumption at curves, in example by using GIS. Traffic calming measures and signalized intersections should be modeled if energy predictions are to be made. This thesis found that for traffic calming measures, only modelling the bump centerline and the speed reduction would give accurate results.

6.2.5 Limitations

Multiple limitations have been identified during the performance of this research, affecting the accuracy of the results. Limitations have been found in the method, as well as in gathering the data.

First, finding accurate data has been a challenge. There's no complete dataset of electric vehicles containing the powertrain efficiency, regenerative braking efficiency and power use of auxiliaries. Therefore, parts of the model had to be made based on assumptions. For the environmental variables, wind speed and direction could still not be modeled accurately on large scales and therefore remains a gap in the energy prediction model. Infrastructural data had to be acquired manually. As microscopic traffic models contain a lot of information, modelling the Nieuwegein case was very time consuming. Information about infrastructural design elements was often based on visual observations or assumptions. As there seems to be no guideline to create these microscopic models, and no method has been commercialized to automatically create complete microscopic models, this method doesn't seem to be suitable to use on a larger scale. The development of mesoscopic models, combining the strengths of micro- and macroscopic models, is interesting and should be closely kept an eye on.

The knowledge about traffic behavior and driving styles is still too scarce to create a complete overview of all the effects on energy consumption. Driving styles have been generalized into three categories for this thesis, while in practice many combinations of variables representing the driving style are likely to be possible. Further research into the behavior and decision-making process of a driver would be necessary and it would be interesting to see this knowledge to be combined with energy prediction modelling.

Finally, the driving tests for the validation has been done with only one driver. Testing multiple drivers would be extremely valuable since this would not only create a more reliable validation but could also give new insights in the differences in driving style.

References

- Ge, Q. (2016). *Sensitivity analysis in the calibration of microscopic traffic models: From theory to implementation* (Doctoral dissertation, ETH Zurich). Retrieved from <https://pdfs.semanticscholar.org/c455/200e96219cf2aao47d714879f683dcc72901.pdf>
- Solberg, G. (2011). The magic of tesla roadster regenerative braking. Retrieved from https://www.tesla.com/nl_NL/blog/magic-tesla-roadster-regenerative-braking?redirect=no at 27/02/2019
- Clarke, S. (2017). *How green are electric cars? The Guardian*. Retrieved from <https://www.theguardian.com/football/ng-interactive/2017/dec/25/how-green-are-electric-cars>
- Wang, J., Besselink, I., & Nijmeijer, H. (2017). Battery electric vehicle energy consumption prediction for a trip based on route information. *Proceedings of the Institution of Mechanical Engineers, Part D: Journal of Automobile Engineering*, 232(11), 1528-1542. Retrieved from <https://doi.org/10.1177/02F0954407017729938>
- Wang, J., Besselink, I., & Nijmeijer, H. (2015). Electric vehicle energy consumption modelling and prediction based on road information. *World Electric Vehicle Journal*, 7(3), 447-458. Retrieved from <https://doi.org/10.3390/wevj7030447>
- Woo, J.R., Choi, H., & Joongha, A. (2017). Well-to wheel analysis of greenhouse gas emissions for electric vehicles based on electricity generation mix: A global perspective. *Transportation Research Part D: Transport and Environment*, 51, 340-350. Retrieved from <https://doi.org/10.1016/j.trd.2017.01.005> at 05-02-2019
- Turconi, R., Boldrin, A., & Astrup, T. (2013). Life cycle assessment (LCA) of electricity generation technologies: Overview, comparability and limitations. *Renewable and sustainable energy reviews*, 28, 555-565. Retrieved from <https://doi.org/10.1016/j.rser.2013.08.013> at 04/02/2019
- IEA. (2018). *World Energy Balances 2018*. Retrieved from <https://www.iea.org/statistics/?country=NETHLAND&year=2016&category=Energy%20supply&indicator=TPESbySource&mode=chart&dataTable=BALANCES> at 04/02/2019
- Ministerie van Economische Zaken. (2016). *Energierapport: Transitie naar duurzaam*. Retrieved from <https://www.rijksoverheid.nl/binaries/rijksoverheid/documenten/rapporten/2016/01/18/energi-erapport-transitie-naar-duurzaam/energi-erapport-transitie-naar-duurzaam.pdf> at 04/02/2019
- Ke, W., Zhang, S., He, X., Wu, Y., & Hao, J. (2017). Well-to-wheels energy consumption and emissions of electric vehicles: Mid-term implications from real-world features and air pollution control progress. *Applied energy*, 188, 367-377. Retrieved from <https://dx.doi.org/10.1016/j.apenergy.2016.12.011> at 07/02/2019
- Bauer, C., Hofer, J., Althaus, H. J., Del Duce, A., & Simons, A. (2015). The environmental performance of current and future passenger vehicles: Life cycle assessment based on a novel scenario analysis framework. *Applied energy*, 157, 871-883. Retrieved from <https://doi.org/10.1016/j.apenergy.2015.01.019>
- Faria, R., Marques, P., Moura, P., Freire, F., Delgado, J., & de Almeida, A. T. (2013). Impact of the electricity mix and use profile in the life-cycle assessment of electric vehicles. *Renewable and Sustainable Energy Reviews*, 24, 271-287. Retrieved from <https://doi.org/10.1016/j.rser.2013.03.063> at 07/02/2019
- Bartolozzi, I., Rizzi, F., & Frey, M. (2013). Comparison between hydrogen and electric vehicles by life cycle assessment: A case study in Tuscany, Italy. *Applied energy*, 101, 103-111. Retrieved from <https://doi.org/10.1016/j.apenergy.2012.03.021> at 07/02/2019
- Rogers, E. M. (1962). *Diffusion of innovations*. *The Free Press*. Retrieved from <https://teddykw2.files.wordpress.com/2012/07/everett-m-rogers-diffusion-of-innovations.pdf> at 05/02/2019

- Lin, B., & Wu, W. (2018). Why people want to buy electric vehicle: An empirical study in first-tier cities of China. *Energy Policy*, 112, 233-241. Retrieved from <https://doi.org/10.1016/j.enpol.2017.10.026> at 06/02/2019
- Deloitte. (2019). Battery Electric Vehicles. New market. New entrants. New challenges. Retrieved from <https://www2.deloitte.com/content/dam/Deloitte/uk/Documents/manufacturing/deloitte-uk-battery-electric-vehicles.pdf>
- Denning, L. (2018). All Roads, Electric or Oil, Lead to China. *Bloomberg Opinion. Technology & Ideas*. Retrieved from <https://www.bloomberg.com/opinion/articles/2019-01-31/brexit-leaves-u-k-investors-in-purgatory> at 05/02/2019
- Butler, N. (2018). Why the future of electric cars lies in China. *Financial Times*. Retrieved from <https://www.ft.com/content/1c31817e-b5a4-11e8-b3ef-799c8613f4a1> at 05/02/2019
- Cluzel, C., & Douglas, C. (2012). Cost and performance of EV batteries. Final Report for the Committee on Climate Change. *Element Energy Limited*. Retrieved from <https://www.theccc.org.uk/archive/aws/IA&S/CCC%20battery%20cost%20Element%20Energy%20report%20March2012%20Public.pdf> at 05/02/2019
- Chandler, R. E., Herman, R., & Montroll, E. W. (1958). Traffic dynamics: studies in car following. *Operations research*, 6(2), 165-184. Retrieved from <https://www.jstor.org/stable/167610> at 11/03/2019
- Burghout, W. (2004). *Hybrid microscopic-mesosopic traffic simulation* (Doctoral dissertation, KTH). Retrieved from <https://doi.org/10.1177/0361198105193400123> at 11/03/2019
- Van der Bijl, B. (2018). Nieuw realtime model voor verkeerslichten reduceert wachttijd en CO₂ uitstoot. *Sweco*. Retrieved from <https://www.sweco.nl/nieuws/nieuwsartikelen/nieuw-realtime-model-voor-verkeerslichten-reduceert-wachttijd-en-co2-uitstoot/> at 11/03/2019
- Jonkers, E., Nellthorp, J., Wilmlink, I., & Olstam, J. (2018). Evaluation of eco-driving systems: A European analysis with scenarios and micro simulation. *Case Studies on Transport Policy*, 6(4), 629-637. Retrieved from <http://dx.doi.org/10.1016/j.cstp.2018.08.001> at 11/03/2019
- Hofer, C., Jäger, G., & Füllsack, M. (2018). Large scale simulation of CO₂ emissions caused by urban car traffic: an agent-based network approach. *Journal of Cleaner Production*, 183, 1-10. Retrieved from <https://doi.org/10.1016/j.jclepro.2018.02.113> at 11/03/2019
- Hamdar, S. (2012). Driver behavior modeling. *Handbook of Intelligent Vehicles*, 537-558. Retrieved from https://doi.org/10.1007/978-0-85729-085-4_20 at 11/03/2019
- Fellendorf, M., & Vortisch, P. (2010). Microscopic Traffic Flow Simulator VISSIM. *International Series in Operations Research & Management Science*, 145. Retrieved from https://doi.org/10.1007/978-1-4419-6142-6_2
- Immers, L.H., & Logghe, S. (2002). Traffic Flow Theory. Katholieke Universiteit Leuven. Retrieved from <https://www.mech.kuleuven.be/cib/verkeer/dwn/Huipart3.pdf> at 08/03/2019
- Saifuzzaman, M., & Zheng, Z. (2014). Incorporating human-factors in car-following models: a review of recent developments and research needs. *Transportation research part C: emerging technologies*, 48, 379-403. Retrieved from <http://dx.doi.org/10.1016/j.trc.2014.09.008>
- Barth, M., & Boriboonsomsin, K. (2009). Energy and emissions impacts of a freeway-based dynamic eco-driving system. *Transportation Research Part D: Transport and Environment*, 14(6), 400-410. Retrieved from <https://doi.org/10.1016/j.trd.2009.01.004> at 25-06-2019
- Olstam, J. J., & Tapani, A. (2004). Comparison of Car-following models. *Swedish National Road and Transport Research Institute*. Linköping: Sweden. Retrieved from <https://www.diva-portal.org/smash/get/diva2:673977/FULLTEXT01.pdf> at 17-06-2019
- Gazis, D. C., Herman, R., & Potts, R. B. (1959). Car-following theory of steady-state traffic flow. *Operations research*, 7(4), 499-505. Retrieved from <https://www.jstor.org/stable/166948> at 11/03/2019

- Gipps, P. G. (1981). A behavioural car-following model for computer simulation. *Transportation Research Part B: Methodological*, 15(2), 105-111. Retrieved from http://turing.iimas.unam.mx/sos/sites/default/files/Gipps_ABehaviouralCarFollowingModel.pdf at 11/03/2019
- Nagel, K., & Schreckenberg, M. (1992). A cellular automaton model for freeway traffic. *Journal de physique I*, 2(12), 2221-2229. Retrieved from <https://dx.doi.org/10.1051/jp1:1992277> at 11-03-2019
- Krauss, S., Wagner, P., & Gawron, C. (1997). Metastable states in a microscopic model of traffic flow. *Physical Review E*, 55(5), 5597. Retrieved from <https://doi.org/10.1103/PhysRevE.55.5597> at 11/03/2019
- Treiber, M., Kesting, A., & Helbing, D. (2006). Delays, inaccuracies and anticipation in microscopic traffic models. *Physica A: Statistical Mechanics and its Applications*, 360(1), 71-88. Retrieved from <https://doi.org/10.1016/j.physa.2005.05.001> at 11/03/2019
- PTV Group. (2016). Training PTV VISSIM Basic course. Retrieved at 11/03/2019
- Yang, Q., & Koutsopoulos, H. N. (1996). A microscopic traffic simulator for evaluation of dynamic traffic management systems. *Transportation Research Part C: Emerging Technologies*, 4(3), 113-129. Retrieved from [https://doi.org/10.1016/S0968-090X\(96\)00006-X](https://doi.org/10.1016/S0968-090X(96)00006-X) at 12/03/2019
- Kim, S. J. (2006). Simultaneous calibration of a microscopic traffic simulation model and OD matrix (Doctoral dissertation). Texas A&M University. Retrieved from <https://core.ac.uk/download/pdf/4271380.pdf> at 17-06-2019
- Zhu, M., Wang, X., & Wang, Y. (2018). Human-like autonomous car-following model with deep reinforcement learning. *Transportation research part C: emerging technologies*, 97, 348-368. Retrieved from <https://arxiv.org/ftp/arxiv/papers/1901/1901.00569.pdf> at 17-06-2019
- Ahmed, K. I. (1999). Modeling drivers' acceleration and lane changing behavior. Retrieved from <http://hdl.handle.net/1721.1/96662> at 11/03/2019
- Hidas, P. (2004). Evaluation of lane changing and merging in microsimulation models. In *Australasian Transport Research Forum (ATRF)*, 27. Retrieved from https://atrf.info/papers/2004/2004_Hidas.pdf at 13/03/2019
- Gipps, P. G. (1986). A model for the structure of lane-changing decisions. *Transportation Research Part B: Methodological*, 20(5), 403-414. Retrieved from [https://doi.org/10.1016/0191-2615\(86\)90012-3](https://doi.org/10.1016/0191-2615(86)90012-3) at 11/03/2019
- Toledo, T., Koutsopoulos, H. N., & Ben-Akiva, M. E. (2003). Modeling integrated lane-changing behavior. *Transportation Research Record*, 1857(1), 30-38. Retrieved from <https://doi.org/10.3141/1857-04> at 12/03/2019
- Yang, Q., Koutsopoulos, H. N., & Ben-Akiva, M.E. (1999). A Simulation Laboratory for Evaluating Dynamic Traffic Management Systems. Retrieved from <https://its.mit.edu/sites/default/files/documents/MITSIM1.PDF> at 12/03/2019
- Kesting, A., Treiber, M., & Helbing, D. (2007). General lane-changing model MOBIL for car-following models. *Transportation Research Record*, 1999(1), 86-94. Retrieved from <https://doi.org/10.3141/1999-10>
- Mahapatra, G., & Maurya, A. K. (2013). Study of vehicles lateral movement in non-lane discipline traffic stream on a straight road. *Procedia-social and behavioral sciences*, 104, 352-359. Retrieved from <https://doi.org/10.1016/j.sbspro.2013.11.128> at 13/03/2019
- PTV Group. (n.d.). PTV Vissim FAQs. #VIS19266. Retrieved from <http://vision-traffic.ptvgroup.com/en-us/training-support/support/ptv-vissim/faqs/visfaq/show/VIS19266/> at 22/02/2019
- Lin, N., Liu, H. D., & Gong, C. Q. (2013). Research and Simulation on Drivers' Route Choice Behavior Cognition Model. *arXiv preprint arXiv:1303.2764*. Retrieved from <https://arxiv.org/ftp/arxiv/papers/1303/1303.2764.pdf> at 26-06-2019
- Bert, E., Lavoc, E., Torday, R., Torday, A., & Dumont, A. G. (2005). Calibration of urban network microsimulation models. In *5th Swiss Transport Research Conference, Monte Verita*. Retrieved

from

[http://www.academia.edu/20285280/Calibration of urban network microsimulation models](http://www.academia.edu/20285280/Calibration_of_urban_network_microsimulation_models) at 13/03/2019

Noto, M., & Sato, H. (2000). A method for the shortest path search by extended Dijkstra algorithm. In *Systems, Man, and Cybernetics, 2000 IEEE International Conference on* (Vol. 3, pp. 2316-2320). IEEE. Retrieved from <https://doi.org/10.1109/ICSMC.2000.886462> at 13/03/2019

Dijkstra, E., (1959). A note on two problems in connexion with graphs. *Numerische Mathematik*. 1. 269-271. Retrieved from <http://www-m3.ma.tum.de/foswiki/pub/MN0506/WebHome/dijkstra.pdf> at 13/03/2019

Singal, P., & Chhillar, R. S. (2014). Dijkstra Shortest Path Algorithm using Global Positioning System. *International Journal of Computer Applications*, 101(6), 12-18. Retrieved from <https://pdfs.semanticscholar.org/1540/945b4b16d9b485e410ff4a6730a7c103f399.pdf> at 13-03-2019

Nazari, S., Meybodi, M. R., Salehigh, M. A., & Taghipour, S. (2008, November). An advanced algorithm for finding shortest path in car navigation system. In *Intelligent Networks and Intelligent Systems, 2008. ICINIS'08. First International Conference on* (pp. 671-674). IEEE. Retrieved from <https://doi.org/10.1109/ICINIS.2008.147> at 13/03/2019

Bellman, R. (1958). On a routing problem. *Quarterly of applied mathematics*, 16(1), 87-90. Retrieved from <https://apps.dtic.mil/dtic/tr/fulltext/u2/606258.pdf> at 13/03/2019

Ford Jr, L. R. (1956). *Network flow theory* (No. P-923). Rand Corp Santa Monica Ca. Retrieved from <https://apps.dtic.mil/dtic/tr/fulltext/u2/422842.pdf> at 13/03/2019

Yen, J. Y. (1971). Finding the k shortest loopless paths in a network. *Management Science*, 17(11), 712-716. Retrieved from <https://www.jstor.org/stable/2629312> at 13/03/2019

Ben-Akiva, M.E., Ramming, M.S. & Bekhor, S. (2004). Route Choice Models. In *Human Behavior and Traffic Networks* (pp. 23-45). Retrieved from <https://link.springer.com/content/pdf/10.1007%2F978-3-662-07809-9.pdf> at 13/03/2019

Scholten, J. (2010). Verkeersoverlast inzichtelijk door EnViVer – Vlot en fris op weg. *Dag en Nacht Mobiliteit*. 3. Retrieved from <http://vialis.organiq.nl/site/assets/files/1237/pag.pdf> at 13/03/2019

Gao, Y. (2008). Calibration and comparison of the VISSIM and INTEGRATION microscopic traffic simulation models (Doctoral dissertation). *Virginia Tech*. Retrieved from <https://pdfs.semanticscholar.org/96e2/379081169e217aid7a31b9efb737f7fdob54.pdf> at 17-06-2019

Higgs, B., Abbas, M. M., & Medina, A. (2011). Analysis of the Wiedemann car following model over different speeds using naturalistic data. In *Procedia of RSS Conference* (pp. 1-22). Retrieved from <http://onlinepubs.trb.org/onlinepubs/conferences/2011/RSS/3/Higgs,B.pdf> at 26-06-2019

Boriboonsomsin, K., Barth, M. J., Zhu, W., & Vu, A. (2012). Eco-routing navigation system based on multisource historical and real-time traffic information. *IEEE Transactions on Intelligent Transportation Systems*, 13(4), 1694-1704. Retrieved from <https://doi.org/10.1109/TITS.2012.2204051>

Bysveen, M. (2017). *Vehicle speed prediction models for consideration of energy demand within road design* (Master's thesis, NTNU). Retrieved from <https://pdfs.semanticscholar.org/1178/f0573e729b9329ff3e4914f9410f83d2ae8d.pdf>

Fitzpatrick, K., Carlson, P., Brewer, M. A., Wooldridge, M. D., & Miaou, S. P. (2003). NCHRP report 504: Design speed, operating speed, and posted speed practices. *Transportation Research Board of the National Academies*, Washington, DC. Retrieved from http://onlinepubs.trb.org/onlinepubs/nchrp/nchrp_rpt_504.pdf

Psarianos, B., & Garcia, A. (2011). Speed Models in Europe. In *Transportation Research Board (Ed.), Modeling Operating Speed: Synthesis Report* (pp. 43-75). Washington DC, Washington: TRB. Retrieved from <http://onlinepubs.trb.org/onlinepubs/circulars/ec151.pdf>

- Csikós, A., Viharos, Z. J., Kis, K. B., Tettamanti, T., & Varga, I. (2015, June). Traffic speed prediction method for urban networks—an ANN approach. In *2015 International Conference on Models and Technologies for Intelligent Transportation Systems (MT-ITS)* (pp. 102-108). IEEE. Retrieved from <https://doi.org/10.1109/MTITS.2015.7223243> at 13/03/2019
- Lin, L., Li, J., Chen, F., Ye, J., & Huai, J. (2018). Road traffic speed prediction: a probabilistic model fusing multi-source data. *IEEE Transactions on Knowledge and Data Engineering*, 30(7), 1310-1323. Retrieved from <https://doi.org/10.1109/TKDE.2017.2718525> at 15/03/2019
- Tang, J., Liu, F., Zou, Y., Zhang, W., & Wang, Y. (2017). An improved fuzzy neural network for traffic speed prediction considering periodic characteristic. *IEEE Transactions on Intelligent Transportation Systems*, 18(9), 2340-2350. Retrieved from <https://doi.org/10.1109/TITS.2016.2643005> at 15/03/2019
- Guo, C., Yang, B., Andersen, O., Jensen, C. S., & Torp, K. (2015). Ecomark 2.0: empowering eco-routing with vehicular environmental models and actual vehicle fuel consumption data. *GeoInformatica*, 19(3), 567-599. Retrieved from <https://doi.org/10.1007/s10707-014-0221-7> at 15/03/2019
- Barth, M., An, F., Younglove, T., Scora, G., Levine, C., Ross, M., & Wenzel, T. (2000). The development of a comprehensive modal emissions model. *NCHRP web-only document*, 122, 25-11. Retrieved from http://onlinepubs.trb.org/onlinepubs/nchrp/nchrp_w122.pdf
- EPA. (n.d.-b). Description and History of the MOBILE Highway Vehicle Emission Factor Model. Retrieved from <https://www.epa.gov/moves/description-and-history-mobile-highway-vehicle-emission-factor-model>
- Scora, G., & Barth, M. (2006). Comprehensive Modal Emission Model (CMEM) Version 3.01 User's Guide. *University of California Riverside Center for Environmental Research and Technology*, 23, 24. Retrieved from <https://www.cert.ucr.edu/transportation-systems-vehicle-infrastructure-interaction/innovative-vehicle-evaluation-techniques>
- Morrissey, P., Weldon, P., & O'Mahony, M. (2016). Future standard and fast charging infrastructure planning: An analysis of electric vehicle charging behaviour. *Energy Policy*, 89, 257-270. Retrieved from <https://doi.org/10.1016/j.enpol.2015.12.001>
- Jourard, R., Jost, P., Hickman, J., & Hassel, D. (1995). Hot passenger car emissions modelling as a function of instantaneous speed and acceleration. *Science of the Total Environment*, 169(1-3), 167-174. Retrieved from [https://doi.org/10.1016/0048-9697\(95\)04645-H](https://doi.org/10.1016/0048-9697(95)04645-H)
- Ericsson, E. (2001). Independent driving pattern factors and their influence on fuel-use and exhaust emission factors. *Transportation Research Part D: Transport and Environment*, 6(5), 325-345. Retrieved from [https://doi.org/10.1016/S1361-9209\(01\)00003-7](https://doi.org/10.1016/S1361-9209(01)00003-7)
- Brundell-Freij, K., & Ericsson, E. (2005). Influence of street characteristics, driver category and car performance on urban driving patterns. *Transportation Research Part D: Transport and Environment*, 10(3), 213-229. Retrieved from <https://doi.org/10.1016/j.trd.2005.01.001>
- Fukushima, A., Yano, T., Imahara, S., Aisu, H., Shimokawa, Y., & Shibata, Y. (2018). Prediction of energy consumption for new electric vehicle models by machine learning. *IET Intelligent Transport Systems*, 12(9), 1174-1180. Retrieved from <https://doi.org/10.1049/iet-its.2018.5169> at 15/03/2019
- Pan, C., Dai, W., Chen, L., Chen, L., & Wang, L. (2017). Driving range estimation for electric vehicles based on driving condition identification and forecast. *AIP Advances*, 7(10), 105206. Retrieved from <https://doi.org/10.1063/1.4993945>
- Foiadelli, F., Longo, M., & Miraftabzadeh, S. (2018). Energy Consumption Prediction of Electric Vehicles Based on Big Data Approach. In *2018 IEEE International Conference on Environment and Electrical Engineering and 2018 IEEE Industrial and Commercial Power Systems Europe (EEEIC/I&CPS Europe)* (pp. 1-6). IEEE. Retrieved from <https://doi.org/10.1109/EEEIC.2018.8494573> at 15/03/2019
- Ericsson, E. (2000). *Urban driving patterns-characterisation, variability and environmental implications* (Doctoral dissertation, Lund University). Retrieved at

- Lee, T. K., Adornato, B., & Filipi, Z. S. (2011). Synthesis of real-world driving cycles and their use for estimating PHEV energy consumption and charging opportunities: Case study for Midwest/US. *IEEE Transactions on vehicular technology*, 60(9), 4153-4163. Retrieved from <https://doi.org/10.1109/TVT.2011.2168251>
- Wu, X., Freese, D., Cabrera, A., & Kitch, W. A. (2015). Electric vehicles' energy consumption measurement and estimation. *Transportation Research Part D: Transport and Environment*, 34, 52-67. Retrieved from <https://doi.org/10.1016/j.trd.2014.10.007>
- Genikomsakis, K. N., & Mitrentsis, G. (2017). A computationally efficient simulation model for estimating energy consumption of electric vehicles in the context of route planning applications. *Transportation Research Part D: Transport and Environment*, 50, 98-118. Retrieved from <https://doi.org/10.1016/j.trd.2016.10.014>
- Larminie, J., & Lowry, J. (2012). *Electric vehicle technology explained*. John Wiley & Sons. Retrieved from https://books.google.nl/books?hl=nl&lr=&id=FwXcCmT1OQUC&oi=fnd&pg=PR13&dq=larminie+lowry+2012&ots=q1QFiPncdH&sig=a_x77QZ7CwPKcZ-8JOfxPuprhc#v=onepage&q=larminie%20lowry%202012&f=false
- Irimescu, A., Mihon, L., & Pădure, G. (2011). Automotive transmission efficiency measurement using a chassis dynamometer. *International Journal of Automotive Technology*, 12(4), 555-559. <https://doi.org/10.1007/s12239-011-0065-1> at 15/03/2019
- Argonne National Laboratory. (2015). Downloadable Dynamometer Database (D³) - Test Summary Sheet. Retrieved from <https://app.box.com/embed/s/p26vffirf2yu2bft5s8v2vh5lxy2d5hb/file/36151616214>
- Lohse-Busch, H., Stutenberg, K., Duoba, M., Rask, E., Jehlik, F., & Keller, G. (2013). Chassis Dynamometer Testing Reference Document. *U.S. Department of Energy: Energy Efficiency and Renewable Energy*. Retrieved from <https://anl.app.box.com/s/5tll40tjhhhtoj2tgon4y3fkwdbs4m3> at 24-06-2019
- Xu, G., Xu, K., Zheng, C., Zhang, X., & Zahid, T. (2016). Fully electrified regenerative braking control for deep energy recovery and maintaining safety of electric vehicles. *IEEE Transactions on Vehicular Technology*, 65(3), 1186-1198. Retrieved from <https://ieeexplore.ieee.org/abstract/document/7055278> at 27-02-2019
- Solberg, G. (2007). The magic of tesla roadster regenerative braking. Retrieved from https://www.tesla.com/nl_NL/blog/magic-tesla-roadster-regenerative-braking?redirect=no at 27/02/2019
- Fiori, C., Ahn, K., & Rakha, H. A. (2018). Optimum routing of battery electric vehicles: Insights using empirical data and microsimulation. *Transportation Research Part D: Transport and Environment*, 64, 262-272. Retrieved from <https://doi.org/10.1016/j.trd.2017.08.007> at 04/03/2019
- Llana, C. (2015). A magnetic braking primer: BMW i3 versus Tesla 70D. Retrieved from <https://www.bmwblog.com/2015/07/10/a-magnetic-braking-primer-bmw-i3-versus-tesla-70d/> at 27/02/2019
- Schmitz, M., Jagiellowicz, M., Maag, C., & Hanig, M. (2012). The impact of different pedal solutions for supporting efficient driving with electric vehicles. In *European Conference on Human Centered Design for Intelligent Transport Systems* PV Mora, J.-F. Pace & L. Mendoza, Valencia, Spain (pp. 21-28). Retrieved from http://www2.psychologie.uni-wuerzburg.de/izvw/texte/2012_schmitz_jagiellowicz_maag_hanig_HUMANIST.pdf at 04/03/2019
- Cocron, P., Bühler, F., Franke, T., Neumann, I., Dielmann, B., & Krems, J. F. (2013). Energy recapture through deceleration-regenerative braking in electric vehicles from a user perspective. *Ergonomics*, 56(8), 1203-1215. Retrieved from <http://dx.doi.org/10.1080/00140139.2013.803160> at 27/02/2019

- Lv, C., Zhang, J., Li, Y., & Yuan, Y. (2015). Novel control algorithm of braking energy regeneration system for an electric vehicle during safety-critical driving maneuvers. *Energy conversion and management*, 106, 520-529. Retrieved from <https://doi.org/10.1016/j.enconman.2015.09.062>
- González-Gil, A., Palacin, R., Batty, P., & Powell, J. P. (2014). A systems approach to reduce urban rail energy consumption. *Energy Conversion and Management*, 80, 509-524. Retrieved from <https://doi.org/10.1016/j.enconman.2014.01.060> at 04/03/2019
- Walsh, C., Carroll, S., Eastlake, A., & Blythe, P. (2010). Electric vehicle driving style and duty variation performance study. *University of Sheffield*. Retrieved from <https://pdfs.semanticscholar.org/d8fa/of2fe997b567043624907c602f3ffb235b1.pdf> at 04/03/2019
- Romm, J. J., & Frank, A. A. (2006). Hybrid vehicles gain traction. *Scientific American*, 294(4), 72-79. Retrieved from <http://shadow.eas.gatech.edu/~kcobb/energy/Readings/Romm%20and%20Frank.pdf> at 04/03/2019
- Wager, G., Whale, J., & Braunl, T. (2018). Performance evaluation of regenerative braking systems. *Proceedings of the Institution of Mechanical Engineers, Part D: Journal of Automobile Engineering*, 232(10), 1414-1427. Retrieved from <https://journals.sagepub.com/doi/pdf/10.1177/0954407017728651> at 04/03/2019
- Besselink, I. (2019). Energy Consumption Calculations. Retrieved at 27-02-2019
- Evtimov, I., Ivanov, R., & Sapundjiev, M. (2017). Energy consumption of auxiliary systems of electric cars. In *MATEC Web of Conferences* (Vol. 133, p. 06002). EDP Sciences. Retrieved from https://www.matec-conferences.org/articles/mateconf/pdf/2017/47/mateconf_bultrans2017_06002.pdf at 07/03/2019
- Kavalchuk, I., Arisoy, H., Stojcevski, A., & Oo, A. M. T. (2015). Advanced simulation of power consumption of electric vehicles. *World Academy of Science, Engineering and Technology, International Journal of Electrical, Computer, Energetic, Electronic and Communication Engineering*, 9(1), 53-59. Retrieved from <https://doi.org/10.1109/ICCAD.2014.7001349> at 26/03/2019
- BMW. (2018). Technical specifications. BMW i3 (120 Ah). Retrieved from <https://www.press.bmwgroup.com/global/article/attachment/To284828EN/415571> at 22/02/2019
- Reichmuth, D. (2016). Do Electric Cars Work in Cold Weather? Get the Facts... Retrieved from <https://blog.ucsusa.org/dave-reichmuth/electric-cars-cold-weather-temperatures>
- Vražić, M., Barić, O., & Vrtič, P. (2014). Auxiliary systems consumption in electric vehicle. *Przegląd elektrotechniczny*, 90(12), 172-175. Retrieved from <http://red.pe.org.pl/articles/2014/12/42.pdf>
- Schoettle, B., Sivak, M., & Fujiyama, Y. (2008). LEDs and power consumption of exterior automotive lighting: Implications for gasoline and electric vehicles. Retrieved from <http://hdl.handle.net/2027.42/61187>
- Geringer, B., & Tober, W. K. (2012). Batterieelektrische Fahrzeuge in der Praxis-Kosten, Reichweite, Umwelt, Komfort. Österreichischen Vereins für Kraftfahrzeugtechnik. Retrieved from http://toolbox.electrosuisse.ch/forum/download/id/122_c94bb17a5fce36cf882bd20foe390eaf.pdf
- Jiménez, F., & Cabrera-Montiel, W. (2014). System for road vehicle energy optimization using real time road and traffic information. *Energies*, 7(6), 3576-3598. Retrieved from <https://doi.org/10.3390/en7063576>
- Barkenbus, J. N. (2010). Eco-driving: An overlooked climate change initiative. *Energy Policy*, 38(2), 762-769. Retrieved from <https://doi.org/10.1016/j.enpol.2009.10.021> at 12/02/2019

- De Vlieger, I. (1997). On board emission and fuel consumption measurement campaign on petrol-driven passenger cars. *Atmospheric Environment*, 31(22), 3753-3761. Retrieved from [https://doi.org/10.1016/S1352-2310\(97\)00212-4](https://doi.org/10.1016/S1352-2310(97)00212-4)
- Gundana, D., Dollar, R. A., & Vahidi, A. (2018, November). To Merge Early or Late: Analysis of Traffic Flow and Energy Impact in a Reduced Lane Scenario. In *2018 21st International Conference on Intelligent Transportation Systems (ITSC)* (pp. 525-530). IEEE. Retrieved from <https://doi.org/10.1109/ITSC.2018.8569407> at 11/03/2019
- Kedar-Dongarkar, G., & Das, M. (2012). Driver classification for optimization of energy usage in a vehicle. *Procedia Computer Science*, 8, 388-393. Retrieved from <https://doi.org/10.1016/j.procs.2012.01.077> at 04/03/2019
- Fonseca, N., Casanova, J., & Espinosa, F. (2010). Influence of driving style on fuel consumption and emissions in diesel-powered passenger car. Retrieved from <https://core.ac.uk/download/pdf/11999517.pdf> at 06/03/2019
- Reymond, G., Kemeny, A., Droulez, J., & Berthoz, A. (2001). Role of lateral acceleration in curve driving: Driver model and experiments on a real vehicle and a driving simulator. *Human factors*, 43(3), 483-495. Retrieved from <https://doi.org/10.1518/027001872001775898188> at 25-06-2019
- KNMI. (2018). Weerstatistieken De Bilt – 2018. Retrieved from <https://weerstatistieken.nl/de-bilt/2018>
- KNMI. (2019). Langjarig gemiddelden – normale waarden temperatuur. Retrieved from <https://www.knmi.nl/nederland-nu/weer/waarschuwingen-en-verwachtingen/normalentabel> at 03-06-2019
- Blocken, B. (2014). 50 years of computational wind engineering: past, present and future. *Journal of Wind Engineering and Industrial Aerodynamics*, 129, 69-102. Retrieved from <https://doi.org/10.1016/j.jweia.2014.03.008> at 03-06-2019
- Michelin. (2003). The tyre: Rolling resistance and fuel savings. Clermond-Ferrand: Société de Technologie Michelin. Retrieved from http://www.dimnp.unipi.it/guiggiani-m/Michelin_Tire_Rolling_Resistance.pdf at 08/03/2019
- Ejsmont, J., Goubert, L., Ronowski, G., & Świeczko-Żurek, B. (2016). Ultra low noise poroelastic road surfaces. *Coatings*, 6(2), 18. Retrieved from <https://www.mdpi.com/2079-6412/6/2/18> at 07/03/2019
- Ejsmont, J., Świeczko-Żurek, B., Ronowski, G., & Taryma, S. (2015). Results of rolling resistance laboratory drum tests. Retrieved from <http://www.rosanne-project.eu/ajax/DownloadHandlerFM.php/downloadFile?id=11823> at 07/03/2019
- Ejsmont, J., Mioduszewski, P., Ronowski, G., Taryma, S., & Świeczko-Żurek, B. (2015). Final report on noise and rolling resistance. Retrieved from http://persuade.fehrl.org/?m=3&mode=download&id_file=18280 at 07/03/2019
- Goubert, L., & Sandberg, U. (2016). Construction and Performance of Poroelastic Road Surfaces Offering 10 dB of Noise Reduction. Retrieved from http://persuade.fehrl.org/?m=3&mode=download&id_file=18291 at 07/03/2019
- Sandberg, U., Świeczko-Żurek, B., Ejsmont, J. A., & Ronowski, G. (2013). Tyre/road noise reduction of poroelastic road surface tested in a laboratory. In *Proc. of Acoustics* (pp. 1-8). Retrieved from http://www.acoustics.asn.au/conference_proceedings/AAS2013/papers/p98.pdf at 07/03/2019
- Bendtsen, H. (2015). Performance of PERS on the road [PowerPoint]. Retrieved from http://persuade.fehrl.org/index.php?m=3&mode=download&id_file=17326 at 07/03/2019
- Groenendijk, J. (2010). Een goed of een slecht wegdek... wie betaalt de rekening? Retrieved from <http://www.asfaltblij.nl/media/1432/2010-een-goed-of-een-slecht-wegdek-wie-betaalt-de-rekening.pdf> at 07/03/2019
- Rijkswaterstaat. (n.d.). Zoab. Retrieved from <https://www.rijkswaterstaat.nl/wegen/wegbeheer/aanleg-wegen/zoab.aspx> at 07/03/2019

- Liu, K., Yamamoto, T., & Morikawa, T. (2017). Impact of road gradient on energy consumption of electric vehicles. *Transportation Research Part D: Transport and Environment*, 54, 74-81. Retrieved from <https://doi.org/10.1016/j.trd.2017.05.005> 18-06-2019
- Johnson, L., & Nedzesky, A. J. (2004). A comparative study of speed humps, speed slots and speed cushions. In *ITE Annual Meeting*. Retrieved from https://nacto.org/docs/usdg/study_speed_humps_speed_slots_and_speed_cushions_johnson.pdf at 25/02/2019
- Gupta, A. (2014). Study on speed profile across speed bumps. Retrieved from <http://ethesis.nitrkl.ac.in/5881/1/e-74.pdf> at 25/02/2019
- Ahn, K., & Rakha, H. (2009). A field evaluation case study of the environmental and energy impacts of traffic calming. *Transportation Research Part D: Transport and Environment*, 14(6), 411-424. Retrieved from https://www.researchgate.net/publication/248320070_A_field_evaluation_case_study_of_the_environmental_and_energy_impacts_of_traffic_calming at 25/02/2019
- Struyk Verwo Infra. (n.d.). CROW Gerelateerde Verkeersdrempels & -plateaus. Retrieved from <https://www.struykverwoinfra.nl/files/publicaties/Folder-Verkeersdrempels-en-plateaus.pdf> at 08/03/2019
- Smeed, R. J. (1949). Some statistical aspects of road safety research. *Journal of the Royal Statistical Society. Series A (General)*, 112(1), 1-34. Retrieved from <https://www.jstor.org/stable/2984177> at 11/03/2019
- C/CAG of San Mateo County. (2005). Final Congestion Management Program for 2005. Retrieved from <http://ccag.ca.gov/programs/transportation-programs/congestion-management/> at 08/03/2019
- Rijkswaterstaat. (2018). Handboek Autonetwerken 3.3. Retrieved at 25/02/2019
- Sugiyama, Y., Fukui, M., Kikuchi, M., Hasebe, K., Nakayama, A., Nishinari, K., ... & Yukawa, S. (2008). Traffic jams without bottlenecks—experimental evidence for the physical mechanism of the formation of a jam. *New journal of physics*, 10(3), 033001. Retrieved from <https://iopscience.iop.org/article/10.1088/1367-2630/10/3/033001/meta> at 08/03/2019
- Hoogendoorn, S., & Knoop, V. (2013). Traffic flow theory and modelling. In van Wee, B., Annema, J.A., & Banister, D. (Eds.), *The Transport System and Transport Policy: An Introduction* (pp. 125-159). Cheltenham, UK: Edward Elgar Publishing. Retrieved from http://victorknoop.eu/research/papers/chapter_vanwee.pdf at 25/02/2019
- Schoenmakers, M.J. (2018). Automated Vehicles and Infrastructure Design. Retrieved from <https://www.ofcoursecme.nl/?mdocs-file=3999> at 25/02/2019
- Heijne, S. (2014). Veel te dicht op elkaar, maar toch veilig. *De Volkskrant*. Retrieved from <https://www.volkskrant.nl/nieuws-achtergrond/veel-te-dicht-op-elkaar-maar-toch-veilig~bfff95839/> at 08/03/2019
- University of Alabama. (n.d.). How to Conduct a Literature Review: Types of Literature Reviews. *University Libraries*. Retrieved from <https://guides.lib.ua.edu/c.php?g=39963&p=253698> at 05-06-2019
- Actueel Hoogtebestand Nederland. (n.d.). AHN Viewer. Retrieved from <https://ahn.arcgisonline.nl/ahnviewer/> at 22-05-2019
- Syntus Utrecht. (2018). Syntus Provincie Utrecht 2017-2018. Retrieved from https://www.syntusutrecht.nl/getmedia/126c200d-7279-49ba-8313-3ee369d7fb9a/Syntus_Provincie_Utrecht_2017_2018_v5b.pdf at 05-06-2019
- Huisman, H. (2018). Verkeersmodel Regio Utrecht VRU3.4: Technische rapportage en verantwoording. *Gemeente Utrecht*. Retrieved from <https://www.utrecht.nl/fileadmin/uploads/documenten/bestuur-en-organisatie/publicaties/onderzoek-en-cijfers/2018-10-rapport-verkeersmodelregio-utrecht-VRU3-4.pdf> at 05-06-2019

- AlleCijfers.nl. (2019). Informatie buurt Fokkesteeg. Retrieved from <https://allecijfers.nl/buurt/fokkesteeg-nieuwegein/>
- GreenChoice. (n.d.). Salderingsregeling Zonnepanelen. Retrieved from <https://www.greenchoice.nl/zonnepanelen/salderingsregeling/> at 28-05-2019
- Fastned. (2019). Prijzen Nederland en Duitsland. Retrieved from <https://fastned.nl/nl/kies-je-prijsplan> at 28-05-2019
- Westeneng, A. (2019). De kosten voor het opladen van een elektrische auto kunnen enorm verschillen – zo duur is het vergeleken met rijden op diesel en benzine. *Business Insider*. Retrieved from <https://www.businessinsider.nl/opladen-elektrische-auto-kosten-benzine-diesel/> at 28-05-2019
- Klut, A. (2016). Wat kost het opladen van een elektrische auto? *Change magazine*. Retrieved from http://www.changemagazine.nl/klimaatkennis/mobiliteit_en_energie/wat-kost-het-opladen-van-een-elektrische-auto at 28-05-2019
- Mathieu, L. (2018). Roll-out of public EV charging infrastructure in the EU. Is the chicken and egg dilemma resolved? *Transport & Environment*. Retrieved from https://www.transportenvironment.org/sites/te/files/publications/Charging%20Infrastructure%20Report%20September%202018_FINAL.pdf at 28-05-2019
- Carbon Expert. (n.d.). Carbon Allowances. Retrieved from <https://carbonexpert.ro/en/co2-emissions/what-are-co2-emissions-allowances/> at 28-05-2019
- Markets Insider. (2019). CO₂ European emission allowances price chart. Retrieved from <https://markets.businessinsider.com/commodities/historical-prices/co2-emissionsrechte/euro> at 28-05-2019
- ElectricityMap. (2019). Nederland. Retrieved from <https://www.electricitymap.org/?page=country&solar=false&remote=true&wind=false&countryCode=NL> at 28-05-2019
- Stern, N., & Stiglitz, J. E. (2017). Report of the high-level commission on carbon prices. *International Bank for Reconstruction and Development and International Development Association / The World Bank*. Retrieved from https://static1.squarespace.com/static/54ff9c5ce4b0a53deccfb4c/t/59b7f2409f8dce5316811916/1505227332748/CarbonPricing_FullReport.pdf at 28-05-2019
- CBS. (2017). Personenautoverkeer. Retrieved from <https://www.cbs.nl/nl-nl/maatschappij/verkeer-en-vervoer/transport-en-mobiliteit/mobiliteit/verkeer/categorie-verkeer/personenautoverkeer> at 28-05-2019
- Than, K. (2015). Estimated social cost of climate change not accurate, Stanford scientists say. *Stanford Report*. Retrieved from <https://news.stanford.edu/news/2015/january/emissions-social-costs-011215.html> at 28-05-2019
- Litman, T. (2009). Transportation cost and benefit analysis II–travel time costs. *Victoria Transport Policy Institute, Victoria, Canada*. Retrieved from <http://www.vtpi.org/tca/tca0502.pdf> at 29-05-2019
- Wardman, M., & Toner, J. (2018). Is generalised cost justified in travel demand analysis?. *Transportation*, 1–34. Retrieved from <https://link.springer.com/article/10.1007%2Fs11116-017-9850-7> at 29-05-2019
- McEvoy, J., Prince, A., & Ferreira, L. (1995). Generalised cost parameters for travel demand forecasting in queensland. *Road and Transport Research*, 4 (2), 76-87. Retrieved from <http://railknowledgebank.com/Presto/content/GetDoc.axd?ctID=MjEiZTI4YzctZjc1YSooMzQ4LTkyY2UtMDJmNTgxYjg2ZDA5&rID=NDkwNA==&pID=MTQ3Ng==&attchmnt=VHJlZQ==&uSesDM=False&rIdx=MTIyNTg=&rCFU> at 29-05-2019
- Persoon Advies. (2017). Wat kost een werknemer in vaste dienst u in 2018? Retrieved from <https://www.persoonadvies.nl/site/nl/organisatie/blog/detail/wat-kost-een-werknemer-in-vaste-dienst-u-in-2018/nl-63-453> at 29-05-2019

- Tentoo. (n.d.). Wat kost personeel? Retrieved from <https://www.tentoo.nl/personeelskosten> at 29-05-2019
- CBS. (2016). Uurloon. Retrieved from <https://www.cbs.nl/nl-nl/visualisaties/dashboard-arbeidsmarkt/ontwikkeling-cao-lonen/toelichtingen/uurloon> at 29-05-2019
- Raijmakers, K. (2019). Travelers' preferences towards Eindhoven city center: Implications of Mobility as a Service in the built environment. Retrieved from <https://www.ofcoursecme.nl/?mdocs-file=4825> at 21-06-2019
- MeteoGroup. (n.d.). Klimaat Nederland. Retrieved from <http://www.weer.nl/verwachting/klimaat/nederland/nederland/1813809/> at 03-06-2019
- Spritmonitor. (n.d.). Electricity consumption: BMW – i3. Retrieved from <https://www.spritmonitor.de/en/overview/6-BMW/1312-i3.html?fueltype=5&page=4> at 13/02/2019
- Eboli, L., Mazzulla, G., & Pungillo, G. (2017). How drivers' characteristics can affect driving style. *Transportation research procedia*, 27, 945-952. Retrieved from <https://doi.org/10.1016/j.trpro.2017.12.024> at 06/03/2019
- Hoelen, A. (2019). Nieuwe laadpalen in Utrecht: een eitje bakken met stroom uit je auto. NOS. Retrieved from <https://nos.nl/artikel/2277087-nieuwe-laadpalen-in-utrecht-een-eitje-bakken-met-stroom-uit-je-auto.html> at 24-06-2019
- Cuijpers, M., Staats, M., Bakker, W., & Hoekstra, A. (2016). Eindrapport Toekomstverkenning elektrisch vervoer. Retrieved from <https://www.rijksoverheid.nl/binaries/rijksoverheid/documenten/rapporten/2016/12/06/eindrapport-toekomstverkenning-elektrisch-vervoer/eindrapport-toekomstverkenning-elektrisch-vervoer.pdf>
- ACEA. (2018). Electric cars: unrealistic CO₂ targets proposed by EU Parliament ignore lack of charging points. Retrieved from <https://www.acea.be/press-releases/article/electric-cars-unrealistic-co2-targets-proposed-by-eu-parliament-ignore-lack>
- Jochem, P., Doll, C., & Fichtner, W. (2016). External costs of electric vehicles. *Transportation Research Part D: Transport and Environment*, 42, 60-76. Retrieved from https://ac.els-cdn.com/S1361920915001467/1-s2.0-S1361920915001467-main.pdf?_tid=b153e785-fc56-40a7-85e6-31559e6536a9&acdnat=1548504749_e2847a51635658cd15315bede814dcab
- IPCC. (2014). *Climate Change 2014: Mitigation of Climate Change. Contribution of Working Group III to the Fifth Assessment Report of the Intergovernmental Panel on Climate Change*. Cambridge University Press, Cambridge, United Kingdom and New York, NY, USA. Retrieved from https://www.ipcc.ch/site/assets/uploads/2018/02/ipcc_wg3_ar5_full.pdf
- EPA. (n.d.). *Smog, Soot, and Other Air Pollution from Transportation*. United States Environmental Protection Agency. Retrieved from <https://www.epa.gov/transportation-air-pollution-and-climate-change/smog-soot-and-local-air-pollution>
- OECD/IEA. (2018). Global EV Outlook 2018. Towards cross-modal electrification. Retrieved from <https://www.connaissancedesenergies.org/sites/default/files/pdf-actualites/globalevoutlook2018.pdf>
- Tate, E.D., Harpster, M.O., & Savagian, P.J. (2008). *The Electrification of the Automobile: From Conventional Hybrid, to Plug-in Hybrids, to Extended-Range Electric Vehicles*. SAE International Journal of Passenger Cars – Electronic and Electrical Systems. 1(2008-01-0458), 156-166. Retrieved from https://www.researchgate.net/publication/259032607_The_Electrification_of_the_Automobile_From_Conventional_Hybrid_to_Plug-in_Hybrids_to_Extended-Range_Electric_Vehicles
- Brady, J. (2010). *Electric Car Cultures: An ethnography of the everyday use of electric vehicles in the UK* (Doctoral dissertation, Durham University). Retrieved from http://etheses.dur.ac.uk/690/1/ELECTRIC_CAR_CULTURES.pdf?DDD5

- Sonnenschein, J. (2010). Preparing for The Roll-Out of Electric Vehicles: Exploring how cities can become plug-in ready. *IIIEE Theses*. Retrieved from <http://lup.lub.lu.se/luur/download?func=downloadFile&recordId=174741&fileId=1747418>
- Wynn, T., & Lafleur, S. (2009). A free market perspective on electric vehicles. *Cascade Policy Institute*. Portland: Oregon. Retrieved at <https://docplayer.net/8378981-A-free-market-perspective-on-electric-vehicles.html>
- Nilsson, M. (2011). *Electric vehicles: the phenomenon of range anxiety*. Lindholmen Science Park, Sweden. Retrieved from <https://cordis.europa.eu/docs/projects/cnect/5/249105/080/deliverables/001-ThephenomenonofrangeanxietyELVIRE.pdf>
- Shahan, Z. (2017). How Many Cars Do Electric Car Drivers Have? (CleanTechnica #EV Report). Retrieved from <https://cleantechnica.com/2017/06/15/many-cars-electric-car-drivers/>
- Khan, M., & Kockelman, K. M. (2012). Predicting the market potential of plug-in electric vehicles using multiday GPS data. *Energy Policy*, 46, 225-233. Retrieved from https://ac.els-cdn.com/S0301421512002601/1-s2.0-S0301421512002601-main.pdf?_tid=ac270ce6-7334-4bc6-8f97-a17e6a5744a2&acdnat=1548513478_cdc3c9c49cb6939b296b552e08fb61b5
- Yong, J. Y., Ramachandaramurthy, V. K., Tan, K. M., & Mithulananthan, N. (2015). A review on the state-of-the-art technologies of electric vehicle, its impacts and prospects. *Renewable and Sustainable Energy Reviews*, 49, 365-385. Retrieved from <https://doi.org/10.1016/j.rser.2015.04.130>
- Fagnant, D. J., & Kockelman, K. (2015). Preparing a nation for autonomous vehicles: opportunities, barriers and policy recommendations. *Transportation Research Part A: Policy and Practice*, 77, 167-181. Retrieved from <https://doi.org/10.1016/j.tra.2015.04.003>
- Hollweck, B., Moullion, M., Christ, M., Kolls, G., & Wind, J. (2018). Energy Analysis of Fuel Cell Electric Vehicles (FCEVs) under European Weather Conditions and Various Driving Behaviors. *Fuel Cells*, 18(5), 669-679. Retrieved from <https://doi.org/10.1002/fuce.201700227> at 01-07-2019
- Jiménez, F., & Cabrera-Montiel, W. (2014). System for road vehicle energy optimization using real time road and traffic information. *Energies*, 7(6), 3576-3598. Retrieved from <https://doi.org/10.3390/en7063576>
- Tang, J., Zhang, S., Chen, X., Liu, F., & Zou, Y. (2018). Taxi trips distribution modeling based on Entropy-Maximizing theory: A case study in Harbin city—China. *Physica A: Statistical Mechanics and its Applications*, 493, 430-443. Retrieved from <https://doi.org/10.1016/j.physa.2017.11.114>
- Long, J., Szeto, W. Y., & Ding, J. (2019). Dynamic traffic assignment in degradable networks: paradoxes and formulations with stochastic link transmission model. *Transportmetrica B: Transport Dynamics*, 7(1), 336-362. Retrieved from <https://doi.org/10.1080/21680566.2017.1405749>
- Wang, Q., & Sun, H. (2019). Traffic structure optimization in historic districts based on green transportation and sustainable development concept. *Advances in Civil Engineering*, 2019. Retrieved from <https://doi.org/10.1155/2019/9196263>
- Langbroek, J. H., Franklin, J. P., & Susilo, Y. O. (2016). The effect of policy incentives on electric vehicle adoption. *Energy Policy*, 94, 94-103. Retrieved from <https://doi.org/10.1016/j.enpol.2016.03.050>
- De Myttenaere, A., Golden, B., Le Grand, B., & Rossi, F. (2016). Mean absolute percentage error for regression models. *Neurocomputing*, 192, 38-48. Retrieved from <https://arxiv.org/pdf/1605.02541.pdf>
- Shitzer, A. (2006). Wind-chill-equivalent temperatures: regarding the impact due to the variability of the environmental convective heat transfer coefficient. *International journal of biometeorology*, 50(4), 224-232. Retrieved from <https://doi.org/10.1007/s00484-005-0011-x>

Ericsson, E., Larsson, H., & Brundell-Freij, K. (2006). Optimizing route choice for lowest fuel consumption–potential effects of a new driver support tool. *Transportation Research Part C: Emerging Technologies*, 14(6), 369–383. Retrieved from <https://doi.org/10.1016/j.trc.2006.10.001>

Appendices

- A** Routes in Nieuwegein
- B** VISSIM model of Nieuwegein
- C** Desired speed distributions
- D** Driving tests
- E** Nieuwegein results: Scenario 1
- F** Nieuwegein results: Scenario 2
- G** Nieuwegein results: Scenario 3
- H** Nieuwegein results: Scenario 4

Appendix A - Routes in Nieuwegein

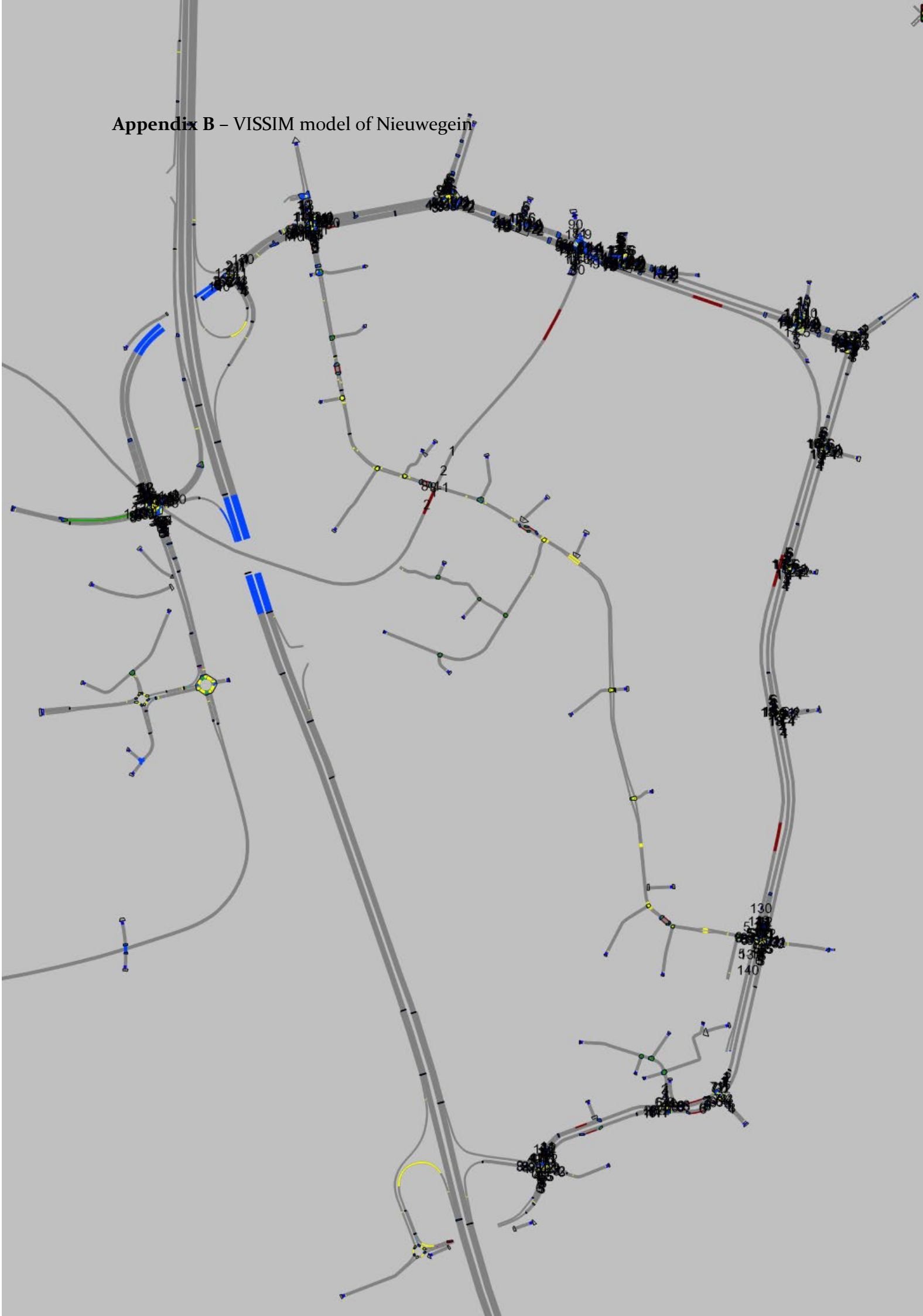


City center route

Residential route

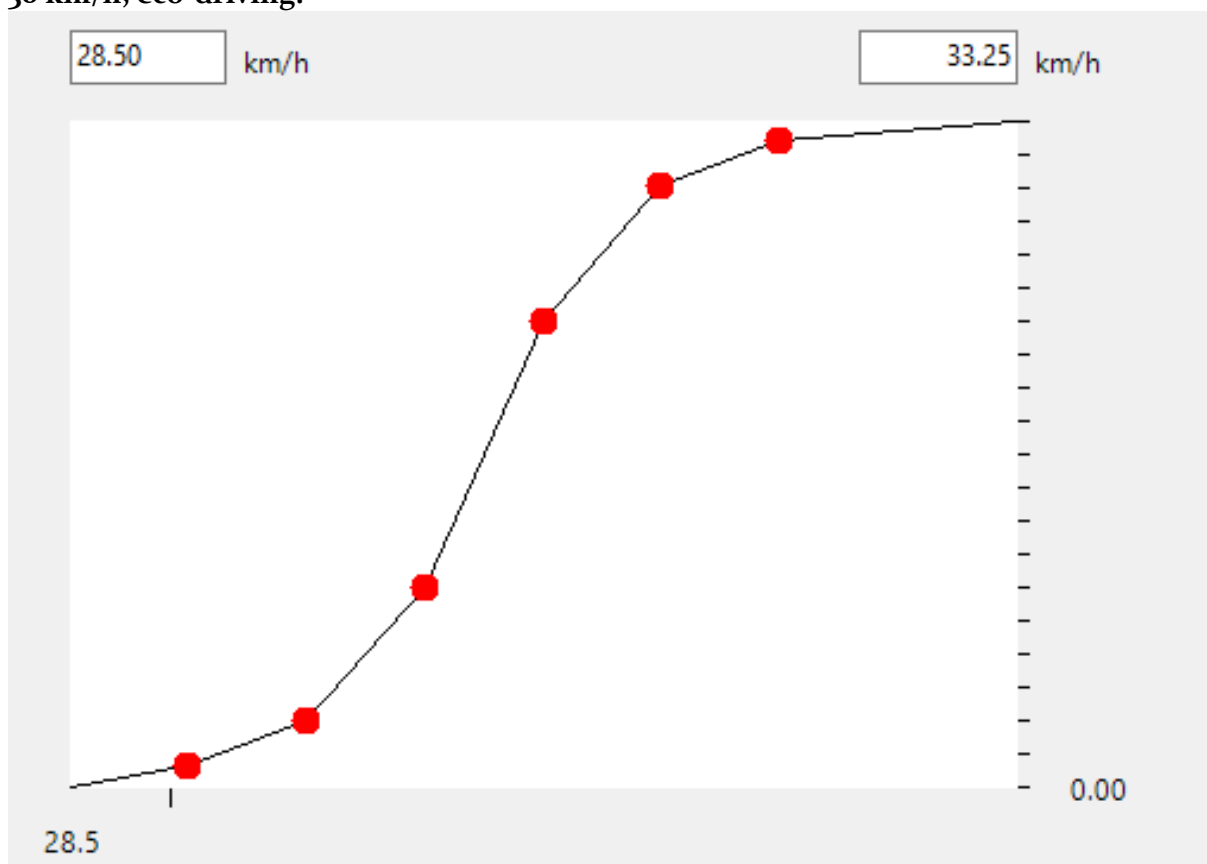
Motorway route

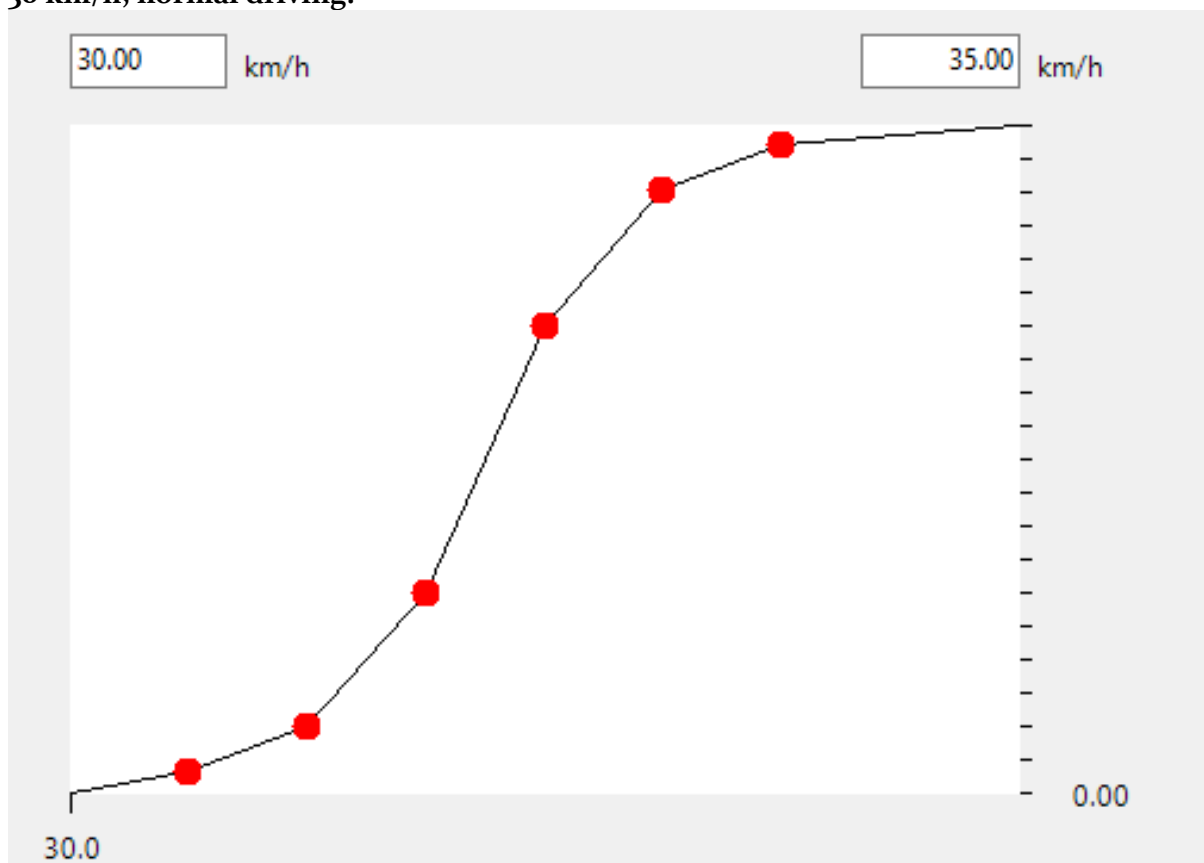
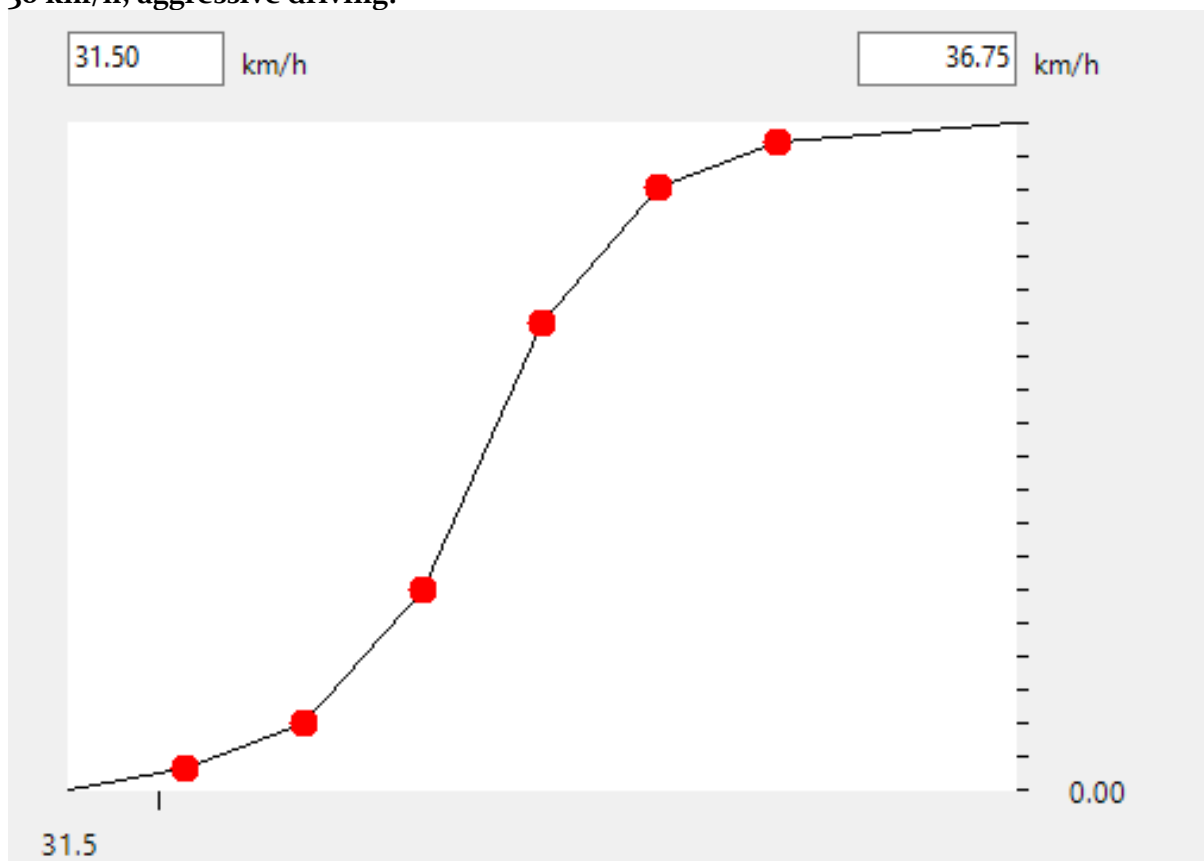
Appendix B – VISSIM model of Nieuwegein



Appendix C - Desired speed distributions

30 km/h, eco-driving:



30 km/h, normal driving:**30 km/h, aggressive driving:**

Appendix D – Driving tests

Driving test period #1

Date: 11-06-2019
 Car: BMW i3
 Passengers: Driver only
 Lights on: Yes, daytime
 Climate system on: No

Trip #	Route	Average speed [km/h]	Average consumption [kWh/100km]	Driving style	Notes
1	Residential	28,0	10,1	Eco	
2	City center	36,6	11,2	Normal	
3	Motorway	46,1	12,6	Eco	
4	Residential	39,2	10,4	Normal	
5	City center	34,3	15,3	Aggressive	Many traffic lights turned red
6	Motorway	51,6	13,6	Aggressive	Regen efficiency better than expected
7	Residential	39,3	15,2	Aggressive	
8	City center	32,0	10,1	Eco	
9	Motorway	47,8	11,4	Normal	
10	Residential	40,8	17,8	Aggressive	
11	City center	37,4	17,3	Aggressive	
12	Motorway	44,1	15,2	Aggressive	Congestion
13	Residential	28,8	8,6	Eco	Extreme eco-driving, other vehicles annoyed by me
14	City center	29,0	10,9	Normal	Congestion
15	Motorway	41,8	12,6	Normal	No congestion

Driving test period #2

Date: 12-06-2019
 Car: BMW i3
 Passengers: Driver only
 Lights on: Yes, daytime
 Climate system on: No

Trip #	Route	Average speed [km/h]	Average consumption [kWh/100km]	Driving style	Notes
16	Residential	27,0	9,5	Eco	
17	City center	38,3	11,3	Normal	
18	Motorway	53,2	12,7	Normal	
19	Residential	35,0	10,4	Normal	
20	City center	34,6	12,7	Eco	
21	Motorway	45,3	11,1	Eco	
22	Residential	34,7	10,2	Normal	
23	City center	44,8	10,7	Normal	Rain
24	Motorway	45,6	14,9	Normal	Rain
25	Residential	30,9	10,9	Normal	Rain

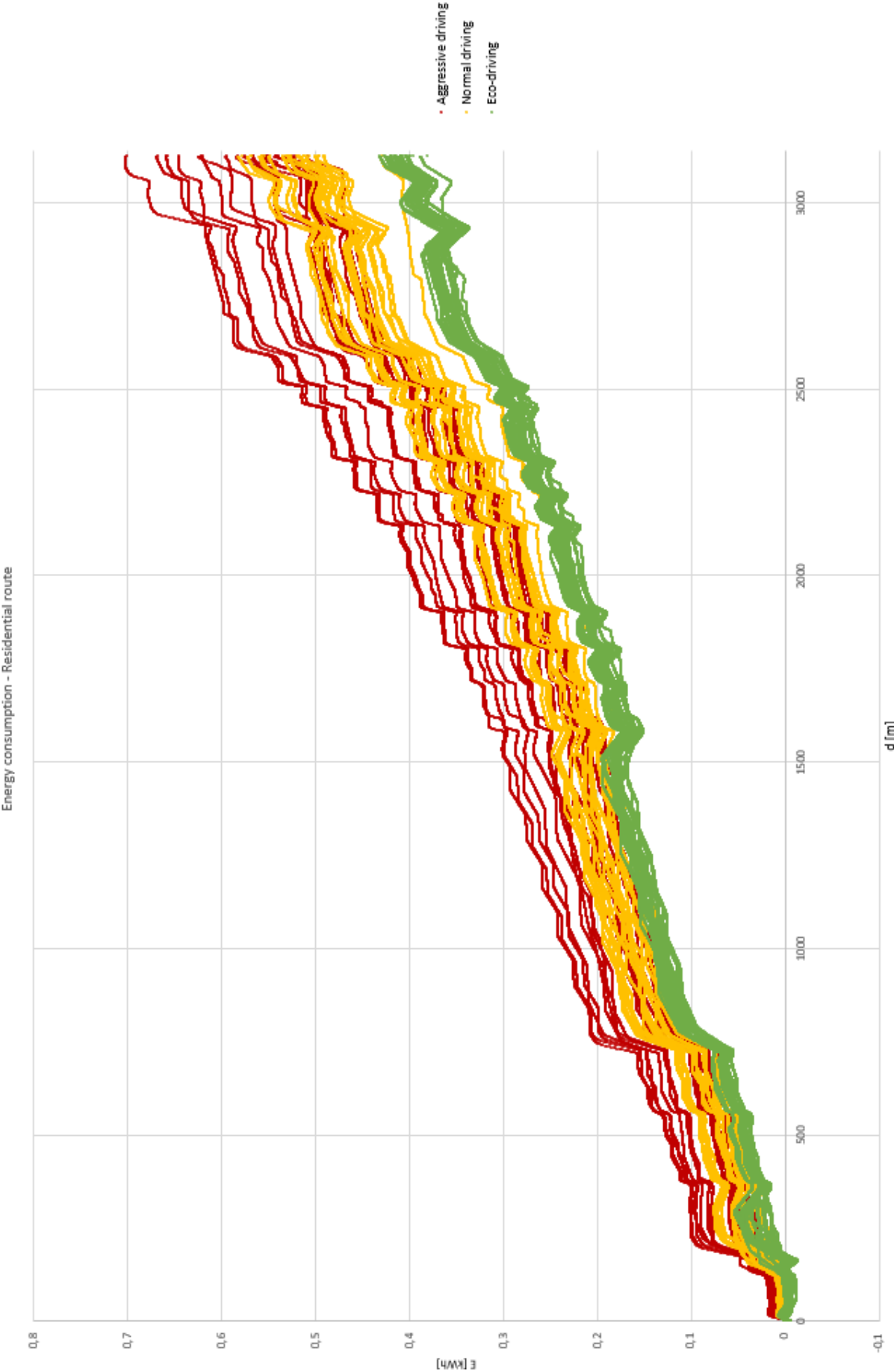
Driving test period #3

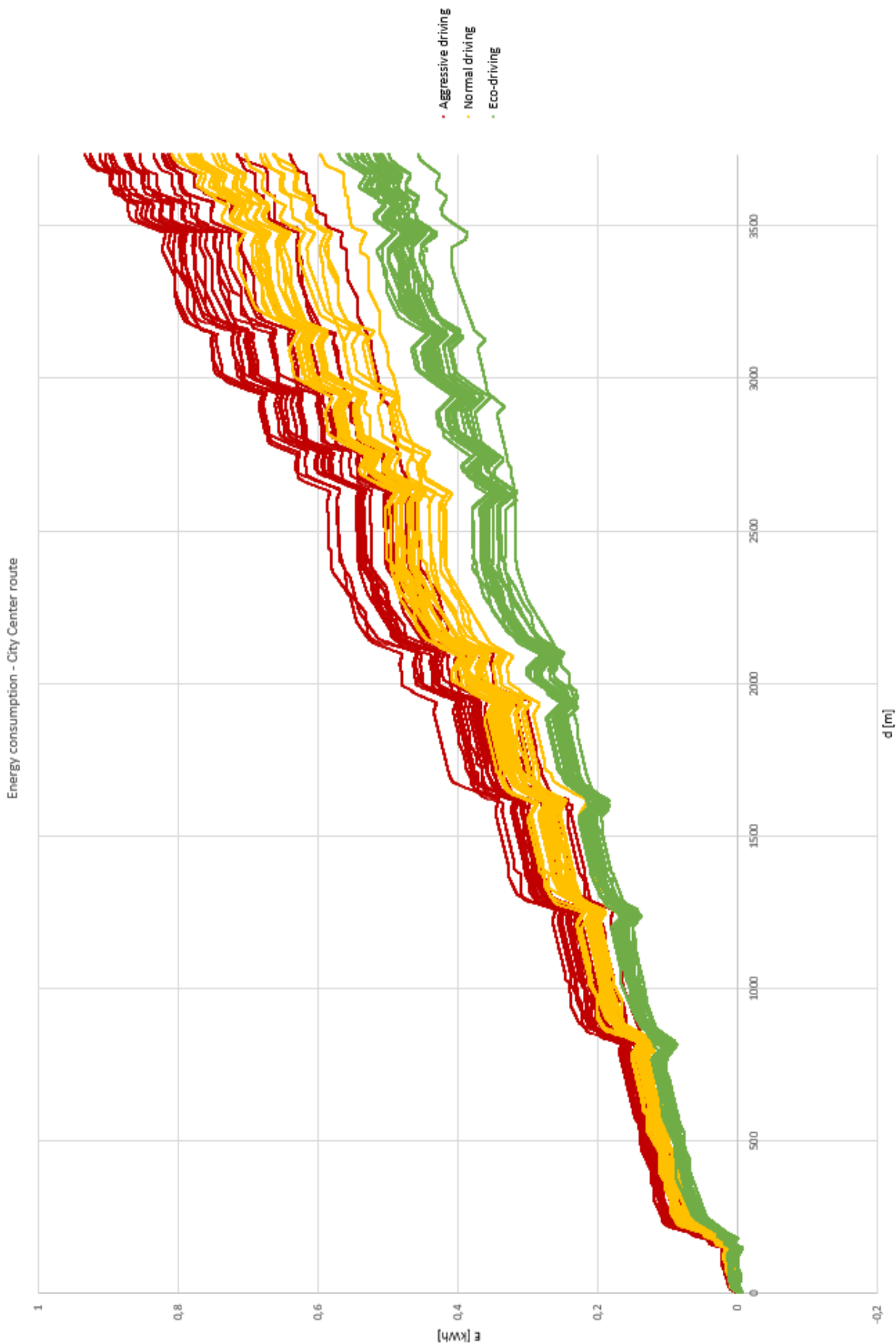
Date: 12-06-2019
Car: BMW i3
Passengers: Driver only
Lights on: Yes, daytime
Climate system on: Yes

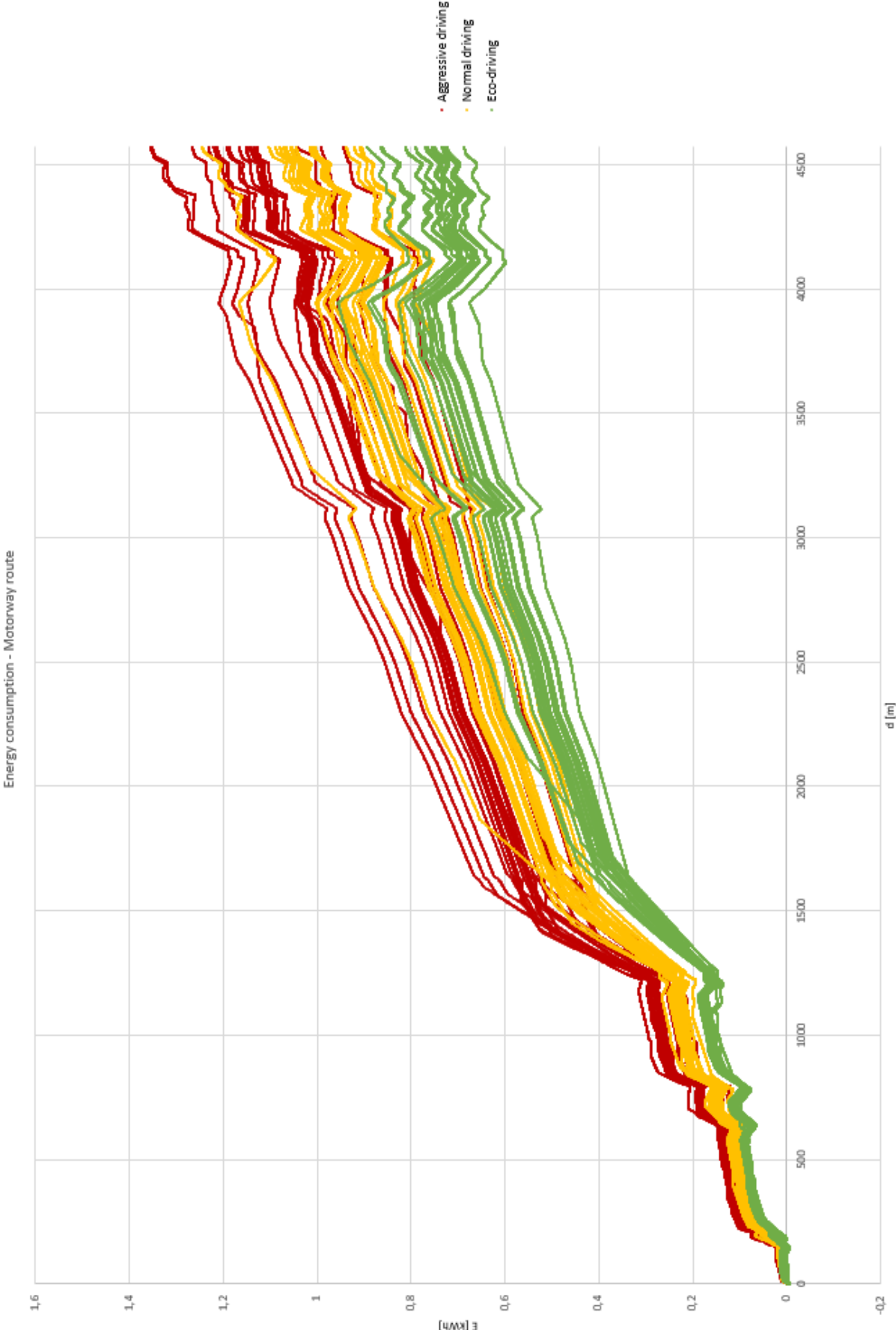
Trip #	Route	Average speed [km/h]	Average consumption [kWh/100km]	Driving style	Notes
26	City center	40,0	16,9	Normal	
27	Motorway	48,8	20,3	Normal	
28	Residential	33,1	14,7	Normal	
29	City center	35,7	24,0	Aggressive	
30	Motorway	49,3	22,6	Aggressive	
31	Residential	33,3	21,6	Aggressive	

Appendix E – Nieuwegein results: Scenario 1

	Eco-driving	Normal driving	Aggressive driving
Residential route			
d [m]	3140	3140	3140
t [s]	344.92	322.475	325.47
E [kWh]	0.41039327	0.52418624	0.580296431
E/d [kWh/km]	0.13069849	0.166938293	0.184807781
E*t [kWh*s]	141.552848	169.0369576	188.8690794
E*t^2 [kWh*s^2]	48824.4083	54510.19291	61471.21929
Range [km]	289.980387	227.0299962	205.0779457
City center route			
d [m]	3735	3735	3735
t [s]	318.745	298.53	279.585
E [kWh]	0.51566825	0.731335853	0.843954242
E/d [kWh/km]	0.13806379	0.195806119	0.225958298
E*t [kWh*s]	164.366675	218.3256922	235.9569468
E*t^2 [kWh*s^2]	52391.0559	65176.76888	65970.02296
Range [km]	274.510794	193.5588136	167.7300651
Motorway route			
d [m]	4570	4570	4570
t [s]	277.585	257.76	242.765
E [kWh]	0.76572959	1.024617428	1.1645837
E/d [kWh/km]	0.16755571	0.224205127	0.25483232
E*t [kWh*s]	212.555047	264.1053883	282.720162
E*t^2 [kWh*s^2]	59002.0928	68075.80489	68634.56014
Range [km]	226.193428	169.0416298	148.7252483

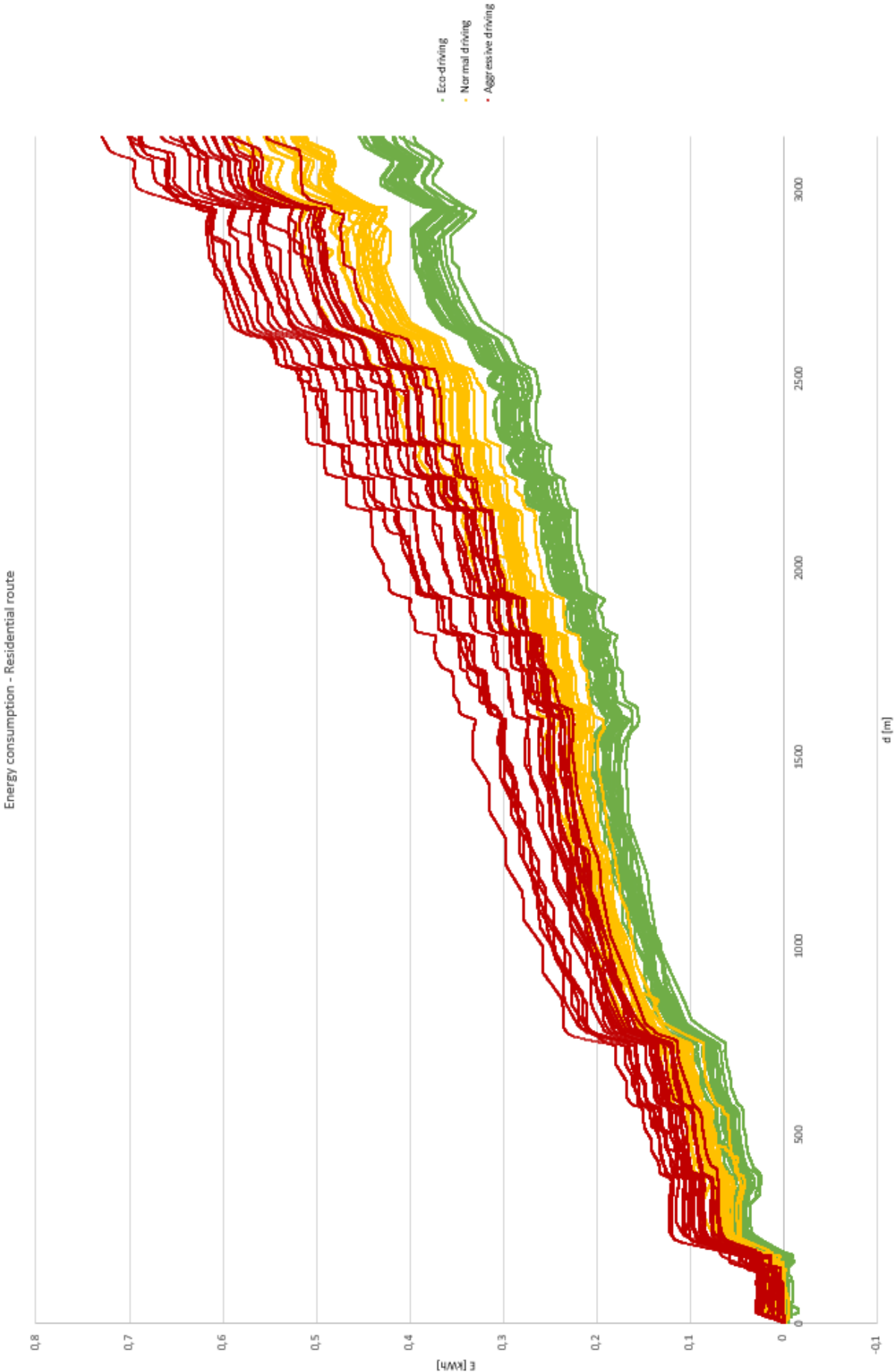


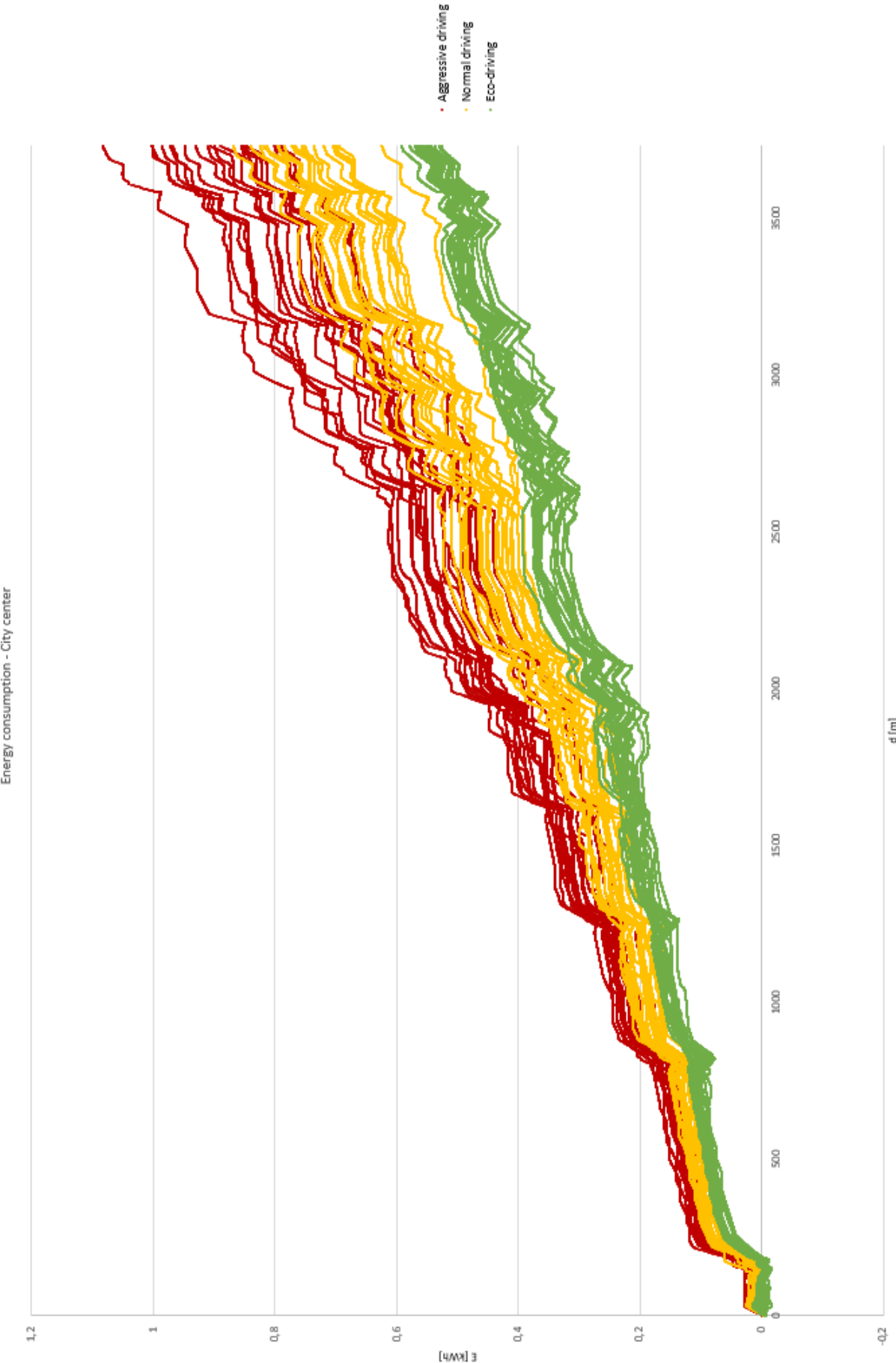


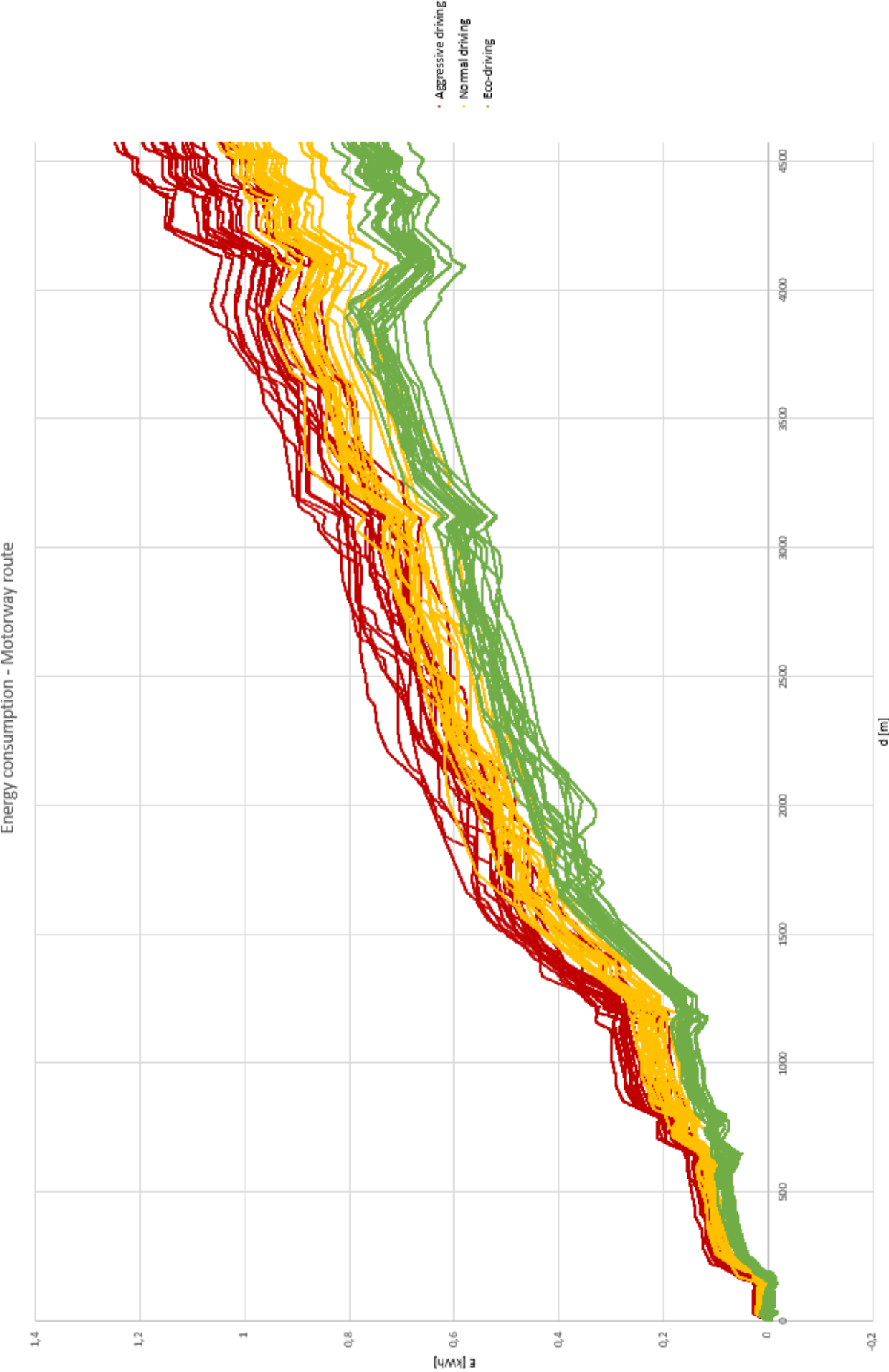


Appendix F – Nieuwegein results: Scenario 2

	Eco-driving	Normal driving	Aggressive driving
Residential route			
d [m]	3140	3140	3140
t [s]	414.18	414.32	381.205
E [kWh]	0.42546668	0.536528976	0.639040056
E/d [kWh/km]	0.13549894	0.170869101	0.203515941
E*t [kWh*s]	176.21979	222.2946852	243.6052644
E*t^2 [kWh*s^2]	72986.7127	92101.13398	92863.54483
Range [km]	279.706979	221.807219	186.2261981
City center route			
d [m]	3735	3735	3735
t [s]	481.06	463.36	433.025
E [kWh]	0.55146503	0.75552778	0.907089911
E/d [kWh/km]	0.14764793	0.202283207	0.242862091
E*t [kWh*s]	265.287768	350.0813521	392.7926087
E*t^2 [kWh*s^2]	127619.333	162213.6953	170089.0194
Range [km]	256.691707	187.3610789	156.0556438
Motorway route			
d [m]	4570	4570	4570
t [s]	362.695	350.205	335.575
E [kWh]	0.76090369	0.97932554	1.129687344
E/d [kWh/km]	0.16649971	0.214294429	0.247196355
E*t [kWh*s]	275.975964	342.9647007	379.0948306
E*t^2 [kWh*s^2]	100095.102	120107.953	127214.7478
Range [km]	227.628019	176.8594741	153.3194125

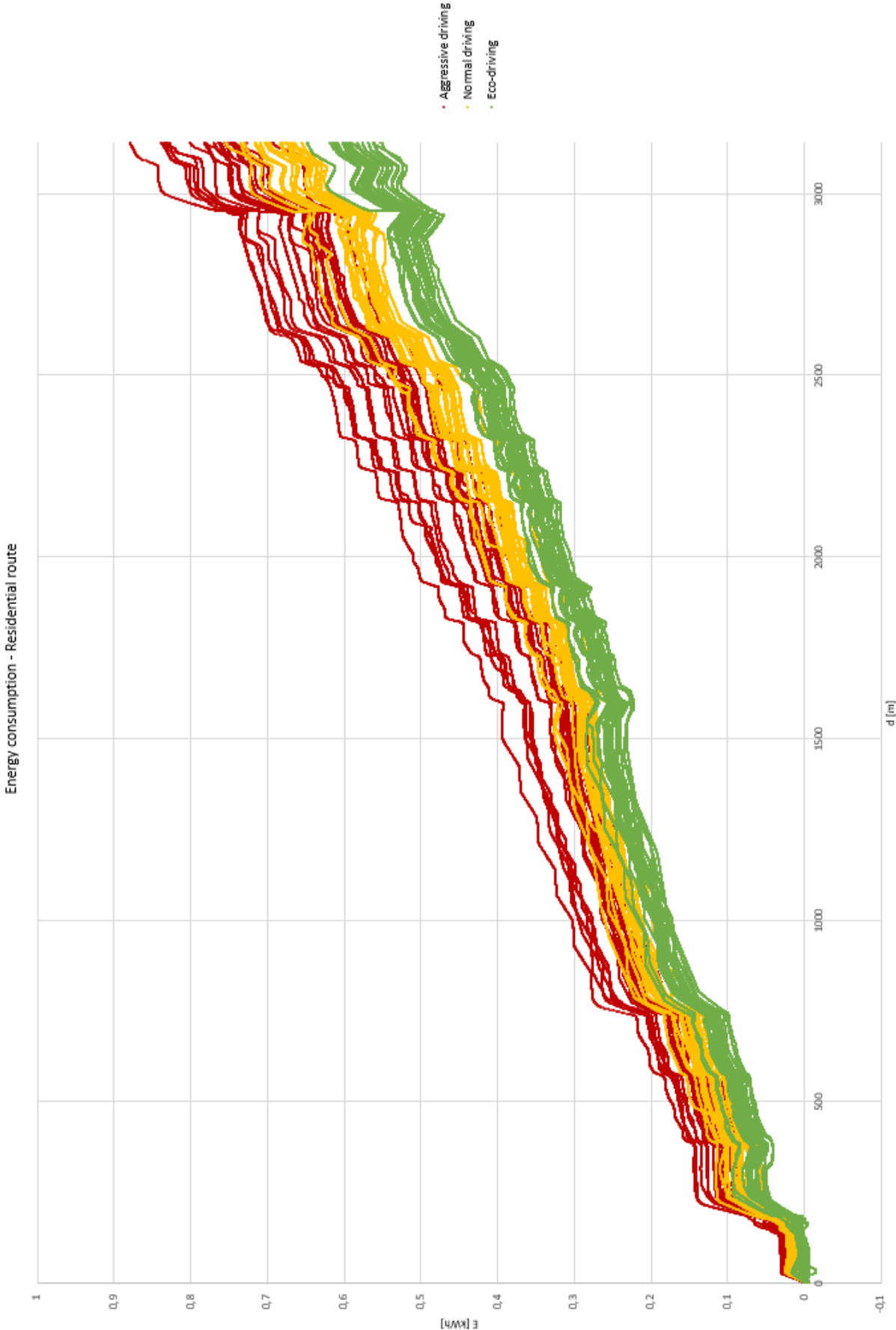


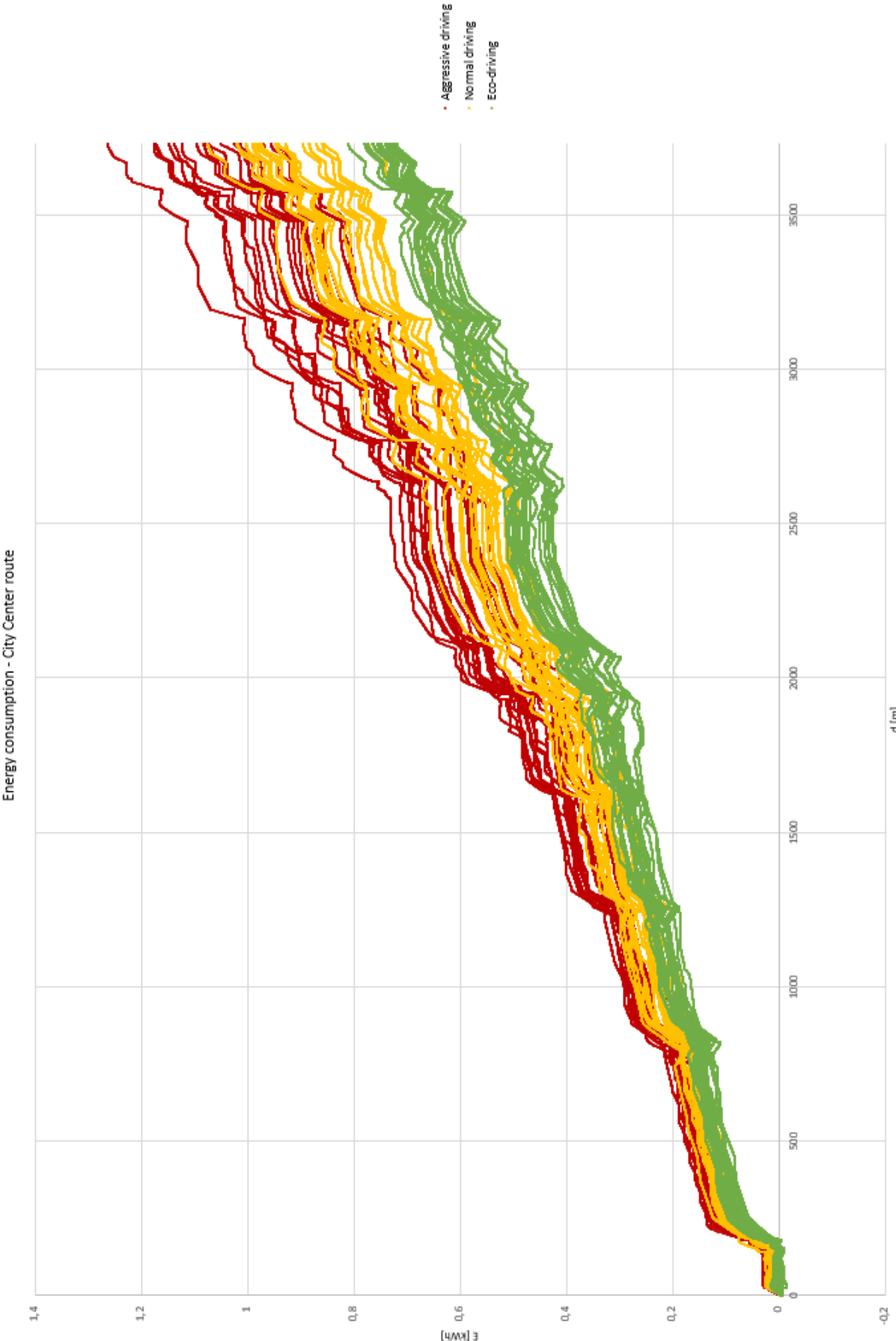


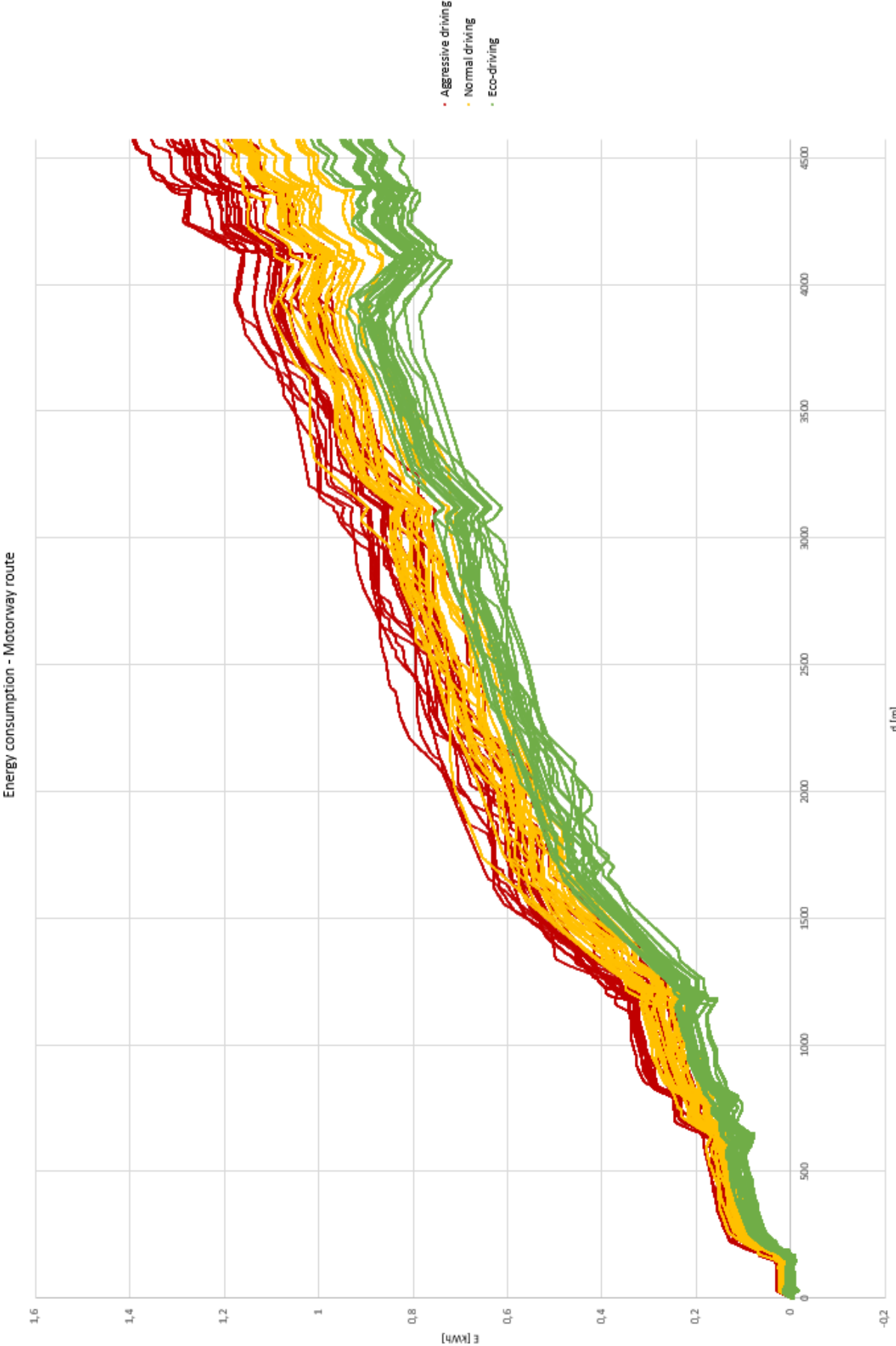


Appendix G – Nieuwegein results: Scenario 3

	Eco-driving	Normal driving	Aggressive driving
Residential route			
d [m]	3140	3140	3140
t [s]	414.18	414.32	381.205
E [kWh]	0.59076163	0.692971374	0.783010985
E/d [kWh/km]	0.18814065	0.22069152	0.249366556
E*t [kWh*s]	244.681652	287.1118995	298.4877025
E*t^2 [kWh*s^2]	101342.247	118956.2022	113785.0046
Range [km]	201.445039	171.7329237	151.9850964
City center route			
d [m]	3735	3735	3735
t [s]	481.06	463.36	433.025
E [kWh]	0.74395834	0.941761585	1.077179287
E/d [kWh/km]	0.19918563	0.252145003	0.288401415
E*t [kWh*s]	357.888599	436.3746478	466.4455605
E*t^2 [kWh*s^2]	172165.89	202198.5568	201982.5889
Range [km]	190.274767	150.3103358	131.4140569
Motorway route			
d [m]	4570	4570	4570
t [s]	362.695	350.205	335.575
E [kWh]	0.92436281	1.135182434	1.278167014
E/d [kWh/km]	0.20226757	0.248398782	0.279686436
E*t [kWh*s]	335.261769	397.5465644	428.9208956
E*t^2 [kWh*s^2]	121597.767	139222.7946	143935.1295
Range [km]	187.375561	152.5772376	135.5088953

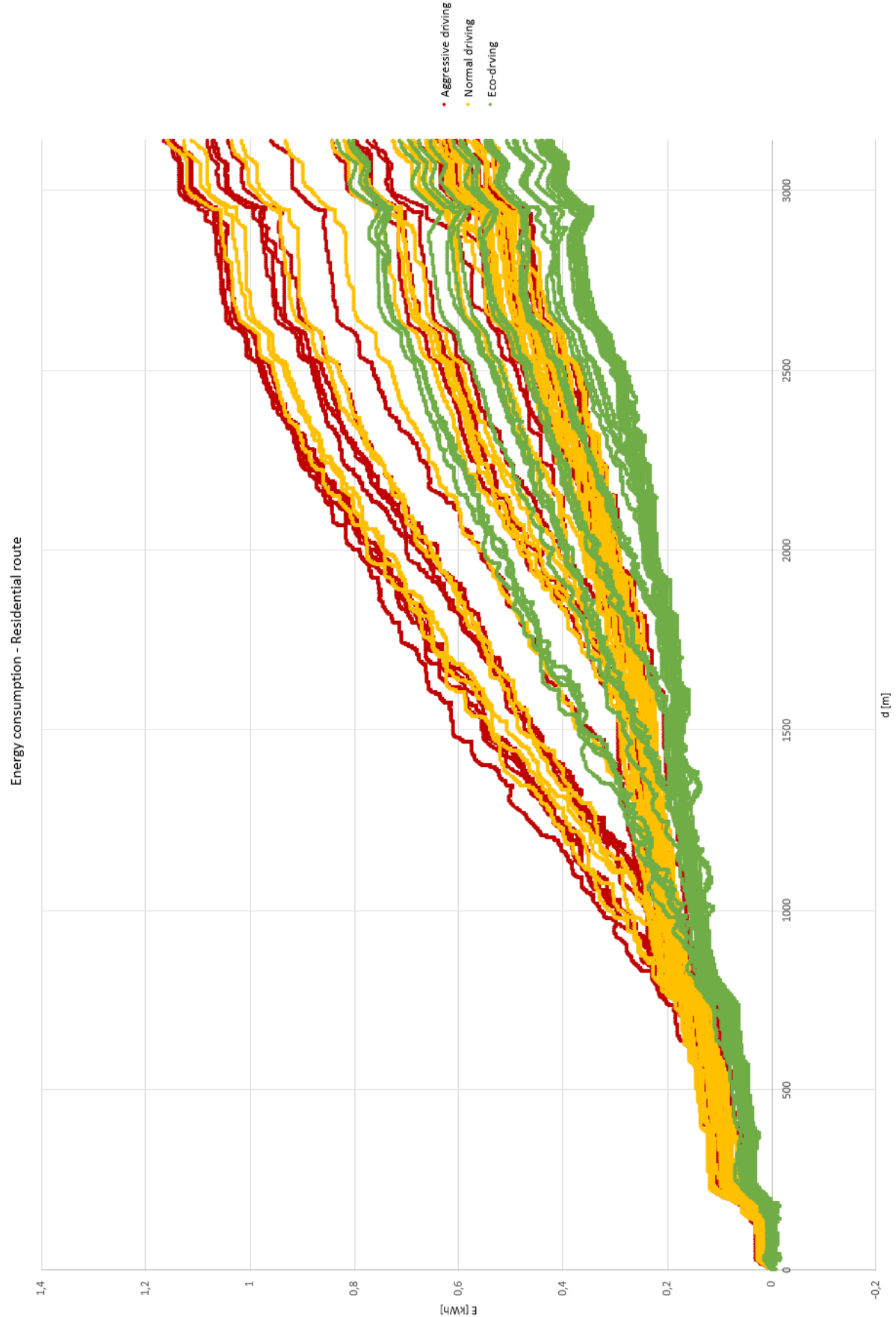


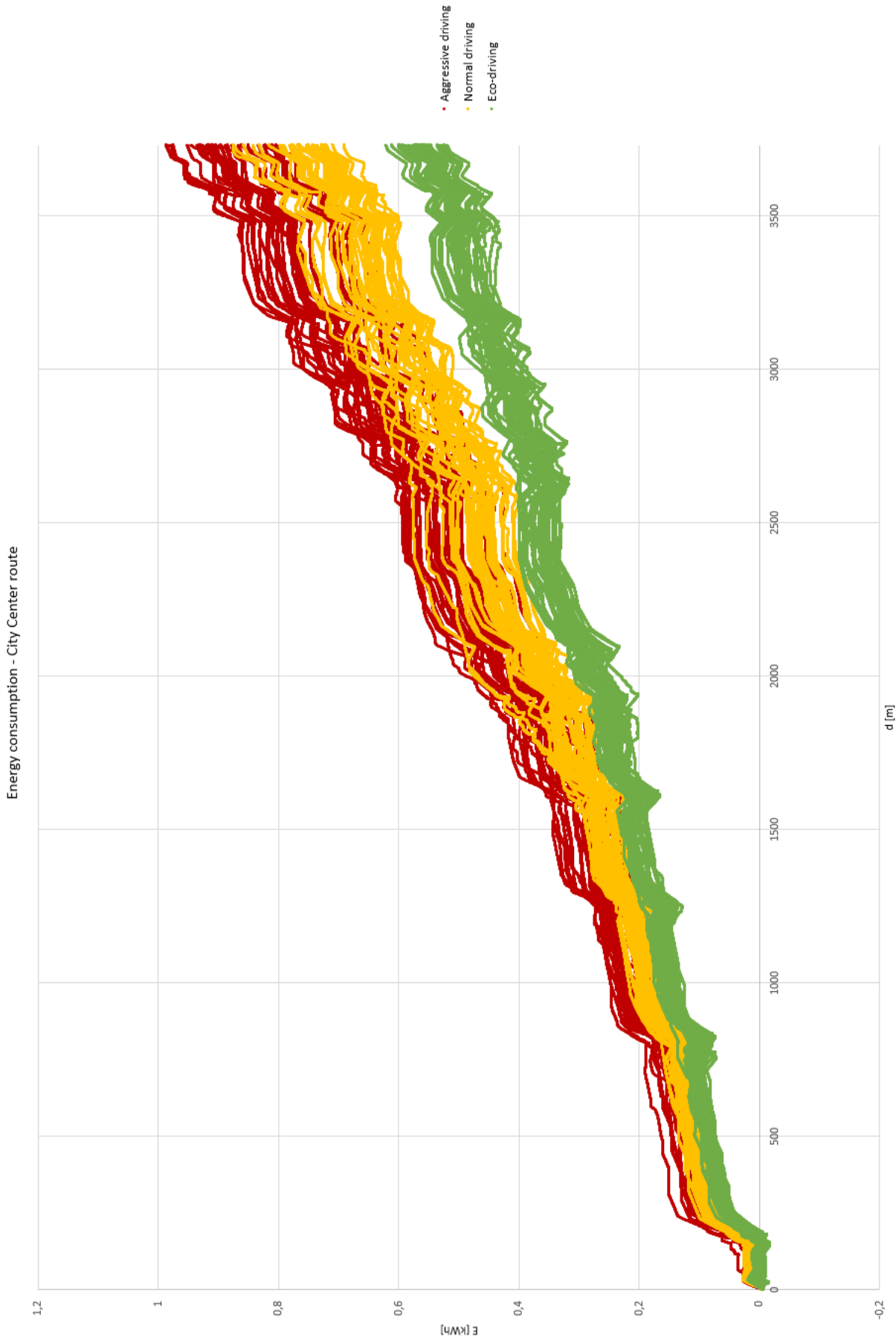




Appendix H – Nieuwegein results: Scenario 4

	Eco-driving	Normal driving	Aggressive driving
Residential route			
d [m]	3140	3140	3140
t [s]	428.935	415.07	412.34
E [kWh]	0.42879198	0.534452521	0.614096772
E/d [kWh/km]	0.13655796	0.170207809	0.195572221
E*t [kWh*s]	183.923889	221.8352081	253.2166632
E*t^2 [kWh*s^2]	78891.3933	92077.13982	104411.3589
Range [km]	277.537839	222.6689841	193.7903036
City center route			
d [m]	3735	3735	3735
t [s]	482.9	474.235	471.895
E [kWh]	0.55761208	0.759879525	0.890448075
E/d [kWh/km]	0.14929373	0.203448333	0.238406446
E*t [kWh*s]	269.270875	360.3614666	420.1979946
E*t^2 [kWh*s^2]	130030.905	170896.0201	198289.3326
Range [km]	253.861967	186.2880829	158.9722117
Motorway route			
d [m]	4570	4570	4570
t [s]	411.305	400.835	384
E [kWh]	0.8153217	1.060815588	1.041444728
E/d [kWh/km]	0.17840737	0.232125949	0.227887249
E*t [kWh*s]	335.345891	425.2120162	399.9147757
E*t^2 [kWh*s^2]	137929.442	170439.8585	153567.2739
Range [km]	212.435166	163.2734303	166.3103142







Thank you for reading.

Improving the range of EVs through urban data

The impacts of environmental variables and route choice on the energy efficiency of electric vehicles

A.J.A. Donkers

a.j.a.donkers@student.tue.nl

